

3D ICHNOFABRICS

IN SHALE GAS RESERVOIRS

By

@ Małgorzata Bednarz

A thesis submitted to the School of Graduate Studies
in partial fulfillment of the requirements for the degree of

Doctor of Philosophy

Department of Earth Sciences

Memorial University of Newfoundland

October 2014

St. John's

Newfoundland

Abstract

This PhD research project uses three-dimensional ichnology to address issues of shale-hydrocarbon reservoir quality and provides new tools for ichnofabric analysis and ichnotaxonomic considerations. The study presents deterministic (devoid of conceptual simplifications and interpretations) visualizations of the true spatial geometry of the aff. *Chondrites*, aff. *Phycosiphon* and *Nereites* trace fossils and models the three-dimensional arrangements of the burrow components. The volumetric reconstructions of the real geometry of the trace fossils allowed for their comparison with the previously established visualizations and for reconsideration of pre-existing palaeobiological models. To date three-dimensional understanding of the majority of trace fossils is presented as conceptual drawings available only on two-dimensional media. Such reconstructions are extrapolated mainly from observations of cross sections of burrows from core and outcrop and do not allow for realistic volumetric quantification and full elucidation of complex trace fossil geometries in the context of the host-sediment. The new methodology based on precise serial grinding and volume-visualization presented herein addresses this gap in ichnological knowledge, and is especially useful for examination of the ichnofabric contained in mudstones and muddy siltstones where the application or non-destructive methods of 3D reconstructions as CT scanning or MRI is impossible owing to the rock petrological characteristics (e.g., low burrow-matrix density difference). Volumetric calculations formulated in this study allowed for quantitative characterization of the fundamental attributes of the trace fossils and ichnofabric. The

quantitative analytical methods of three-dimensional ichnology presented herein considerably improve our understanding of the petrophysical characteristics of the bioturbated mudstone and therefore they significantly inform the quality of shale gas reservoirs.

Five bioturbated samples of organic-rich mudstones collected from shale-gas reservoir type facies of different ages (from Yorkshire [UK], Northumberland [UK], Baja California [Mexico] and Muddy Creek Canyon [Utah]) were reconstructed in 3D at a 1:1 scale. Visualization and volumetric analysis of the spatial distribution and architecture of burrows in reconstructed phycosiphoniform and aff. *Chondrites* ichnofabrics provides insights into the effects of these taxa on the rheological and petrophysical characteristics of mudstones. It has been demonstrated in the course of this thesis that, in addition to creating significant volumes of silty (clay-poor) zones of enhanced porosity and permeability, trace fossils propagate in all directions infiltrating substantial spatial volume of “tight” matrix and generate horizontally and vertically connected frameworks of densely packed quartzose strips, thereby improving permeability isotropy ($k_h \approx k_v$) and increasing stress isotropy. It is illustrated herein that shale ichnofabrics can create extensive fracture-prone planes of weakness in sediments that are of importance to hydraulic fracturing methods. Burrows similar to *Phycosiphon* and *Chondrites* significantly increase the surface area of the interface between the organic-rich matrix and silty burrow fills, thereby increasing the potential for diffusive transport of hydrocarbon molecules from the “tight” matrix to wellbore-connected volumes. By creating dense, highly interconnected brittle boxworks, ichnofabrics also have the

potential to improve the fracturability of reservoir mudstones by affecting fracture-spacing and fracture connectivity. The burrow spacing approach developed and employed in this study may form the basis for future modeling of fracture spacing and assessment of fracture complexity in stimulated hydrocarbon-charged shale intervals with bioturbation.

Acknowledgements

I would like to thank my parents, Alicja and Maciej Bednarz, for all the help and advice they gave me during my doctoral studies and who supported all of my decisions. Their love and understanding has been critical to my success and to the completion of this degree. I would like to thank them for motivating me and helping me to stay focused. I love you Mum and Dad. This project would never be completed without the faith, support and love that my family gave me throughout the last six years. My extended acknowledgements go to my sister Magdalena Mildner and my niece Emilia Mildner.

I would like to thank my supervisor Prof. Duncan McIlroy for his vital guidance, support and the chance to pursue research on such a timely and interesting topic.

It is a pleasure to formally thank some of those who have generously shared their time and wisdom with me in recent years. I extend my gratitude to my examiner Prof. Andreas Wetzel (University of Basel) for many enlightening discussions; as well as Prof. Alfred Uchman (Jagiellonian University) and Dr. Liam Herringshaw (Durham University). I acknowledge help within Memorial from my supervisory committee Prof. Susan Ziegler and Dr. Richard Callow, my internal reviewers Prof. Suzanne Dufour and Prof. Richard Hiscott. My thanks also go to Prof. Marek Michalik (Jagiellonian University).

Completing this work would not have been possible without help from a number of colleagues. I am thankful to Dario Harazim, Chris Phillips, Nikki Tonkin and Mary Laeman, who supported me when it was needed. I am also grateful to my friend Stefanie Lode who offered me a friendly atmosphere at her home just before my defence; her hospitality gave me a much needed respite. Thank you for being patient and understanding.

Without the help of my friends Margaret and Thomas Michalak I would have never been able to establish myself in Canada, even for a short time.

I especially appreciate the support and help of my best friends Weronika Górczyk (who inspired me to start my doctoral studies) and Magdalena Tomaszek, as they believed in me during hard times even when I lost hope.

John Max Wojnowski is acknowledged here for saving me when no one else could in very difficult times.

Last, but certainly not least, I would like to thank my friend Tomasz Tomaszek (Tomahavek) for his love, support and friendship during this long-lasting project.

I gratefully acknowledge the financial support I received from the Natural Science and Engineering Research Council of Canada (NSERC) as well as various student grants sponsored by AAPG and The Canadian Society for Unconventional Gas (CSUG).

Table of Contents

Abstract	ii
Acknowledgements	v
Table of Contents	vi
List of Tables	xiii
List of Figures	xiii
List of Appendices	xv
Co-authorship Statement.....	xvii

CHAPTER 1

Shale-gas reservoirs and ichnofabric: introduction and overview.....	1-1
1.1. Project overview and problem statement.....	1-1
1.1.1. Shale gas reservoir lithofacies variability and mudstone fabric as a first control on reservoir petrophysical properties	1-4
1.1.2. Most frequent ichnofabric-forming trace fossils in shale gas facies.....	1-7
1.1.3. Importance of deterministic three-dimensional reconstruction of ichnofabric in shale gas reservoir facies.....	1-13
1.1.4. Three-dimensional reconstructions in ichnology	1-15
1.2. Three-dimensional reconstruction of ichnofabric in shale gas reservoir facies: thesis aim and scope	1-18

1.2.1. Methodology formulation for the deterministic 3D reconstructions of ichnological specimens.	1-18
1.2.2. What do the common shale-gas reservoir trace fossils look like in 3D?	1-20
1.2.3. What effect do the common shale-gas reservoir trace fossils have on reservoir quality? Ichnofabric-associated porosity, permeability and fracturability	1-21
1.3. Objectives and analytical approaches	1-23
1.4. References	1-25

CHAPTER 2

Automated precision serial grinding and volumetric three-dimensional reconstruction of large ichnological specimens	2-1
2.1. Abstract	2-1
2.2. Introduction	2-2
2.3. Methodology	2-4
2.3.1. Sample preparation	2-4
2.3.2. Serial grinding set-up	2-6
2.3.3. Photography	2-7
2.3.4. Digital image-processing and interpretation	2-8
2.3.5. Burrow selection methods	2-8
2.3.6. 3D modeling	2-10
2.3.6.1. Volume visualization and polygonal surface extraction	2-10
2.3.6.2. 3D modeling software and polygonal mesh optimization	2-11

2.3.6.4. Popularization of 3D interactive models.....	2-20
2.4. Applications and future work.....	2-20
2.5. Conclusion	2-23
2.6. Acknowledgements.....	2-24
2.7. References.....	2-25
2.8. Appendices.....	2-27

CHAPTER 3

Three-dimensional reconstruction of “phycosiphoniform” burrows: implications for identification of trace fossils in core3-1

3.1. Abstract.....	3-1
3.2. Introduction.....	3-2
3.3. Phycosiphoniform burrows in marine ichnofabrics.....	3-5
3.4. Interpreted three-dimensional morphology of <i>Phycosiphon incertum</i>	3-8
3.4.1. The mud-filled “marginal burrow”	3-9
3.4.2. Spreiten and halos in <i>Phycosiphon</i>	3-12
3.5. Palaeobiology of the <i>Phycosiphon</i> trace-maker.....	3-13
3.5.1. Style of feeding	3-13
3.6. Interpretation of three-dimensional morphology from cross sections of phycosiphoniform burrows	3-14
3.6.1. Interpreting “frogspawn texture” as <i>Phycosiphon</i> -generated ichnofabrics.....	3-15
3.7. Methods.....	3-17

3.7.1. Serial grinding.....	3-17
3.7.2. Image processing.....	3-19
3.7.3. Three-dimensional rendering	3-19
3.8. Three-dimensional morphology of the Rosario Formation phycosiphoniform	
burrows	3-21
3.8.1. Nature of the halo in the Rosario phycosiphoniform burrows.....	3-25
3.9. Conclusion	3-26
3.10. Acknowledgements.....	3-28
3.11. References.....	3-28

CHAPTER 4

Effect of phycosiphoniform burrows on shale hydrocarbon reservoir quality 4-1

4.1. Abstract	4-1
4.2. Introduction.....	4-2
4.3. Phycosiphoniform trace fossils in shale-gas reservoir facies	4-6
4.3.1. Typical settings of <i>Phycosiphon</i> -like trace fossils occurrence	4-6
4.3.2. Gas shale facies with recognized occurrence of <i>Phycosiphon</i> -like	
trace fossils.....	4-8
4.3.3. Effects of phycosiphoniform burrows on permeability and fracturability.....	4-8
4.4. Methods.....	4-10
4.4.1. Three-dimensional methods in ichnology.....	4-10
4.4.2. Serial grinding.....	4-11

4.4.3. Image processing.....	4-12
4.4.4. Three-dimensional modeling and volume measurements.....	4-13
4.4.5. Quantitative ichnological methods.....	4-13
4.4.5.1. Burrow lengths and orientations	4-14
4.4.5.2. Volumetric considerations	4-17
4.5. Examined phycosiphoniform burrow types	4-18
4.5.1. Phycosiphoniform burrows from the Upper Cretaceous Rosario Formation, Baja California, Mexico (Ph1)	4-19
4.5.2. <i>Phycosiphon sensu stricto</i> from the Lower Jurassic Staithes Sandstone Formation, Yorkshire coast, UK	4-24
4.5.3. <i>Nereites</i> isp. from the Mississippian Yoredale Sandstone Formation, Northumberland, UK.....	4-28
4.6. Impact of phycosiphoniform ichnofabric on shale-gas reservoir quality	4-31
4.6.1. Porosity and permeability of reservoir mudstone	4-32
4.6.2. Brittleness of reservoir mudstone	4-33
4.6.3. Shale-gas reservoir capacity.....	4-35
4.6.4. Gas storativity and deliverability	4-35
4.7. Conclusion	4-37
4.8. Acknowledgements.....	4-40
4.9. References.....	4-40
4.10. Appendices.....	4-46

CHAPTER 5

Organism-sediment interactions in shale-hydrocarbon reservoir facies - three-dimensional reconstruction of complex ichnofabric geometries and pore-networks.....	5-1
5.1. Abstract	5-1
5.2. Introduction.....	5-2
5.3. Main ichnofabric-forming trace fossils in hydrocarbon shale facies	5-5
5.3.1. <i>Chondrites</i> ichnofabrics	5-8
5.3.2. Phycosiphoniform ichnofabric	5-9
5.4. Methods.....	5-10
5.4.1. Volumetrics	5-10
5.5. Results.....	5-15
5.5.1. Examined aff. <i>Chondrites</i> ichnofabric	5-16
5.5.1.1. <i>Chondrites</i> -like ichnofabric from Upper Cretaceous Mancos Shale, Muddy Creek, Utah	5-16
5.5.1.2. <i>Chondrites</i> -like ichnofabric from the Lower Jurassic Staithes Sandstone Formation, Yorkshire coast, UK	5-20
5.5.2. Examined <i>Phycosiphon</i> -like ichnofabrics.....	5-23
5.5.2.1. Phycosiphoniform burrows from the Upper Cretaceous Rosario Formation, Baja California, Mexico	5-23
5.5.2.2. <i>Phycosiphon sensu stricto</i> from the Lower Jurassic Staithes Sandstone Formation, Yorkshire coast, UK	5-25

5.5.2.3. <i>Nereites</i> isp. from the Mississippian Yoredale Sandstone Formation, Northumberland, UK	5-26
5.6. Discussion - The effect of ichnofabric on mudstone properties and shale reservoir potential	5-27
5.6.1. Porosity and permeability of the bioturbated reservoir facies	5-27
5.6.2. Brittleness of bioturbated shale.....	5-31
5.6.3. Impact of ichnofabric on fracture spacing and complexity.....	5-33
5.6.4. Impact on fluid flow within bioturbated shale	5-34
5.7. Conclusion	5-36
5.8. References	5-38
5.9. Appendices.....	5-50

CHAPTER 6

Three-dimensional reconstruction of ichnofabrics in shale gas reservoirs:

discussion and conclusions	6-1
6.1. Achievements of the thesis and summary of conclusions	6-2
6.1.1. Formulation of methodology for the deterministic volumetric 3D reconstructions and analysis of ichnological specimens.	6-2
6.1.2. Understanding morphological diversity of common shale-gas reservoir trace fossils in the light of their 3D reconstructions	6-5
6.1.3. Understanding the impact of trace fossils on shale–hydrocarbon reservoir	6-10
6.2. Avenues for future research	6-12

6.3. References.....	6-14
----------------------	------

List of Tables

CHAPTER 2

Table 2.1. Software used for visualization, modeling and viewing of 3D models.	2-21
---	------

CHAPTER 4

Table 4.1. Measurements of examined phycosiphoniform burrows.	4-22
--	------

Table 4.2. <i>Phycosiphon</i> -like bioturbation types.....	4-39
---	------

CHAPTER 5

Table 5.1. Organic-rich shale intervals with recognized presence of trace fossils	5-7
---	-----

Table 5.2. Measurements of examined three-dimensional ichnofabric.	5-19
---	------

List of Figures

CHAPTER 1

Fig. 1.1. Trace fossils that are typical for shale-hydrocarbon facies	1-10
---	------

CHAPTER 2

Fig. 2.1. Set-up and procedure for precise, computer-controlled, serial grinding.....	2-5
---	-----

Fig. 2.2. Selection of features in two samples of serially ground trace fossil.	2-9
Fig. 2.3. Application of artificial colors for visual enhancement of burrow.	2-12
Fig. 2.4. Polygonal surface extraction of reconstructed <i>Phycosiphon</i> -like burrow	2-13
Fig. 2.5. Mesh simplification of reconstructed trace fossils.	2-14
Fig. 2.6. 3D model of reconstructed ichnofabric composed of <i>Nereites</i> burrows.	2-18

CHAPTER 3

Fig. 3.1. Siltstone from Cretaceous Rosario Formation, Mexico.	3-4
Fig. 3.2. Locality map showing the field locality (in Baja California, Mexico)	3-6
Fig. 3.3. Conceptual model showing the orientation of a <i>Phycosiphon</i> burrow lobe.....	3-10
Fig. 3.4. Multiple phases of foraging by an unknown vermiform organism.	3-11
Fig. 3.5. Idealized 3D conceptual model showing the <i>Phycosiphon</i> structure.	3-16
Fig. 3.6. Image processing stages during three-dimensional reconstruction	3-20
Fig. 3.7. 3D reconstruction of phycosiphoniform from Rosario Formation.....	3-22
Fig. 3.8. 3D reconstruction of the lobe of the phycosiphoniform burrow	3-23
Fig. 3.9. Reconstructed phycosiphoniform burrow with associated halo	3-24

CHAPTER 4

Fig. 4.1. 3D reconstruction of a burrow from Mexico (Ph1 b01)	4-16
Fig. 4.2. Photographs of example slices of examined samples	4-20
Fig. 4.3. 3D reconstruction of phycosiphoniform burrows from Rosario Formation....	4-23
Fig. 4.4. Relationship between tortuosity and the volume of halo material.	4-25
Fig. 4.5. 3D reconstruction of <i>Phycosiphon s.s.</i> burrows from Yorkshire, UK.	4-27
Fig. 4.6. 3D reconstruction of <i>Nereites</i> Northumberland, UK	4-30

Fig. 4.7. Types of material in bioturbated mudstone	4-34
--	------

CHAPTER 5

Fig. 5.1. Variables used to assess volumetric characteristics of fabrics.	5-12
Fig. 5.2. Examined <i>Phycosiphon</i> -like and <i>Chondrites</i> -like ichnofabric.....	5-13
Fig. 5.3. 3D models of examined ichnofabrics.	5-18
Fig. 5.4. Composite master shafts of burrows of aff. <i>Chondrites</i> from Staithes.	5-22
Fig. 5.5. Chart illustrating relation of volume exploited to surface area	5-29
Fig. 5.6. Stages of the fluid flow within bioturbated, gas-charged tight mudstone.....	5-30

List of Appendices

CHAPTER 2

Appendix 2.1. Example of interactive 3D model embedded in the PDF file.	2-28
---	------

CHAPTER 3

Appendix 3.1. Multiple phases of phycosiphoniform burow formation.....	3-32
Appendix 3.2. 3D reconstruction of phycosiphoniform burrow core and halo	3-33

CHAPTER 4

Appendix 4.1. Symbols and equations.....	4-47
Appendix 4.2. Description of samples containing phycosiphoniform burrows.....	4-48

Appendix 4.2.	3D interactive models of reconstructed phycosiphoniform burrows	4-49
----------------------	--	------

CHAPTER 5

Appendix 5.1.	Interactive, simplified 3D models of examined ichnofabric	5-51
----------------------	---	------

Appendix 5.2.	Calculation of burrow spacing (BS).....	5-52
----------------------	---	------

Co-authorship Statement

This doctoral thesis is composed of six chapters. Chapters 2, 3, 4 and 5 are written in manuscript format and each of them has already been, or will be, submitted to an international scientific journal, as indicated at each title page.

Chapter 1 provides context for the dissertation, reviews existing knowledge in the field of study and defines the specific problems to be addressed (in the following chapters, and is entirely written by me with editorial help). Chapters 2 to 5 are written as focused research papers that present the research completed as part of this doctoral dissertation (in collaboration with Prof. D. McIlroy and other members of the research group). Chapter 6 integrates the individual objectives, summarizes the overall findings of this study, describes the project significance and outlines potential avenues for future research. It is entirely written by me with some editorial help.

Chapter 2, Bednarz et al., in press

The final shape of the manuscript is a collaborative effort of the members of the MUN Ichnology Research Group. I have provided guidelines for the method of sample preparation, serial grinding, digital image-processing, volume visualisation process and the volumetric analysis of the reconstructed ichnological data. Chris Boyd and Dr. Liam Herringshaw provided advice on professional photography in order to obtain high resolution images suitable for further digital analysis. Mary Leaman provided illustrations of the volume-visualised *Ophiomorpha*. Elisabeth Kahlmeyer assisted with

sample preparation and digital data management. Supervisory support was given by Dr. Liam Herringshaw and Prof. Duncan McIlroy

Chapter 3 (Bednarz and McIlroy 2009)

The reconstructed sample was collected by Prof. Duncan McIlroy, who also provided information on the sedimentological context of the Rosario Formation, editorial and supervisory support.

Chapter 4 (Bednarz and McIlroy 2012) is a case-study based manuscript. Prof. Duncan McIlroy provided samples from the UK and Mexico and field supervision in the UK along with editorial and supervisory support.

Chapter 5 (Bednarz and McIlroy in prep)

Samples were collected by Prof. Duncan McIlroy and myself during the field trips to the UK in 2009 and Utah in 2010. Dr. Liam Herringshaw, although not an author, provided help and advice with sample collection during field-work in Utah. Prof. Duncan McIlroy provided expert knowledge, guidance, and constructive editorial comments during construction of the manuscripts.

Funding for this work was mainly provided in the form of a grant from the National Sciences and Engineering Research Council of Canada (NSERC) and the Canada Research Chair (CRC) Program, awarded to Prof. Duncan McIlroy. Additional research funding was awarded to me from the American Association of Petroleum Geologists (AAPG), and the Canadian Society for Unconventional Gas (CSUG).

CHAPTER 1

Shale-gas reservoirs and ichnofabric: introduction and overview

1.1. Project overview and problem statement

Shale gas reservoirs are unconventional reservoir systems of continuous gas accumulations found within very fine-grained sedimentary rocks characterized by ultra-low matrix permeability. Hydrocarbon-bearing shale deposits can function as both hydrocarbon source and reservoir that can also simultaneously act as a seal, making exploitation technically challenging and dependent on the fracturability of mudstone (e.g., Wylie et al. 2007; Jenkins and Boyer 2008; Ding et al. 2012; Bust et al. 2013).

With improved understanding of mudstone petrophysics and the development of the production technologies, shale gas initially became an important source of hydrocarbons in the USA, and its production is now in prospect worldwide. Currently the gas from shale formations is estimated to constitute 32 % (7.299 trillion cubic feet) of the total technically recoverable natural gas resources identified to date in 42 countries around the globe (U.S. Energy Information Administration [EIA] 2013). Shale gas reservoirs are technically challenging and commercially economic shale-gas production presently takes

place only in 3 countries: United States, Canada and China with 39%, 15% and 1% of their national natural gas production respectively (U.S. Energy Information Administration [EIA] 2013). The highly successful exploitation of American shale-gas reservoirs (particularly Barnett Shale) had a profound influence on the development of shale/tight oil reservoirs worldwide, especially when the shale reservoir is capable of producing both: gas and oil (e.g., Woodford Shale and the Eagle Ford Shale, [U.S. Geological Survey, 2013]). Considering the uncertainty of long-term availability of gas and oil from currently known conventional reservoirs, shale-gas and shale-oil are at high demand at present, and will probably remain so in the short-medium term. This is especially true, since natural gas is, in addition, a clean-burning fossil fuel.

The processes of gas release from mudstone followed by the transport of gas molecules through a mudstone matrix, and also the production mechanisms are still not well understood (e.g., Ballard et al. 1994; Javadpour et al. 2007; Fan et al. 2010; Monteiro et al. 2012; Swami 2012; Swami et al. 2012). This is a consequence of the fact that mudstones are some of the most heterogeneous sedimentary rocks and include relevant lithological variability even at the microscopic scale. Comprehensive understanding of a shale-gas reservoir is possible if it is analyzed not only at a macroscopic scale but also from the millimetre scale, and even down to the molecular level. An appreciation of a mudstone's mineralogy, macro- and micro-fabric, nano-porosity and characteristics of pore-throats is essential (e.g., Schieber 2003; Javadpour et al. 2007; Macquaker et al. 2007; Ross and Bustin 2009, Bustin 2012; Chalmers et al. 2012a, b; Loucks et al. 2012; Spaw 2012; 2013a, b). The heterogeneous nature of the mudstones that comprise shale-

gas reservoirs makes each shale-gas reservoir unique, requiring a bespoke approach to the assessment of its economic value and the choice of development of production strategy (Jarvie et al. 2007; Deville et al. 2011; Bust et al. 2013).

The presence of reservoir–quality enhancing trace fossils in various types of conventional hydrocarbon reservoirs has been widely studied and documented (e.g., Gingras et al. 1999, 2004, 2012 and references therein; Pemberton and Gingras 2005; McIlroy 2004; Tonkin et al. 2010; Spila et al. 2007). Ichnological analysis in shale-hydrocarbon reservoirs has been primarily aimed at elucidation of palaeoenvironment of deposition, and for stratigraphic prediction through application of sequence stratigraphic principles (e.g., Cluff 1980; Wetzel and Uchman 1998a; Hovikoski et al. 2008; McIlroy 2008; Pervesler et al. 2008; Lemiski et al. 2011; Angulo and Buatois 2012a, b; Gingras et al. 2012; Egenhoff and Fishman 2013). The impact of ichnofabric on shale-hydrocarbon reservoir quality (mainly on shale reservoir permeability) has been studied in some producing and prospective shale-hydrocarbon reservoirs (Hovikoski et al. 2008; Lemiski et al. 2011, Gingras et al. 2012; La Croix et al. 2013, Spaw 2012, 2013a). These studies provide important insights through measurements of burrow-matrix permeability differences, however they do not provide deterministic volumetric analyses of the ichnofabric. Such a volumetric approach would allow quantitative assessment and prediction of the portion of the reservoir that is enhanced (in terms of porosity and permeability but also of fracturability) by trace fossils (Bednarz and McIlroy 2012; cf. La Croix et al. 2012). This study addresses this gap in knowledge by deterministic (devoid of conceptual simplifications and interpretations) volumetric analyses of ichnofabrics that

are typical of organic-rich shale-hydrocarbon reservoir deposits. The results of the deterministic burrow modelling allow quantitative investigation of actual volumes and authentic spatial distributions of the permeable and brittle components of shale-gas facies trace fossils. This study of shale-hydrocarbon reservoir ichnofabrics is the first step towards development of a new understanding of reservoir properties in terms of porosity, permeability and fractureability.

1.1.1. Shale gas reservoir lithofacies variability and mudstone fabric as a first control on reservoir petrophysical properties

Shale-gas and shale-oil reservoirs are self-sourcing reservoirs composed of organic-rich very fine-grained sedimentary facies characterized by predominant content of clay minerals and other clay-size particles (< 0.063 mm; cf. Macquaker and Adams 2003). These facies are informally named “shales” and are complex heterogeneous mixtures of clay minerals, quartz, carbonates, feldspars and heavy minerals of detrital, biogenic or authigenic origin that may constitute a wide range of lithologies including e.g., mudstones, siltstones, claystones, marlstones or limestones (Bustin 2012; Bust et al. 2013). The word “shale” is used in a broad sense in petroleum industry even though the classification of clay-rich and mud-rich rocks has received more attention by academics (e.g., Potter et al. 1980). Since practical application of this ichnological research pertains to gas extraction from rocks classified as shales by industrial colleagues, the author has decided to consider a wide variety of silt- and clay-rich rocks (mudrocks, both fissile and non-fissile) as shales in this thesis.

Gas-shales composed of organic-rich facies (including so called “black shales”) are still poorly understood (Schieber 2003; Javadpour et al. 2007; Josh et al. 2012). This lack of understanding results probably mainly from the fact that hand specimens of such fine grained rocks appear to be homogeneous and lacking in clearly visible heterogeneity of fabric and mineralogy at the hand sample scale. In addition, for years they have been uncritically considered to have been deposited in prevailing anoxic bottom water conditions typical of stratified and stagnant water-masses (cf. Schieber 2003 and references therein). The necessity of anoxia for the formation of black shale deposition has however been challenged (e.g., Schieber 1994, 2003, 2011; Wetzel and Uchman 1998b; Macquaker et al. 1999; Macquaker and Bohacs 2007; Schieber et al. 2007; Rodríguez-Tovar and Uchman 2010; Ghadeer and Macquaker 2012). Presence of bioturbation and bottom current activity in organic-rich deposits is, currently implied to be rather the norm than an exception. The homogeneity of mudstones is considered to be due to the effects of compaction, comparative lithological homogeneity in terms of grain size, and a lack of macroscopic sedimentary structures (Schieber 2003, Macquaker and Bohacs 2007; cf. Chamberlain 1978; Wetzel and Uchman 1998a, b; Jacobi et al. 2008; Callow and McIlroy 2011; Egenhoff and Fishman 2013).

The distribution of mineral grains and organic matter particles in mudstones comprise the macroscopic- and microscopic-fabrics (including ichnofabric) that determine the petrophysical and geomechanical properties of mudstones (e.g., porosity, permeability and brittleness; Josh et al. 2012 and references therein). The brittleness of a mudstone depends on the brittle mineral content (mainly quartz, feldspars or carbonates) relative to

the clay mineral content (e.g., Jacobi et al. 2008; Rickman et al. 2008; Bust et al. 2013). In shale-hydrocarbon reservoirs the brittleness of the shale facies determines their fracturability, and therefore potential as productive reservoirs. Because of the ultra-low matrix permeability (measured in nano- to milli-Darcy) and complex gas release processes in shale-hydrocarbon reservoirs, successful production is dependent not only upon locating sufficient gas volume within a brittle horizon, but also on the complexity, spacing and conductivity of the induced fractures (e.g., Wylie et al. 2007; Jacobi et al. 2008; Cipolla et al. 2009, 2010; Fan et al. 2010; Palmer and Moschovidis 2010; Bustin and Bustin 2012; Swami 2012; Bust et al. 2013). Ichnofabric is potentially the most influential and volumetrically significant contributor to the spatial distribution and architecture of the quartzose and/or silt-rich zones within bioturbated mudstones and consequently directly affects natural and/or induced fracture development. Associations of burrows with quartz-rich components can create tortuous planes of weakness within a clay-rich mudstone matrix, thereby considerably enhancing fracture spacing and consequently the surface area of mudstone connected to the well-bore.

Endobenthic burrowing organisms re-distribute mineral grains within the host sediment and can directly influence the porosity and permeability of the resultant rock (e.g., Gingras et al. 1999, 2002, 2004, 2012; Pemberton and Gingras 2005; Tonkin et al. 2010; Bednarz and McIlroy 2012). Burrow fills in mudstones are commonly more porous and permeable than the host sediment (e.g., Hovikoski et al. 2008, Leminski et al. 2011, Bednarz and McIlroy 2009, 2012; Gingras et al. 2012, 2013; Harazim 2013) in terms of bulk permeability relative to unbioturbated horizons. This is because of the permeability

isotropy resulting from closely spaced silt- and sand-rich burrow-fills that may be considerably more permeable than the host sediment (e.g., Gingras et al. 2013). Such burrow-enhanced permeability is considered to be capable of sustaining gas production even without well-stimulation providing that there is significant vertical permeability, k_v (Gingras et al. 2013; cf. also Bednarz and McIlroy 2012; La Croix 2012). Recognition of mudstone ichnofabrics and other macro- and micro-fabrics is therefore a requisite for complete appreciation of shale gas reservoirs facies and is integral to assessment and prediction of shale porosity, permeability and stress-strain behavior (Jacobi et al. 2008; Bustin 2012; Bustin and Bustin 2012; Chalmers et al. 2012b; Josh et al. 2012; Spaw 2013a, b).

1.1.2. Most frequent ichnofabric-forming trace fossils in shale gas facies

Bioturbation of muddy deposits may result in significant spatial reorganisation of sediment grains consequently causing substantial heterogeneity of lithified shales, and thereby influence their petrophysical properties. Porosity, permeability and brittleness of bioturbated shales can therefore be significantly influenced by the volume and/or spatial distribution of burrows present. For this reason, recognizing and understanding the presence of trace fossils in shale-gas facies may meaningfully inform quality of reservoir in shales, especially in cases where burrows contribute in formation of, or constitute, the sediment fabric. Ichnofabric-forming trace fossils are defined as burrows that occur within and/or process large volumes of sediment and have strong lithological contrast to the host rock matrix (Callow and McIlroy 2011). In contrast to weakly-penetrating

(interface) trace fossils, makers of ichnofabric-forming burrows process (mix, ingest, segregate or introduce) significantly larger volumes of sediment (McIlroy 2007; Callow and McIlroy 2011). The net effect of this is that the burrowing organisms may influence reservoir quality through the generation and/or improvement of permeable and/or brittle zones and by increasing vertical connectivity.

Ichnofabric is common in black and dark organic-rich shale facies that have in the past been uncritically associated with the anoxic and life-depleted environments (Schieber 2003). The ability of benthic organisms to tolerate, and even prosper, in dysoxic, anoxic and euxinic environments has been proven through biological and ichnological studies (e.g., Bromley and Ekdale 1984; Ekdale and Mason 1988; Seilacher 1990; Fu 1991; Wetzel and Uchman 1998a; Schieber 2003; Dufour and Felbeck 2003; Stewart et al. 2005; Arndt-Sullivan et al. 2008; Dando et al. 2008; Middelburg and Levin 2009). This capability of surviving in black-shale depositional environments and sediments is primarily associated with interrelated characteristics of feeding strategy (e.g., deposit feeding [makers of *Phycosiphon* and *Nereites*] or chemosymbiotic adaptations [makers of *Chondrites*, *Trichichnus*, *Zoophycos*]), respiration adaptations and burrow architecture (open stationary burrows [e.g., *Chondrites*, *Trichichnus*, *Zoophycos*] or burrows without connection to the water-sediment surface [e.g., *Phycosiphon* and *Nereites*]) or short-term re-oxidation events (e.g., Wetzel and Uchman 1998a). It was recently demonstrated that deposition of organic-rich sediments and even black shales is not limited to deep-water anoxic settings in low energy environments, and deposition of organic matter is driven mainly by large primary production, low rates of remineralization in the water column,

and rapid sedimentation in wide range of depths in marine and lacustrine settings (e.g., Wetzel and Uchman 1998b; Schieber 2003; Bohacs et al. 2005, Macquaker and Bohacs 2007). Trace fossils have been recorded from almost all shale gas reservoirs in the USA and Canada, and in multiple organic-rich fine-grained successions worldwide. The lack of recognition of trace fossils in other shale-gas facies may yet be because of their small size, low density and low color contrast, and the necessity of focussed unconventional methods to determine their presence (e.g., microscopy and polishing; Callow and McIlroy 2011; Bednarz and McIlroy 2012 and references therein; La Croix et al. 2013).

The most abundant ichnofabric-forming trace fossils in shale-gas facies are: *Chondrites*, *Planolites*, *Phycosiphon*, *Nereites*, *Zoophycos*, *Trichichnus* (Fig. 1.1). All the above ichnotaxa are often suggested to indicate anoxic (i.e., *Trichichnus* and *Chondrites*; Bromley and Ekdale 1984) or dysoxic (oxygen-poor) conditions during bioturbation. These trace fossils are commonly assigned to *Nereites* and *Zoophycos* ichnofacies indicating event/turbiditic softgrounds and non-event dysoxic or anoxic and/or euxinic conditions respectively with *Chondrites*, *Phycosiphon* and *Planolites* being facies-breaking trace fossils (Seilacher 1967, 2007; McIlroy 2008).

This work addresses deterministic three-dimensional reconstruction of *Phycosiphon*, *Nereites* and *Chondrites* ichnofabrics from samples collected from organic-rich rocks that are analogous to the shale-gas facies in order to examine how their presence, volume and distribution may impact reservoir quality.

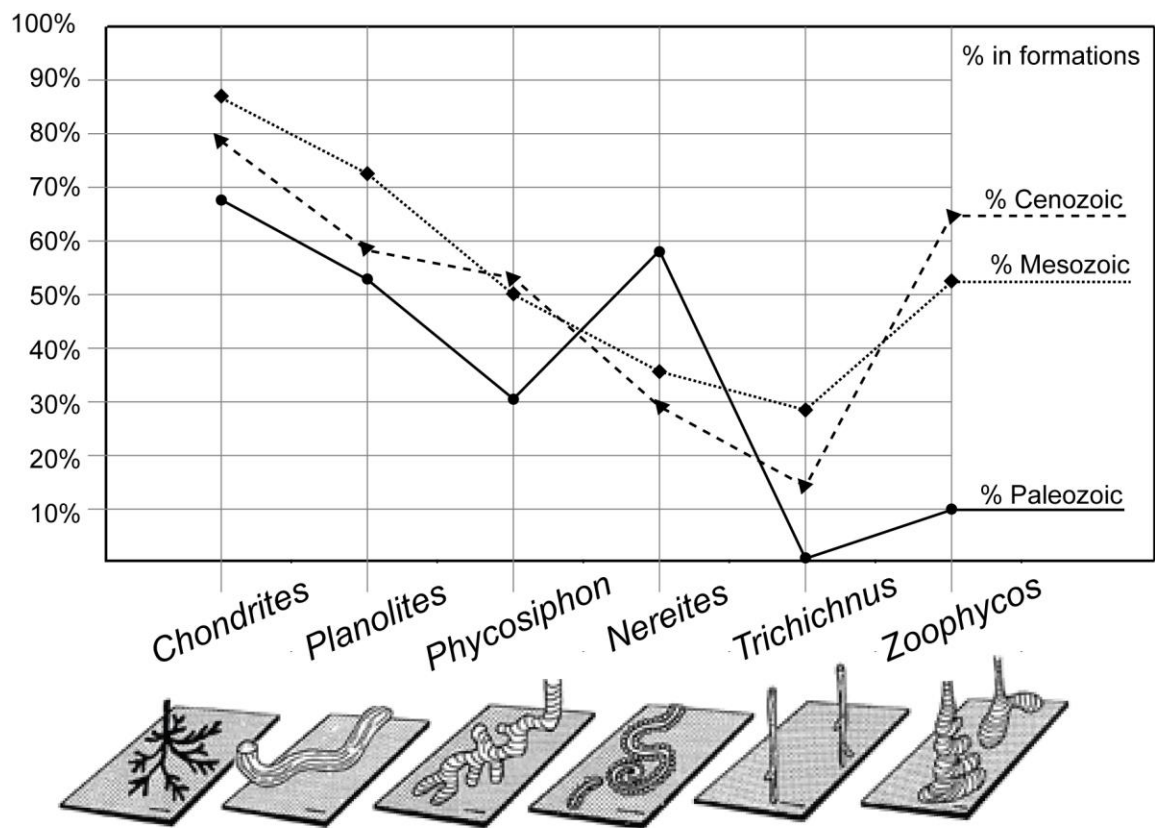


Fig. 1.1. Trace fossils that are typical for shale-hydrocarbon facies (graphic visualizations taken from Wetzel and Uchman 1998a).

The plot represents most frequently occurring ichnofabric-forming ichnotaxa against percentage of turbidite-bearing formations containing the trace or similar (after Callow and McIlroy 2011).

Phycosiphon (including its junior synonym *Anconichnus*, see Wetzel and Bromley 1994), *Nereites* (including its several junior synonyms *Helminthoida*, *Spirophycus*, *Scalarituba*, etc. Uchman 1995) and other *Phycosiphon*-like trace fossils (i.e., phycosiphoniform burrows, Bednarz and McIlroy 2009, 2012) have in cross section a dark to black clayey fecal core surrounded by a light silt-grade quartzose halo (e.g., Wetzel and Bromley 1994; Bromley 1996; Wetzel 2002) in various ratios and arrangement (Bednarz and McIlroy 2009, 2012). Phycosiphoniform burrows occur mostly in silt- or very fine sand-bearing mudstones. The vermiform producers of these complex trace fossils employed a similar deposit-feeding strategy of selectively ingesting organic matter and clay particles from ambient silty sediment (e.g., Wetzel and Bromley 1994; Bromley 1996). The similarity of the palaeobiological models and ecological niche of the opportunistic *Phycosiphon* and *Nereites* ichnotaxa are additionally accentuated by the fact that *Nereites*, that was more frequent in Paleozoic formations, was supplanted by *Phycosiphon* in Mesozoic and Cenozoic turbidite-bearing successions (Fig. 1.1; Callow and McIlroy 2011). Although both frequently co-occur in sedimentary record, only *Nereites* is suggested to indicate the position of the redox boundary, and typically occurs just above it (Wetzel 2002, 2010) whereas *Phycosiphon* is suggested to represent opportunistic feeding within oxygenated food-rich deposits (e.g., Wetzel and Uchman 1998b; 2001). Both ichnotaxa can, contrary to previous consensus, be inclined from the horizontal, a behaviour that may be controlled by the food distribution, and redox boundary fluctuations (Uchman 1995; Wetzel and Bromley 1994; Wetzel 2002, 2010; cf. Bednarz and McIlroy 2009, 2012). The considerable degree of verticality of the

Phycosipon-like and *Nereites* burrows is particularly influential as it generates and/or contributes to permeability isotropy that is vital for successful production from shale-gas reservoir (Bednarz and McIlroy 2012).

Chondrites and *Chondrites*-like burrows are complex root-like systems of tunnels branching from more or less vertical master shaft that was open to the sediment-water interface (e.g., Osgood 1970; Wetzel 1983; Löwemark et al. 2006; Wetzel and Reisdorf 2007; Pervesler et al. 2008; Pemberton et al. 2009). This trace fossil is common in black and organic-rich mudstones and is considered to be a result of the burrowing activity of a chemosymbiotic organism and is commonly inferred to be an indicator of anoxic and euxinic sediments or even anoxic bottom-water conditions (Bromley and Ekdale 1984; Fu 1991; c.f. Dufour and Felbeck 2003; Seilacher 1990; Savrda and Bottjer 1991). Tunnels of *Chondrites* burrows in mudstones are small in diameter (usually around 1 mm) and passively in-filled with (usually) silty or sandy material. *Chondrites* has been recognized in number of source rocks and shale facies and it is usually present in dense occurrences penetrating the sediment to depths of tens of centimetres (e.g., McBride and Picard 1991; Seilacher 2007; Spaw 2012, 2013a). *Chondrites* is the most frequently documented ichnofabric-forming trace fossils of turbiditic/deep marine successions through the entire Phanerozoic (Fig. 1.1, Callow and McIlroy 2011).

The abovementioned ichnotaxa can be subdivided into 1) the traces that maintained an open connection to the sea floor (*Chondrites*, *Trichichnus* and *Zoophycos*) and 2) those that do not (*Phycosiphon* and *Nereites*) and whose trace-makers could either function in

anoxic muddy sediments or require oxygenated pore waters to respire (e.g., Wetzel and Uchman 1998a).

The recently recognized ubiquity of these ichnotaxa within hydrocarbon-charged facies worldwide creates a need to investigate their volumetrics and determine the influence that these trace fossils might have on shale reservoir quality in terms of petrophysics and reserves estimates (c.f. Schieber 2003; Pemberton and Gingras 2005; Meyer and Krause 2006; Tonkin et al. 2010; Bednarz and McIlroy 2012).

1.1.3. Importance of deterministic three-dimensional reconstruction of ichnofabric in shale gas reservoir facies

Three-dimensional ichnofabrics are necessary to understand the density of bioturbation, the spatial distribution of burrows and their connectivity. To date this has largely been done only from two-dimensional illustrations. Three-dimensional (3D) deterministic reconstructions are devoid of the imperfections of extrapolations from two dimensional models, e.g., the presence of “dead ends”, and “eddies” extrapolated from planar illustrations and simulations (e.g., Spila et al. 2007 in reference to two dimensional analysis of the fluid transport through vertically connected burrows of *Phycosiphon*) which do not allow for connectivity in the third dimension. Relative to conceptual 3D models of ichnotaxa, deterministic 3D reconstructions allow for critical verification and reassessment of paleobiological models for the ichnotaxon as well as quantitative documentation of parameters such as bioturbation index, connectivity, burrow length,

depth etcetera (e.g., Naruse and Nifuku 2008; Bednarz and McIlroy 2009, 2012; Platt et al. 2010; cf. La Croix et al. 2012). Most importantly computer-modeled 3D reconstructions of ichnological specimens allows deterministic volumetric analysis and measurements of individual burrow and bulk ichnofabric volumes, along with surface area of the burrow-sediment interface, and calculations of burrow density in three-dimensional space (Bednarz and McIlroy 2012; cf. La Croix et al. 2012). Deterministic 3D models of ichnofabric such as those created in this study may become an easily accessible tool for realistic volumetric evaluation of the potential ichnological influence on reservoir quality.

Trace fossils in mudstones are usually silt-rich tortuous tubes and strips of complex three-dimensional morphology and are inherently more porous and permeable (if not cemented) than the surrounding clay-rich matrix (e.g., Wetzel and Uchman 1998a; Lemiski et al. 2011; Bednarz and McIlroy 2012; La Croix et al. 2012). The complex three-dimensional architecture of ichnofabrics can provide spatially complex planes of weakness in a sediment, as determined by the mineralogical contrast between silt/sand filled trace fossils and the organic- and clay-rich host sediment (Bednarz and McIlroy 2012). Such biogenic fracture-prone interfaces may increase fracture-spacing during reservoir stimulation. Detailed modeling and prediction of induced fracture orientation and distribution is required to maximize the reservoir area that is connected to the wellbore (e.g., Cipolla et al. 2009; Bust et al. 2013). Investigation and understanding of the three-dimensional distribution, architecture and spatial connectivity of the quartz-rich ichnofabric in gas-shales provides the basis for the prediction and subsequent generation

of high fracture complexity and dense fracture spacing if bioturbated horizons are targeted for stimulation. It is considered that bioturbated intervals may become significant targets for hydraulic fracturing because of the potential for intense fracturing around burrows that may maximize the well-reservoir contact.

1.1.4. Three-dimensional reconstructions in ichnology

Until comparatively recently ichnology has been a rather palaeontological endeavour, using a lot of the conventional tools of straightforward observation of fossils collected from outcrop specimens or interpreted from 2D slabs of core. The ability to “see” the fossils in three dimensions, along with their relationship to the host sediment (e.g., sediment disturbance or geochemical changes in the near burrow environment) has resulted in significant leaps in understanding of the behaviour of the trace maker (Bednarz and McIlroy 2012; Šimo and Tomašových 2013). This methodology has the power to better inform the ichnologists regarding trace-maker behaviour. Digital methods of 3D reconstruction allow for creation and population of interactive models i.e., models that can be manipulated by the reader in 3D. If embedded and shared in common digital formats (e.g., PDF files, PowerPoint presentations or media formats supported by Internet browsers) such 3D reconstructions can take communication of results in ichnology to a new level, enabling readers to not only understand the fossils from 2D screen grabs, but to also explore and investigate the models themselves.

To date 3D visualisation of majority of trace fossils are presented as conceptual drawings and are available only on 2D (printed) media. Such reconstructions illustrate a high degree of accuracy in reference to the general burrow system architecture and gave a starting point for all later ichnological research and analysis (e.g., Wetzel and Uchman 1998a; Seilacher 2007). These reconstructions are extrapolated mainly from observations of cross sections of burrows in core or outcrop and also from manual serial polishing of small, hand-size samples, which technique allows for exposing consecutive cross sections' shapes. Elucidation of the geometry of trace fossils in mudstones starts with the problems of their recognition owing to low colour contrast, small size, and sediment compaction and weathering of the host sediment (cf. Wetzel and Uchman 1998a). Conceptual reconstructions account for much of the current basis for ichnotaxonomy as well as paleoenvironmental and paleobiological analysis in ichnology. However they do not allow for full elucidation of complex trace fossil geometries in the context of the host-sediment.

Deterministic 3D visualisations of trace fossils from core (mainly unlithified sediments) and hand-size samples were firstly undertaken through usage of X-ray imaging followed by CT-scanning (e.g., Wetzel and Werner 1980; Wetzel 1983, 1984, 2008, 2010; Fu and Werner 1994; Löwemark, 2003, 2007 and references therein). The low X-ray contrast of most mudstone components precludes recognition of some trace fossils in lithified mudstones using X-radiography. In other cases, even if the resolution of the CT-scanning technique is high enough (fraction of millimetre) the images do not provide sufficiently detailed illustration of these complex structures (e.g., Wetzel and Uchman 1998a). Trace

fossils preserved in pyrite are an exception to this rule (Löwemark 2003, 2007 and references therein). Small to microscopic burrows as well as pore distribution can be visualized with microtomography technique (Micro-CT) with micron- to millimetre scale density (Gingras et al. 2007). Polishing of freshly excavated surface has proven to be the best practice for detailed examination of trace fossils in hand-size samples of mudstones (Uchman 1995, Wetzel and Uchman 1998a). If coupled with computer-controlled constantly maintained interval of serial sectioning it introduces a base for deterministic volumetric reconstructions (Bednarz and McIlroy 2012, based on Sutton et al. 2001).

Deterministic volumetric 3D models of ichnofabric offer possibilities to proceed with all sorts of measurements and calculations that the researcher needs having certainty that the analyses reflect the true rock-sourced ichnological data. Quantitative and volumetric analyses of the deterministic 3D reconstruction of the ichnofabric will allow for realistic assessment of biogenic structures that enhance fluid flow and fracturability within bioturbated shale gas reservoir facies.

This work presents the step-by-step methodology that was employed to reconstruct three-dimensional geometry and analysis of individual burrows and ichnofabric from collected bioturbated shale samples.

1.2. Three-dimensional reconstruction of ichnofabric in shale gas reservoir facies: thesis aim and scope

This PhD thesis aims to bridge the gap in knowledge of the three-dimensional ichnology and the importance of trace fossil in reservoir studies by investigating the impact of ichnofabric on shale-hydrocarbon reservoir quality. This is approached through detailed analysis of the deterministic 3D reconstructions of typical mudstone trace fossils, and by formulating a methodology to examine the above. Three-dimensional reconstructions of *Phycosiphon*, *Nereites* and *Chondrites* are the basis for palaeobiological and taxonomic reconsideration of these taxa.

1.2.1. Methodology formulation for the deterministic 3D reconstructions of ichnological specimens. (Chapter 2)

The goals of the study presented in chapter 2 are:

- 1) To find the procedure for precise three-dimensional reconstruction of individual burrows and ichnofabric hosted in mudstones and large samples of other lithologies. Chapter 2 investigates methodology of precision automated serial grinding method that is the most effective in gaining highly detailed analysis of the internal and external structure of trace fossils hosted within fine-grained sediments. This is particularly true of mudstones where conventional methods of three-dimensional studies, e.g., CT scanning, MRI (magnetic resonance imaging) or MLT (multi-stripe laser triangulation scanning) are ineffective. Further the study presents the approach

to convert the visualized volume to the 3D polygonal mesh that is the basis for quantitative volumetric analyses.

- 2) To standardize procedures so that all the samples are treated the same way and the results are comparative.
- 3) To create methodologies for calculation of volumetric analysis relevant to 3D ichnological data.
- 4) To review, and provide useful terminology for, descriptive and volumetric analysis of 3D ichnofabric and individual trace fossils.
- 5) To develop techniques for sharing interactive 3D models that other ichnologists can manipulate and examine the reconstructions.
- 6) To provide tools for geologists to examine and estimate the impact and volumetric content of ichnofabric within bioturbated reservoir rocks.

Except for chapter 2, the methodology description is otherwise presented in general manner in all the three remaining manuscripts (chapter 3, 4, 5) for their completeness as stand-alone publications. In these chapters, additional means of volumetric calculations and analyses of the 3D models are presented that aim to clarify publication-specific considerations.

1.2.2. What do the common shale-gas reservoir trace fossils look like in 3D?

(Chapters 3, 4, 5)

The work addresses deterministic three-dimensional reconstruction of *Phycosiphon*, *Nereites* and *Chondrites* ichnofabrics from samples collected from organic-rich successions that are analogous to the shale-gas facies. Volumetric and descriptive analyses are applied to the reconstructed models in order to visualise and understand ichnofabric spatial geometry.

The creation of 3D reconstructions of the ichnofabrics presented in this study aims to:

1) Elucidate the geometry of the internal structure of the burrows of studied trace fossils.

The geometric and volumetric inter-relationships of the compositional elements (i.e., core and halo) of three examined phycosiphoniform burrow types are investigated in chapters 3 and 4. The structure of the material composing *Chondrites* burrows is presented in chapter 5. Improved knowledge of the variability with phycosiphoniform taxa with respect to their core-halo relation is aimed to improve their identification from cross sections in core or outcrop, and furthermore in studies of reservoir quality.

2) Visualize the true spatial geometry of the trace fossils, and the entire ichnofabric, built with the natural association of multiple burrow specimens.

Reconstruction and analysis of burrows' general shapes and geometry and recognition of potential repetitive architectural patterns within the burrow natural associations were presented in chapters 3, 4 and 5 for phycosiphoniform traces

and in chapter 5 for *Chondrites*. Volumetric reconstructions of the real trace fossils allowed for their comparison with the established visualizations based on the core observations and for revision of the ichnotaxons' palaeobiological models. This study aims to present the real distribution of burrows composing the ichnofabric in order to examine the importance of ichnofabric with respect to shale gas/oil reservoir quality.

1.2.3. What effect do the common shale-gas reservoir trace fossils have on reservoir quality? Ichnofabric-associated porosity, permeability and fracturability. (Chapters 4, 5)

Within bioturbated, low-matrix-permeability mudstones fluid flow is possible only through conduits formed by the natural or induced fractures or by the silty and sandy burrows before the fluid reaches the well. The work investigates the effects of phycosiphoniform and aff. *Chondrites* ichnofabrics on the petrophysical characteristics of mudstones such as transmissibility and distribution of fluid flow conduits. Mudstone (ichno)fabric can control petrophysical characteristics such as porosity, permeability and brittleness. To examine ichnofabric in the light of these interrelated characteristics this study deterministically models:

1) The manner in which burrow components are arranged in three dimensions.

The vertical connectivity of burrows in ichnofabrics is investigated in order to examine the degree to which silty burrow material is interconnected in relation to the estimated burrow density (chapters 4 and 5). Vertically connected burrows

built of silt-grained material may create primary porous and permeable flow paths that would result in effective flow of fluids through ambient ultra-low permeable matrix. Strong vertical components of the interconnected ichnofabrics may enhance, or even create isotropy and homogeneity relative to laminated strata by breaching horizontal permeability barriers and linking more permeable horizons (improving k_v).

2) The volume of the ichnofabric that is distributed within a given volume of the bioturbated mudstone.

Calculations of the volume of the ichnofabric that is composed of silty material will shed a light on the real volumes that are available for enhanced fluid flow through an ichnofabric (chapters 4 and 5). Volumetric assessment of the ichnofabric is undertaken to show what portion of the bulk volume of brittle minerals (quartz, feldspars or carbonates) is present within the mudstone in concentrated form (i.e., in clay-cleaned zones of burrow tubes and strips). Such quartzose and/or feldspar-rich zones are inherently brittle and thus susceptible for natural or induced fracture development, what may be particularly important for facies of low bulk quartz (or other brittle mineral) content.

3) The surface area and distribution of the ichnofabric within a given volume of the bioturbated mudstone.

The calculations of the volume and reconstruction of the geometry of burrow shapes and ichnofabric spatial arrangement when analyzed together, allow for understanding of the relation of bioturbation density to the distribution of the

quartzose material. The tortuous and chaotic nature of the biologically-generated shapes creates a vast surface area of the ichnofabric in relation to the containing volume of the sediment.

The short distance between kerogen particles and permeable flow conduits (fracture or permeable burrow tube), or brittle porous material (e.g., the burrow) is critical for economic production from mudstones. The spatial architecture of ichnofabric tends to partition the ultra-low permeable matrix into small volumes, thereby shortening the communication distance between a released hydrocarbon molecule and fracture networks. Chapter 5 investigates distribution and density of the ichnofabric network in order to examine the potential of this network to enhance induced or natural fracture spacing.

1.3. Objectives and analytical approaches

In order to answer the abovementioned research questions stated in this study, this PhD project was designed with the following objectives:

- 1) To deterministically reconstruct three-dimensional architecture of *Phycosiphon* and *Chondrites* ichnofabric contained in organic-rich shale facies from different locations and age.
- 2) To analyze the modeled 3D reconstructions by application of volumetric analytical methods in order to understand and comprehensively describe the structure and spatial architecture of the ichnofabric.

- 3) To analyze and describe the impact of the examined ichnofabric on shale-hydrocarbon quality.

The following approaches and methods were used to address the objectives:

- a) Collection of bioturbated hand-sized samples of organic-rich bioturbated mudstones from shale gas equivalent facies during field trips.

The five collected samples of ichnofabric were assigned to two groups of trace fossils:

I. *Phycosiphon*-like trace fossils group with *Phycosiphon sensu stricto* from the Jurassic Staithes Sandstone Formation, *Phycosiphon*-like trace fossil from the Upper Cretaceous Rosario Formation, Baja California, Mexico and *Nereites* from The Mississippian Yoredale Sandstone Formation, Craster, Northumberland, UK. The three trace fossils were assigned to the informal group of phycosiphoniform burrows (*Phycosiphon*-like burrows) because of the significant similarity of their vertical cross sections (Bednarz and McIlroy 2009; 2012).

II. *Chondrites*-like trace fossils group with *Chondrites sensu stricto* from Jurassic Staithes Sandstone Formation and *Chondrites*-like trace fossil from the Upper Cretaceous Mancos Shale, Ferron Sandstone Formation, Muddy Creek, Utah.

- b) Petrographic analysis of the samples (thin sections and visual description)

- c) Serial grinding, photography and digital processing (volume visualization and 3D model production)
- d) Quantitative volumetric analyses of the 3D models of the reconstructed ichnofabric.

1.4. References

- Angulo, S., and L.A. Buatois, 2012a, Ichnology of a Late Devonian–Early Carboniferous low-energy seaway: The Bakken Formation of subsurface Saskatchewan, Canada: Assessing paleoenvironmental controls and biotic responses, *Palaeogeography, Palaeoclimatology, Palaeoecology*, v. 315–316, p. 46–60, doi: 10.1016/j.palaeo.2011.11.007.
- Angulo, S., and L.A. Buatois, 2012b, Integrating depositional models, ichnology, and sequence stratigraphy in reservoir characterization: The middle member of the Devonian–Carboniferous Bakken Formation of subsurface southeastern Saskatchewan revisited, *AAPG Bulletin*, v. 96, no. 6, p. 1017–1043
- Arndt-Sullivan, C., J.,P. Lechaire, and H. Felbeck, 2008. Extreme tolerance to anoxia in the *Lucinoma aequizonata* symbiosis, *Journal of Shellfish Research*, v. 27, no. 1, p. 119–127.
- Ballard, T.J., S.P. Beare, and T.A. Lawless, 1994, Fundamentals of Shale Stabilisation: Water Transport Through Shales, *SPE Formation Evaluation*, v. 9, no. 2, p. 129–134.
- Bednarz, M., and D. McIlroy, 2009, Three-dimensional reconstruction of "phycosiphoniform" burrows: implications for identification of trace fossils in core: *Palaeontologia Electronica* v. 12, no. 3. http://palaeo-electronica.org/2009_3/195/index.html
- Bednarz, M., and D. McIlroy, 2012, Effect of phycosiphoniform burrows on shale hydrocarbon reservoir quality: *AAPG Bulletin*, v. 96, no. 10, p. 1957–1977, doi:10.1306/02221211126.
- Bohacs, K.M., G. J. Grabowski Jr, A.R. Carroll, P. J. Mankiewicz, K. J. Miskell-Gerhardt, J.R. Schwalbach, M. B. Wegner, and J. A. Simo, 2005, Production, destruction, and dilution: The many paths to source rock development, in N. B. Harris, ed., *The deposition of organic carbon-rich sediments: Models, mechanisms, and consequences: SEPM, Special Publication 82*, p. 61–101.
- Bromley, R. G., 1996, *Trace fossils: Biology, taphonomy and applications*: London, Chapman and Hall, 361 p.

- Bromley R.G. and A.A Ekdale, 1984, *Chondrites*; a trace fossil indicator of anoxia in sediments: *Science*, v. 224, no. 4651, p. 872-874.
- Bust, V.K., A.A. Majid, J.U. Oletu, and P.F. Worthington, 2013, The petrophysics of shale gas reservoirs: Technical challenges and pragmatic solutions: *Petroleum Geoscience*, v. 19, no 2, p. 91–103, DOI: 10.1144/petgeo2012-031.
- Bustin, R.M., 2012, Shale gas and shale oil petrology and petrophysics: *International Journal of Coal Geology*, v. 103, p. 1-2.
- Bustin, A.M.M. and R.M. Bustin, 2012, Importance of rock properties on the producibility of gas shales: *International Journal of Coal Geology*, v. 103, p. 132-147.
- Callow, R.H.T., and D. McIlroy, 2011, Ichnofabrics and ichnofabric forming trace fossils in Phanerozoic turbidites: *Bulletin of Canadian Petroleum Geology*, v. 59, no. 2, p. 103-111.
- Chamberlain, C.K., 1978, Recognition of trace fossils in cores; trace fossil concepts: *SEPM Short Course*, v. 5, p. 133-183.
- Chalmers, G.R., R.M. Bustin, and I.M. Power, 2012a, Characterization of gas shale pore systems by porosimetry, pycnometry, surface area, and field emission scanning electron microscopy/transmission electron microscopy image analyses: examples from the Barnett, Woodford, Haynesville, Marcellus, and Doig units: *AAPG Bulletin*, v. 96, no. 6 p. 1099–1119, DOI:10.1306/10171111052.
- Chalmers, G.R., D.J. Ross, and R.M. Bustin, 2012b, Geological controls on matrix permeability of Devonian Gas Shales in the Horn River and Liard basins, northeastern British Columbia, Canada: *International Journal of Coal Geology*, v. 103, p: 120-131.
- Cipolla, C.L., E.P. Lolon, and M.J. Mayerhofer, 2009, Reservoir Modeling and Production Evaluation in Shale-Gas Reservoirs: Conference Paper, International Petroleum Technology Conference, 7-9 December 2009, Doha, Qatar, doi:10.2523/13185-MS.
- Cipolla, C., M. Mack, and S. Maxwell, 2010, Reducing Exploration and Appraisal Risk in Low-Permeability Reservoirs Using Microseismic Fracture Mapping: Conference Paper, Canadian Unconventional Resources and International Petroleum Conference, 19-21 October 2010, Calgary, Alberta, Canada, doi: 10.2118/137437-MS.
- Cluff, R.M., 1980, Paleoenvironment of the New Albany Shale Group (Devonian-Mississippian) of Illinois: *Journal of Sedimentary Petrology*, September, 1980, v. 50, no. 3, p.767-780.

- Dando P.R., A.J. Southward, E.C. Southward, P. Lamont, R. Harvey, 2008, Interactions between sediment chemistry and frenulate pogonophores (Annelida) in the north-east Atlantic: Deep-Sea Research, v. 55, p. 966 – 996.
- Deville, J.P., B. Fritz, M. Jarrett, 2011, Development of Water-Based Drilling Fluids Customized for Shale Reservoirs: Society of Petroleum Engineers International Symposium on Oilfield Chemistry, The Woodlands, Texas, USA, 11-13 April 2011, doi:10.2118/140868-PA
- Ding, W., C. Li, Ch. Li, C. Xu, K. Jiu, W. Zeng, and L. Wu, 2012, Fracture development in shale and its relationship to gas accumulation: Geoscience Frontiers, v. 3, no. 1, p: 97-105.
- Dufour, S.C., and H. Felbeck, 2003, Sulphide mining by the super-extensile foot of symbiotic thyasirid bivalves: Nature, v. 426, p. 65-67.
- Egenhoff S.O., and N.S. Fishman, 2013, Traces in the dark: sedimentary processes and facies gradients in the upper shale member of the Upper Devonian-Lower Mississippian Bakken Formation, Williston Basin, North Dakota, U.S.A: Journal of Sedimentary Research, v. 83, p. 803 – 824.
- Ekdale, A.A. and T.R. Mason, 1988. Characteristic trace-fossil associations in oxygen-poor sedimentary environments: Geology, v.16, p.720-723.
- Fan, L., J.W. Thompson, and J.R. Robinson, 2010, Understanding Gas Production Mechanism and Effectiveness of Well Stimulation in the Haynesville Shale Through Reservoir Simulation: Conference Paper, Canadian Unconventional Resources and International Petroleum Conference, 19-21 October 2010, Calgary, Alberta, Canada, Society of Petroleum Engineers, doi: 10.2118/136696-MS
- Fu, S., 1991, Funktion, Verhalten und Einteilung fucoider und lophocteniider Lebensspuren. Cour. Forsch. Inst. Senckenberg 135, p. 1–79.
- Fu, S., and F. Werner, 1994, Computed tomography: application in studying biogenic structures in sediment cores: Palaios, v. 9, p. 116-119
- Ghadeer, S.G., and J.H.S. Macquaker, 2012, The role of event beds in the preservation of organic carbon in fine-grained sediments: Analyses of the sedimentological processes operating during deposition of the Whitby Mudstone Formation (Toarcian, Lower Jurassic) preserved in northeast England: Marine and Petroleum Geology, v. 35, no 1, p. 309-320.
- Gingras, M. K., S. G. Pemberton, C. A. Mendoza, and F. Henk, 1999, Assessing the anisotropic permeability of *Glossifungites* surfaces: Petroleum Geoscience, v. 5, p. 349–357, doi:10.1144/petgeo.5.4.349.
- Gingras, M. K., C. A. Mendoza, and S. G. and Pemberton, 2004, Fossilized worm burrows influence the resource quality of porous media: AAPG Bulletin, v. 88, p. 875– 883, doi:10.1306/01260403065.

- Gingras, M. K., S. G. Pemberton, F. Henk, J. A. MacEachern, C. Mendoza, B. Rostron, R. O'Hare, M. Spila, and K. Konhauser, 2007, Applications of ichnology to fluid and gas production in hydrocarbon reservoirs, in J. A. MacEachern, S. G. Pemberton, M. K. Gingras, K. L. Bann, eds., *Applied ichnology: SEPM Short Course Notes* 52, p. 131–147.
- Gingras M.K., G. Baniak, J. Gordon, J. Hovikoski, K.O. Konhauser, A. La Croix, R. Lemiski, C. Mendoza, S.G. Pemberton, C. Polo, and J-P. Zonneveld, 2012, Porosity and Permeability in Bioturbated Sediments, In: *Developments in Sedimentology: Trace Fossils as Indicators of Sedimentary Environments*, Eds. Knaust, D. and Bromley, R.G., v. 64, p. 837-868.
- Gingras, M. K., Angulo, S., and L.A. Buatois, 2013, Biogenic Permeability in the Bakken Formation: Search and Discovery Article #50905, Extended abstract, AAPG Annual Convention and Exhibition, Pittsburgh, Pennsylvania, May 19-22, 2013.
- Harazim, D., 2013, High-energy seafloor processes and biological reworking as first-order controls on mudstone composition and geochemistry: Ph.D. Thesis, Memorial University of Newfoundland, Canada.
- Hovikoski, J., R. Lemiski, M. K. Gingras, S. G. Pemberton, and J. A. MacEachern, 2008, Ichnology and sedimentology of a mud-dominated deltaic coast: Upper Cretaceous Alderson Member (Lea Park Formation), western Canada: *Journal of Sedimentary Research*, v. 78, no. 12, p. 803–824, doi:10.2110/jsr.2008.089.
- Jacobi, D., M. Gladkikh, B. LeCompte, G. Hursan, F. Mendez, J. Longo, S. Ong, M. Bratovich, G. Patton, B. Hughes, and P. Shoemaker, 2008, Integrated Petrophysical Evaluation of Shale Gas Reservoirs: Conference Paper, CIPC/SPE Gas Technology Symposium 2008 Joint Conference, 16-19 June 2008, Calgary, Alberta, Canada, Society of Petroleum Engineers doi: 10.2118/114925-MS.
- Jarvie, D. M., R. J. Hill, T. E. Ruble, and R.M. Pollastro, 2007, Unconventional shale-gas systems; the Mississippian Barnett Shale of North-central Texas as one model for thermogenic shale-gas assessment: Special issue; Barnett Shale: *AAPG Bulletin*, v. 91, no. 4, p. 475-499.
- Javadpour, F., D. Fisher, and M. Unsworth, 2007, Nanoscale Gas Flow in Shale Gas Sediments, *Journal of Canadian Petroleum Technology*, vol. 46, no. 10, p. 55-61; doi: 10.2118/07-10-06.
- Jenkins, C.D., and C. M. Boyer, 2008, Coalbed and shale gas reservoirs: *Journal of Petroleum Technology*, v. 60, no. 2, p. 92-99.
- Josh, M., L. Esteban, C. Delle Piane, J. Sarout, D.N. Dewhurst, M.B. Clennell, 2012, Laboratory characterisation of shale properties, *Journal of Petroleum Science and Engineering*, Volumes 88–89, June 2012, pp: 107-124

- La Croix, A.D., M.K. Gingras, S.E. Dashtgard, and S.G. Pemberton, 2012, Computer modeling bioturbation: The creation of porous and permeable fluid-flow pathways, *AAPG Bulletin*, v. 96, no. 3, pp. 545–556.
- La Croix, A.D., M.K. Gingras, S.G. Pemberton, C.A. Mendoza, J.A. MacEachern, R.T. Lemiski, 2013, Biogenically enhanced reservoir properties in the Medicine Hat gas field, Alberta, Canada: *Marine and Petroleum Geology*, v. 43, p. 464-477.
- Lemiski, R.T., J. Hovikoski, S.G. Pemberton, and M.K. Gingras, 2011, Sedimentological, ichnological and reservoir characteristics of the low-permeability, gas-charged Alderson Member (Hatton gas field, southwest Saskatchewan): Implications for resource development: *Bulletin of Canadian Petroleum Geology*, v. 59, p. 27–53, doi:10.2113/gscpgbull.59.1.27.
- Loucks, R.G., R.M. Reed, S.C. Ruppel, and U. Hammes, 2012, Spectrum of pore types and networks in mudrocks and a descriptive classification for matrix-related mudrock pores: *AAPG Bulletin*, v. 96, no. 6, p. 1071–1098, DOI:10.1306/08171111061.
- Löwemark, L., 2003, Automatic image analysis of X-ray radiographs: a new method for ichnofabric evaluation: *Deep Sea Research Part I*, v. 50, no. 6, p. 815–827.
- Löwemark, L., Y. Lin, H.F. Chen, T.N. Yang, C. Beier, F. Werner, C.Y. Lee, S.R. Song, and S. J. Kao, 2006, Sapropel burn-down and ichnological response to late Quaternary sapropel formation in two similar to 400 ky records from the eastern Mediterranean Sea: *Palaeogeography Palaeoclimatology Palaeoecology*, v. 239, no. 3-4, p. 406-425 DOI: 10.1016/j.palaeo.2006.02.013.
- Löwemark, L., 2007, Importance and usefulness of trace fossils and bioturbation in paleoceanography, In: W. Miller, III (Ed), *Trace fossils: Concepts, Problems, Prospects*, p. 413-427 Elsevier; Amsterdam.
- Macquaker, J.H.S., M.A. Keller, and K.G. Taylor, 1999, Sequence Stratigraphic Analysis of the Lower Part of the Pebble Shale Unit, Canning River, northeastern Alaska: Chapter SS (Sequence Stratigraphy of the Pebble Shale Unit), in *The Oil and Gas Resource Potential of the Arctic National Wildlife Refuge 1002 Area, Alaska*, by ANWR Assessment Team: U.S. Geological Survey Open-File Report 98-34, Version 1.0, p. SS1-SS28.
- Macquaker, J.H.S., and A.E. Adams, 2003, Maximizing information from fine-grained sedimentary rocks; an inclusive nomenclature for mudstones: *Journal of Sedimentary Research*, v. 73, no. 5, p. 735-744.
- Macquaker, J. H. S., and K. M. Bohacs, 2007, On the accumulation of mud: *Science*, v. 318, no. 5857, p. 1734–1735, doi:10.1126/science.1151980.
- Macquaker, J.H.S., K.G. Taylor, and R.L. Gawthorpe, 2007, High-resolution facies analyses of mudstones; implications for paleoenvironmental and sequence stratigraphic interpretations of offshore ancient mud-dominated successions:

- Journal of Sedimentary Research, v. 77, no. 4, p. 324-339, doi:10.2110/jsr.2007.029.
- McBride, E.F., and M.D. Picard, 1991, Facies implications of *Trichichnus* and *Chondrites* in turbidites and hemipelagites, Marnosoarenacea Formation (Miocene), Northern Apennines, Italy: *Palaaios*, v. 6, p. 281-290.
- McIlroy, D., 2004, Some ichnological concepts, methodologies, applications and frontiers, in D. McIlroy, ed., *The application of ichnology to paleoenvironmental and stratigraphic analysis: Geological Society (London) Special Publication 228*, p. 3–29.
- McIlroy, D. 2007, Lateral variability in shallow marine ichnofabrics: implications for the ichnofabric analysis method: *Journal of the Geological Society*, v. 164; p. 359-369.
- McIlroy, D., 2008, Ichnological analysis: The common ground between ichnofacies workers and ichnofabric analysts: *Palaeogeography, Palaeoclimatology, Palaeoecology*, v. 270, no. 3–4, 15 p: 332–338.
- Meyer, R., and F.F. Krause, 2006, Permeability anisotropy and heterogeneity of a sandstone reservoir analogue: an estuarine to shoreface depositional system in the Virgelle Member, Milk River Formation, Writing-on-Stone Provincial Park, southern Alberta: *Bulletin of Canadian Petroleum Geology*, v. 54, p: 301-318.
- Middelburg, J., J., and L. A. Levin, 2009 Coastal hypoxia and sediment biogeochemistry: *Biogeosciences*, v. 6, p. 1273-1293.
- Monteiro, P.J.M., C.H. Rycroft, and G. Isaakovich Barenblatt, 2012, A mathematical model of fluid and gas flow in nanoporous media: *Proceedings of the National Academy of Sciences (PNAS)*, v. 109 no. 5, doi: 10.1073/pnas.1219009109.
- Naruse, H., and K. Nifuku, 2008, Three-dimensional morphology of the ichnofossil *Phycosiphon incertum* and its implication for paleoslope inclination: *Palaaios*, v. 23,no. 5, p. 270–279, doi:10.2110/palo.2007.p07-020r.
- Osgood, R.G. Jr. 1970. Trace fossils of the Cincinnati area: *Palaeontographica Americana*, v. 6, no. 41, p. 328-340.
- Palmer, I., and Z. Moschovidis, 2010, New Method To Diagnose and Improve Shale Gas Completions: Conference Paper, SPE Annual Technical Conference and Exhibition, 19-22 September 2010, Florence, Italy, Society of Petroleum Engineers, doi: 10.2118/134669-MS
- Pemberton, S. G., and M. K. Gingras, 2005, Classification and characterizations of biogenically enhanced permeability: *AAPG Bulletin*, v. 89, p. 1493–1517, doi:10.1306/07050504121.

- Pemberton, S.G., J.A. MacEachern, M.K., Gingras, and K.L. Bann, 2009. *Atlas of Trace Fossils: The Recognition of Common Trace Fossils in Outcrop and Cores*, Elsevier Science Ltd., ISBN 9780444532329.
- Pervesler, P., A. Uchman, and J. Hohenegger, 2008, New methods for ichnofabric analysis and correlation with orbital cycles exemplified by the Baden-Sooss section (Middle Miocene, Vienna Basin, Lower Austria): *Geologica Carpathica*, v. 59, no.5, p. 395-409.
- Platt, B. F., S. T. Hasiotis, and D.R. Hirmas, 2010, Use of low-cost multistripe laser triangulation (MLT) scanning technology for three-dimensional, quantitative paleoichnological and neoichnological studies: *Journal of Sedimentary Research*, v. 80, no. 7, p. 590–610, doi:10.2110/jsr.2010.059.
- Potter, P. E., J. B. Maynard, and W. A. Pryor, 1980, *Sedimentology of Shale*: New York Springer-Verlag, 306 p.
- Rickman, R., M. Mullen, E. Petre, B. Grieser, and D. Kundert, 2008, A Practical Use of Shale Petrophysics for Stimulation Design Optimization: All Shale Plays Are Not Clones of the Barnett Shale: Society of Petroleum Engineers, SPE Annual Technical Conference and Exhibition, 21-24 September 2008, Denver, Colorado, USA, Conference Paper, doi: 10.2118/115258-MS.
- Rodríguez-Tovar, F.J. and A. Uchman, 2010, Ichnofabric evidence for the lack of bottom anoxia during the Lower Toarcian Oceanic Anoxic Event (T-OAE) in the Fuente de la Vidriera section, Betic Cordillera, Spain: *Palaaios*, v. 25, p.576-587.
- Ross, D.J.K., and R.M. Bustin, 2009, The importance of shale composition and pore structure upon gas storage potential of shale gas reservoirs: *Marine and Petroleum Geology*, v. 26, p. 916-927, doi:10.1016/j.marpetgeo.2008.06.004.
- Savrda C.E. and D.J. Bottjer, 1991, Oxygen-related biofacies in marine strata: An overview and update. In: Tyson R.V. & Pearson T.H. (Eds.): *Modern and ancient continental shelf anoxia*. Geol. Soc. London Spec. Publ. No. 58, 202-219.
- Schieber, J., 1994, Reflection of deep vs shallow water deposition by small scale sedimentary features and microfabrics of the Chattanooga Shale in Tennessee: *Canadian Society of Petroleum Geologists*, v. 17, p. 773-784.
- Schieber, J., 2003, Simple gifts and hidden treasures – Implications of finding bioturbation and erosion surfaces in black shales: *The Sedimentary Record*, v. 1, p. 4-8.
- Schieber, J., 2011, Reverse engineering mother nature — Shale sedimentology from an experimental perspective: *Sedimentary Geology*, v. 238, no. 1-2, p. 1-22.
- Schieber, J., J. Southard, and K. Thaisen, 2007, Accretion of mudstone beds from migrating floccule ripples: *Science*, v. 318, no. 5857, p. 1760-1763, doi: 10.1126/science.1147001.

- Seilacher, A., 1967, Bathymetry of trace fossils: *Marine Geology*, v. 5, no. 5–6, p. 413–428
- Seilacher, A., 1990, Aberrations in bivalve evolution related to photo- and chemosymbiosis: *Historical Biology*, v. 3, p. 289-311.
- Seilacher, A., 2007, *Trace Fossil Analysis*: Springer-Verlag, Berlin, Heidelberg, New York, 226p.
- Šimo, V., and A. Tomašových, 2013, Trace-fossil assemblages with a new ichnogenus in “spotted” (Fleckenmergel—Fleckenkalk) deposits: a signature of oxygen-limited benthic communities: *Geologica Carpathica*, v. 64, no. 5, p. 355-374 doi: 10.2478/geoca-2013-0024
- Spaw, J.M., 2012, Identification, integration and upscaling of mudrock types - a pathway to unlocking shale plays: SPE/EAGE European Unconventional Resources Conference and Exhibition, 20-22 March, Vienna, Austria, doi.org/10.2118/153111-MS.
- Spaw, J.M., 2013a, Recognition of ichnofacies distributions and their contributions to matrix heterogeneity in mudstones: Unconventional Resources Technology Conference (URTeC), Denver, Colorado, USA, 12-14 August 2013.
- Spaw, J.M., 2013b, Microfacies analysis: an integrated petrologic approach to characterizing mudrock heterogeneity: Unconventional Resources Technology Conference (URTeC), Denver, Colorado, USA, 12-14 August 2013.
- Spila, M. V., S. G. Pemberton, B. Rostron, and M. K. Gingras, 2007, Biogenic textural heterogeneity, fluid flow and hydrocarbon production: Bioturbated facies, Ben Nevis Formation, Hibernia field, offshore Newfoundland, in J. A. MacEachern, K. L. Bann, M. K. Gingras, and G. S. Pemberton, eds., *Applied ichnology: SEPM Short Course Notes* 52, p. 363–380.
- Stewart, F.J., I.L. Newton, and C.M. Cavanaugh, 2005, Chemosynthetic endosymbioses: adaptations to oxic-anoxic interfaces. In: *Trends Microbiology*, vol. 13, no.9, p. 439-48.
- Sutton, M.D., D.E.G. Briggs, D.J. Siveter, and D.J. Siveter, 2001, Methodologies for the visualization and reconstruction of three-dimensional fossils from the Silurian Herefordshire Lagerstätte: *Palaeontologia Electronica*, v. 4, no. 1, p. 1-17, 1MB; http://palaeo-electronica.org/2001_1/s2/issue1_01.htm
- Swami, V., 2012, Shale Gas Reservoir Modeling: From Nanopores to Laboratory: Society of Petroleum Engineers, Conference Paper, SPE Annual Technical Conference and Exhibition, 8-10 October 2012, San Antonio, Texas, USA. doi.org/10.2118/163065-STU
- Swami, V., C.R. Clarkson, and A. Settari, 2012, Non-Darcy Flow in Shale Nanopores: Do We Have a Final Answer?: SPE Canadian Unconventional Resources

- Conference, 30 October-1 November 2012, Calgary, Alberta, Canada, Society of Petroleum Engineers, doi: 10.2118/162665-MS
- Tonkin, N.S., D. McIlroy, R. Meyer, and A. Moore-Turpin, 2010, Bioturbation influence on reservoir quality; a case study from the Cretaceous Ben Nevis Formation, Jeanne d'Arc Basin, offshore Newfoundland, Canada: AAPG Bulletin, v. 94, no. 7, p. 1059-1078, doi:10.1306/12090909064
- U.S. Energy Information Administration, 2013, Technically recoverable shale oil and shale gas resources: an assessment of 137 shale formations in 41 countries outside the United States. Retrieved from <http://www.eia.gov/analysis/studies/worldshalegas/pdf/fullreport.pdf> (accessed March 20, 2014)
- U.S. Geological Survey, 2013, National Assessment of Oil and Gas Project: Map of Assessed Shale Gas in the United States, 2012. Retrieved from http://pubs.usgs.gov/dds/dds-069/dds-069-z/DDS-69-Z_pamphlet.pdf (accessed March 20, 2014)
- Uchman, A., 1995, Taxonomy and palaeoecology of fiysch trace fossils: The Mamoso-arenacea Formation and associated facies (Miocene, Northern Appenines, Italy): *Bergingeria*, v. 15, p. 1-114.
- Wetzel, A., 1983, Biogenic structures in modern slope to deep-sea sediments in the Sulu Sea Basin (Philippines): *Palaeogeography, Palaeoclimatology, Palaeoecology*, v. 42, p. 285-304.
- Wetzel, A., 1984, Bioturbation in deep-sea fine-grained sediments: influence of sediment texture, turbidite frequency and rates of environmental change: *Geological Society, London, Special Publications*, v. 15; p. 595-608, doi:10.1144/GSL.SP.1984.015.01.37.
- Wetzel, A., 2002, Modern Nereites in the South China Sea: Ecological associations with redox conditions in the sediment: *Palaios*, v. 17, p. 507-515.
- Wetzel, A., 2008, Recent bioturbation in the deep South China Sea: a uniformitarian ichnologic approach: *Palaios*, 2008, v. 23, p. 601-615, doi: 10.2110/palo.2007.p07-096r
- Wetzel, A., 2010, Deep-sea ichnology: Observations in modern sediments to interpret fossil counterparts: *Acta Geologica Polonica*, v. 60, no. 1, p. 125-138
- Wetzel, A., and F. Werner, 1980, Morphology and ecological significance of *Zoophycos* in deep-sea sediments off NW Africa: *Palaeogeography, Palaeoclimatology, Palaeoecology*, v. 32, p. 185-212, doi:10.1016/0031-0182(80)90040-1.
- Wetzel, A., and R.G. Bromley, 1994, *Phycosiphon incertum* revisited: *Anconichnus horizontalis* is junior subjective synonym: *Journal of Paleontology*, v. 68, no. 6, p.1396-1402.

- Wetzel, A., and A. Uchman, 1998 a, Biogenic sedimentary structures in mudstones - an overview, In: Schieber, J., Zimmerle, W. & Sethi, P.S. (eds.), *Shales & Mudstones. I. Basin Studies, Sedimentology, and Paleontology*. E. Schweitzerbart, Stuttgart, p. 351-369. Stuttgart.
- Wetzel, A., and A. Uchman, 1998 b, Deep-sea benthic food content recorded by ichnofabrics: A conceptual model based on observations from Paleogene flysch, Carpathians, Poland: *Palaios*, v. 13, no. 6, p. 533-546.
- Wetzel, A., and A. Uchman, 2001, Sequential colonization of muddy turbidites in the Eocene Beloveza Formation, Carpathians, Poland: *Paleogeography, Paleoclimatology, Paleoecology*, v. 168, no. 1-2, p. 171-186, doi:10.1016/S0031-0182(00)00254-6.
- Wetzel, A., and A. G. Reisdorf, 2007, Ichnofabrics elucidate the accumulation history of a condensed interval containing a vertically emplaced ichthyosaur skull, In: Bromley et al. (eds): p. 241-251. *Ichnology at the Crossroads: A Multidimensional Approach to the Science of Organism- Substrate Interactions*: SEPM Special Publication, no. 88: Society for Sedimentary Geology, Tulsa, Oklahoma.
- Wylie, G., M. Eberhard, and M. Mullen, 2007, Special report: unconventional gas technology - 1: Advances in fracs and fluids improve tight-gas production, *Trends In Unconventional Gas: Oil and Gas Journal*, 17 December, 2007, Retrieved from: <http://www.halliburton.com/public/common/trends.pdf> (accessed March 20, 2014).

CHAPTER 2

Automated precision serial grinding and volumetric three-dimensional reconstruction of large ichnological specimens

Małgorzata Bednarz, Liam G. Herringshaw, Christopher Boyd, Mary Leaman,
Elisabeth Kahlmeyer and Duncan McIlroy

In press with *Post-Ichnia 2012 Volume - Book of collected papers*,
Memorial University of Newfoundland and Geological Association of Canada

2.1. Abstract

To obtain deterministic three-dimensional reconstructions of large or complex trace fossils and to quantify the reconstructed models volumetrically, two stages are necessary: a laboratory stage, involving precision serial grinding and high-resolution digital photography, and a computer analysis stage, where burrow volumes are visualized and analysed. It is shown that the techniques can be used successfully for bioturbated rocks that have little or no density contrast between the matrix and the burrows, upon which non-destructive techniques, such as CT scanning, are ineffective. To demonstrate the technique, several trace fossil samples (phycosiphoniform burrows, *Nereites*, *Chondrites* and *Ophiomorpha*) were reconstructed in 3 dimensions using the described method. The

serial grinding method employing automated, computer-controlled machinery followed by detailed computer analysis, enables volume calculations to be determined precisely for a single burrow, burrow networks and ichnofabrics.

2.2. Introduction

Serial grinding has been used to reconstruct the three-dimensional morphology of palaeontological specimens for over a century (e.g., Sollas 1903; Stensjø 1927; Ager 1965, Tipper 1976; Herbert and Jones 2001; Watters and Grotzinger 2001). With the advent of low-cost digital photography and fast, high quality image-processing software, however, the approach has become increasingly accessible, and the techniques developed by Sutton et al. (2001a, 2001b, 2005, 2006) for studying the body fossils of the Herefordshire Lagerstätte have proved particularly influential. With the high resolution, easily manipulable images produced, and the wealth of morphological data that can be garnered, this approach has now been applied to a variety of fossil material (e.g., Rahman and Zamora 2009; Maloof et al. 2010).

Despite its potential value in elucidating morphology and sedimentological impact, serial grinding and computer modeled 3D reconstruction has been little used in ichnology. Exceptions are the trace fossil studies of Naruse and Nifuku (2008), Bednarz and McIlroy (2009, 2012), Michalík and Šimo (2010) and Boyd et al. (2012). Other studies have used serial polishing to examine ichnofabrics and ichnofossils, but without the creation of 3-D computer modeled volumetric reconstructions.

Serial grinding and 3D reconstruction of trace fossils and ichnofabrics in large rock samples has never been attempted, but such work is critical to full morphological characterization of many ichnotaxa (cf. McIlroy et al. 2009). Since trace fossils can comprise volumetrically significant components of many sedimentary rocks—affecting sedimentological properties at a reservoir scale (Buatois et al. 2002; Gingras et al. 2004; Burns et al. 2005; Gordon et al. 2010; Tonkin et al. 2010; Bednarz and McIlroy 2012) it is vital to understand their three-dimensional morphology.

Volumetric 3D reconstruction of such trace fossils has the potential to provide new insights into reservoir characterization. Several techniques have been used previously to obtain spatial models of the burrowing activity of living animals, or to measure the volumes of trace fossils and ichnofabrics. These include computed axial tomographic (CT) scanning (e.g., Dufour et al. 2005; Herringshaw et al. 2010), magnetic resonance imaging (MRI) (e.g., Gingras et al. 2002), multi-stripe laser triangulation scanning (MLT) (Platt et al. 2010) and serial grinding (Naruse and Nifuku 2008; Bednarz and McIlroy 2009, 2012; Michalík and Šimo, 2010; Boyd et al. 2012). All these methods have their limitations, depending upon the examined rock or sediment properties. The density contrast between matrix and burrow is commonly low, and it can be difficult to determine the true morphology of a trace fossil from two-dimensional cross-sections. As such, only destructive serial grinding can be employed satisfactorily to obtain a volumetric 3D reconstruction of a burrow (cf. Gingras et al. 2002; Naruse and Nifuku 2008; Bednarz and McIlroy 2012). In most palaeontological and ichnological studies, the serial grinding has been carried out manually (e.g., Wetzel and Uchman 1998; Sutton et

al. 2001; Bednarz and McIlroy 2009). While this is acceptable for small specimens, such an approach is not appropriate for larger ones, as it is too unwieldy and imprecise.

By using serial grinding to produce high resolution reconstructions, new information can also be obtained on the ecology of the tracemaker and the sedimentological impact of bioturbation. Furthermore, such studies can be used to resolve ichnotaxonomic issues by resolving trace fossil morphology within the host sediment. This approach to ichnological and ichnotaxonomic research is particularly relevant if applied to specimens from the type locality (Boyd et al. 2012).

The aim of this paper is to present methodology used to model trace fossils in three dimensions in order to apply a deterministic volumetric approach that is beneficial in ichnotaxonomy and also in bioturbated reservoir studies.

2.3. Methodology

2.3.1. Sample preparation

Large blocks containing multiple or single trace fossils of various size can be trimmed in the field using a hand-held rock saw, if care is taken to leave sufficient matrix around the trace fossil. In our study, to create a regular shape for precise image alignment, each block was placed in a box and plaster of Paris poured around it (cf. Bednarz and McIlroy 2009, 2012; Boyd et al. 2012). Once the plaster is set, the block can be removed from the box, and cut into a rectangular prism with a laboratory rock saw. The regular outline of the block is used as the basis for image registration (see below; Fig. 2.1A).

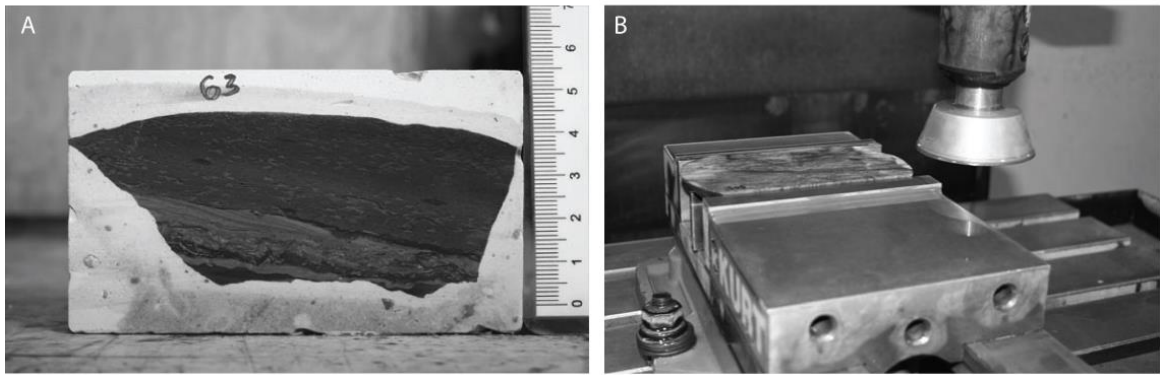


Fig. 2.1. Set-up and procedure for precise, computer-controlled, serial grinding of ichnological samples. **A.** Freshly exposed surface of sample embedded in plaster of Paris, ready for photography. **B.** HAAS VF-3 CNC Vertical Machining Center, showing diamond-tipped rotating blade with sample clamped in place prior to grinding.

For further accuracy of image alignment, vertical holes can be drilled into the block (cf. Sutton et al. 2001a). Prior to photography (see below), visual contrast between the ichnofabric and the rock matrix can be enhanced considerably by wetting the ground surface of the specimen with water or a light oil (cf. Bromley 1981). To prevent disintegration of the plaster of Paris from frequent moistening, non fossil-bearing surfaces of the block can be coated with plain, transparent lacquer.

2.3.2. Serial grinding set-up

Serial grinding was carried out using a Haas VF3 VOP-C Vertical Machining Center (20hp vector dual drive, 1000 IPM), capable of grinding to a precision of 0.001 inches (0.025 mm). Specimens were clamped in place (Fig. 2.1B), with the gantry raised by remote control to the start position, and then raised by the required increment after each grinding run. The most effective grinding element was found to be a diamond disc (diameter = 70 mm).

The increment of rock removed during each serial grinding run can be varied according to the dimensions and expected complexity of the material studied. For example, phycosiphoniform burrows with a diameter of 2–3 mm were serially ground at increments of 0.2 mm; whereas a block containing *Diplocraterion* with a width of ~60 mm and an estimated depth of over 100 mm, was serially ground at increments of 0.4 mm. The choice of serial grinding interval resolution depends also on the purpose of the reconstruction, with coarser increments used for gross-scale reconstructions, and finer

increments used to provide highly detailed reconstructions and to enable volume measurements of small specimens.

2.3.3. Photography

Canon 30D and 50D digital SLR cameras were used to photograph the specimens after each grinding run. For accuracy in the subsequent registration process (see below), it is crucial to maintain the distance between the freshly exposed sample surface being photographed, and the objective (lens) of the camera being used. Owing to the fact that the sample decreases in thickness after each run of the grinding tool, the camera–specimen surface distance was adjusted each time to ensure consistency.

The photographs should be taken under invariant lighting conditions that best illuminate the ichnofabrics. To test this, a series of photographs of the same sample surface should be taken under different conditions, after the first serial grinding run. Lighting conditions to consider include photography under ambient lighting, under flash lighting, and under controlled directional lighting. It is essential to avoid shadows across the sample, which might obscure important features or be confused subsequently as being of lithological origin.

If contrast is insufficient when the rock surface is dry, it may be necessary to wet the surface to enhance the contrast: this is particularly true of finer-grained rocks, or specimens where the trace fossil fill is of a similar colour to the matrix. Successively ground surfaces should be consecutively numbered using a permanent marker or pencil, and photographed with a scale bar (Fig. 2.1A).

2.3.4. Digital image-processing and interpretation

Images can be processed with a range of filters (e.g., brightness, contrast) in a 2D graphic software package such as Adobe Photoshop to enhance the contrast between the burrow and the matrix. Depending on the characteristics of the sample, the photographs may need to be changed to greyscale to do this effectively.

In the worked examples considered here, each photograph of the serially ground sample was stacked consecutively as layers in a single Photoshop file (.PSD). The first photograph in the series was used as a base layer, and all other layers were registered (aligned) with this base layer. Each successive layer was named using the number of the serial grinding run captured in the photograph.

2.3.5. Burrow selection methods

Once all images are aligned, the image stack was cropped to focus on the area of interest. The burrows can be selected, either by mouse or tablet pen, using one of the many tools in Photoshop (e.g., Magic Wand or Pen). The choice of tool depends upon the nature of the burrows (Fig. 2.2A and D). If the burrows are large and the contrast between them and the matrix is sufficient, the Magic Wand tool can be used. If the burrows are small, however, and the contrast between the trace fossil and matrix minimal, the Magic Wand tool might select a range of pixels that do not belong to the burrow, introducing errors (cf. Fig. 2.2B and E) and overly complex 3D isosurfaces (see below). The most accurate – but time-consuming – method of burrow selection is to use the “Brush” and “Magnetic

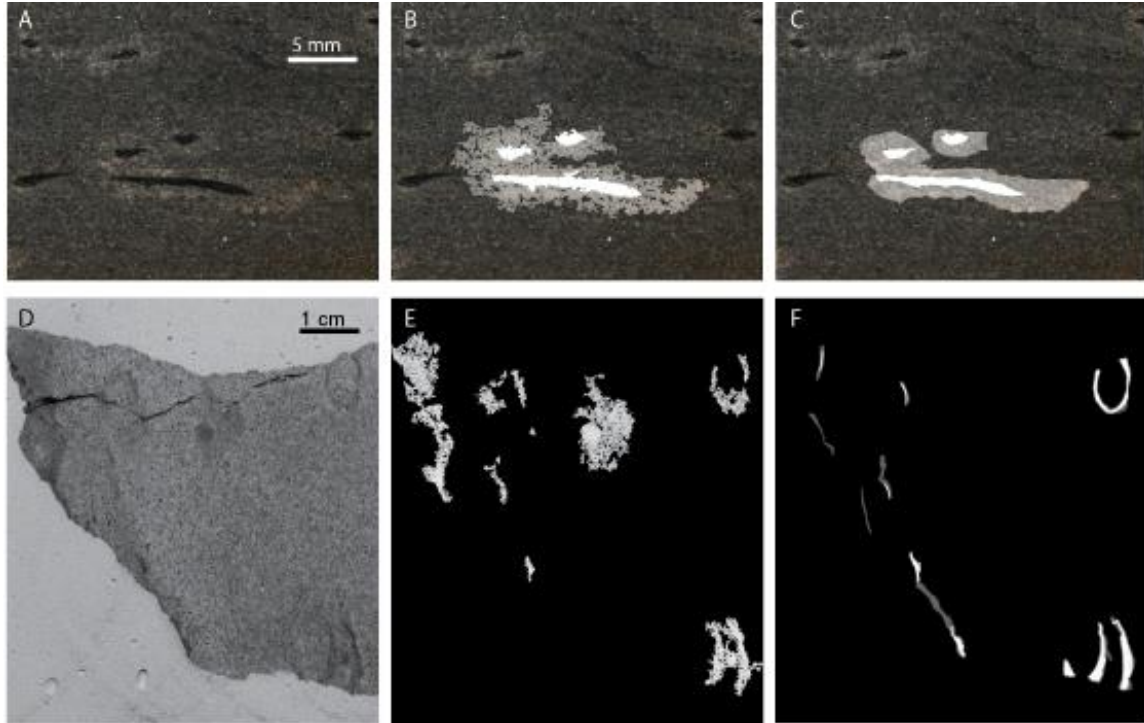


Fig. 2.2. Selection of features in two samples of serially ground trace fossil: phycosiphoniform burrows (**A, B, C**; composed of two elements: core and halo) and *Ophiomorpha* burrows (**D, E, F**). Phycosiphoniform burrow core shown in white in images B and C; burrow halo in grey. **A, D.** Images showing polished surface of ichnological samples, prior to burrow selection. **A,** black shapes represent burrow cores surrounded by haloes of lighter-coloured material in low contrast to matrix material. **D,** dark grey areas represent muddy lining/fill of *Ophiomorpha* burrows. **B, E.** Shapes of burrows obtained using Magic Wand selection tool; pixelization of burrows visible, resulting from imprecise nature of the tool. **C, F.** Burrow shapes obtained using Magnetic Lasso and Brush tools. Smooth outlines representing burrow margins are most suitable for subsequent interpretation by 3D rendering software.

Lasso” tools with a tablet pen (Fig. 2.2C and F). These tools enable the most accurate selection of burrow shape and minimize production of spurious burrow margins.

When the examined ichnotaxon is known to be composed of more than one element (e.g., *Nereites*, Fig. 2.2A-C; cf. Bednarz and McIlroy, 2009, 2012), all elements can be selected and saved separately. This makes it possible to reconstruct different elements of the same burrow separately in 3D. In addition, modeling different components of the burrow separately in the same 3D volume enables artificial colouring of the different components of the trace fossil, and can be used for volume measurements of these separated elements and their comparisons. The burrow selection layers are then saved as grey-scaled images, with white silhouettes on a black background.

2.3.6. 3D modeling

In our study, stacks of the images to be reconstructed were imported into the commercial edition of one of two 3D volume visualization software packages: VG Studio Max 1.2, and VolView 2.0. Both programs can reconstruct spatial geometry from a sequence of 2D images representing the cross-sections of any object or structure, by the process of voxel (volume element) rendering. When importing raster image formats such as .JPG or .PNG into the programs sample spacing values (x, y and z) must be provided manually.

2.3.6.1. Volume visualization and polygonal surface extraction

The burrow volumes are visualized as 3D objects by the software on the basis of the greyscale iso-values of the voxels in merged 2D slices. Volume generation is calculated

by the connection of voxels with the same grey intensity in each consecutive image (iso-grey-value surface; Fig. 2.3B). Thus obtained, the 3D volumes of the trace fossils can be artificially coloured to better visualize different elements of the trace fossil (e.g., Fig. 2.3A and C).

Volumetric studies of trace fossils and ichnofabrics require that the external morphology of the reconstructed burrows be “polygonized”. The polygonal models of reconstructed burrows are generated from the volumetric data sets through isosurface extraction (Fig. 2.4A). Polygonal surface extraction is based on the grey-scale or opacity iso-value that is chosen to be the most accurate representation of the object being reconstructed (Fig. 2.4B). The polygonal mesh created is exported at 1:1 scale into the .SLT file format (Stereo Lithography 3D object) that can be opened and edited by most 3D modeling programs (e.g., Autodesk 3ds Max).

2.3.6.2. 3D modeling software and polygonal mesh optimization

The mesh of the generated polygonized objects reflects the three-dimensional morphology of the modeled trace fossil. The mesh originally generated by the software is dense, composed of millions of triangle-shaped polygons, and usually contains duplicated vertices and faces as well as isolated fragments and open holes. As a result, the file containing the mesh is usually very large and needs considerable system and graphic card memory to be opened and edited. Therefore it must be optimized, simplified and/or remeshed to reduce the number of polygons (decimation) (Fig. 2.5). The surface of the polygonized trace fossil must also be smoothed to account for the unknown distribution

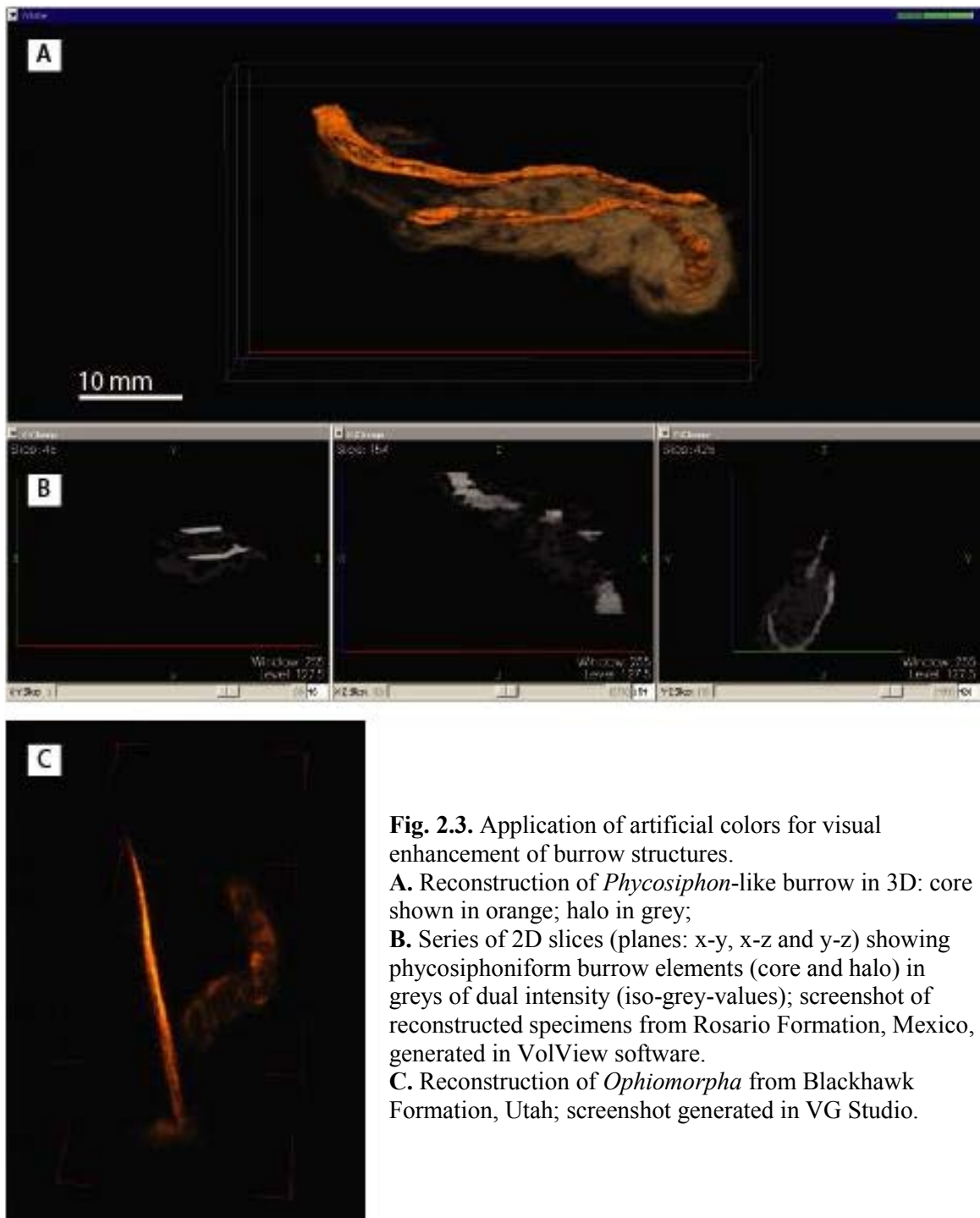


Fig. 2.3. Application of artificial colors for visual enhancement of burrow structures.

A. Reconstruction of *Phycosiphon*-like burrow in 3D: core shown in orange; halo in grey;

B. Series of 2D slices (planes: x-y, x-z and y-z) showing phycosiphoniform burrow elements (core and halo) in greys of dual intensity (iso-grey-values); screenshot of reconstructed specimens from Rosario Formation, Mexico, generated in VolView software.

C. Reconstruction of *Ophiomorpha* from Blackhawk Formation, Utah; screenshot generated in VG Studio.

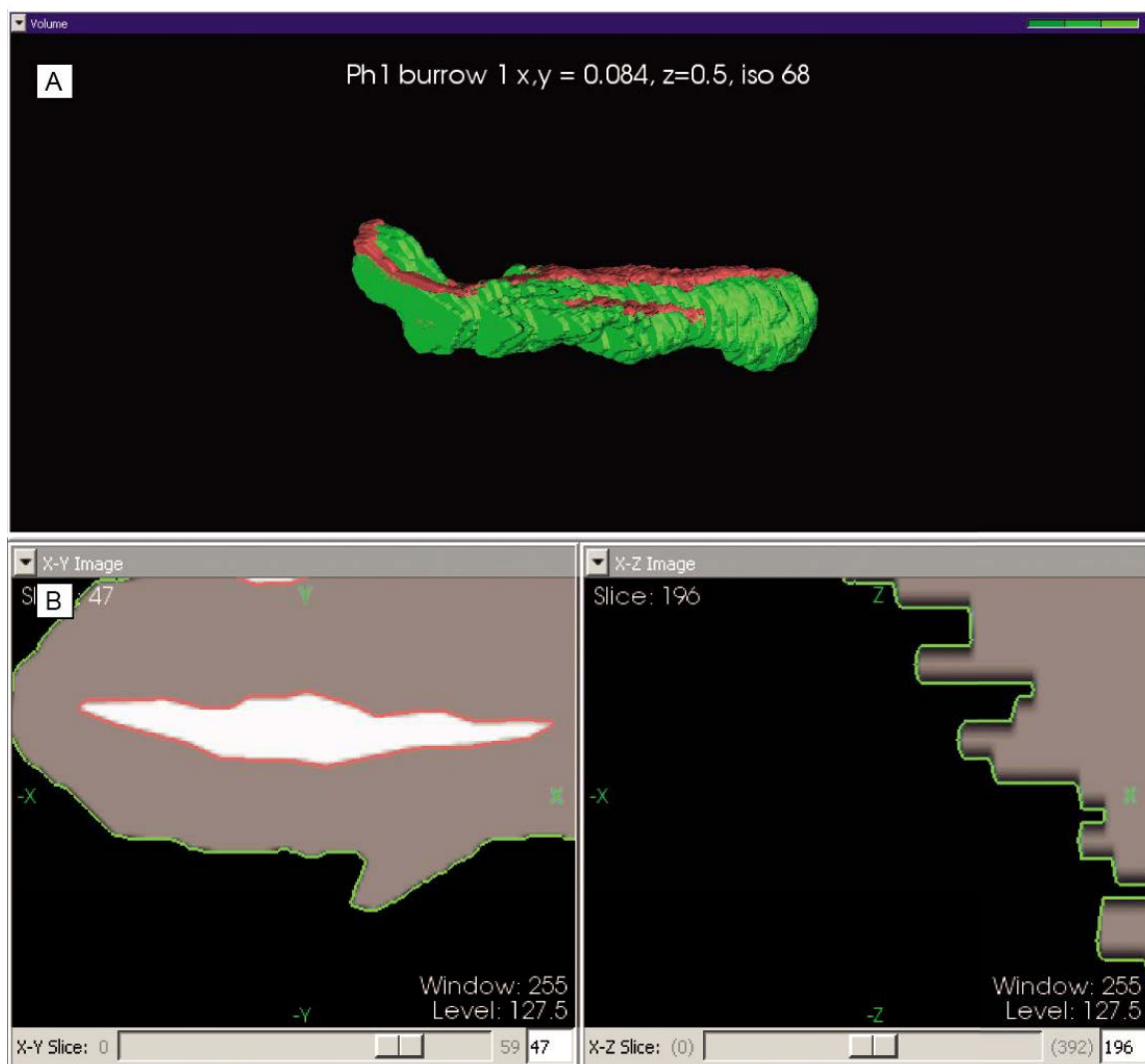


Fig. 2.4. Polygonal surface extraction of reconstructed *Phycosiphon*-like burrow from Rosario Formation, Mexico, based on iso-grey-values; screenshots generated in VolView software. **A.** Resultant polygonal surface showing core (red) and halo (green); **B.** Surface component lines applied to iso-grey-values of distinct burrow elements (core and halo) in each of 2D slices (planes: x-y and x-z).

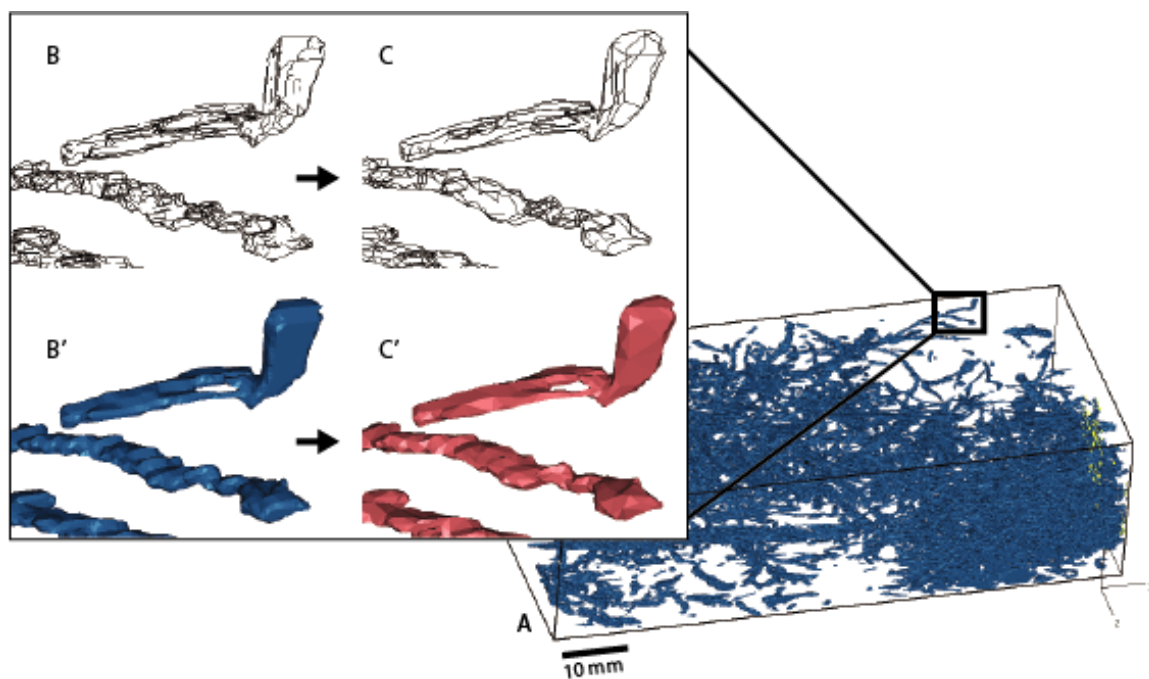


Fig. 2.5. Mesh simplification of reconstructed trace fossils. **A.** Polygonized 3D model of *Chondrites* ichnofabric. Mesh was exported as .STL file from VolView software and was 314 MB in non-simplified mesh format. **B, B'.** Zoomed-in selection of non-simplified polygonized mesh; **C, C'.** Zoomed-in selection of simplified polygonized mesh (decimated, optimized, smoothed). Resultant simplified mesh file size reduced to 68 MB.

of the trace fossil surface between the known two dimensional planes (the two images representing the two surfaces of the rock exposed during two consecutive serial grinding runs), which have been averaged in the process of creating voxels.

In this study, the first stage of simplification was achieved in the volume-visualizing software prior to exporting the mesh. Further simplification and optimization can be accomplished using most 3D modeling programs (e.g., MeshLab v1.2.2 or Autodesk 3ds Max). The resultant 3D objects were further modified by: 1) the application of artificial colours to the specified volumes of distinct transparency (representing different density or porosity within the specimen); 2) the cropping of reconstructed volumes along specified planes; 3) the isolation of discrete burrows as detached objects; and 4) the rotation and animation of objects.

Volumetric binary data obtained through digital reconstruction can be exported to many file types that maintain the 3D structure. This enables further examination using freeware, such as Right Hemisphere Deep View, GLC_Player, Cortona3D Viewer and Acrobat Reader. Exporting burrow reconstructions to widely used, interactive file formats allows for further investigation of 3D morphology by the creation of artificial cross-sections, animations, visualization of connected high porosity zones in three dimensions, and the measurement of volumes of the different burrow components (c.f. Bednarz and McIlroy 2012).

2.3.6.3. Volumetrics in ichnology

Once a polygonized surface is created, it is possible to apply a volumetric approach to the three-dimensional models characterizing the reconstructed burrow or ichnofabric. The volume or surface area of the polygonized ichnological model can be measured directly by VolView, or by using a third-party program such as Autodesk 3ds Max.

Recent studies have reviewed volumetric approaches in ichnology (see Platt et al. 2010; Bednarz and McIlroy 2012). Distances and angles can be measured in any 3D modeling or volume-visualizing software. From a volumetric perspective, the most valuable measurements are those of surface area and volumes of the examined burrow or ichnofabric, which are either given in metric units or as relative magnitudes in percentages.

Surface area (*SA*, after Platt et al. 2010) is a measurement of the polygonal surface area generated by the volume-visualizing software. It is crucial to measure the optimized polygonal mesh to avoid flawed results, such as those caused by overlapping polygons (Platt et al. 2010).

There are two main volumes that describe any burrow or ichnofabric. These are: 1) the volume of a prism bounding the ichnofabric or the whole preserved burrow or partly preserved burrow, or *volume available* (*VA*, after Platt et al. 2010); and 2) the volume of the burrow or ichnofabric itself, or *volume utilized* (*VU*, after Platt et al. 2010).

Volume available (VA) is the volume of the smallest rectangular prism (width = a , height = b and length = c) that encloses the burrow, preserved part of the burrow or burrow association (Fig. 2.6):

$$(1) \quad VA = a \cdot b \cdot c$$

The volume of the entire burrow or burrow association is the VU , calculated using the 3D software, and it describes the amount of the sediment reworked by the trace maker.

On the basis of these volumes, further measurements can be made. These describe and quantify the characteristics of the measured burrow or ichnofabric in relation to the main volumes (VA and VU), as follows:

Volume exploited (VE) describes burrow density and the efficiency of space usage by the trace maker, reflecting the percentage of the volume of the sediment that was reworked by the trace maker. It is calculated using the following equation (after Platt et al. 2010):

$$(2) \quad VE = VU \cdot 100 / VA$$

Volume component percentage ($\%Vcomp$) represents the volumetric contribution of a particular component ($Vcomp$) of the burrow or ichnofabric, when reconstructed separately (e.g., the core or halo of *Phycosiphon*). $\%Vcomp$ is calculated as a percentage of the VA :

$$(3) \quad \%Vcomp = Vcomp \cdot 100 / VA$$

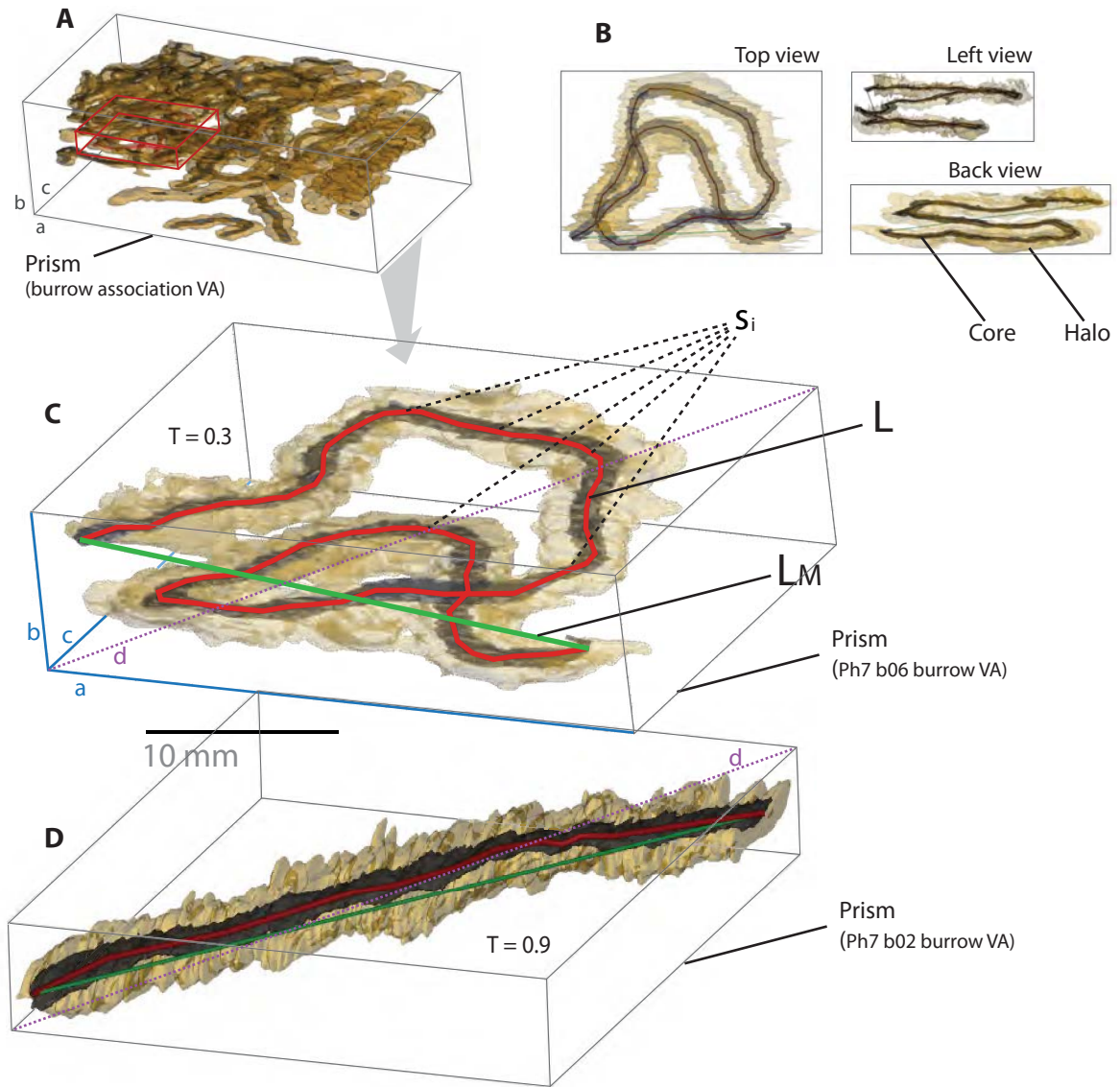


Fig. 2.6. 3D model of reconstructed ichnofabric composed of *Nereites* burrows (Lower Carboniferous Yoredale Sandstone Formation, Northumberland, UK).

A. Reconstruction of burrow network; **B.** Individual burrow (Ph7 b06) isolated from reconstructed burrow network, shown in top, lateral, and back views; **C.** Reconstruction of burrow Ph7 b06, showing tortuosity value (T) = 0.3; **D.** Reconstruction of burrow Ph7 b02 from the same sample, showing tortuosity value (T) = 0.9. Symbols: VA – Volume Available; s_i – straight elements composing burrow length line; L – burrow length; T – tortuosity index; a , b , c – prism dimensions; d – space diagonal within prism.

If the length of all components of the burrow (L) is known (by measurement using the 3D modeling software), the tortuosity index (T) can be calculated.

The *tortuosity index* (T) is the ratio between the diagonal length (d) of a rectangular prism bounding the burrow, and the total length of the burrow (or the length of a specific burrow component) (L):

$$(4) \quad T = d/L$$

When calculated for a burrow that does not branch or intersect itself at any point (i.e., a string, as observed in ichnotaxa such as *Phycosiphon*, *Helminthoida*, *Nereites* and *Spirorhapha*), the T value can illustrate the degree of burrow sinuosity and how densely it is packed in three dimensions (through consideration of value of d within the equation; Equation 4). In cases when the burrow is branched or intersects itself, the T value indicates how densely the burrow is packed within the burrow-bounding 3D prism, but not necessarily its curvature (e.g., *Chondrites*, *Thalassinoides*, *Ophiomorpha*). T values vary between 0 and 1, with straight burrows having a T value equal one or close to one (e.g., $T=0.9$ for an individual *Nereites* burrow; Fig. 2.6D), and highly tortuous/densely packed burrows having a T value that approaches zero (e.g., $T=0.3$ for a highly tortuous burrow in Fig. 2.6C).

Measurements of lengths and angles can be made in the 3D modeling software while examining the polygonal mesh of the models. A variety of possible measurements can be applied to different trace fossils, such as examining the branching angles of *Chondrites*, or the inclination of a burrow relative to the bedding.

2.3.6.4. Popularization of 3D interactive models

To enable the most comprehensive use and investigation of 3D ichnological models, it is beneficial to generate file formats that can display any polygonal mesh in an interactive 3D environment, and which can be opened with a dedicated 3D viewer installed on the user's computer system (see Table 2.1 for popular 3D software). The best formats for this are .PDF with 3D models embedded, .STL, .OBJ and .WRL files. WRL and PDF files also offer the possibility of publishing the interactive reconstructions on the internet, and are therefore the most desirable file formats in terms of rapid sharing and dissemination of 3D models and data (see example of interactive 3D model embedded in the PDF file in Appendix 1). All the file formats listed above can be generated in most forms of 3D modeling software, such as Autodesk 3ds Max.

2.4. Applications and future work

Three-dimensional reconstructions of trace fossils and ichnofabrics give ichnologists the possibility to review or determine the true morphology and geometry of any ichnological specimen. Deterministic calculations of the true volumes and surface areas of trace fossils also provide new insights of significance to reservoir studies (Bednarz and McIlroy 2012). When evaluating ichnological impact on reservoir quality, the volumetric assessment of the trace fossils or ichnofabrics is probably the most significant factor. Depending on the characteristics of the reconstructed trace fossils, their volumetric description can help determine reservoir quality. *Phycosiphon*-like burrows, for example, can significantly increase the reservoir quality of mudstones in unconventional shale-gas

Table 2.1. List of 3D software used for visualizing, modeling and viewing 3D models.

Software	Type	Website	License
VGStudio Max	3D volume visualizing (reconstruction)	www.volumegraphics.com	commercial
VolView	3D volume visualizing (reconstruction)	www.kitware.com	commercial
Autodesk 3ds Max	3D modeling software	www.autodesk.com	commercial
MeshLab	3D modeling software	meshlab.sourceforge.net	freeware
DeepView	3D viewer	www.righthemisphere.com	freeware
GLC_Player	3D viewer	www.glc-player.net	freeware
Cortona3D Viewer	3D viewer	www.cortona3d.com	freeware
Adobe Acrobat Reader	PDF reader with 3D viewer	www.adobe.com	freeware

plays as their silt-rich burrow haloes can create porous and permeable zones within otherwise impermeable host rocks (Bednarz and McIlroy 2012). Three-dimensional visualization of such biogenic pore networks is thus highly relevant to hydrocarbon reservoir characterization. Future work on 3D reconstructions is likely to enhance the availability/accessibility of 3D models and streamline their generation to make them a widely used tool for ichnologists and petroleum geologists.

Three-dimensional reconstructions of trace fossils and other ichnologically generated sedimentary fabrics have the potential to greatly inform ichnotaxonomic studies, as well as palaeobiological and palaeoecological models accounting for the processes of burrow formation and modification. At present, with few exceptions (*Macaronichnus*: Gingras et al. 2002; phycosiphoniforms: Nifuku and Naruse 2008; Bednarz and McIlroy, 2009, 2012; *Zavitokichnus*: Michalík and Šimo 2012; *Ophiomorpha*: Boyd et al. 2012), the true and deterministic morphology of many common, ichnofabric-forming trace fossils is not known. It has been shown recently that there are at least three trace fossils that produce similar “frogspawn” ichnofabrics in vertical cross-section, while having considerably different three-dimensional geometries (Bednarz and McIlroy 2009, 2012).

The method described herein may have limitations when applied to totally bioturbated sediments, especially if employed for ichnotaxonomic studies. High bioturbation index and/or presence of burrows that intersect each other may considerably reduce the lucidity of the component single burrows and thus influence the resultant reconstruction of the burrows’ spatial morphology.

However in terms of resolution, the presented methodology employing high-res photography and a chosen computer controlled serial grinding machinery can be used to make extremely precise reconstructions because of the fact that the diamond-coated grinding tip can remove a rock layer as thin as 1 micron (c.f. Maloof et al. 2010). Although time consuming, manual selection of the ichnofossil's shape components gives the confidence that the obtained spatial structure is not flawed by the elements that could be erroneously interpreted as a burrow's elements by the automatic selection tools which usage may result in incorrect spatial structure and further volumetric measurements.

2.5. Conclusion

Automated, computer-controlled, serial grinding allows for highly precise abrasive removal of extremely thin, parallel portions of examined rock samples (up to 1 micron). This method creates the possibility of obtaining – through digital photography – a large number of high-resolution images showing the three-dimensional structure of ichnological specimens. The reconstruction process necessitates the careful, and time-consuming, manual selection of burrows within these photographic images using 2D software. This precision, however, plays a vital role in the subsequent reconstruction of the trace fossils with volume-visualizing software. After the volume has been reconstructed, it is possible to produce a polygonal mesh of the trace fossil surface that can be the basis for volumetric analysis. Quantification of many burrow or ichnofabric parameters can then be done once the polygonal mesh is produced, including: 1) burrow

dimensions; 2) the volume of sediment that the trace-maker reworked; 3) the surface area of the burrow; and 4) burrow tortuosity.

When the 3D models are exported to popular file formats, they can be made widely accessible to researchers, giving the opportunity for further analytical work. This volumetric approach to ichnology is likely to have a particularly significant impact in petroleum geology, where the characterization of trace fossils has already proven to have a major effect on the permeability and fracturability characteristics of reservoir intervals (Buatois et al. 2002; Gingras et al. 2004; Burns et al. 2005; Gordon et al. 2010; Tonkin et al. 2010; Bednarz and McIlroy 2012).

2.6. Acknowledgements

This work is supported by a NSERC, RDC and by the award of a Canada Research Chair to Duncan McIlroy. Technical support from Jennifer Dunne of the Department of Technical Services, Memorial University, who assisted through many hours of rock grinding and problem solving, is gratefully appreciated.

2.7. References

- Ager, D.V., 1965, Serial grinding techniques. p. 212–224. In Kummel, B. and Raup, D. (eds.), *Handbook of Paleontological Techniques*. W. H. Freeman, New York.
- Bednarz, M., and D. McIlroy, 2009, Three-dimensional reconstruction of “phycosiphoniform” burrows: Implications for identification of trace fossils in core: *Paleontologia Electronica*, v. 12, no. 3, http://palaeo-electronica.org/2009_3/195/index.html (accessed August 20, 2011).
- Bednarz, M., and D. McIlroy, 2012, Effect of phycosiphoniform burrows on shale hydrocarbon reservoir quality: *AAPG Bulletin*, v. 96, no. 10, p. 1957–1977, doi:10.1306/02221211126.
- Boyd, C., McIlroy, D., Herringshaw, L., and Leaman, M., 2012, The recognition of *Ophiomorpha irregulaire* on the basis of pellet morphology: restudy of material from the type locality: *Ichnos*, v. 19, no. 4, p. 185–189.
- Bromley, R.G., 1981, Concepts in ichnotaxonomy illustrated by small round holes in shells: *Acta Geologica Hispanica*, v. 16, p. 55–64.
- Buatois, L.A., M.G. Mángano, A. Alissa, and T.R. Carr, 2002, Sequence stratigraphic and sedimentologic significance of biogenic structures from a late Paleozoic reservoir, Morrow Sandstone, subsurface of southwest Kansas, USA: *Sedimentary Geology*, v. 152, p. 99–132.
- Burns, F.E., S.D. Burley, R.L. Gawthorpe, and J.E. Pollard, 2005, Diagenetic signatures of stratal surfaces in the Upper Jurassic Fulmar Formation, central North Sea, UKCS: *Sedimentology*, v. 52, p. 1155–1185.
- Dufour, S. C., G. Desrosiers, B. Long, P. Lajeunesse, M. Gagnoud, J. Labrie, P. Archambault, G. Stora, 2005, A new method for three-dimensional visualisation and quantification of biogenic structures in aquatic sediments using axial tomodensitometry: *Limnol. Oceanogr. Methods* v. 3, p. 372–380.
- Gingras, M. K., B. Macmillan, B. J. Balcom, T. Saunders, and S. G. Pemberton, 2002, Using Magnetic Resonance Imaging and petrographic techniques to understand the textural attributes and porosity distribution in *Macaronichnus*-burrowed sandstone: *Journal of Sedimentary Research*, v. 72, no. 4, p. 552–558.
- Gingras, M. K., C. A. Mendoza, and S. G. Pemberton, 2004, Fossilized worm burrows influence the resource quality of porous media: *AAPG Bulletin*, v. 88, no. 7, p. 875–883.
- Gordon, J.B., S.G. Pemberton, M.K. Gingras, and K.O. Kornhauser, 2010, Biogenetically enhanced permeability: A petrographic analysis of *Macaronichnus segregatus* in the Lower Cretaceous Bluesky Formation, Alberta, Canada: *AAPG Bulletin*, v. 94, p. 1779–1795.

- Herbert, M., J. and C. B. Jones, 2001, Contour correspondence for serial section reconstruction: complex scenarios in palaeontology: *Computers & Geosciences*, v. 27, p. 427–440.
- Herringshaw, L.G., O.A. Sherwood, D. McIlroy, 2010, Ecosystem engineering by bioturbating polychaetes in event bed microcosms: *Palaios*, v. 25, p. 46–58.
- Maloof, A. C., C. V. Rose, R. Beach, B. M. Samuels, C. C. Calmet, D. H. Erwin, G. R. Poirier, N. Yao, and F. J. Simons, 2010, Possible animal-body fossils in pre-Marinoan limestones from South Australia: *Nature Geoscience*, v. 3, p. 653–659.
- Michalík, J., and V. Šimo, 2010, A new spreite trace fossil from Lower Cretaceous limestone (Western Carpathians, Slovakia): *Earth and Environmental Science Transactions of the Royal Society of Edinburgh*, v. 100, no. 4, p. 417–427.
- Naruse, H., and K. Nifuku, 2008, Three-dimensional morphology of the ichnofossil *Phycosiphon incertum* and its implication for paleoslope inclination: *Palaios*, v. 23, no. 5, p. 270–279, doi:10.2110/palo.2007.p07-020r.
- Platt, B. F., S. T. Hasiotis, and D.R. Hirmas, 2010, Use of low-cost multistripe laser triangulation (MLT) scanning technology for three-dimensional, quantitative paleoichnological and neoichnological studies: *Journal of Sedimentary Research*, v. 80, no. 7, p. 590–610, doi:10.2110/jsr.2010.059.
- Rahman, I.A., and S. Zamora, 2009, The oldest cinctan carpoid (stem-group Echinodermata), and the evolution of the water vascular system: *Zoological Journal of the Linnean Society*, v. 157, p. 420–432.
- Sollas, W. J., 1903, A method for the investigation of fossils by serial sections: *Proceedings of the Royal Society of London*, v. 72, p. 98.
- Stensio E. A. 1927, The Downtonian and Devonian vertebrates of Spitzbergen: *Skrift, Svalbard Nordishavet*, v. 12: p. 1–31.
- Sutton, M.D., D.E.G. Briggs, David J. Siveter, and Derek J. Siveter, 2001a, Methodologies for the visualization and reconstruction of three-dimensional fossils from the Silurian Herefordshire Lagerstätte: *Paleontologia Electronica*, v. 4, no. 1, p. 1–17, http://palaeo-electronica.org/2001_1/s2/issue1_01.htm (accessed August 10, 2010).
- Sutton, M.D., D.E.G. Briggs, David J. Siveter, and Derek J. Siveter, 2001b, An exceptionally preserved vermiform mollusc from the Silurian of England: *Nature*, v. 410, p. 461–463.
- Sutton, M.D., D.E.G. Briggs, David J. Siveter, and Derek J. Siveter, 2005. Silurian brachiopods with soft-tissue preservation, *Nature*, v. 436, p. 1013–1015.

- Sutton, M.D., D.E.G. Briggs, David J. Siveter, and Derek J. Siveter, 2006. Fossilized soft tissues in a Silurian platyceratid gastropod: *Proceedings of the Royal Society B*, v. 273, p. 1039–1044.
- Tipper, J. C., 1976, The study of geological objects in three dimensions by the computerised reconstruction of serial sections: *Journal of Geology*, v. 84, p. 476-484
- Tonkin, N. S., D. McIlroy, R. Meyer, and A. Moore-Turpin, 2010, Bioturbation influence on reservoir quality: A case study from the Cretaceous Ben Nevis Formation, Jeanne d'Arc Basin, offshore Newfoundland, Canada: *AAPG Bulletin*, v. 94, no. 7, p. 1059–1078, doi:10.1306/12090909064.
- Watters, W. A., and J. P. Grotzinger, 2001, Digital reconstruction of calcified early metazoans, terminal Proterozoic Nama Group, Namibia: *Paleobiology*, v. 27, no. 1, p. 159–171.
- Wetzel, A., and A. Uchman, 1998, Deep-sea benthic food content recorded by ichnofabrics: A conceptual model based on observations from Paleogene flysch, Carpathians, Poland: *Palaos*, v. 13, no. 6, p. 533–546, doi:10.2307/3515345.

2.8. Appendices

In order to control an interactive model (Appx 2.1):

1) click on the chosen three-dimensional reconstruction to activate the interactive content; 2) Use tools that are listed on the bar at the top of the activated area; 3) choose between available views to explore spatial geometry of the three-dimensional object and their chosen components; 4) use Model Tree panel in order to display or hide chosen components.

Appendix 2.1.

Interactive 3D reconstruction of aff. *Chondrites* from the Lower Jurassic Staithes Sandstone Formation, Yorkshire coast, UK. Scale: 10 mm.

CHAPTER 3

Three-dimensional reconstruction of “phycosiphoniform” burrows: implications for identification of trace fossils in core

Małgorzata Bednarz and Duncan McIlroy

Published in *Palaeontologia Electronica* (2009) Volume 12 (3)

3.1. Abstract

Phycosiphon-like trace fossils are some of the most common and important ichnofabric forming trace fossils in marine facies. This study aims to reconstruct the three-dimensional morphology of a *Phycosiphon*-like trace fossil from Cretaceous turbidites in Mexico in order to test the validity of criteria used to recognize such fossils in vertical cross-sections such as are seen in cores through hydrocarbon reservoir intervals. The geometry of the trace fossil was computer-modeled using series of consecutive images obtained by serial grinding. The recognition of *Phycosiphon* in cross section is usually based on comparison with hypothetical cross sections of bedding-parallel specimens. This study critically reassesses *Phycosiphon*-like burrows in the light of existing conceptual and deterministic models, for comparison with three-dimensional

reconstruction of *Phycosiphon*-like trace fossils from the Cretaceous Rosario Formation of Baja California, Mexico.

Observed morphological differences between our material and typical *Phycosiphon* suggest that the characteristic “frogspawn” ichnofabric that is usually attributed to *Phycosiphon* (*sensu stricto*) can be produced by other similar taxa. Our palaeobiological model for the formation of the studied *Phycosiphon*-like trace fossil is fundamentally different to that proposed for *Phycosiphon*, but produces remarkably similar vertical cross sections. We consider that identification of *Phycosiphon incertum* in core is not possible without detailed 3D examination of burrow geometry. We propose the term “phycosiphoniform” for this group of ichnofabric-forming trace fossils.

3.2. Introduction

Phycosiphon-like trace fossils are perhaps the most common group of trace fossils identified in vertically slabbed cores of mud-rich sedimentary rocks in petroleum fields worldwide (e.g., Bockelie 1991; Goldring et al. 1991; Wetzel and Bromley 1994; Bromley 1996; Pemberton and Gingras 2005). We herein use the term “phycosiphoniform” to encompass all burrows that, when seen in cross sectional view, have a *Phycosiphon*-like core of clay-grade material surrounded by a bioturbated zone of clay-poor silt or very-fine-grained sand that is inferred to have been produced during deposit feeding. The ichnofabric generated is commonly termed frogspawn texture (Fig. 3.1). Phycosiphoniform trace fossils are found in a range of marine depositional environments from marginal- to deep-marine settings in rocks ranging in age from the

Palaeozoic to the recent (e.g., Goldring et al. 1991; Fu 1991; Wetzel and Bromley 1994; McIlroy 2004b). The trace maker(s) of phycosiphoniform burrows are unknown small, probably vermiform, deposit feeding organisms, which are common in clay-rich siltstones (Kern 1978; Wetzel and Bromley 1994; Bromley 1996).

While phycosiphoniform burrows are common in the rock record, there is little consistency in the literature regarding the ichnogenic assignment of such burrows. A number of taxa with phycosiphoniform cross section have been recognised from core including: *Phycosiphon incertum* (Wetzel and Bromley 1994; McIlroy 2004b, 2007); *Helminthopsis* (Dafoe and Pemberton 2007; forms lacking a halo); *Helminthoidichnites* isp. (MacEachern et al. 2007); *Anconichnus* (Kern 1978; latterly synonymized with *Phycosiphon* by Wetzel and Bromley 1994); *Nereites* isp. (Wetzel 2002); *Cosmorhaphis* isp. (e.g., MacEachern et al. 2007). Most Palaeozoic occurrences of burrows in vertical cross section with a mudstone core and silty halo have been assigned to *Nereites*.

Since the behaviour of all of these phycosiphoniform trace fossils is conventionally interpreted to be systematic, selective deposit feeding, precise ichnogenic identification is perhaps not necessary for palaeoenvironmental analysis. In ichnofacies studies, which rely partly upon assessment of ichnogenic diversity, a full appreciation of ichnodiversity can be integral (MacEachern et al. 2007; McIlroy 2008), and thus in need of careful consideration. The three-dimensional geometry and full range of potential vertical cross sections of most phycosiphoniform taxa are imperfectly known. This work focuses on reviewing existing data on the most commonly recognised phycosiphoniform burrow *Phycosiphon incertum* Fisher-Ooster 1858 for comparison with our 3D

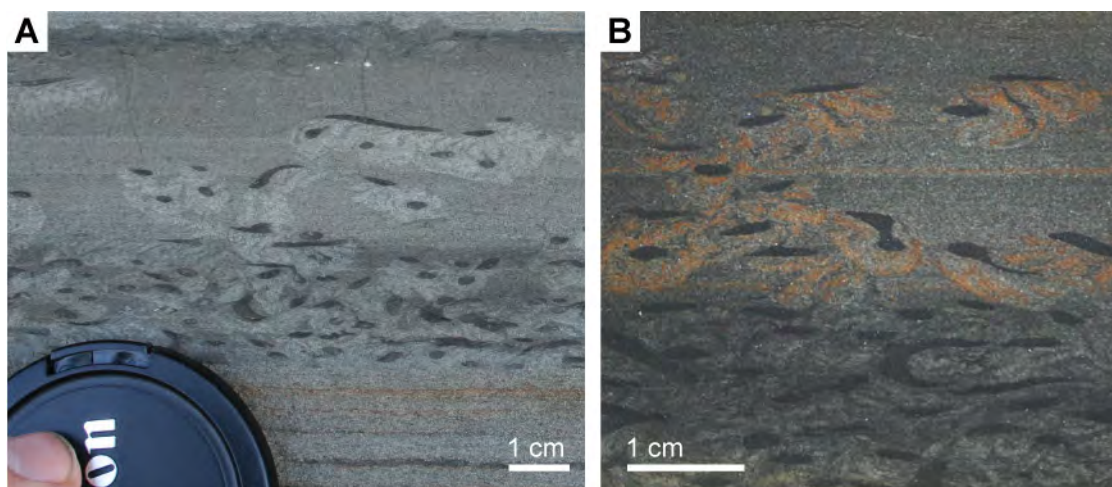


Fig. 3.1. Siltstone from Cretaceous Rosario Formation, Mexico, containing phycosiphoniform burrows with “frogspawn texture” in vertical section.

A. Outcrop photograph; **B.** Photograph of cut and ground surface of the sample examined during three-dimensional reconstruction of burrows. The halo is accentuated by diagenetic pyrite precipitation. Note that the burrow halo is predominantly located below the black mudstone core.

reconstruction of well-preserved phycosiphoniform burrows from the late Cretaceous of Mexico. The phycosiphoniform trace fossil reconstructed herein was studied from a hand specimen containing many phycosiphoniform trace fossils from a succession of well exposed slide blocks in a slope channel complex from coastal exposures of the Upper Cretaceous Rosario Formation in the coastal outcrop at Cajilola, close to the town of El Rosario, Mexico (Fig. 3.2). The ichnofabric is distinctive in containing anomalously large, slightly atypical, phycosiphoniform burrows. The host-sediment is a laminated turbidite siltstone. The burrow cores were subject to differential compaction relative to the host sediment, with the plane of flattening being parallel to bedding (Fig. 3.1).

3.3. Phycosiphoniform burrows in marine ichnofabrics

Phycosiphoniform trace fossils are an important component of most post-Palaeozoic shallow marine ichnological assemblages, particularly those with a mixture of clay and silt grade material (Goldring et al. 1991; Fu 1991). The recognition of *Phycosiphon incertum* has been greatly encouraged by publication of a series of representative hypothetical cross sections based on bedding-parallel specimens (Bromley 1996). We consider it likely that all phycosiphoniform burrows result from deposit feeding by organisms that selectively ingest clay grade material in order to process microbial biomass, particulate or dissolved organic matter, bio-films on sediment grains and the associated meiofaunal/interstitial biomass. The clay grade material ingested is concentrated into a faecal strand, surrounded by a zone of biologically processed sediment (silt to very fine grained sand) that has been cleaned of clay-grade material.

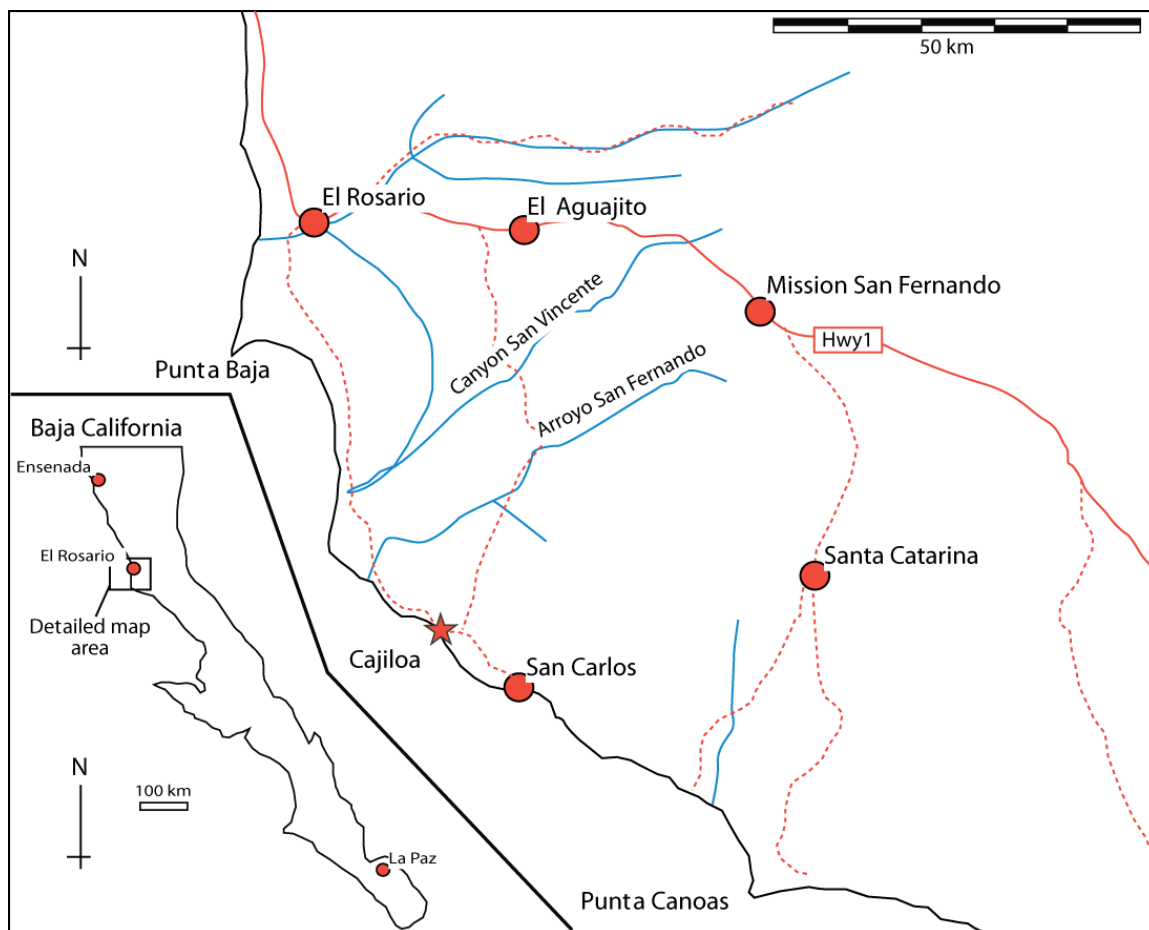


Fig. 3.2. Locality map showing the field locality (Cajilola marked with a star) relative to the town of Rosario in Baja California (Mexico). Redrafted with permission of Ben Kneller, University of Aberdeen unpublished field guide.

Published occurrences of *Phycosiphon* are commonly taken to include older literature mentioning the trace fossil *Anconichnus horizontalis*, which was described exclusively from vertical and horizontal cross sections in slabbed material (Kern 1978). The synonymization of *A. horizontalis* with *Phycosiphon incertum* (Wetzel and Bromley 1994), based on revision of the type material of *A. horizontalis*, and emendation of the original diagnosis of *P. incertum* to include non-bedding-parallel specimens has been widely adopted. As a result, *Anconichnus* is seldom referred to in modern literature.

In most cases, phycosiphoniform burrows are found as part of diverse ichnofabrics developed in shallow marine depositional environments (Goldring et al. 1991; Bockelie 1991; MacEachern et al. 2007). In ichnotaxonomically diverse shallow marine ichnofabrics, *Phycosiphon incertum* is generally a late-stage component of the ichnofabric, cross-cutting and reworking earlier burrow fills (e.g. Goldring et al. 1991; McIlroy 2007). Modern *Phycosiphon incertum* are common in deep marine settings (Wetzel 2008), though the trace maker is not as yet identified. Where phycosiphoniform burrows are found in mono-taxic assemblages, the depositional environment is typically inferred to have been stressed. Examples of stressful depositional environments with mono-taxic assemblages of phycosiphoniform trace fossils include tide dominated deltaic deposits, in association with fluid mud deposits (McIlroy 2004b), and dysoxic mudstones (Bromley and Ekdale 1984, 1986; Ekdale and Mason 1988).

3.4. Interpreted three-dimensional morphology of *Phycosiphon incertum*

The trace fossil *Phycosiphon* was first described by Fisher-Ooster (1858) from Gurnigel Flysch strata of Maastrichtian age (van Stuijvenberg 1979) in the western part of Switzerland (see Wetzel and Bromley 1994). The species was created by monotypy (Fisher-Ooster 1858). Study of topotype material facilitated the proposition of an emended diagnosis as follows: “*Extensive small-scale spreite trace fossils comprising repeated narrow, U-shaped lobes enclosing a spreite in millimetre to centimetre scale, branching regularly or irregularly from an axial spreite of similar width. Lobes are protrusive, mainly parallel to bedding/seafloor. However, the plane enclosing their width may lie horizontally, obliquely or even vertically to bedding/seafloor.*” (Wetzel and Bromley 1994, p. 1400).

In emending the diagnosis, the authors allowed for a strong vertical component to the fecal string, which is not evident in the type material. A vertical or oblique looped fecal string is present in other similar material collected from modern depositional settings (Wetzel and Wijayananda 1990; Wetzel and Bromley 1994). The diagnostic spreite have not, however, been fully documented from such material. The re-description of the type material by Wetzel and Bromley (1994) included review of *Anconichnus* Kern 1978, recognizing the latter as junior synonym of their emended *Phycosiphon* (i.e. *Anconichnus* is interpreted to be a morphotype of *Phycosiphon* with oblique to vertically oriented spreiten-bearing limbs). Supplementary block diagram models for *Phycosiphon* are needed to encompass cross-sections of non-bedding-parallel burrows (Fig. 3.3).

3.4.1. The mud-filled “marginal burrow”

The most visually striking part of *Phycosiphon*, and all phycosiphoniform burrows in cross section, is the marginal burrow, which is generally filled with dark clay-grade material, is usually less than 1mm in diameter and is surrounded by a silty halo. The marginal burrow has not been demonstrated to self-cross (Bromley 1996). The marginal burrow of any given lobe of *Phycosiphon sensu lato* may be in any orientation relative to bedding (Kern 1978; Wetzel and Wijayananda 1990; Wetzel and Bromley 1994; Bromley 1996; Fig. 3.3). Detailed three-dimensional imaging of the marginal burrow of a phycosiphoniform burrow has been undertaken recently (Naruse and Nifuku 2008), demonstrating that the sub-horizontal to oblique limbs may lie above one another. Neither a siltstone halo nor spreiten were reconstructed, perhaps because of a lack of lithological contrast. These burrows have been assigned to *Phycosiphon incertum* (Naruse and Nifuku 2008), though we consider that the lack of a full complement of ichnotaxobases precludes confident ichnotaxonomic assignment of this material.

Existing models for the orientation of lobes in *Phycosiphon incertum* (Wetzel and Bromley 1994) suggest that: 1) oblique lobes are most common in sandstone; 2) the same taxon in laminated siltstones and mudstones produces bedding-parallel lobes [comparable to the type material]; and 3) lobes in homogeneous silty mudstones are commonly randomly oriented. The marginal tube of *Phycosiphon* is looped, and defines the outer margin of spreiten-bearing regions that are discussed in detail below. A series of these curved probes are developed on one margin of the trace fossil in bedding-parallel material (Fig. 3.4). The tube, which is surrounded by very thin “mantle” of coarser

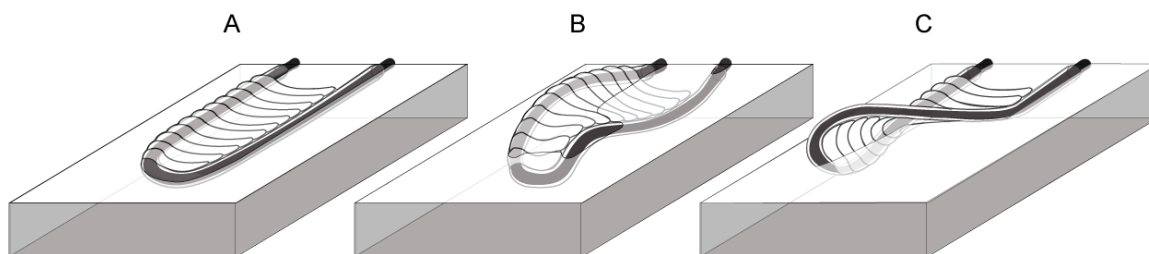


Fig. 3.3. Conceptual model showing the non-planar orientation of a single *Phycosiphon* burrow lobe with the mantle and spreite shown as being transparent to facilitate viewing of the central mudstone strand. **A.** Lobe parallel to the bedding plane; **B – C.** Possible variations of twisted *Phycosiphon* burrow lobes. This model is an expanded version of the bedding plane conceptual model (Bromley 1996), but incorporating the possible twisting allowed by the emended diagnosis of Wetzel and Bromley (1994).

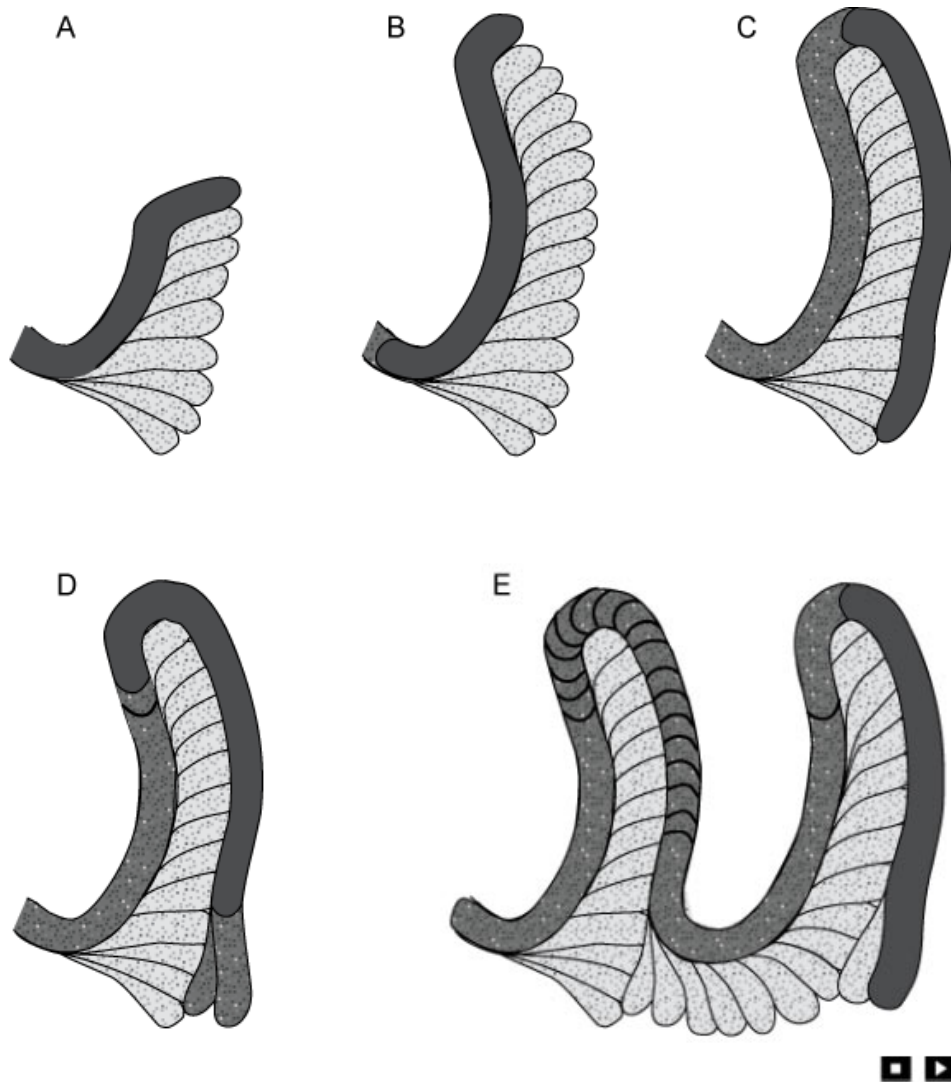


Fig. 3.4. Reconstruction showing how multiple phases of foraging by an unknown vermiform organism creates phycosiphoniform looped burrows composed of marginal tube and spreiten (based upon Wetzel and Bromley 1994; Bromley 1996; Seilacher 2007). Different shades of grey represent distribution of silt-sized (light grey) and clay-sized (dark grey) material.

A. Foraging organism creates feeding probes lateral to the marginal tube. **B.** Successive probes are made until the organism has produced a marginal tube the length of its body. **C.** Outer margin of the loop is produced by the organism moving along previously produced probes. **D.** Second loop is started after the organism body is straight one again. **E.** Animation (embedded in the PDF and in appendix 3.1) presenting multiple phases of phycosiphoniform trace fossil formation. (Click to activate the animation).

grained sediment (from which the original clay-grade material has been removed by the activity of the trace maker), is generally considered to be composed of fecal material selectively collected by deposit feeding activity in the central spreiten-bearing region.

3.4.2. Spreiten and haloes in *Phycosiphon*

Spreiten are positioned inside of the marginal tube and are considered to consist of zones of sediment that have been processed during feeding. The outer curves of the spreite are orientated in the direction of progressive feeding (e.g., Wetzel 1983; Wetzel and Bromley 1994; Bromley 1996; Seilacher 2007; Fig. 3.4A - E). It is anticipated that individual spreite would be meniscate if vertically sectioned through the axis of a lobe. Such a cross-section has never been figured, perhaps due to either a lack of lithological contrast between spreite or the small size of most *Phycosiphon*.

In some cases the mud-filled tube and mantle are not associated with a spreiten bearing loop. This phenomenon was attributed to locomotory behaviour by the trace making organism in its search for a new region of rich organic detritus (Wetzel and Bromley 1994). It is implied that when an organic-rich area is found by the trace maker, that the full spreiten-forming behaviour would resume.

The preservation of spreiten and mantle is highly dependent upon sufficient grain size contrast in the bioturbated sediment. If there is no variability in grain size in the host sediment there is little potential for spreiten formation. It has also been considered that spreiten are best preserved at sand-mud interfaces (Fu 1991). The clay-rich marginal tube is commonly the most prominent feature seen in field material. Some degree of mantle

and spreiten preservation is generally seen in cross-section. The marginal tube is commonly filled with dark coloured clay-grade material and is surrounded by a thin, pale mantle of coarser grains, lithologically similar to the spreiten (Wetzel and Bromley 1994). The combination of pale mantle and spreiten material around the dark mudstone core gives rise to the colloquial term “frogspawn texture” (Bromley 1996; Fig. 3.1).

3.5. Palaeobiology of the *Phycosiphon* trace-maker

3.5.1. Style of feeding

The *Phycosiphon*-making organism was sensitive to grainsize variability of the host sediment, and is not found in sediments coarser than fine grained sandstone (Ekdale and Lewis 1991, in reference to *Anconichnus*). The trace maker is considered to selectively ingest the clay-grade material from the sediment, leaving clean, coarser grained spreite or halos, and depositing behind it a continuous clay-rich fecal string. This is perhaps analogous to the selective deposit feeding behaviour of *Euzonus mucronata* which is known to produce *Macaronichnus*-like burrows (cf. Gingras et al. 2002a, b). The depth to which *Phycosiphon* is thought to bioturbate is up to 15 cm below the sediment-water interface in a wide range of bathymetric conditions from shallow marine to bathyal and perhaps even abyssal depths (Wetzel and Bromley 1994).

The presence of a meniscate backfill in the marginal tube, strongly supports its origin as a faecal string (Ekdale and Lewis 1991 in reference to *Anconichnus* [= *Phycosiphon*]). The

trace maker was probably a vermiform organism that produced a series of closely spaced feeding probes lateral to the marginal tube (in the centre of what is eventually a feeding loop; Fig. 3.4A). Each probing, feeding activity leaves a tubular zone of manipulated sediment that is cleaned of clay-grade material (upon which the trace maker feeds). Successive probes are made until the organism has produced a marginal tube the length of its body (Fig. 3.4B). The trace maker is then inferred to burrow along the outer margin of the earlier probes, to produce the outer margin of a loop (Fig. 3.4C). When the body of the trace maker is once again straight, either lateral probes are produced at the start of a second loop (Fig. 3.4D) or the organism abandons the region and moves in search of a new food-rich region (based upon Wetzel and Bromley 1994; Bromley 1996; Seilacher 2007). When considered together these multiple phases of burrowing can be seen to leave behind a phycosiphoniform trace fossil (Fig. 3.4E - animation).

3.6. Interpretation of three-dimensional morphology from cross sections of phycosiphoniform burrows

Bridging the gap from the two dimensional cross-sections commonly seen in core and slabbed material to a three-dimensional interpretation of morphology is a significant challenge for applied ichnologists (McIlroy 2004a, 2008, Bromley and Pedersen 2008). The starting point for this process has to be reliable three-dimensional reconstructions of known taxa; preferably type material. To address the issue of identifying phycosiphoniform burrows from cross-sectional views we will review and update the

model for *Phycosiphon incertum* for comparison with our phycosiphoniform material from Mexico.

3.6.1. Interpreting “frogspawn texture” as *Phycosiphon*-generated ichnofabrics

Phycosiphon is a morphologically complex trace fossil in three dimensions; consequently it has a diverse range of expressions in vertical cross section. These vertical cross sections can closely resemble other phycosiphoniform burrows (e.g., *Helminthoidichnites* cf. Chamberlain 1978; *Nereites* cf. Wetzel 2002). The characteristic frogspawn fabric (Bromley 1996) is produced by cross sections of the marginal tube (“embryo”) and the spreite or mantle (“jelly”). A number of vertical cross sections of bedding parallel *Phycosiphon* have been figured by Bromley (1996), and are supplemented by our digitally dissected deterministic model (Fig. 3.5A–3.5C). Since the emendation of the ichnogeneric diagnosis for *Phycosiphon* (Wetzel and Bromley 1994) includes the possibility of non bedding-parallel lobes, we have created a 3D digital model of *Phycosiphon* inclined 17° from the vertical, and created virtual vertical cross sections from it (Fig. 3.5E). The resultant cross-sections include the comma-shaped cross sections so common in outcrop material but not explained by pre-existing hypothetical models (Bromley 1996). The vertically stacked, bent paired marginal tubes not linked to a cross section by Bromley (1996), can also be explained by our model (Fig. 3.5E).

Comparison of our three-dimensional model, and cross sections obtained from it (Figs 3.3 and 3.5), with published cross sections of *Phycosiphon* (Goldring et al.1991; Wetzel and Bromley 1994; Bromley 1996; Naruse and Nifuku 2008) allows us to confidently

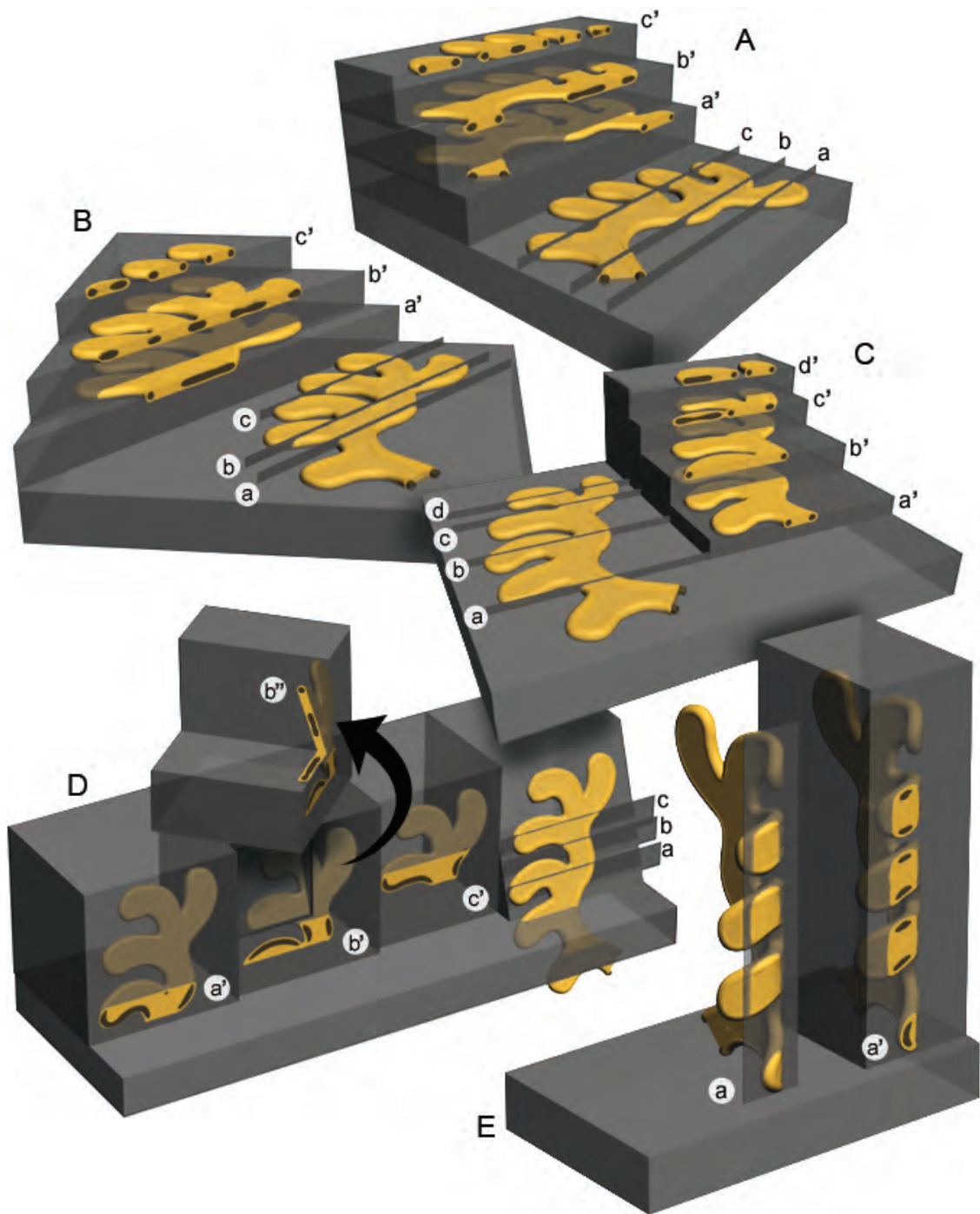


Fig. 3.5. Idealized 3D conceptual model showing the antler-like morphology of *Phycosiphon* structure cut to show the expected vertical cross sections.

Each of the boxes A-E show the 3D form of *Phycosiphon* in different orientations along with the location of labelled cut sections which are alphabetically linked to the vertical cross-sections which are analogous to the common sections seen in petroleum cores. **A-C.** Burrow loop parallel to bedding plane and intersected with perpendicular planes to show cross sectional views. **D.** Burrow inclined 17 degrees from the vertical and cut by vertical planes to show cross sectional views. **E.** Burrow vertical to bedding plane, with bent lobes, cut in the vertical plane to show cross sectional views.

state that the model of Bromley (1996) has the potential to produce the full range of *Phycosiphon* cross sections seen in vertical sections from core. It is thus entirely possible that the *Phycosiphon* trace maker deposit fed in vertical, oblique or bedding parallel orientations as well as the horizontal orientation seen in the type material. Not encompassed by our three-dimensional model, are twisted lobes, though it is inferred that those would produce broadly similar vertical cross-sections to those in Figs 3.5D-E.

3.7. Methods

Creation of three-dimensional conceptual models of trace fossils differs greatly from the process of direct reconstruction of the three-dimensional morphology of fossil material based on serial grinding and tomography. This paper aims to produce a three-dimensional deterministic model of some phycosiphoniform burrows from turbiditic siltstone of Cretaceous Rosario Formation and compare them to the *Phycosiphon* model of Bromley (1996). The approach used involves the use of serial grinding and computed tomography as outlined below.

3.7.1. Serial grinding

Three-dimensional geometry of the studied burrows was systematically exposed through serial grinding of the hand specimen. This approach has been successfully employed for three-dimensional imaging of body fossils (e.g., Baker 1978; Hammer 1999; Sutton et al. 2001), ichnofabric (Wetzel and Uchman 1998, 2001), and trace fossils (Naruse and Nifuku 2008). Serial grinding allowed us to obtain a sequence of regularly spaced images

of the resultant vertical cross sections. The photographic dataset thus created is the basis for subsequent computer-based three-dimensional reconstructions.

To aid in creating parallel regularly-spaced cross sections, the irregularly-shaped sample of turbiditic siltstone was placed in a tight fitting box and set in plaster of Paris. When the plaster was set, and regular 0.5 mm increments inscribed on the outer surface of the rectangular block, it was then ready to be serially ground. The regular outline of the block was essential to create reference points, for alignment of the photographic images to be used in digital analysis. The 0.5 mm spacing of images was chosen to capture a sufficiently large number of data-points to allow gridding of surfaces, and reconstruction of the burrows. A total of 59 images were acquired through a 29.5 mm thick slab of the sample. The consecutive series of photographs were taken from parallel surfaces with a digital camera, which was stationed an identical distance above the sample surface, under the same lighting and zoom conditions for every surface. The camera was attached to a photographic stand with height controlling screw feed.

Ichnofabrics have not generally been studied using a serial grinding approach. In contrast to body fossil material, trace fossil fabrics are commonly complex, tortuous, and without sharply defined limits (both morphologically and mineralogically). A particular problem is that burrows may branch and inter-penetrate, making closely spaced slicing essential, and poses particular challenges in image processing (discussed below). The size of the block studied is larger than has typically been studied by palaeontologists, but did not pose any particular methodological problems.

3.7.2. Image processing

The set of sequential slice images acquired through serial grinding technique was processed to select the regions to be studied. The phycosiphoniform burrows studied include a dark mud core and a halo of coarser sediment, which in the present material is accentuated through the presence of pyrite (Figs 3.1, 3.6). To obtain adequate contrast, the images were made into gray scales (Fig. 3.6B). All images were put into a single Photoshop document in consecutive order. Discrete burrow cores were chosen as the objects for tracing the location of the chosen burrow. The burrow core was tracked through each consecutive image and manually selected using layer masking to hide all other burrow cores and halo that might confuse the reconstruction of the chosen burrow (Fig. 3.6C). A masking layer was used to allow retention of the original, gray scaled images, including location of adjacent burrows, should it become subsequently desirable to study adjacent burrows. The layered Photoshop document was then cropped to the smallest size that encompassed the isolated burrow core. Each layer, representing the equidistant ground surfaces, was saved as JPEG image in the same directory with a numeric name that indicates its position in the sequence. This set of image-processed two-dimensional binary images was used for the subsequent three-dimensional reconstruction.

3.7.3. Three-dimensional rendering

The set of the binary images was imported to the commercial edition of VolView 2.0 software. Consecutive, gray scaled intersections of burrow core were converted by the

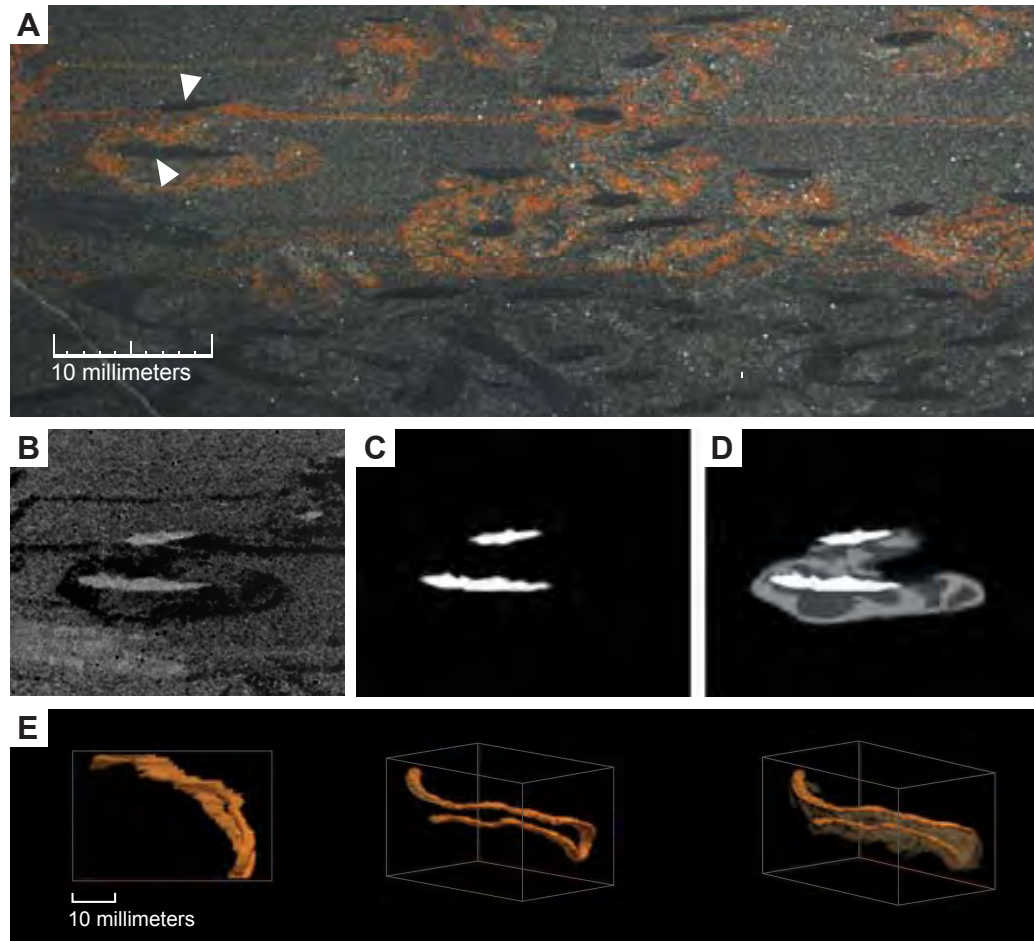


Fig. 3.6. Image processing stages during three-dimensional reconstruction of phycosiphoniform burrow from Rosario Formation.

A. Investigated material from Rosario Formation containing phycosiphoniform forms. Each photograph obtained during serial grinding was aligned and cropped. The continuous burrow cores were selected manually as the object of study (indicated by white arrows). **B.** To improve contrast, images were converted to gray scale. **C.** Distinct burrow cores were manually selected using layer masks in Photoshop and hiding all other burrow cores in the investigated area of the original images. Selected cores were tracked on all processed images. Images were then cropped to size that encompassed isolated burrow cores on all processed images. **D.** For additional reconstruction of burrow with its surrounding halos, areas of the halos were manually marked on all sequential images uncovering it from the masked layer. **E.** Three-dimensional visualization of phycosiphoniform burrow obtained through volume rendering of sequential images imported to VolView software.

software to the volume shape that represents the three-dimensional geometry of the examined phycosiphoniform burrow. Artificial colors were attributed to the reconstructed burrow core and to the halo in order to aid illustration (Figs 3.6E, 3.7, 3.8 and 3.9). Three-dimensional reconstruction of the phycosiphoniform burrow from examined rock was additionally saved as movie file that shows the burrow rotating around the axis that is perpendicular to the bedding plane (see attached animation files, Figure 3.7D and 3.9.4).

3.8. Three-dimensional morphology of the Rosario Formation phycosiphoniform burrows

By choosing a sparsely bioturbated portion of the ichnofabric, it was possible to identify a single isolated burrow. The burrow consists of a single loop shaped clay-filled tube that is identifiable in the series of ground vertical cross sections. This isolated burrow was subjected to detailed 3-dimensional reconstruction of both the mud-filled burrow core (Fig. 3.7B-C) and the burrow halo (Fig. 3.7A). The volume of rock subjected to three-dimensional reconstruction, and containing the fossil burrow was 40.9 mm in length (X axis), 21.9 mm in height (Y axis) and 29.5 mm thick (Z axis) (Figs 3.7-3.9). The two limbs mud-filled burrow core that describe the shape of the lobe are parallel to each other in vertical section and vary in diameter between 3 and 4 mm. Slight thickening in tube width is noted in the distal portion of the loop that cannot be attributed to compaction. Thickening of this part of the tube was described as one of the diagnostic characteristics of *Phycosiphon* (Wetzel and Bromley 1994). The paired limbs of the

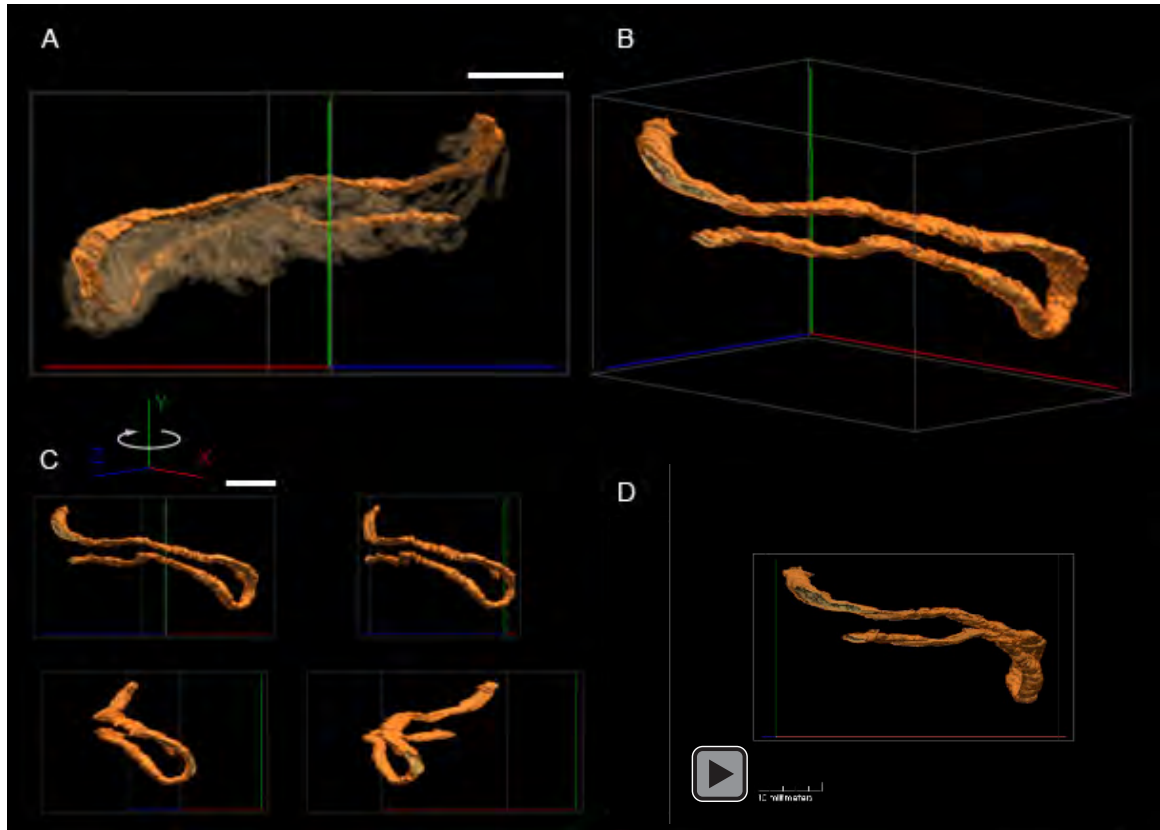


Fig. 3.7. Three-dimensional reconstruction of phycosiphoniform burrow from Rosario Formation, Mexico. **A.** Burrow core with surrounding halo. **B-C.** Burrow core without the halo. **D.** Animation of rendered reconstruction of the phycosiphoniform burrow core (embedded in the PDF and in appendix 3.2 A; click to activate the animation). Scale bars = 10 mm.

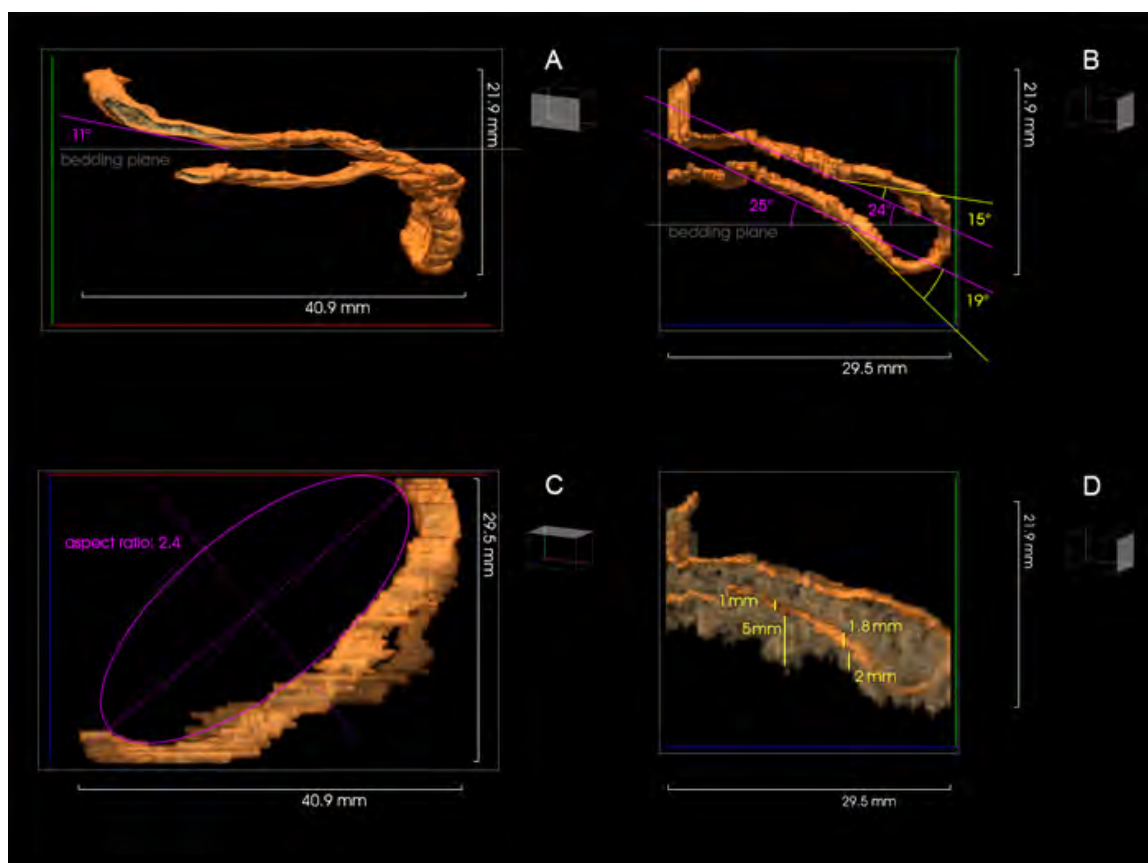


Fig. 3.8. Three-dimensional reconstruction of the lobe of the phycosiphoniform burrow from Rosario Formation, Mexico.

A. The longer arm of the lobe descends gently downward for about 30% of the lobe length and is inclined in about 11° to the bedding plane. Then in about next 30% of lobe length both arms continue more or less parallel to the stratification in order to incline in $24 - 25^\circ$ downward to the sediment. **B.** In about last 15% of lobe length the arms incline for further 15 – 19% each in opposite directions (upward and downward) and then direct back to create the apex of the lobe(so in the last part of formed loop the arms are the most distant from each other before they connect in the apex). **C.** Whole lobe is bent in the horizontal direction along a half-ellipse of an aspect ratio of 2.4. **D.** The halo can be several times thicker than the burrow core.

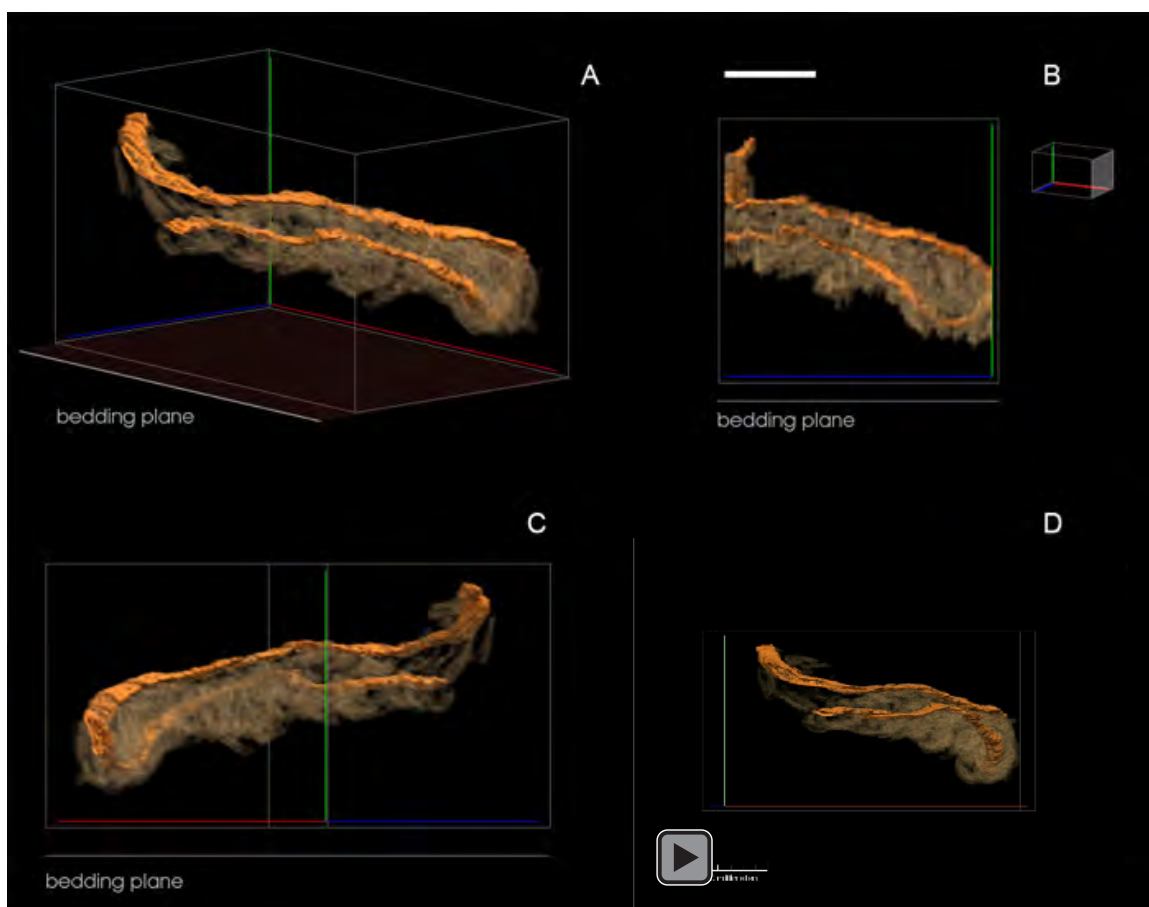


Fig. 3.9. Reconstructed phycosiphoniform burrow with associated halo from Rosario Formation, Baja California, Mexico.

Coarser grained material of the halo propagates downward from the line of each lobe arm (in direction to bedding plane) and fills the space between the lobe arms. **A-C.** Different views of reconstructed burrow with surrounding halo in relation to the bedding plane. **D.** Animation of rendered reconstruction of burrow with the associated halo (embedded in the PDF and in appendix 3.2 B; click to activate the animation) Scale bar = 10 mm.

examined form are not in the same horizontal plane, and the terminal portion of the loop is at a steep angle to the limbs.

3.8.1. Nature of the halo in the Rosario phycosiphoniform burrows

Our 3-D reconstruction of phycosiphoniform burrows from the Rosario Formation, Baja California, Mexico, demonstrates that the reworked silt-rich, clay-poor material that forms the halo around the clay-filled burrow core is dominantly present below the level of the clay-filled burrow (Fig. 3.9). This is also a feature of most natural vertical cross sections studied in the field (Fig. 3.1A). The halo is demonstrably meniscate, as determined from cross sectional views, but especially through three-dimensional reconstruction (Fig. 3.9). It is also noted that the burrow halos of adjacent burrow limbs are closely juxtaposed with little if any undisturbed host sediment between them (Fig. 3.9). The halo around phycosiphoniform burrow cores has been described from other occurrences (Wetzel and Wijayananda 1990; Ekdale and Lewis 1991), but has not previously been reconstructed in three dimensions.

A similar halo associated with a phycosiphoniform burrow (attributed to *Anconichnus*) was interpreted as an early diagenetic oxidation halo (Ekdale and Lewis 1991). This feature was subsequently reinterpreted as being due to bioturbation, specifically the formation of spreiten in accord with newer conceptual models (Wetzel and Bromley 1994; Bromley 1996). Three-dimensional reconstruction of the Rosario Formation phycosiphoniform fossil, with its associated coarser-grained structure, demonstrates that the coarser-grained material is indeed asymmetric and lies below the level of each of the

two lobe arms (Fig. 3.9). This asymmetry is also visible from vertical surfaces prepared in the laboratory and in natural outcrop (Fig. 3.1). The burrow halo is characteristically pyrite rich (Fig. 3.1B). Pyritization is interpreted to have been caused by sulphate-reducing bacteria during early diagenesis. The marked color contrast between the pyritized halo and clay-rich burrow cores relative to the surrounding rock matrix allowed us to distinguish the three components of the fabric for the purpose of image analysis.

The presence of the coarser-grained (silt-sized) material, not only between lobe arms, but also external to the marginal tube (Fig. 3.9) precludes the presence of spreite, and allows rejection of the possibility that the phycosiphoniform trace fossil reconstructed herein is *Phycosiphon*. In the accepted conceptual model of Bromley (1996; Figs 3.3-3.5), spreiten are predicted only between arms of a single lobe and between marginal burrows. The behavioural model proposed for *Phycosiphon* (Bromley 1996) precludes the possibility of formation of the halo/spreiten below the level of a marginal tube that borders the *Phycosiphon* structure. Spreiten are demonstrably not present in our material from Rosario Formation. Instead, the phycosiphoniform cross sections are inferred to have been formed by bulk sediment processing at the anterior of the burrow during continuous burrowing rather than successive probing as is proposed for *Phycosiphon s.s.*

3.9. Conclusion

Mud-rich siltstones from Rosario Formation are characterized by dense monospecific assemblages of phycosiphoniform burrows, and are analogous to many shale-gas reservoir facies. Local concentrations of burrowing may reflect patches of labile organic

matter. The phycosiphoniform burrow-makers are thought to be selective deposit feeders that ingested clay-grade material and left a clean mud-poor feeding halo of processed sediment.

Our image analysis of two dimensional slices allows reconstructing the three-dimensional geometry of the phycosiphoniform trace fossil. The reconstructed burrow is unlike *Phycosiphon* (*sensu lato*), but produces very similar “frogspawn texture” ichnofabrics. The cross-sections of our burrow system are distinguished from those of *Phycosiphon s.l.* in that the halo is generally present only beneath the level of clay-rich burrow cores.

The examined phycosiphoniform burrow geometry presents the following characteristics that allow differentiation from *Phycosiphon incertum*: 1) Arms of the single lobe are parallel in the vertical plane (Fig. 3.8A, B) and the lobe is seen to bend into a half ellipse when viewed in the plane of the lobe (Fig. 3.8C); 2) In side view, the lobe arms extend parallel to bedding and are steeply bent downward at the termination of the loop (Fig. 3.8A); 3) in axial view, the lobe is steeply inclined relative to the bedding plane (Fig. 3.8B); 4) The halo of the burrow is present only below the level of the burrow core and completely fills the space between the lobe arms (Figs 3.1 and 3.9); 5) The halo can be several times thicker than the burrow core (Fig. 3.8D); 6) No spreiten have been observed.

Our palaeobiological model for the formation of the studied phycosiphoniform trace fossil is fundamentally different to that proposed for *Phycosiphon*, but produces remarkably similar vertical cross sections. We consider that identification of *Phycosiphon incertum* in core is not possible without detailed three-dimensional examination of

burrow geometry. We propose the term “phycosiphoniform” to describe this group of ichnofabric-forming trace fossils. We consider that, at present, our material should be left in open nomenclature pending thorough three-dimensional analysis of the type material of other phycosiphoniform burrows including *Anconichus horizontalis*. We note that there are many possible burrow geometries that can produce phycosiphoniform cross sections, but that much work needs to be done before many taxa can be convincingly recognized in vertical cross section.

3.10. Acknowledgements

Preliminary discussion with Andreas Wetzel and Richard Bromley are acknowledged with thanks. Mark Sutton kindly provided initial guidance in the art of serial grinding and tomographic reconstruction. Material from Cajilloa, Baja California was collected with Ben Kneller, whose help and logistical support are much appreciated. Support for this research came from an NSERC grant to DMc, the SLOPES consortium and the award of Canada Research Chair to DMc. We would like to recognize the contribution of Dr. Wetzel and an anonymous reviewer which helped us to clarify our arguments.

3.11. References

- Baker, P. G., 1978, A technique for the accurate reconstruction of internal structures of micromorphic fossils: *Palaeontology*, v. 19, p. 565-584.
- Bockelie, J. F., 1991, Ichnofabric mapping and interpretation of Jurassic reservoir rocks in the Norwegian North Sea: *Palaios*, v. 6, p. 206-215.
- Bromley, R. G., 1996, *Trace fossils: Biology, taphonomy and applications*: London, Chapman and Hall, 361 p.

- Bromley, R. G. and A. A. Ekdale, 1984, *Chondrites*; a trace fossil indicator of anoxia in sediments: *Science*, v. 224, p.872-874.
- Bromley, R. G. and A. A. Ekdale, 1986, Composite ichnofabrics and tiering of burrows: *Geological Magazine*, v. 123, p.59-65.
- Bromley, R. G. and G. K. Pedersen, 2008, *Ophiomorpha irregulaire*, Mesozoic trace fossil that is either well understood but rare in outcrop or poorly understood but common in core: *Palaeogeography, Palaeoclimatology, Palaeoecology*, v. 270, p. 295-298.
- Chamberlain, C. K., 1978, Recognition of trace fossils in cores; trace fossil concepts: *SEPM Short Course*, v. 5, p. 133-183.
- Dafoe, L. T., S. G. Pemberton, and J. MacEachern, 2007, Characterizing Subtle Deltaic Influences in the Shallow Marine (Lower Cretaceous) Viking Formation at Hamilton Lake, Alberta, Canada: 2007 AAPG Annual Convention and Exhibition, Abstracts volume, Abstracts: Annual Meeting - American Association of Petroleum Geologists, 2007.
- Ekdale, A. A., and D. W. Lewis, 1991, Trace fossils and paleoenvironmental control of ichnofacies in a late quaternary gravel and loess fan delta complex, New Zealand: *Palaeogeography, Palaeoclimatology, Palaeoecology*, v. 81, p. 253-279.
- Ekdale, A. A. and T. R. Mason, 1988, Characteristic trace-fossil associations in oxygen-poor sedimentary environments: *Geology*, v. 16, p. 720-723.
- Fischer-Ooster, C., 1858, Die fossilen Fucoiden der Schweizer Alpen, nebst Erörterungen über deren geologisches: Alter. Huber, Bern, 74 p.
- Fu, S., 1991, Funktion, Verhalten und Einteilung fucoider und lophocteniider Lebensspuren: *CFS.Courier Forschungsinstitut Senckenberg*, v. 135, 79 p.
- Gingras, M.K., B., Macmillan, B.J., Balcom, T. Saunders, and S.G. Pemberton, 2002a, Using magnetic resonance imaging and petrographic techniques to understand the textural attributes and porosity distribution in *Macaronichnus*-burrowed sandstone: *Journal of Sedimentary Research*, v. 72, p. 552-558.
- Gingras, M.K., B. Macmillan, B.J. Balcom, 2002b, Visualizing the internal physical characteristics of carbonate sediments with magnetic resonance imaging and petrography: *Bulletin of Canadian Petroleum Geology*, v. 50, p. 363-369.
- Goldring, R., J. E. Pollard, and A. M. Taylor, 1991, *Anconichnus horizontalis*; a pervasive ichnofabric-forming trace fossil in post-paleozoic offshore siliciclastic facies: 13th International Sedimentological Congress, Ichnologic Symposium: *Palaaios*, v. 6, p. 250-263.
- Hammer, Ø. 1990. Computer-aided study of growth patterns in tabulate corals, exemplified by *Catenipora heintzi* from Ringerike, Oslo Region: *Norsk Geologisk Tidsskrift*, v. 79, p. 219-226.

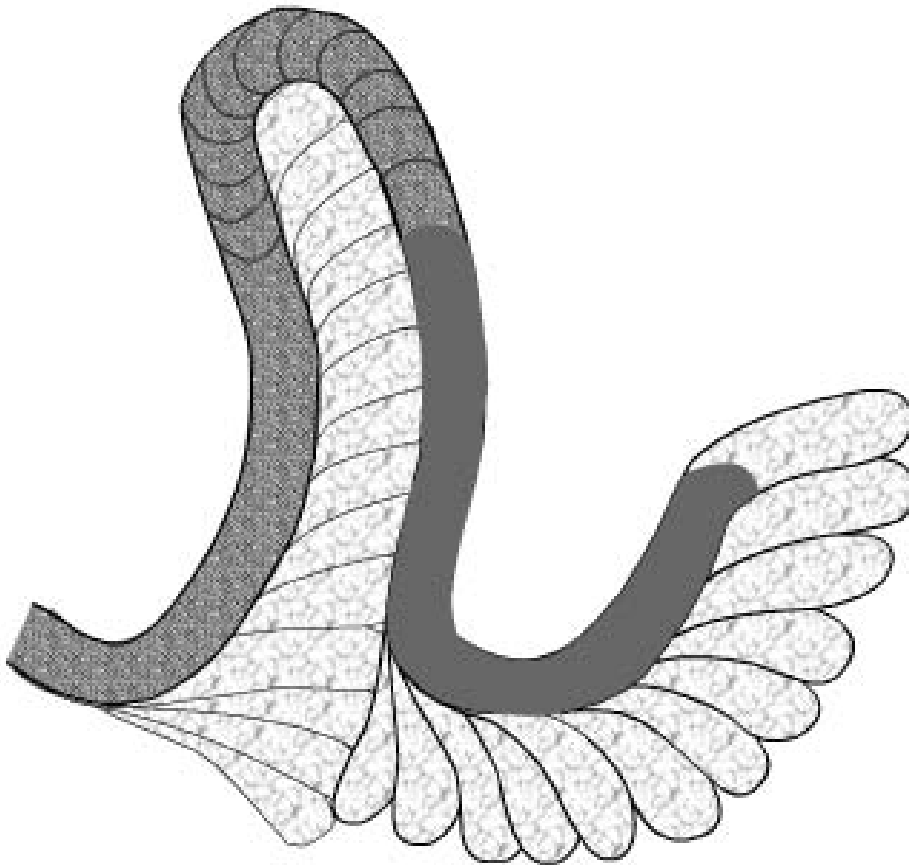
- Kane, I.A., B.C., Kneller, M., Dykstra, A. Kassem, and W.D. McCaffrey, 2007, Anatomy of a submarine channel-levee: An example from Upper Cretaceous slope sediments, Rosario Formation, Baja California, Mexico: *Marine and Petroleum Geology*, v. 24, p. 540-563.
- Kern, J. P., 1978, Paleoenvironment of new trace fossils from the Eocene Mission Valley Formation, California: *Journal of Paleontology*, v. 52, p. 186-194.
- MacEachern, J.A., S.G., Pemberton, M.K. Gingras, and K.L. Bann, 2007a, The ichnofacies paradigm: a fifty-year retrospective, p. 52–77 in Miller, W. (ed.), *Trace Fossils. Concepts, Problems, Prospects*: Elsevier, Amsterdam.
- MacEachern, J.A., S.G., Pemberton, M.K., Gingras, K.L. Bann, and L.T. Dafoe, 2007b, Uses of trace fossils in genetic stratigraphy, p. 110–134 in Miller, W. (ed.), *Trace Fossils. Concepts, Problems, Prospects*: Elsevier, Amsterdam.
- MacEachern, J.A., K.L., Bann, M.K., Gingras, S.G., Pemberton, M.K., Gingras, 2007, The ichnofacies paradigm: high-resolution paleoenvironmental interpretation of the rock record, p. 27–64. In: MacEachern, J.A., Pemberton, S.G., Gingras, M.K., Bann, K.L. (eds.), *Applied Ichnology: SEPM Core Workshop*.
- McIlroy, D., 2004a, Some ichnological concepts, methodologies, applications and frontiers, p 3–27. In: McIlroy, D. (ed.), *The Application of Ichnology to Palaeoenvironmental and Stratigraphic Analysis*: Geological Society, London, Special Publications, 228p.
- McIlroy, D., 2004b, Ichnology and facies model of a tide-dominated delta: Jurassic upper Ror and Ile Formations of Kristin Field, Halten Terrace, Offshore Mid-Norway, p 237–272. In: McIlroy, D. (ed.), *The Application of Ichnology to Palaeoenvironmental and Stratigraphic Analysis*: Geological Society, London, Special Publications, 228p.
- McIlroy, D., 2007, Lateral variability in shallow marine ichnofabrics; implications for the ichnofabric analysis method: *Journal of the Geological Society of London*, v. 164, p. 359-369.
- McIlroy, D., 2008, Ichnological analysis: The common ground between ichnofacies workers and ichnofabric analysts: *Palaeogeography, Palaeoclimatology, Palaeoecology*, v. 270, p. 332-338.
- Naruse, H., and K. Nifuku, 2008, Three-dimensional morphology of the ichnofossil *Phycosiphon incertum* and its implication for paleoslope inclination: *Palaios*, v. 23, p. 270-279.
- Pemberton, S. G., and M. K. Gingras, 2005, Classification and characterizations of biogenically enhanced permeability: *AAPG Bulletin*, v. 89, p. 1493-1517.
- Seilacher, A., 2007, *Trace fossil analysis: Federal Republic of Germany (DEU)*, Springer, Berlin.

- Sutton, M.D., D.E.G. Briggs, David J. Siveter, and Derek J. Siveter, 2001, Methodologies for the Visualization and Reconstruction of Three-dimensional Fossils from the Silurian Herefordshire Lagerstätte: *Palaeontologia Electronica*, v. 4, no.1, http://palaeo-electronica.org/2001_1/s2/issue1_01.htm
- Van Stuivenberg, J., 1979, Geology of the Gurnigel area (Prealps, Switzerland). *Beiträge zur Geologischen Karte der Schweiz*, 151:111, Bern (Schweizerische Geologische Kommission).
- Wetzel, A., 1983, Biogenic sedimentary structures in a modern upwelling area: the NW African continental margin, p.123-44, In: Thiede, J. and Suess, E. (eds.), *Sedimentary Records of Ancient Coastal Upwelling*: Plenum Press, New York.
- Wetzel, A., 2002, Modern *Nereites* in the South China Sea- ecological association with redox conditions in the sediment: *Palaaios*, v. 17, p. 507-515.
- Wetzel, A., 2008, Recent bioturbation in the deep South China Sea: a uniformitarian ichnologic approach: *Palaaios*, v. 23, p. 601-615.
- Wetzel, A., and R. G. Bromley, 1994, *Phycosiphon incertum* revisited: *Anconichnus horizontalis* is junior subjective synonym: *Journal of Paleontology*, v. 68, p. 1396-1402.
- Wetzel, A., and A. Uchman, 1998, Deep-sea benthic food content recorded by ichnofabrics: A conceptual model based on observations from Paleogene flysch, Carpathians, Poland: *Palaaios*, v 13, p. 533–546.
- Wetzel, A., and A. Uchman, 2001, Sequential colonization of muddy turbidites in the Eocene Beloveža Formation, Carpathians, Poland: *Palaeogeography, Palaeoclimatology, Palaeoecology*, v. 168, p.171–186.
- Wetzel, A., and N. P. Wijayananda, 1990, Biogenic sedimentary structures in outer Bengal fan deposits drilled during LEG 116, 15–24. In: Cochran J.R. and Stow D.A.V., (eds.), *Proceedings of the Ocean Drilling Program, Scientific Results 116*.

Appendix 3.1.

Animation showing how multiple phases of foraging by an unknown vermiform organism create phycosiphoniform looped burrows composed of marginal tube and spreiten (based upon Wetzel and Bromley 1994; Bromley 1996; Seilacher 2007). Different shades of grey represent distribution of silt-sized (light grey) and clay-sized (dark grey) material.

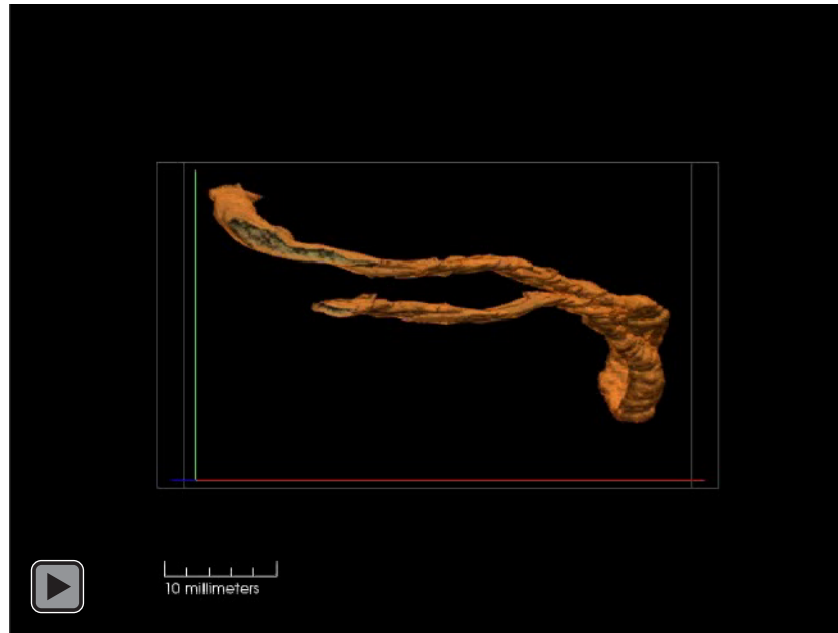
Click to activate the animation.



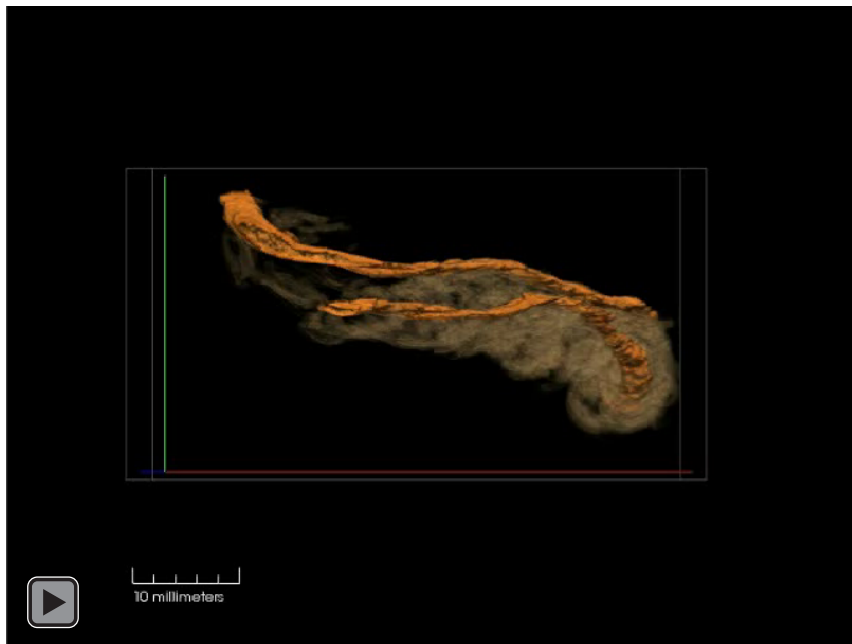
Appendix 3.2.

Three-dimensional reconstruction of phycosiphoniform burrow from Rosario Formation, Mexico.
Scale bars = 10 mm.

A. Animation of rendered reconstruction of the phycosiphoniform burrow core. Click to activate the animation.



B. Animation of rendered reconstruction of the burrow core with the associated halo. Click to activate the animation.



CHAPTER 4

Effect of phycosiphoniform burrows on shale hydrocarbon reservoir quality

Małgorzata Bednarz and Duncan McIlroy

Published in *AAPG Bulletin* (2012) Volume 96 (10)

4.1. Abstract

Unconventional gas (tight-gas, coal-bed methane and shale-gas) has become an increasingly significant source of energy. Economic production from such low permeability reservoirs relies upon identifying regions of the reservoir that will yield the highest gas production rates. Currently available gas recovery technologies are highly dependent on the fracturability of the reservoir. Zones of enhanced brittleness and permeability within shale-gas reservoir horizons are a pre-requisite for successful shale-gas recovery. Such brittle zones are directly linked with increased quartz and/or carbonate content within the mudstone. In mudstones with high clay mineral content, quartz may be concentrated and redistributed as a result of burrowing activities of infaunal organisms. High quality porosity and permeability zones in shale-petroleum

reservoirs may be present in the form of silty and sandy tortuous strips of selectively concentrated grains of quartz that constitute burrow halos. Grain-selective burrows therefore can improve reservoir capacity, permeability and fracturability and thus control the storativity of the shale-petroleum reservoir. This study presents three-dimensional reconstructions of three different types of *Phycosiphon*-like burrows and investigates the possible fluid flow paths caused by the ichnofabric. The volumetric approach to the bioturbation generated by phycosiphoniform burrows makers used herein shows that the volume of sediment that becomes more porous and more permeable media within such bioturbated interval can range from 13-26% of the total volume. The quartzose strips of sediment caused by bioturbation are highly tortuous and interconnected vertically and horizontally, thereby increasing both horizontal and vertical permeability. Additionally, the quartz-frameworks created by the burrows may locally increase fracturability within otherwise non-brittle mudstones.

4.2. Introduction

Shale-gas and other shale-hosted hydrocarbon -reservoirs are unconventional hydrocarbon resources that rely upon the connectivity of porosity and fractures—both natural and induced—in organic-rich mudstones and very fine-grained strata over very large geographic areas. The host sediment is typically an ultra-low permeability organic-rich mudstone and/or siltstone with poor vertical permeability, and rich in biogenic and/or thermogenic gas that is tightly bound within the host sediment (Curtis 2002). Shale gas and other shale petroleum facies are commonly composed of inter-bedded

successions of dominantly fine-grained rocks (siltstones and mudstones) of variable but generally low permeability (e.g. Lemiski et al. 2011). Economic production from such heterogeneous, low-permeability but volumetrically large reservoirs relies not only upon locating the organic-rich mudstone, but also upon identification of stratigraphic intervals within the reservoir that are sufficiently fracturable and permeable to allow exploitation (Jenkins and Boyer 2008). The highest rate of gas or liquid petroleum production is required to create maximally effective fields. Currently available shale gas and oil-shale recovery technologies are largely dependent on the fracturability of the reservoir to connect zones with the potential to have a high gas yield. Such high-yield zones include permeable siltstone laminae and beds that allow production of fluids from the otherwise largely impermeable mudstone (Jenkins and Boyer 2008). Zones of enhanced brittleness and permeability within shale petroleum reservoir horizons are a prerequisite for effective development of shale-gas reservoirs, and are directly linked to the quartz content of the mudstone (Narr and Currie 1982). In mudstones and siltstones with high clay mineral content, silt-grade quartz grains may be preferentially sorted from the clay-rich host sediment and concentrated in burrow fills and burrow linings during the grain-selective deposit feeding activities of infaunal organisms (Bednarz and McIlroy 2009). We therefore predict that zones of intense bioturbation in shale-gas reservoir facies have the potential to significantly influence the rheological and petrophysical properties of the reservoir, by enhancing fracturability and primary porosity. Burrow-related zones of enhanced porosity and permeability in shale-gas reservoirs are typically in the form of

tortuous burrows that have hitherto received little attention in terms of their three-dimensional geometries (Bednarz and McIlroy 2009).

A number of recent studies have considered the influence that burrows have on the reservoir properties of the host sediment in carbonate facies (e.g., Gingras et al. 1999, 2004; Keswani and Pemberton 2007) and in sandstones (e.g., Pemberton and Gingras 2005; Gordon et al. 2010, Tonkin et al. 2010). In carbonate facies, burrows can remain completely open during burial and diagenesis, forming entirely open pipeworks. Similar large burrows in sandstones filled with coarse grained poorly sorted sandstone have also been considered to be reservoir enhancing (Pemberton 1992; Gingras et al. 1999, 2004, 2007; Pemberton and Gingras 2005; Tonkin et al. 2010). Not all burrows are reservoir enhancing, and many types of trace fossils are expected to reduce the connectivity of primary sedimentological porosity (e.g., Pemberton and Gingras 2005; Tonkin et al. 2010). There has been little consideration of how burrows orientated oblique-to-bedding in shale petroleum reservoirs might influence the efficiency of gas or liquid recovery.

There are few focused studies of the ichnology of shale-gas reservoirs (Pemberton and Gingras 2005; Hovikoski et al. 2008; Lemiski et al. 2011). Within some mudstones, siltstones and sandstones with low net-permeability, fluid flow is considered to be possible through conduits, formed by induced fracturing, that connect isolated high porosity trace fossils such as *Phycosiphon*, *Zoophycos* and *Chondrites* (Pemberton and Gingras 2005, Spila et al. 2007; Lemiski et al. 2011). Such burrows, when present in shale-gas reservoirs, can constitute a significant volume of the reservoir, enough to sustain an economically significant flow (Pemberton and Gingras 2005). *Zoophycos*,

Chondrites and *Phycosiphon* are extremely efficient sediment processors. Large *Zoophycos* can reach length of 1 m in vertical extension and maximal horizontal extent being 1m² (Wetzel and Werner 1980). The sediment-processing capacity of *Phycosiphon*-like burrows is assessed herein for the first time.

In this paper we present results from the volumetric consideration of three *Phycosiphon*-like burrows (termed phycosiphoniform because of unresolved taxonomic issues; see Bednarz and McIlroy 2009). Several phycosiphoniform burrows were collected to encapsulate the same sort of deposit feeding/sediment cleaning behavior in rocks of different ages, but from facies similar to shale-gas reservoir facies. Our study is built around deterministic, three-dimensional, volumetric reconstructions of the investigated phycosiphoniform burrows. The three-dimensional volume rendered computer models, when linked to a petrological and petrophysical understanding of burrow geometry, is the only realistic basis for consideration of probable fluid flow paths within very fine-grained siliciclastic facies. For this reason understanding of the structure and distribution of phycosiphoniform burrows is essential for estimations of primary porosity in bioturbated shale-petroleum reservoirs.

Earlier two dimensional models of petroleum flow through the sand-rich burrow haloes of *Phycosiphon incertum* illustrate the possible pathways of fluid flow through bioturbated low matrix permeability facies (Spila et. al. 2007). The two dimensional representation of hydrocarbon migration was based on capillary threshold pressure assessed by a computer program on a base of Invasion Percolation Techniques (Carruthers 2003, MPath software). This method is based on the assignment of capillary

threshold pressure values to the pixels visible on an examined image dependently on their color intensity. It is considered that such two-dimensional model of migration trajectories creates an erroneous impression of the flow paths and their connectivity and gives flawed reservoir characterization. This is due to the limitation of the non-volumetric nature of the flow paths illustrated on planar surfaces. In three dimensions most phycosiphoniform burrows are highly interconnected with very few if any blind-ends. This work reconstructs in three dimensions three phycosiphoniform burrows to enable realistic consideration of gas and liquid migration within shale-petroleum reservoir.

The three-dimensional reconstructions generated using volumetric computational tools, along with an interactive three-dimensional viewer, allow critical reappraisal of the pre-existing understanding of the important trace fossils in gas shale-petroleum facies. Once produced, the deterministic three-dimensional models can be artificially sliced to provide a range of templates for identification of all possible cross sections of the burrow. Our novel approach to three-dimensional ichnology and ichnofabric analysis has created the possibility to undertake precise realistic three-dimensional ichnology, and apply it to the recognition of trace fossils in a core or outcrop.

4.3. Phycosiphoniform trace fossils in shale-gas reservoir facies

4.3.1. Typical settings of *Phycosiphon*-like trace fossils occurrence

Phycosiphoniform trace fossils are found in many marine mudstones, siltstones and very fine sandstones (Ekdale and Lewis 1991; Bednarz and McIlroy 2009).

Phycosiphoniform-bearing fine-grained rocks (especially from distal turbiditic and pelagic settings) are usually considered from the greenish grey color, and total organic carbon (TOC) content, to have been oxygenated during, and shortly after their deposition (e.g. Wetzel and Uchman 2001; Taylor et al. 2003). We note however that the dark color of a mudstone does not necessarily reflect the degree of pore water anoxia. Elevated rates of deposition can cause dilution of organic matter preventing its burn-down and simultaneous preservation of oxygenated interstitial pore waters (Wetzel and Uchman 2001; Bohacs et al. 2005). Availability of oxygen at least at the water-sediment interface or in pore waters of organic matter-rich deposits provides incentives for colonization of the sediment by small burrowing organisms such as the phycosiphoniform trace makers. The makers of phycosiphoniform burrows are generally considered to be opportunistic, grain-selective deposit-feeders that rapidly process sediment, both as early colonizers, but especially as late-stage mid-tier deposit feeders that rework previously created burrow fills (e.g. Goldring et al. 1991; Wetzel and Bromley 1994; Bromley 1996; Savrda et al. 2001; Wetzel and Uchman 2001; Taylor et al. 2003; McIlroy 2004; Bednarz and McIlroy 2009).

The small size of the trace fossils that commonly typify mudstones makes detailed morphological study difficult, and is probably the reason that such subtle bioturbation is not usually considered in detail during evaluation of shale-gas reservoir quality. Trace fossils in mudstones are only easily studied on cut and polished surfaces that may not be available in conventional preparation of cores from shale gas reservoirs. The impact of bioturbation on reservoir facies is especially important in shale-gas reservoir evaluation,

as increased heterogeneity can have significant influence on gas flow, deliverability and reservoir capacity (Lemiski et al. 2011).

4.3.2. Gas shale facies with recognized occurrence of *Phycosiphon*-like trace fossils

Phycosiphon-like trace fossils are probably the most frequent ichnofabric-forming trace fossils in clay-rich sedimentary rocks including shale-gas reservoirs (e.g., Bockelie 1991; Caplan and Bustin 2001; Goldring et al., 1991; Wetzel and Bromley 1994; Bromley 1996; Pemberton and Gingras 2005). The characteristic two-dimensional (2D) geometry of phycosiphoniform burrows in vertical cross section (a central, clay-grade core surrounded by clean quartzose halo of silt to very fine sand) has typically, perhaps uncritically, been identified as *Phycosiphon* isp. in several shale-gas and oil-shale reservoir intervals including the Alderston member of the Lea Park Formation (Western Canada Sedimentary Basin, SK, Canada), the Bakken Formation (Williston Basin, SK, Canada, MT, ND, USA), Barnett Shale (Fort Worth Basin, TX, USA), Mancos Shale (Unita Basin, UT, USA) and others (e.g. Hovikoski et al. 2008; Kohlruss and Nickel 2009; Lemiski et al. 2011; Macquaker et al. 2007; Sonnenberg and Pramudito 2009; Ottmann and Bohacs 2010).

4.3.3. Effects of phycosiphoniform burrows on permeability and fracturability

Phycosiphoniform trace fossils are unified by their small size, usually less than 5mm in diameter, with a quartzose halo of silt-grade material around a clay-rich core (Bednarz

and McIlroy 2009). Three-dimensional reconstruction of field samples of such burrows has revealed that there is considerable variability within this group of trace fossils. Recent work has shown that the distinctive “frogspawn ichnofabric” usually attributed to *Phycosiphon* (*sensu stricto*) can be produced by other similar taxa (Bednarz and McIlroy 2009). Changes in rheology and petrophysical properties associated with these burrows are of fundamental importance to shale-gas reservoirs. The impact of the burrows on reservoir quality can only be meaningfully assessed in the light of three-dimensional morphological understanding. We consider that all phycosiphoniform burrows are likely to significantly increase the heterogeneity of otherwise ultra-low permeability mudstones, increasing fracturability (by creating quartz frameworks) and porosity (where there is no quartz cementation during diagenesis). In sandstones the same trace fossils have been found to reduce porosity and permeability by about 33% (Tonkin et al. 2010).

Shale petroleum facies are typically subject to compaction, which is variable in intensity depending on the burial history. Compaction affects the geometric relationships within ichnofabrics of shale gas facies, with the smallest compaction being observed in reservoirs that produce biogenic gas. In this study we do not analyze the degree of the compaction of the bioturbation and its impact on the burrows’ geometry. The influence of compaction and thus progressive change in burrow morphology was not considered herein. If our data on volumetric relationships were to be applied to reservoir units, the calculated percentage relationships of volumes would have to account for compaction. The degree of compaction could perhaps be estimated from the aspect ratio of the burrow core, which is typically found to be circular in cross section. The quartzose portions of

phycosiphoniform burrows (the halos) are likely to have less potential for burial compaction than the clay-rich matrix. Experimentation on differential compaction of this nature has not yet been applied to trace fossil studies.

4.4. Methods

4.4.1. Three-dimensional methods in ichnology

Three-dimensional visualization of trace fossils has formerly been a challenge to ichnologists owing to the lack of the availability of computational tools required for compilation of a series of two dimensional cross sections of burrows into a three-dimensional volumetric environment. Previously published 3D reconstructions, in the form of sketches, have typically been a reflection of the author's extrapolation from common 2D burrow cross sections (commonly with a fair degree of skill; e.g. Wetzel and Bromley 1994; Bromley 1996). With computerization, and the availability of tools primarily used in medical science, new technologies for reliable three-dimensional visualizations have become available. Three-dimensional, volumetric reconstruction of trace fossils is new and has not yet been widely used. Non destructive techniques used include Magnetic Resonance Imaging of *Macaronichnus* (Gingras et al. 2002); X-Ray analysis of *Zoophycos* (Wetzel and Werner 1980; Löwemark and Schäfer 2003) and *Monesichnus* (Genise and Laza 1998); vertebrate trackways, footprints and terrestrial trace fossils have also been studied using Multi-stripe Laser Triangulation Scanning (MLT) (Platt et al. 2010). At present, all available non-destructive techniques used to

acquire three-dimensional representation of the fossils based on variations in density that characterize the scanned medium (X-Ray CT scanning) or require full exposure of the examined surface of the fossil and do not provide data on the burrow fill (Multistripe Laser Triangulation Scanning, Platt et al. 2010). The effectiveness of CT scanning for imaging trace fossil fabrics in mudstones is limited by the minimal density contrast between the burrow fill and the rock matrix (cf. Gingras et al. 2002; Naruse and Nifuku 2008). Because of our focus on linking detailed geometries to lithology, the examined phycosiphoniform burrows were serially ground and then photographed at closely-spaced intervals and the resultant data were incorporated into the 3D models presented below. Our ongoing work will extend this approach to other common trace fossils from the same fine-grained unconventional reservoir facies.

4.4.2. Serial grinding

Systematic serial grinding has been effectively used in past to obtain three-dimensional models of body fossils (e.g., Baker 1978; Hammer 1999; Sutton et al. 2001, Watter and Grotzinger 2001, Maloof et al. 2010, Schmidting and Marshall 2010) as well as endogenic trace fossils (e.g., Genise and Laza 1998; Wetzel and Uchman 1998, 2001; Naruse and Nifuku 2008; Bednarz and McIlroy 2009). The technique of serial grinding involves sequential abrasive removal of a thin layer of a material from a planar surface of the rock with maintaining constant displacement (Sutton et al. 2001). It results in exposure of parallel regularly spaced surfaces in order to obtain a sequence of photographs of the resultant vertical cross sections of examined objects. The set of

consecutive digital images thus created is the basis for the computer-based 3D reconstructions (Sutton et al. 2001; Naruse and Nifuku 2008; Bednarz and McIlroy 2009).

Serial grinding was conducted manually (Ph1 sample) and with the usage of HAAS VF-3 CNC Vertical Machining Center (samples: Ph3, Ph7). The machine provides precision computer-controlled surface grinding through use of diamond tip. The serial grinding increment was set to 0.2 mm for samples Ph3 and Ph7. Sample Ph1 was ground manually with the increment of 0.5 mm.

4.4.3. Image processing

Each set of digital images that represents the ground sample was processed in the 2D image processing software Adobe Photoshop (cf. Sutton et al. 2001; Naruse and Nifuku 2008; Bednarz and McIlroy 2009).

Phycosiphoniform burrows are typically composed of dark grey mud cores surrounded by halos of lighter and coarser-grained sediment. Both of these burrow components have color contrast relative to the host sediment and are clearly visible in the photographic datasets collected. The burrow cores and the halos were tracked separately through each consecutive image and manually selected with tablet pen. The stacks of images with thus created shapes of either cores or halos were saved in gray scale that is the most suitable color scheme for their interpretation in contemporary 3D volumetric software such as VGStudio Max or VolView.

4.4.4. Three-dimensional modeling and volume measurements

The processed two dimensional photographic images were the basis for three-dimensional modeling. After providing information about spatial slices' displacement and units of measurement, the image stack was imported into volume-visualizing software VolView 2.0 and/or VGStudio MAX 1.2.1. The gray scaled representations of burrow cross sections were converted by the software to a volume that reflects the real size and proportions of the examined volume of the rock. For the purpose of volume measurements, both burrow cores and burrow halos of phycosiphoniform ichnofabric were reconstructed separately (e.g. cores were reconstructed based on the set of images of manually selected cores with halos deliberately omitted). This approach allowed for detailed 3D reconstruction of the volume and geometry of each of the two main parts of phycosiphoniform burrows (core and halo).

The three-dimensional volumes of core and burrow halo were measured in mm³ using VolView 2.0 and/or Autodesk 3ds MAX 2009. This study presents deterministic three-dimensional reconstruction not only of the clay-rich burrow core (cf. Naruse and Nifuku 2008) but in addition also reconstructs the burrow halo composed of the coarser-grained material. It is the burrow halo that provides potential fluid flow paths within the bioturbated mudstones, enhancing the sediment's potential as a shale gas reservoir.

4.4.5. Quantitative ichnological methods

Quantitative methods in ichnology and their application in regards to the newly explored 3D reconstructions of trace fossils have been recently reviewed (Platt et al. 2010).

Quantitative ichnology has previously been limited to two dimensions due to the lack 3D reconstructions (cf. Taylor and Goldring 1993; Droser and Bottjer 1986). Three-dimensional reconstructions such as presented herein allow deterministic measurement of several parameters of trace fossils and ichnofabrics, including burrow size and geometry and the volumes of various components of ichnofabrics (Appx 4.1). Application of 3D volumetric methods for any trace fossil investigation brings new insight into the ichnological interpretation and understanding of the examined sedimentary fabric.

4.4.5.1. Burrow lengths and orientations

Maximum burrow depth (D_{max}) is the vertical distance from the burrow opening to the bottommost termination of the burrow measured perpendicular to the original bedding plane (Hembree and Hasiotis 2006; Platt et al. 2010).

Tortuosity index (T) is an important variable allowing for estimation of a degree of curvature of a burrow. It may be measured as the ratio of the length of the space diagonal (d) of a box bounding the spatial line representing the burrow core in 3D and the total length of the burrow core (L_C ; Equation 1, Fig 4.1B, C). From this data length of the burrow core segments is considered in relation to the volume of the sediment that the core is enclosed within (i.e. the volume of the box is represented by its space diagonal).

(1) Tortuosity index:
$$T = d/L_C$$

(2) Space diagonal:
$$d = \sqrt{a^2 + b^2 + c^2}$$

(3) Burrow core length
$$L_C = \sum_{i=0}^n s_i = s_1 + s_2 + s_3 + \dots + s_n$$

The length of the burrow core (L_C) represents the actual burrow length and it is a sum of all segments consisting central line of the burrow core (Equation 3, Fig. 4.1C, after Platt et al. 2010). The equation 1 shows that the burrow is straight when its tortuosity index is equal 1 (the length of the burrow core and the space diagonal are equal), and (highly) tortuous when the tortuosity index approaches 0 (burrow core is more than two times longer than the space diagonal). Tortuosity of the burrow, along with the tortuosity index, can also be illustrated by the burrow length index (L_i , Equation 4), which is the ratio between the burrow marginal length (L_M) and the total burrow length (L_C).

(4) Burrow length index:
$$L_i = L_M / L_C$$

Burrow marginal length (L_M , Fig. 1 B) is the shortest distance from the center of the opening ellipse (cross section representing the beginning of the burrow core in the rock) to the center of the closing ellipse of the burrow. Similarly to the tortuosity index, the burrow length index indicates the straight burrow when the burrow length index (L_i) is approaching 1, and the most tortuous (or looped) when approaching 0 (however this cannot be assumed without considering the tortuosity index simultaneously because the burrow length index (L_i) is independent of the position of the burrow within the bounding box).

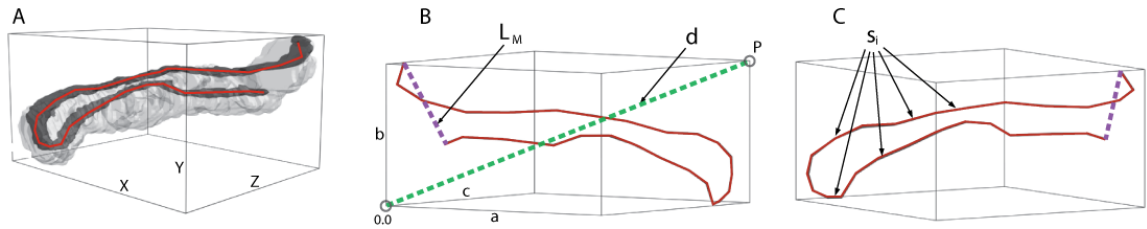


Fig. 4.1. Three-dimensional reconstruction of a phycosiphoniform burrow from Mexico (Ph1 b01) as an example showing the approach used to measure the dimensions of the trace fossils and/or ichnofabrics in three dimensions.

A. Entire reconstructed burrow (core with halo) enclosed in a box (a smallest rectangular cuboid bounding the entire examined burrow) inscribed in the x , y , and z Cartesian coordinate system.

B, C. Visualization showing the central axis of the fecal core of a phycosiphoniform burrow within a box of the dimensions: length (a), height (b), and depth (c) that are parallel with the X , Y , and Z axes. The a , b , and c lines start from the origin of the Cartesian coordinate system (0.0) and their lengths determine the position of point P (a , b , c). The shortest distance from the origin of the coordinate system (0.0) to point P is equal to the space diagonal length of the box (d). The horizontal plane x , z is parallel with bedding; s_i = segments (straight lines) of the central line of the burrow core that are used to approximate the actual burrow length; L_M = marginal length, which is the distance between the burrow opening and burrow closing.

4.4.5.2. Volumetric considerations

Volumetric assessment of the bioturbation within a rock is probably the most significant factor with respect to reservoir quality evaluation and further production from the reservoir. The ability to give reliable 3D volume estimations creates both a new tool for the realistic calculation of likely reservoir volumes, and also the basis for determination of the most permeable and/or fracturable volumes within a reservoir zone.

Volume Available (VA , after Platt et al. 2010) is the volume of the smallest box enclosing the burrow or burrows association (the box in Fig. 4.1A). In reservoir studies the volume available could be simply determined by multiplying the bioturbated core interval's height, width and depth.

Volume Utilized (VU , after Platt et al. 2010) is the volume of the entire examined burrow or burrows association. In other words it is the volume of the sediment reworked by the trace maker. In case of phycosiphoniform trace makers VU is the volume of summarized volumes of the core (Vc) and the halo (Vh).

Volume Exploited (VE) describes efficiency of space usage by the trace maker(s) and also burrow(s) density according to the equation 5 (after Platt et al. 2010; Equation 5). It reflects the percentage of the sediment that was reworked by the trace maker in relation to the volume available:

(5) Volume exploited:
$$VE = \frac{VU \cdot 100}{VA}$$

In shale gas reservoir studies the most important volume within bioturbated intervals is volume of the halo (Vh) produced by the *Phycosiphon*-like burrow makers. It can be

presented as percentage of halo contribution ($\%Vh$) within the volume available (Equation 6):

(6) Volume halo percentage $\%Vh = Vh \cdot 100 / V_A$

The $\%Vh$ corresponds with the variable of *Core Multiplicand* for halo estimation (CM) described as (Equation 7):

(7) Core multiplicand $CM = Vh / Vc$

Core multiplicand illustrates how many times the volume of fracture-able and permeable halo material is larger than the volume of impermeable core. CM variable is found to be independent from tortuosity and volume available and is more or less constant for each type of phycosiphoniform burrow examined in this study. Thus, if the type of *Phycosiphon*-like burrows is correctly identified in the core, the CM variable will allow for estimation of what percent of permeable and brittle material is present within the sample even during a naked eye observation when bioturbation index is simultaneously assessed.

4.5. Examined phycosiphoniform burrow types

Three examples of *Phycosiphon*-like trace fossils were subjected to three-dimensional examination (Fig. 4.2, Appx 4.2). The rock samples containing trace fossils in question were collected from the following localities:

- 1) The Upper Cretaceous Rosario Formation, Baja California, Mexico
(sample Ph1);
- 2) The Lower Jurassic Staithes Sandstone Formation, the Yorkshire coast, UK
(sample Ph3);
- 3) The Mississippian Yoredale Sandstone Formation, Craster, Northumberland UK
(sample Ph7).

Each of the studied rock samples was subject to serial grinding and 3D reconstruction of the ichnofabric they contained. The 3D reconstructions presented in this paper include:

- 1) reconstruction of bioturbated box enclosing all burrows present in selected volume;
- 2) several individual burrows reconstructed separately (Appx 4.3). Reconstructed 3D ichnofabrics and burrows were subjected to quantitative analysis (Tab. 4.1). The examined samples were collected from deep marine sedimentary facies that are comparable in grainsize to many shale hydrocarbon reservoirs (e.g. Hovikoski et al. 2008; Kohlruss and Nickel 2009; Lemiski et al. 2011; Macquaker et al. 2007; Sonnenberg and Pramudito 2009; Ottmann and Bohacs 2010).

4.5.1. Phycosiphoniform burrows from the Upper Cretaceous Rosario Formation, Baja California, Mexico (Ph1)

A sample containing many phycosiphoniform burrows (Ph1) was collected from coastal exposures of the Upper Cretaceous Rosario Formation. The *Phycosiphon*-like burrows from the Rosario Formation are hosted in laminated turbidite siltstone (see Bednarz and

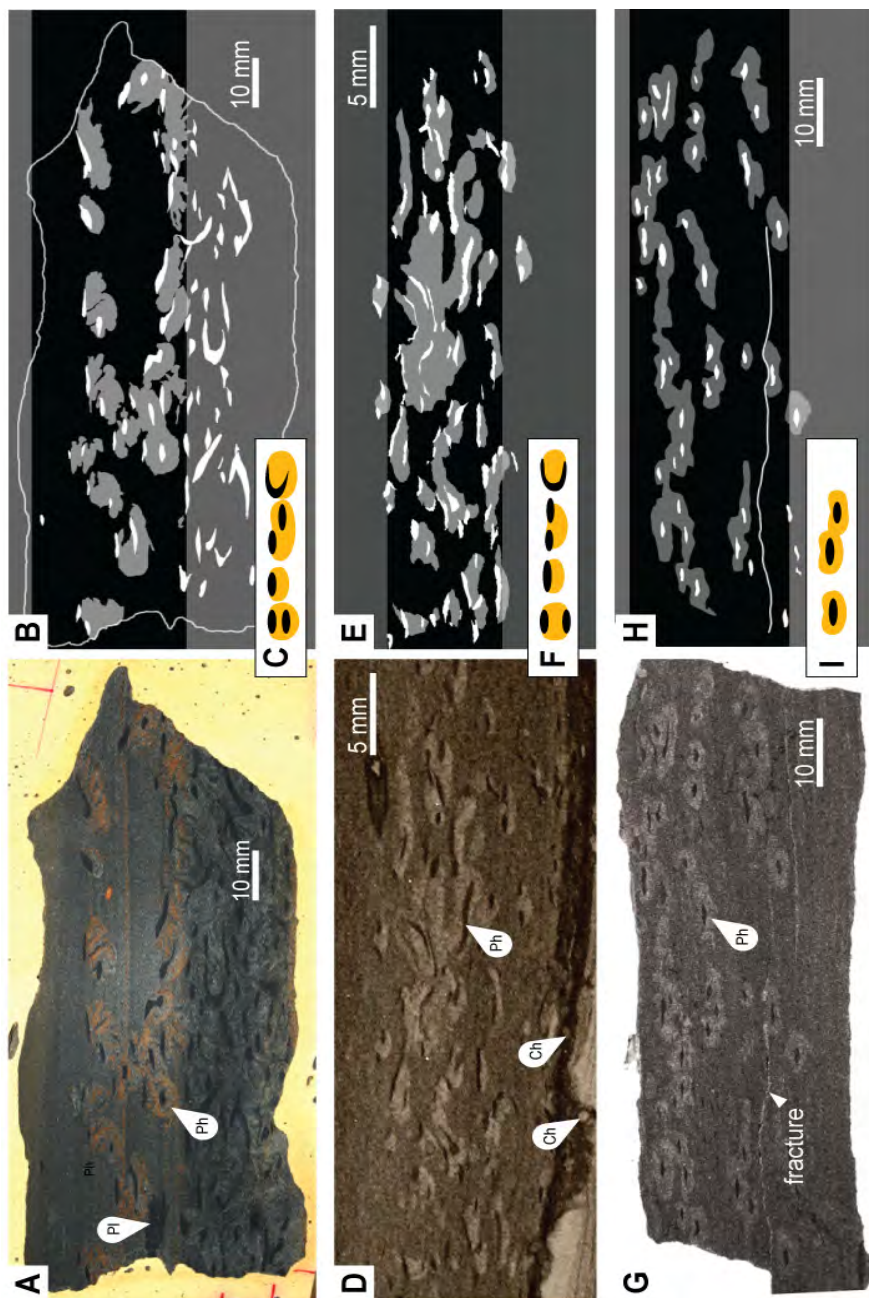


Fig. 4.2. A, D, and G. Photographs of example slices of examined samples with *Phycosiphon*-like burrows and images of sample cross section (B, E, H) with manually drawn burrow cores (white shapes) and burrow halos (gray shapes). Shaded top and bottom stripes border boxes with reconstructed bioturbation. White boxes (C, F, I) present idealized cross sections of the referring phycosiphoniform burrows; black spots represent burrow cores. Phycosiphoniform burrows from: A, B, C: Rosario Formation, Mexico (Ph1); D, E, F: Staithes, United Kingdom (Ph3); G, H, I: Craster, United Kingdom (Ph7). Ph = phycosiphoniform burrow; Pl = *Planolites*; Ch = *Chondrites*.

McIlroy 2009). Bioturbation is intense at the bottom of the sample (BI6 or 95%) and in the upper part it shows well preserved burrows of lower burrow density (BI3 or 35%). A single burrow of *Planolites* was found in the sample (Fig. 4.2A). In vertical cross section the ichnofabric presents the characteristic “frogspawn texture” of phycosiphoniform burrows, that is composed here of anomalously large trace fossils. The average major axis of the burrow cores is 5.3 mm, with the longest exceeding 1 cm (>0.4 in.).

The burrow halo is principally located below each black muddy core and also entirely fills the area between the lobe arms (see also Bednarz and McIlroy 2009). All burrow lobes are essentially perpendicular to the paleo-horizontal (vertical loops), usually around 2 cm (~0.8 in.) in vertical extent (burrow depth) and bent in horizontal plane. Five separate burrows were examined separately, all except one (Ph1 b04) form vertical loops (Fig. 4.3). No dominantly horizontal loops were observed in the examined sample volume.

Volumetric assessment of bioturbation in a selected part of the rock sample (with BI3 or 35%) indicates, that the proportion of halo and core volumes in the sample stays around the same value as for a single burrow: core multiplicand equals 6.5, but the percent of the volume of the halo material in relation to the matrix material is considerably larger (Tab. 4.1). The measurements show that the volume of the reworked material (V_U) ranges around 20% on average and the volume of the halo ($\%V_h$) around 17% on average (Tab. 4.1). The percent contribution of halo volume of a single burrow of this type of phycosiphoniform depends on the burrow tortuosity. Percent contribution of halo volume ($\%V_h$) of a looped burrow with $T \sim 0.5$ (e.g., burrows: Ph1 b03 and Ph1 b05, Tab. 4.1) is

Table 4.1. Measurements of examined three-dimensional reconstructions of studied phycosiphoniform burrows.

V_c = volume of the burrow core(s); V_h = volume of the burrow halo(s); VU = volume utilized (equivalent of merged V_h and V_c); VA = volume available; VE = volume exploited; Bioturbation index; T = tortuosity index; L_i = burrow length index; L_c = core length; L_M = marginal length; CM = core multiplicand; d = space diagonal; N/A = not applicable.

Phycosiphoniforms		Vc			Vh			VU		VA	Prism dimensions (VA)			BI	T	Li	Lc	d of prism Lc	Lm	Average major axis of cross section ellipse of the burrow core	Vertical halo connectivity (height, y)
		mm ³	%Vc (% of VA)	CM	mm ³	%Vh (% of VA)	% of VU	mm ³	VE (% of VA)	mm ³	x	y	z			mm	mm		mm	mm	mm
	Burrow	mm ³	%Vc (% of VA)	CM	mm ³	%Vh (% of VA)	% of VU	mm ³	VE (% of VA)	mm ³	mm					mm	mm		mm	mm	mm
Ph1 Mexico	Ph1 b01	288.1	1.3	6.2	1785.2	8.4	86.1	2073.3	9.7	21343.7	36.6	19.8	29.5	n/a	0.46	0.13	97.7	44.9	12.3		
	Ph1 b02	153.9	5.4	5.0	773.8	26.9	83.4	927.8	32.3	2873.5	25.3	13.3	8.6	n/a	0.49	0.12	43.1	21.3	5.2		
	Ph1 b03	183.1	1.9	8.0	1463.4	14.9	88.9	1646.4	16.8	9807.6	31.8	11.7	26.3	n/a	0.53	0.31	60.5	32.0	19.0		
	Ph1 b04	184.4	0.9	9.3	1709.3	8.0	90.3	1893.7	8.8	21450.7	44.1	17.8	27.4	n/a	0.90	0.88	50.8	45.7	44.7		
	Ph1 b05	225.0	3.6	5.0	1127.1	18.3	83.4	1352.1	21.9	6164.7	34.3	10.1	17.8	n/a	0.52	0.11	60.0	31.1	6.7		
	Average		2.6	6.7		15.3	86.4		17.9												
	Ph1 Bioturbated prism	3910.1	2.6	6.5	25257.7	16.7	86.6	29167.8	19.3	151078.8	152.0	33.7	29.5	III	n/a		n/a	n/a	n/a	5.3	33.7
Ph3 Staithes	Ph3 b01	3.9	1.7	5.4	20.7	8.9	84.3	24.6	10.6	231.7	11.8	3.4	5.8	n/a	0.33	0.26	35.6	11.9	9.2		
	Ph3 b02	1.9	4.2	3.8	8.3	15.6	81.0	10.2	22.2	46.0	10.7	2.2	1.9	n/a	0.56	0.24	16.8	9.4	4.1		
	Ph3 b03	5.8	1.5	4.4	25.2	6.7	81.4	31.0	8.3	374.7	17.7	2.9	7.3	n/a	0.50	n/a	35.3	17.6	n/a		
	Ph3 b04	5.5	1.3	5.8	32.0	7.8	85.3	37.5	9.2	408.2	15.8	4.4	5.9	n/a	0.31	n/a	46.4	14.3	9.7		
	Ph3 b05	1.6	9.2	2.7	4.5	25.1	73.1	6.1	34.4	17.8	3.7	4.3	1.1	n/a	0.51	0.19	9.1	4.6	1.7		
	Ph3 b06	1.7	3.6	3.4	6.0	12.6	77.5	7.8	16.2	47.9	5.5	5.9	1.5	n/a	0.48	n/a	14.8	7.1	n/a		
	Ph3 b07	2.2	2.4	6.1	13.6	14.5	85.9	15.8	16.9	93.8	6.8	7.0	2.0	n/a	0.56	0.32	13.8	7.8	4.5		
	Average		3.4	4.5		13.0	81.2		16.8												
	Ph3 Bioturbated prism	151.2	5.4	4.8	720.3	25.9	82.7	871.5	31.3	2785.9	39.5	6.0	11.8	IV	n/a		n/a	n/a	n/a	1.38	6.0
Ph7 Craster	Ph7 b01	45.7	2.6	5.5	253.1	14.4	84.7	298.7	17.0	1759.7	26.1	5.7	11.9	n/a	0.64	0.43	32.4	20.9	14.0		
	Ph7 b02	71.8	1.0	7.3	522.5	7.1	87.9	594.3	8.1	7339.7				n/a	0.98	0.98	44.5	43.9	43.6		
	Ph7 b03	98.9	0.8	8.1	799.6	6.2	89.0	898.5	6.9	12955.5	63.9	7.3	27.6	n/a	0.91	0.87	69.9	63.5	60.5		
	Ph7 b04	42.6	0.6	14.1	602.2	8.8	93.4	644.8	9.5	6821.6	29.8	7.0	32.6	n/a	0.41	0.36	99.2	40.4	35.4		
	Ph7 b05	111.9	0.5	8.5	948.3	4.3	89.4	1060.3	4.8	21968.4	54.6	11.5	35.1	n/a	0.58	0.44	96.9	55.9	42.7		
	Ph7 b06	75.7	1.0	8.3	627.6	8.4	89.2	703.2	9.4	7506.1	34.2	9.1	24.0	n/a	0.30	0.24	119.0	35.5	28.8		
	Ph7 b07	61.9	0.9	7.5	461.8	6.7	88.2	523.7	7.6	6932.5	23.3	6.0	49.5	n/a	0.89	0.86	58.7	52.2	50.5		
	Ph7 b08	55.0	0.8	11.2	617.1	9.0	91.8	672.1	9.8	6860.4	41.5	8.6	19.3	n/a	0.76	0.69	52.0	39.4	36.1		
	Average		1.0	8.8		8.1	89.2		9.1												
	Ph7 Bioturbated prism	1938.8	1.4	7.8	18136.1	13.3	90.3	20074.9	14.7	136416.4	98.6	27.9	49.6	III	n/a		n/a	n/a	n/a	2.37	27.9

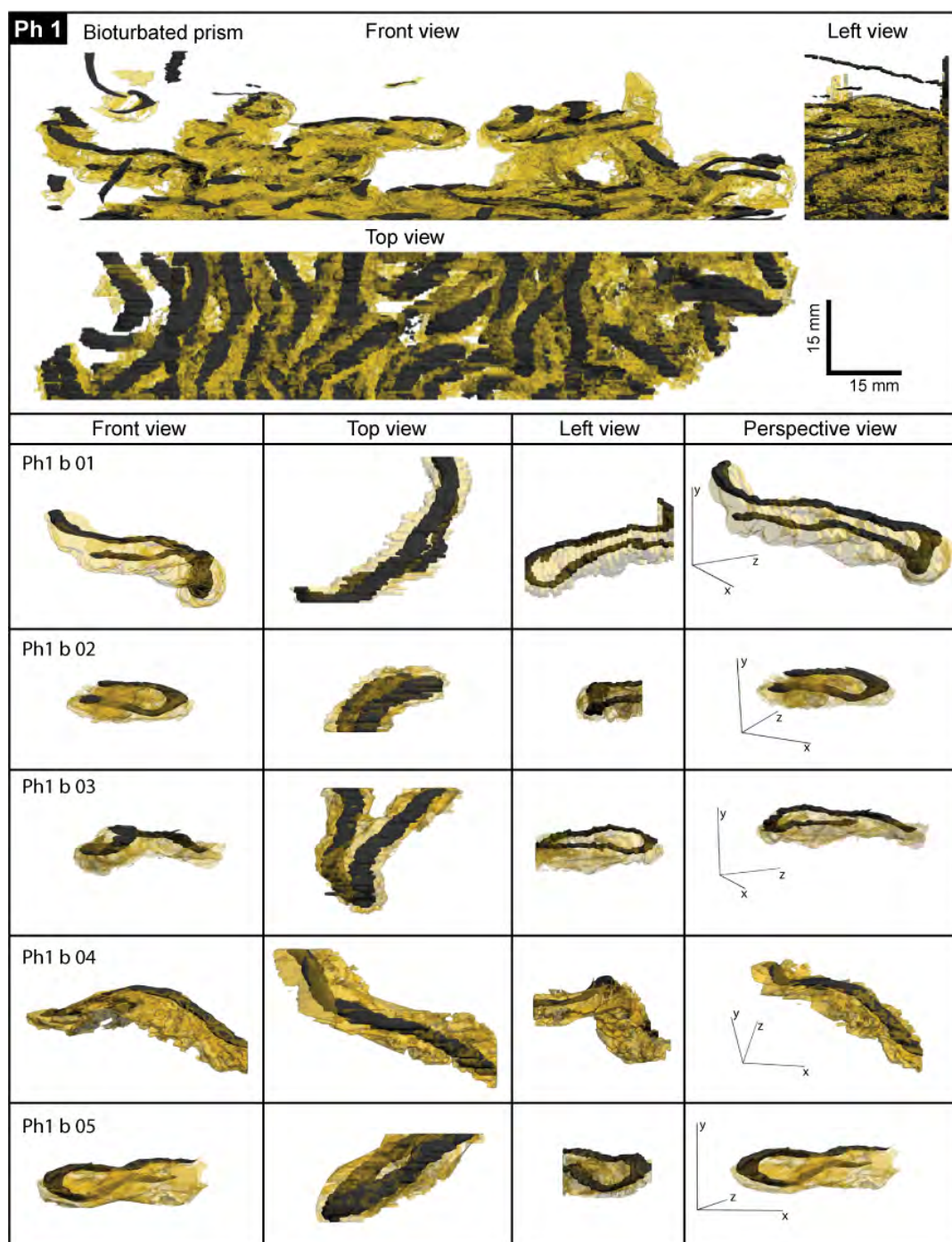


Fig. 4.3. Three-dimensional reconstruction of phycosiphoniform burrows from Rosario Formation, Mexico (Ph1). At the top: Bioturbated box with 3D reconstruction of all burrows present in the chosen part of the rock volume. Below: 3D reconstructions of five separate burrows reconstructed individually. Dark-gray color represents burrow cores. Yellow color with transparency represents halos of the burrows.

about two times larger than the halo volume of a straight burrow with T approaching 1 (burrow Ph1 b04, Tab. 4.1, Fig. 4.4).

Almost 17% of the total volume of the reconstructed bioturbated box is composed of coarser-grained halo material, which is additionally connected throughout the sample in the horizontal plane, but—perhaps more importantly—vertical communication is greatly increased (Fig. 4.3, left and front views of bioturbated box). The volumetric ratios of core and halo to matrix material are dependent on the density of bioturbation (BI). As a rule of thumb, the higher the intensity of bioturbation, the higher is the volume of halo material that contributes to the total connected volume. Even with moderate density of bioturbation (35 % bioturbation) the ichnofabric creates a highly interconnected framework of fracture-prone zones and fluid flow conduits, and the volume of permeable material can reach as much as 17%.

4.5.2. *Phycosiphon sensu stricto* from the Lower Jurassic Staithes Sandstone Formation, Yorkshire coast, UK

A second sample with phycosiphoniform burrows (Ph3) was collected from the lower part of the Jurassic Staithes Sandstone Formation, North Yorkshire, UK. The *Phycosiphon*-like trace fossils are hosted in a fine grained siltstone which is underlain by a bioclastic sandstone (Fig. 4.2D). Rare *Chondrites* burrows were observed in the darker mudstone immediately above the shelly layer (Fig. 4.2D). The sample was found to contain a second type of *Phycosiphon*-like burrows. The characteristic phycosiphoniform

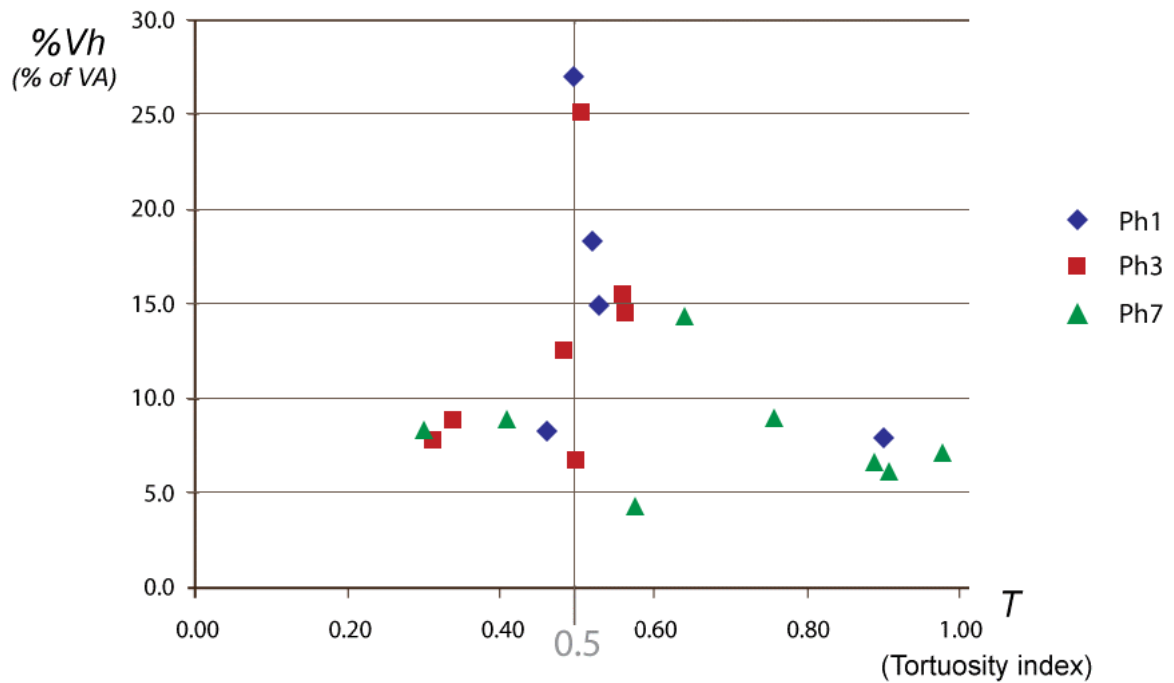


Fig. 4.4. Relationship between tortuosity of single burrows and the volume of halo material (V_h) as a component of volume available (V_A) of a single burrow.

The volume of quartzose halo material of Ph1 and Ph3 burrows is largest when the tortuosity index approaches 0.5 (commonly horseshoe-like burrow loops). The volume of halo material from the single burrows of Ph7 is independent of tortuosity as this type of burrow consists of loops that are not infilled by the halo material and the ratio halo-core material stays the same.

frogspawn texture was identified, but the individual burrows were found to have light-grey halos located mostly below elongated cores of dark clay-grade sediment (Fig. 4.2D, E). The average dimension of major axis of the elliptical transverse cross section of the dark mudstone core ellipses was 1.38 mm; much smaller than the other phycosiphoniform trace fossils considered herein. In the cross sections studied, the core ellipses are usually paired as a result of the geometry of this type of phycosiphoniform burrow being based on lobes (Fig. 4.2E, F).

Three-dimensional reconstruction shows that the burrows are looped in either the horizontal plane (Fig. 4.5: Ph3 b03, Ph3 b05, Ph3 b07), vertical direction (Fig. 4.5: Ph3 b02), or sometimes in both directions within a single burrow (Fig. 4.5: Ph3 b01, Ph3 b04). The halo of the phycosiphoniform in this material is generally enclosed in the area between the paired cores - loops are principally entirely in-filled with halo material (Fig. 4.5). Where the burrow is composed of a single string, the halo is usually located below the muddy core. Because of this, the geometry of this type of *Phycosiphon*-like burrows may be explained by pre-existing paleobiological models for *Phycosiphon incertum* (Bromley 1996; Wetzel and Bromley 1994). This material may be attributed to *Phycosiphon incertum (sensu stricto)*.

Volumetric examination of the reconstructed *Phycosiphon incertum* shows that the volume of the halo material is on average 4.5 times greater than the volume of the burrow core (core multiplicand for halo estimation, Tab. 4.1). The halo of a single burrow occupies an average of 13% of the volume available within the burrow's box, and represents the most permeable zone produced by the burrow maker.

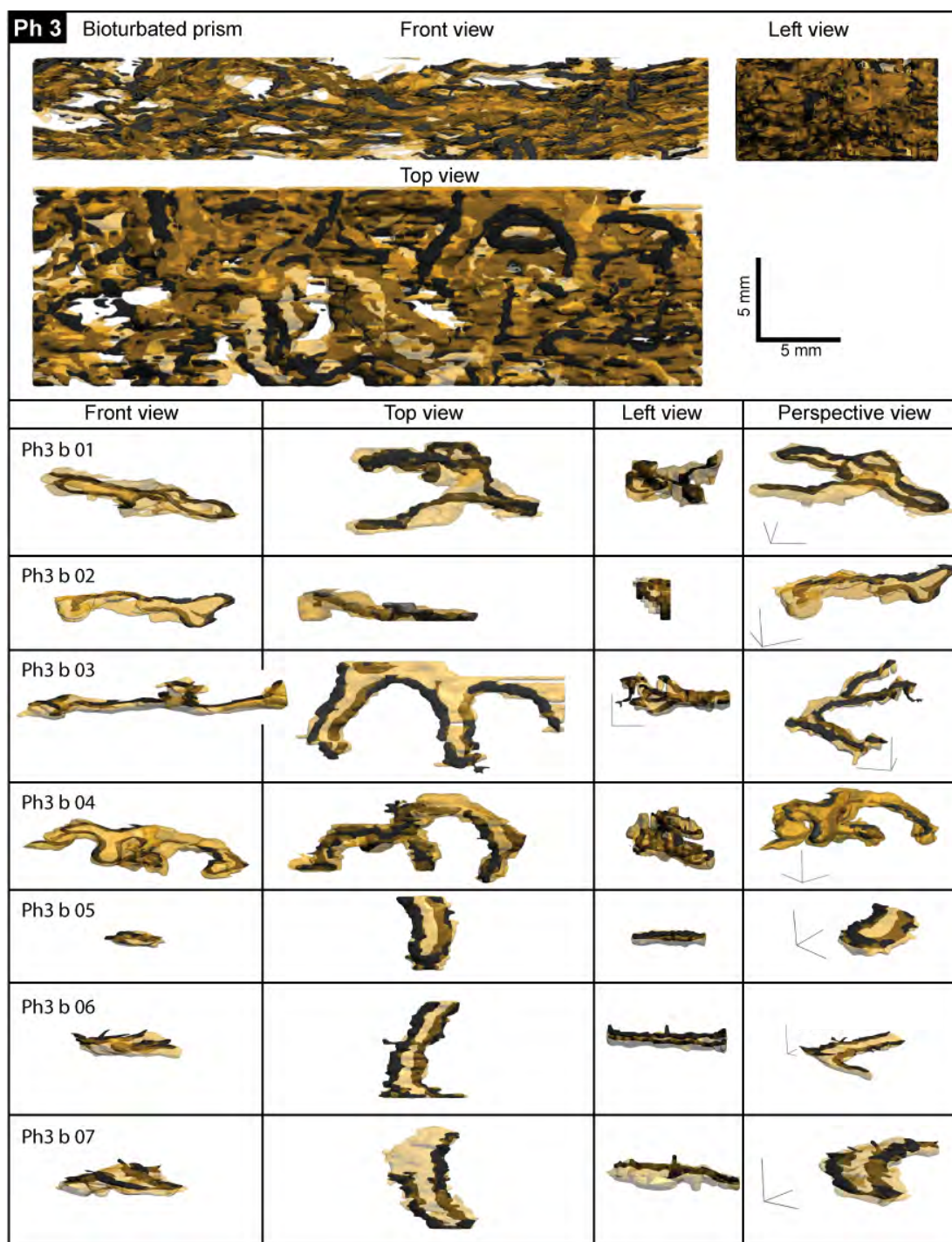


Fig. 4.5. Three-dimensional reconstruction of *Phycosiphon s.s.* burrows from Staithes Sandstone Formation, Yorkshire, UK (Ph3).

At the top: Bioturbated box with 3D reconstruction of all burrows that were present in the chosen part of the rock volume. Below: 3D reconstructions of seven separated burrows reconstructed individually. Dark-gray color represents burrow cores. Yellow color with transparency represents halos of the burrows.

The burrow halo material measured for the entire volume of bioturbated rock sample (BI4 or 65%) constitutes almost 26% of this volume. This high percentage of halo material contribution is a result of overlapping of the volumes available of adjacent single burrows. The halo material is vertically and horizontally connected throughout the reconstructed volume (Fig. 4.5, left and front views of bioturbated box). The net effect from a reservoir perspective is that up to 26% of the reservoir facies has been enhanced in terms of both porosity and permeability (kv and kh). From shale gas reservoir exploitation perspective, an interval bioturbated with this type of phycosiphoniform burrow has good connectivity of quartzose haloes, which may confer improved fracturability and/or greater permeability

4.5.3. *Nereites* isp. from the Mississippian Yoredale Sandstone Formation, Northumberland, UK

Third sample containing *Phycosiphon*-like burrows (Ph7) was collected from the coastal exposure of Mississippian Yoredale Sandstone Formation, close to the village of Craster in Northumberland, UK. The intensity of the bioturbation is low (BI between 2 and 3) and cross-cuts a grey parallel laminated siltstone. The ichnofabric ostensibly resembles the phycosiphoniform “frog-spawn” ichnofabric. Close examination of the cross sections shows that the elliptical, dark grey burrow cores are predominantly isolated (not paired as in *Phycosiphon* s.s.) and are completely surrounded by a light grey halo material. The upper half of the surrounding halo ring is commonly concave to bi-lobed (Fig. 4.2G, H, I). The bi-lobed upper surface of the burrow invites comparison with *Nereites* isp. The

burrows are relatively large, average length of a major axis of the core ellipse in cross section is 2.37 mm, the largest exceed 5 mm in width.

3D reconstructions of single burrows show that this phycosiphoniform burrow type is characterized by the least tortuous burrows considered in this study. Sinuous strings or broadly open loops are the most frequent morphologies (with few exceptions, tortuosity index [T] usually varies between 0.5 - 1, Tab. 4.1). Loops are commonly widely open (Fig. 4.6, e.g., Ph7 b05, Ph7 b06, Ph7 b08, top view) and the inter-burrow portion is not infilled with halo material.

Volumetric data indicate that the volume of a burrow halo is about 8 times larger than the volume of core material (Tab. 4.1, core multiplicand for halo estimation), this is also true for volumes containing multiple burrows (Tab. 4.1, Ph7 bioturbated box). The proportion of halo material in a box of sediment that is between 20 and 40% bioturbated, is 13.3%. That figure is found to be significantly larger than the volume of halo from a single isolated burrow (8.1% on average; Tab. 4.1, Fig. 4.6).

In the reconstructed box, the halo material is connected horizontally and vertically (Fig. 4.6, front and left view of bioturbated box). It is interesting to note that the sample has fractures which run sub-parallel to bedding, but where fractures intersect burrow haloes, the fracture plane is changed (Fig. 4.2G, H). Such burrow-controlled fracturing, if it occurred in the subsurface in a shale gas reservoir would be of significance to improving reservoir connectivity through localization of induced fractures adjacent to the porous burrow haloes. From the perspective of shale gas reservoir exploitation, this type of phycosiphoniform burrow maker has the most significant effect on reservoir properties.

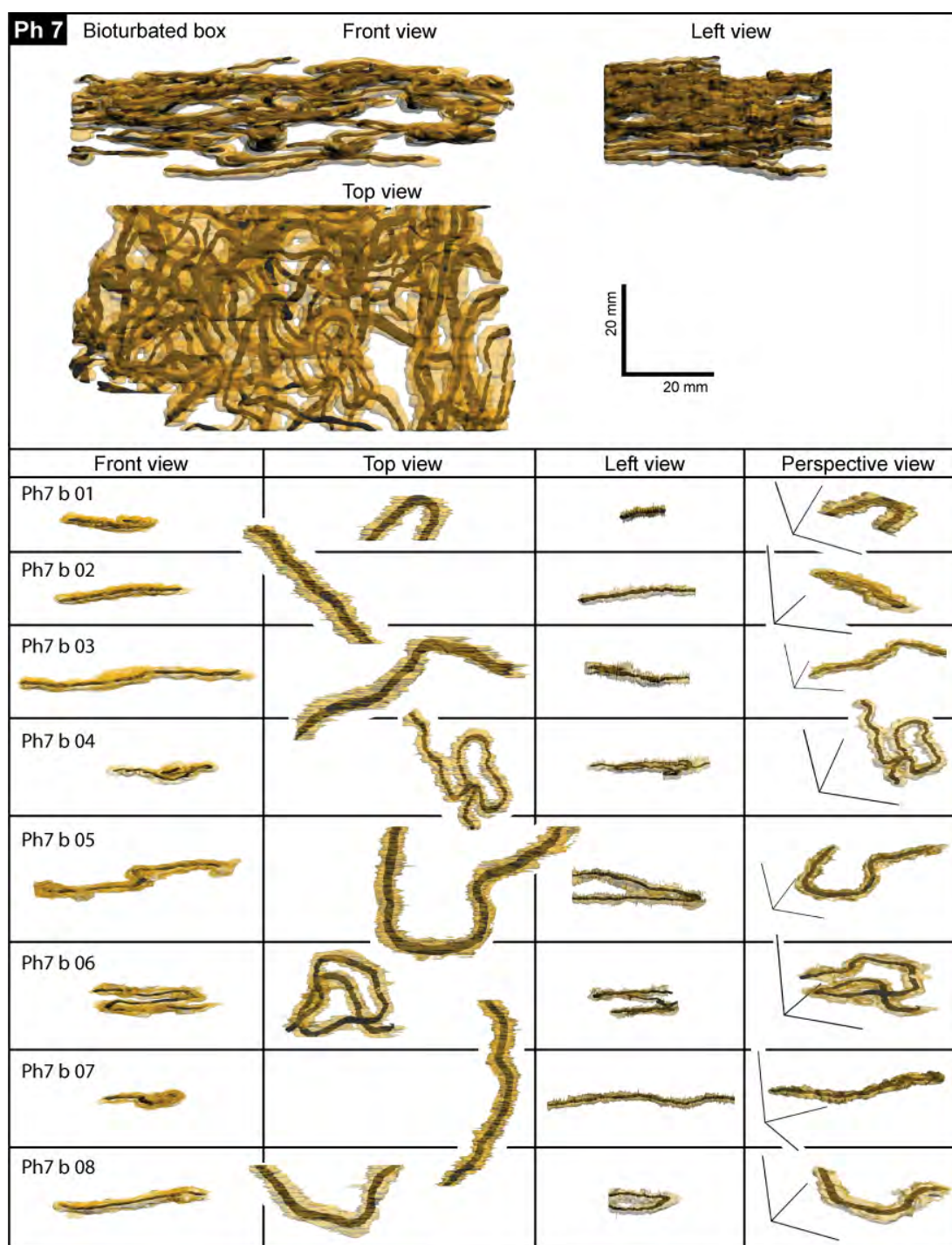


Fig. 4.6. Three-dimensional reconstruction of phycosiphoniform burrows (*Nereites*) from Yoredale Sandstone Formation, Northumberland, UK (Ph7).

At the top: bioturbated box with 3D reconstruction of all burrows that were present in the chosen part of the rock volume. Below: 3D reconstructions of eight separated burrows reconstructed individually. Dark-gray color represents burrow cores. Yellow color with transparency represents halo of the burrows.

The halo material of *Nereites* isp. has a core multiplicand of around 8, significantly improving porosity and permeability relative to unbioturbated sediment. The tortuosity of this type of burrows is not high and the burrows are present mostly as more or less horizontal sinuous strings. Thus the large core multiplicand and relatively large burrow size compensates for the low tortuosity and as a result the volume of halo material, in relation to the rock matrix, is high and the halos of adjacent burrows are connected vertically even within a sparsely bioturbated interval. This fact implies that burrow (more specifically halo) size is of principal importance to porosity and permeability enhancement in shale gas reservoir facies.

4.6. Impact of phycosiphoniform ichnofabric on shale-gas reservoir quality

A complete understanding of mud accumulation mechanisms and generation of biogenic sedimentary fabrics in mudstones is still in its infancy. Recent research on the transport of clay particles, the origin of silt-grade quartz and mineral composition of mudstones has shed new light on the organic-rich mud depositional systems and origin of petroleum source rocks (Schieber et al. 2000, 2007; Macquaker and Bohacs 2007). The burrowing activities and the resulting ichnofabrics in shale-gas facies are commonly un-recognized by petroleum geologists, and are not even completely understood by ichnologists (see Bednarz and McIlroy 2009). Organism-sediment interactions and their effect on sediment fabrics are directly related to hydrodynamic processes and biogeochemical conditions at the seafloor during deposition and through burial until the sediment is buried to a greater

depth than that of endobenthic tiering. The incomplete knowledge of the physical and biological processes acting to produce organic-rich mudstones (or “black shales”) is a major shortcoming in generating models aimed at understanding the distribution and properties of shale-gas facies.

We demonstrate herein that biogenic structures within the sediment can significantly change the final petrophysical properties of shale gas reservoir facies. The biological processes and their impact on sediment properties are outlined below.

4.6.1. Porosity and permeability of reservoir mudstone

Pore sizes in mudstones range typically from 0.3 to 60nm and are the smallest known values for rocks (Best and Katsube 1995). The pores form fluid flow paths with extremely low permeabilities. The permeability of shale gas reservoir mudstones must be enhanced to allow economic production. Permeability can be improved by drilling strategies that access natural fractures (if they exist) or by hydraulically-induced fracturing technology (Curtis 2002). Additional flow conduits within mudstones may be created by burrowing (Gingras et al. 2004a and herein). The tortuous flow-paths, created by grain-selective deposit-feeding organisms, can strongly influence the efficiency of petroleum recovery. It is considered that all the *Phycosiphon*-like trace fossils considered herein have the potential to improve vertical communication in shale gas reservoirs by connecting silt-rich laminae in otherwise impermeable mudstones via their clean silty halos. In addition, the biological concentration of silt grains from muddy host sediment can create additional reservoir volume by bringing the coarsest grains together to form

the burrow halo (Fig. 4.7). Mudstone matrix and burrow cores, due to the significant clay-grade and clay mineral content, have very low porosities and ultra-low permeabilities. Burrow halos can have significantly higher permeability than the core and host sediment. Mudstone bioturbated by *Phycosiphon*-like burrow makers therefore has additional heterogeneity relative to the unbioturbated host-sediment.

The tortuous nature of phycosiphoniform burrows and the strong vertical component to the ichnofabrics they create has the propensity to make ultra-tight mudstones permeable directly through creation of pathways of porous material.

4.6.2. Brittleness of reservoir mudstone

Most shale gas reservoirs rely upon natural and induced fractures to connect zones of porosity in the reservoir facies. Development of fractures depends on the brittleness of a mudstone. The response of brittle rock to stress is manifested by permeability-enhancing brittle deformation due to high shear strength (Nygard et al. 2006). Many mudstones, however, do not behave in a brittle manner but are rather ductile. Propagation of fractures in non-brittle mudstones is ineffective and risky. The mechanical properties of mudstones are strongly related to the presence of quartz, either diagenetic quartz from recrystallization of biogenic opaline silica (e.g. radiolarians or sponges), or as frameworks of quartz grains within the mudstone. Interconnected quartz-rich haloes of phycosiphoniform burrows form a framework of material that have the potential to locally increase brittleness, making the bioturbated, otherwise ductile, mudstone fracture-prone, especially if the burrow halos are diagenetically cemented.

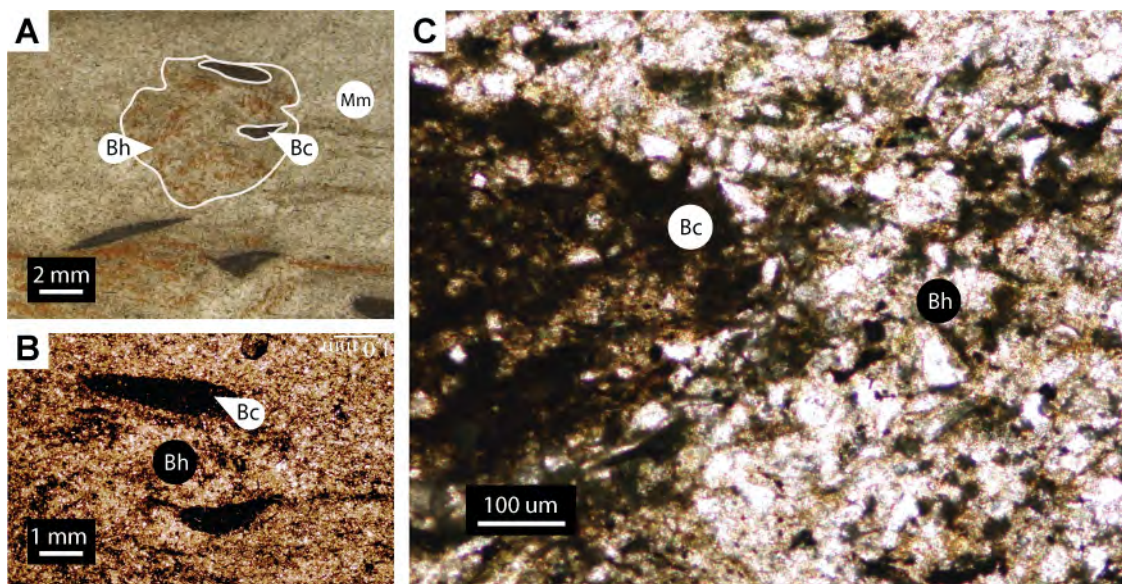


Fig. 4.7. Types of material in bioturbated mudstone distinguished in terms of animal activity alteration. Bc = burrow core composed of clay minerals that have been mineralogically altered; Bh = burrow halo composed of silt- and sand-grade minerals (mainly quartz and feldspars), which have been texturally altered (concentrated); Mm = mudstone matrix, not altered by animal's activity. The image presents phycosiphoniform burrows from Rosario Formation, Mexico (Ph1).

Fracturability of bioturbated shale-gas reservoir intervals may be linked to ichnofabric in some reservoirs.

4.6.3. Shale-gas reservoir capacity

Shale gas reservoirs are considered to be tripartite porosity systems, where gas is stored as: 1) free gas in pore or in natural fracture spaces; 2) adsorbed on kerogen and clays; and 3) absorbed in kerogen or bitumen (e.g., Schettler et al. 1991). Phycosiphoniform burrow halos create natural pore-spaces and can enhance reservoir capacity. If the quartz grain frameworks created by the burrow halo are also loci for fracturing (natural or induced), the burrows may also be responsible for the distribution of fracture porosity in the reservoir. In both cases, pore spaces caused by phycosiphoniform bioturbation could be filled by free gas or organic matter maturation products containing gas. The tortuous geometry of the interconnected phycosiphoniform halos creates a large surface area for release of gas into the porous burrow halos. It is clear that, relative to a laminated shale gas reservoir, a bioturbated shale gas reservoir with phycosiphoniform burrows will have increased reservoir capacity.

4.6.4. Gas storativity and deliverability

Production of gas from ultra-low permeability rocks such as mudstones needs careful reservoir evaluation and engineering. A shale-gas reservoir devoid of natural fractures is dependent upon gas flow through thin, often isolated, silty laminae and beds. Improved connectivity within such reservoirs is integral to their success. Diffusive transport of gas

from the rock matrix to the more porous and permeable burrow halos is increased by the tortuosity of the burrow structures and thus the large surface area of porous zones in the reservoir.

Gas deliverability depends upon the response of the shale-gas reservoir to the applied technology, including injecting of chemical substances, and thus is inseparably related to the wettability of the reservoir rock. Prediction of reservoir wettability is one of the major challenges for petroleum engineers and can be achieved through detailed determination of the petrophysical properties of the reservoir including shale and tight-gas (Al-Garni and Al-Anazi 2008; Rickman and Jaripatke 2010). A comprehensive evaluation of a gas reservoir in mudstone requires thoughtful consideration of its wettability; including appreciation of bioturbated intervals, if present. Burrowing organisms can change mineral grain distributions within the sediment influencing the subsequent distribution of fluids within the reservoir. Biogenic activity of grain-selective burrowers in muds can physically re-organize grain distributions by the separation of clay and silt fractions (Bednarz and McIlroy 2009), and may also affect the clay mineralogy (McIlroy et al. 2003, Needham et al. 2004). Concentration of fine-grained components on the basis of mineralogy and grain size during bioturbation may impact wettability, permeability and porosity distributions. Differences in the wettability of bioturbated mudstone reservoirs may be affected by mineralogical composition of the rock matrix and its composition (Sayyounh et al. 1990). Knowledge of the detailed mineralogy of bioturbated intervals relative to the host sediment will allow the most efficient surfactants (surface-active agents) to be applied to the reservoir. In order to enhance permeability a properly

matched surfactant is required to change water-wet sedimentary facies to become intermediate-wet (Adibhatla et al. 2006).

Consideration of the geometry and mineralogical composition of ichnofabrics dominated by phycosiphoniform burrows in shale-gas reservoir facies allows: 1) better prediction of shale-gas reservoir wettability; and 2) realistic evaluation of the volume of sediment that is available for surfactant-enhanced gas flow through the most permeable regions of shale-gas reservoirs.

4.7. Conclusion

The three-dimensional reconstructions of three examined ichnofabric types generated within muddy sediment by *Phycosiphon*-like burrow makers allow us to make a number of predictions relating to the impact of bioturbation on shale-gas reservoir quality.

1. The three phycosiphoniform burrow types studied all increase the porosity and permeability of the reservoir relative to the unbioturbated portion of the sediment. Increased bioturbation intensity is correlated with improved reservoir quality.
2. Of the burrow parameters studied, burrow (specifically burrow halo) diameter and burrow tortuosity are considered to be the most important in controlling reservoir quality. Large burrow diameters increase reservoir volume, and tortuosity increases also connectivity (particularly important in enhancing kv).
3. The trace fossil *Nereites* was found to have the greatest burrow diameter—halo volume per unit length. The undetermined phycosiphoniform trace fossil and *Phycosiphon*










sensu stricto were well connected in three dimensions owing to the tortuosity of the burrows (see Tab. 4.2).

4. Ichnofabrics dominated by phycosiphoniform burrows typically show good connectivity of biologically enhanced zones of increased porosity. These parameters are directly related to enhanced permeability, increased reservoir capacity, greater storativity and have the potential to increase fracturability.

Together these observations suggest that phycosiphoniform-dominated ichnofabrics would promote fluid flow in otherwise ultra-tight shale-gas reservoir facies.

Table 4.2. *Phycosiphon*-like bioturbation types.

CM = core multiplicand; kv = vertical permeability; BI = bioturbation index; Ph1 = phycosiphoniform ichnofabric from Rosario Formation, Mexico; Ph3 = *Phycosiphon s.s.* from Staithes Sandstone Formation, UK; Ph7 = *Nereites* from Yoredale Sandstone Formation, Craster, UK

		Phycosiphoniform burrow type		
		Ph1	Ph3	Ph7
Vertical cross sections				
Loops view	Top			
	Side			
Core multiplicand (CM, average)		6.5	4.5	8
Vertical permeability (kv) enhancement		High	High	High
Burrow Tortuosity		High	High	Low
Halo material volume (%Vh) / BI in the samples		16.7% / III	25.9% / IV	13.3% / III
Burrow core diameter (average)		5.3 mm	1.4 mm	2.4 mm
Vertical halo vconnectivity in the sample		100%	100%	100%

4.8. Acknowledgements

We acknowledge the many helpful discussions with Dr Liam Herringshaw and Dr Richard Callow. We thank Dr Liam Herringshaw and Christopher Boyd for help with photography. The helpful reviews of Murray K. Gingras, Alfred Lacazette and an anonymous reviewer improved the clarity of our arguments. We thank Frances Whitehurst, AAPG geology consultant, for her comments on the latest version of the manuscript. Duncan McIlroy acknowledges the support of a Canada Research chair and financial funding from an NSERC discovery grant.

4.9. References

- Adibhatla, B., K. K. Mohanty, P. Berger, and C. Lee, 2006, Effect of surfactants on wettability of near-wellbore regions of gas reservoirs: *Journal of Petroleum Science and Engineering*, v. 52, p. 227–236, doi:10.1016/j.petrol.2006.03.026.
- Al-Garni, M. T., and B. D. Al-Anazi, 2008, Investigation of wettability effects on capillary pressure, and irreducible saturation for Saudi crude oils, using rock centrifuge: *Oil and Gas Business*, v. 2008, no. 2, http://www.ogbus.ru/eng/2008_2.shtml (accessed June 20, 2011).
- Baker, P. G., 1978, A technique for the accurate reconstruction of internal structures of micromorphic fossils: *Paleontology*, v. 19, p. 565–584.
- Bednarz, M., and D. McIlroy, 2009, Three-dimensional reconstruction of “phycosiphoniform” burrows: Implications for identification of trace fossils in core: *Paleontologia Electronica*, v. 12, no. 3, http://palaeo-electronica.org/2009_3/195/index.html (accessed August 20, 2011).
- Best, M. E., and T. J. Katsube, 1995, Shale permeability and its significance in hydrocarbon exploration: *The Leading Edge*, v. 14, no. 3, p. 165–170, doi:10.1190/1.1437104.
- Bockelie, J. F., 1991, Ichnofabric mapping and interpretation of Jurassic reservoir rocks in the Norwegian North Sea: *Palaios*, v. 6, no. 3, p. 206–215, doi:10.2307/3514902.

- Bohacs, K.M., G. J. Grabowski Jr, A.R. Carroll, P. J. Mankiewicz, K. J. Miskell-Gerhardt, J.R. Schwalbach, M. B. Wegner, and J. A. Simo, 2005, Production, destruction, and dilution: The many paths to source rock development, in N. B. Harris, ed., The deposition of organic carbon-rich sediments: Models, mechanisms, and consequences: SEPM, Special Publication 82, p. 61–101.
- Bromley, R. G., 1996, Trace fossils: Biology, taphonomy and applications: London, Chapman and Hall, 361 p.
- Caplan, M. L., and R. M. Bustin, 2001, Paleoenvironmental and paleoceanographic controls on black, laminated mudrock deposition: Example from Devonian–Carboniferous strata, Alberta, Canada: *Sedimentary Geology*, v. 145, p. 45–72, doi:10.1016/S0037-0738(01)00116-6.
- Carruthers, D. J., 2003, Modeling of secondary petroleum migration using invasion percolation techniques, in S. Düppenbecker and R. Marzi, eds., *Multidimensional basin modeling: AAPG Datapages Discovery Series 7*, p. 21–37.
- Curtis, J. B., 2002, Fractured shale-gas systems: Unconventional petroleum systems: *AAPG Bulletin*, v. 86, no. 11, p. 1921–1938, doi:10.1306/61EEDDBE-173E-11D7-8645000102C1865D.
- Droser, M. L., and D. J. Bottjer, 1986, A semiquantitative classification of ichnofabric: *Journal of Sedimentary Petrology*, v. 56, p. 558–569.
- Ekdale, A. A., and D. W. Lewis, 1991, Trace fossils and paleoenvironmental control of ichnofacies in a late Quaternary gravel and loess fan-delta complex, New Zealand: *Paleogeography, Paleoclimatology, Paleoecology*, v. 81, p. 253–279, doi:10.1016/0031-0182(91)90150-P.
- Genise, J. F., and J. H. Laza, 1998, *Monesichnus ameghinoi Roselli*: A complex insect trace fossil produced by two distinct trace makers: *Ichnos*, v. 5, p. 213–223, doi:10.1080/10420949809386418.
- Gingras, M. K., S. G. Pemberton, C. Mendoza, and F. Henk, 1999, Modeling fluid flow in trace fossils: Assessing the anisotropic permeability of *Glossifungites* surfaces: *Petroleum Geoscience*, v. 5, p. 349–357, doi:10.1144/petgeo.5.4.349.
- Gingras, M. K., B. Macmillan, B. J. Balcom, T. Saunders, and S. G. Pemberton, 2002, Using magnetic resonance imaging and petrographic techniques to understand the textural attributes and porosity distribution in *Macaronichnus* burrowed sandstone: *Journal of Sedimentary Research*, v. 72, no. 4, p. 552–558, doi:10.1306/122901720552.
- Gingras, M. K., C. A. Mendoza, and S. G. Pemberton, 2004a, Fossilized worm burrows influence the resource quality of porous media: *AAPG Bulletin*, v. 88, no. 7, p. 875–883, doi:10.1306/01260403065.
- Gingras, M. K., S. G. Pemberton, K. Muehlenbachs, and H. Machel, 2004b, Conceptual models for burrow-related, selective dolomitization with textural and isotopic

- evidence from the Tyndall Stone, Canada: *Geobiology*, v. 2, no. 1, p. 21–30, doi:10.1111/j.1472-4677.2004.00022.x.
- Gingras, M. K., S. G. Pemberton, F. Henk, J. A. MacEachern, C. Mendoza, B. Rostron, R. O'Hare, M. Spila, and K. Konhauser, 2007, Applications of ichnology to fluid and gas production in hydrocarbon reservoirs, in J. A. MacEachern, S. G. Pemberton, M. K. Gingras, K. L. Bann, eds., *Applied ichnology: SEPM Short Course Notes* 52, p. 131–147.
- Goldring, R., J. E. Pollard, and A. M. Taylor, 1991, *Anconichnus horizontalis*: A pervasive ichnofabric-forming trace fossil in post-Paleozoic offshore siliciclastic facies: *Palaaios*, v. 6, no. 3, p. 250–263, doi:10.2307/3514905.
- Gordon, J. B., S. G., Pemberton, M. K., Gingras, and K. O. Konhauser, 2010, Biogenically enhanced permeability: A petrographic analysis of *Macaronichnus segregatus* in the Lower Cretaceous Bluesky Formation, Alberta, Canada: *AAPG Bulletin*, v. 94, no. 11, p. 1779–1795, doi:10.1306/04061009169.
- Hammer, Ø., 1999, Computer-aided study of growth patterns in tabulate corals, exemplified by *Catenipora heintzi* from Ringerike, Oslo region: *Norsk Geologisk Tidsskrift*, v. 79, p. 219–226, doi:10.1080/002919699433672.
- Hembree, D. I., and S. T. Hasiotis, 2006, The identification and interpretation of reptile ichnofossils in paleosols through modern studies: *Journal of Sedimentary Research*, v. 76, no. 3, p. 575–588, doi:10.2110/JSR.2006.049.
- Hovikoski, J., R. Lemiski, M. K. Gingras, S. G. Pemberton, and J. A. MacEachern, 2008, Ichnology and sedimentology of a mud-dominated deltaic coast: Upper Cretaceous Alderson Member (Lea Park Formation), western Canada: *Journal of Sedimentary Research*, v. 78, no. 12, p. 803–824, doi:10.2110/jsr.2008.089.
- Jenkins, C. D., and C. M. Boyer, 2008, Coalbed and shale gas reservoirs: *Journal of Petroleum Technology*, v. 60, no. 2, p. 92–99.
- Keswani, A. D., and S. G. Pemberton, 2007, Applications of ichnology in exploration and exploitation of Mississippian carbonate reservoirs, Midale Beds, Weyburn oil field, Saskatchewan (abs.): *Canadian Society of Petroleum Geologists and Canadian Society of Exploration Geophysicists Conference*, Calgary, Alberta, Canada, May 14–17, 2007, 28 p.
- Kohlruss, D., and E. Nickel, 2009, Facies analysis of the Upper Devonian–Lower Mississippian Bakken Formation, southeastern Saskatchewan: Summary of investigations 2009: Saskatchewan, Saskatchewan Geological Survey, Ministry of Energy and Resources, Miscellaneous Report 2009-4.1, Paper A-6, 11 p.
- Lemiski, R. T., J. Hovikoski, S.G. Pemberton, and M.K. Gingras, 2011, Sedimentological, ichnological and reservoir characteristics of the low-permeability, gas-charged Alderson Member (Hatton gas field, southwest Saskatchewan): Implications for resource development: *Bulletin of Canadian Petroleum Geology*, v. 59, p. 27–53, doi:10.2113/gscpgbull.59.1.27.

- Löwemark, L., and P. Schäfer, 2003, Ethological implications from a detailed x-ray radiograph and 14C study of the modern deep-sea *Zoophycos*: Paleogeography, Paleoclimatology, Paleoecology, v. 192, p. 101–121, doi:10.1016/S0031-0182(02)00681-8.
- Macquaker, J. H. S., and K. M. Bohacs, 2007, On the accumulation of mud: Science, v. 318, no. 5857, p. 1734–1735, doi:10.1126/science.1151980.
- Macquaker, J. H. S., K. G. Taylor, and R. L. Gawthorpe, 2007, High-resolution facies analyses of mudstones: Implications for paleoenvironmental and sequence-stratigraphic interpretations of offshore ancient mud-dominated successions: Journal of Sedimentary Research, v. 77, no. 4, p. 324–339, doi:10.2110/jsr.2007.029.
- Maloof, A., C.V. Rose, R. Beach, B. M. Samuels, C. C. Calmet, D. H. Erwin, G. R. Poirier, N. Yao, and F. J. Simons, 2010, Possible animal-body fossils in pre-Marinoan limestones from South Australia: Nature Geoscience, v. 3, p. 653–659, doi:10.1038/ngeo934.
- McIlroy, D., 2004, Some ichnological concepts, methodologies, applications and frontiers, in D. McIlroy, ed., The application of ichnology to paleoenvironmental and stratigraphic analysis: Geological Society (London) Special Publication 228, p. 3–29.
- McIlroy, D., R.H. Worden, and S. J. Needham, 2003, Faeces, clay minerals and reservoir potential: Journal of the Geological Society (London), v. 160, no. 3, p. 489–493, doi:10.1144/0016-764902-141.
- Narr, W., and J. B. Currie, 1982, Origin of fracture porosity: Example from Altamont field, Utah: AAPG Bulletin, v. 66, no. 9, p. 1231–1247.
- Naruse, H., and K. Nifuku, 2008, Three-dimensional morphology of the ichnofossil *Phycosiphon incertum* and its implication for paleoslope inclination: Palaios, v. 23, no. 5, p. 270–279, doi:10.2110/palo.2007.p07-020r.
- Needham, S. J., R. H. Worden, and D. McIlroy, 2004, Animal sediment interaction: The effect of ingestion and excretion by worms on mineralogy: Biogeosciences, v. 1, p. 113–121, doi:10.5194/bg-1-113-2004.
- Nygård, R., M. Gutierrez, R. K. Bratliand, and K. Høeg, 2006, Brittle-ductile transition, shear failure and leakage in shales and mudrocks: Marine and Petroleum Geology, v. 23, no. 2, p. 201–212, doi:10.1016/j.marpetgeo.2005.10.001.
- Ottmann, J. D., and K. M. Bohacs, 2010, The Barnett shale: A sequence-stratigraphic view of depositional controls, reservoir distribution and resource density: AAPG Search and Discovery article 90122: AAPG Hedberg Conference, Austin, Texas, December 5–10, 2010: http://www.searchanddiscovery.com/abstracts/pdf/2011/hedberg-texas/abstracts/ndx_ottmann.pdf (accessed August 20, 2011).

- Pemberton, S. G., 1992, Applications of ichnology to petroleum exploration: SEPM Core Workshop 17, 429 p.
- Pemberton, S. G., and M. K. Gingras, 2005, Classification and characterizations of biogenically enhanced permeability: AAPG Bulletin, v. 89, p. 1493–1517, doi:10.1306/07050504121.
- Platt, B. F., S. T. Hasiotis, and D.R. Hirmas, 2010, Use of low-cost multistripe laser triangulation (MLT) scanning technology for three-dimensional, quantitative paleoichnological and neoichnological studies: Journal of Sedimentary Research, v. 80, no. 7, p. 590–610, doi:10.2110/jsr.2010.059.
- Rickman, R. D., and O. Jaripatke, 2010, Optimizing microemulsion/surfactant packages for shale and tight-gas reservoirs: Society of Petroleum Engineers Deep Gas Conference and Exhibition, Manama, Bahrain, January 24–26, 2010, SPE Paper 131107, p. 1–7, doi:10.2118/131107-MS.
- Savrda, C. E., H. Krawinkel, F. M. G. McCarthy, C. M. G. McHugh, H. C. Olson, and G. Mountain, 2001, Ichnofabrics of a Pleistocene slope succession, New Jersey margin: Relations to climate and sea level dynamics: Paleogeography, Paleoclimatology, Paleoecology, v. 171, no. 1–2, p. 41–61, doi:10.1016/S0031-0182(01)00266-8.
- Sayyounh, M. H., A. S. Dahab, and A. E. Omar, 1990, Effect of clay content on wettability of sandstone reservoirs: Journal of Petroleum Science and Engineering, v. 4, no. 2, p. 119–125, doi:10.1016/0920-4105(90)90020-4.
- Schettler Jr., P. D., C. R. Parmely, and C. Juniata, 1991, Contributions to total storage capacity in Devonian shales: Society of Petroleum Engineers Eastern Regional Meeting, Lexington, Kentucky, October 22–25, 1991, SPE Paper 23422, p. 77–88, doi:10.2118/23422-MS.
- Schieber, J., D. Krinsley, and L. Riciputi, 2000, Diagenetic origin of quartz silt in mudstones and implications for silica cycling: Nature, v. 406, p. 981–985, doi:10.1038/35023143.
- Schieber, J., J. Southard, and K. Thaisen, 2007, Accretion of mudstone beds from migrating floccule ripples: Science, v. 318, no. 5857, p. 1760–1763, doi:10.1126/science.1147001.
- Schmidtling, R. C., and C. R. Marshall, 2010, Three-dimensional structure and fluid flow through the hydrospires of the blastoid echinoderm, *Pentremites rusticus*: Journal of Paleontology, v. 84, no. 1, p. 109–117, doi:10.1666/09-080.1.
- Sonnenberg, S. A., and A. Pramudito, 2009, Petroleum geology of the giant Elm Coulee field, Williston Basin: AAPG Bulletin, v. 93, no. 9, p. 1127–1153, doi:10.1306/052809090006.
- Spila, M. V., S. G. Pemberton, B. Rostron, and M. K. Gingras, 2007, Biogenic textural heterogeneity, fluid flow and hydrocarbon production: Bioturbated facies, Ben

- Nevis Formation, Hibernia field, offshore Newfoundland, in J. A. MacEachern, K. L. Bann, M. K. Gingras, and G. S. Pemberton, eds., *Applied ichnology: SEPM Short Course Notes 52*, p. 363–380.
- Sutton, M. D., D. E. G. Briggs, D. J. Siveter, and D. J. Siveter, 2001, Methodologies for the visualization and reconstruction of three-dimensional fossils from the Silurian Herefordshire Lagerstätte: *Paleontologia Electronica*, v. 4, no. 1, p. 1–17, http://palaeo-electronica.org/2001_1/s2/issue1_01.htm (accessed August 10, 2010).
- Taylor, A., and R. Goldring, 1993, Description and analysis of bioturbation and ichnofabric: *Journal of the Geological Society*, v. 150, no. 1, p. 141–148, doi:10.1144/gsjgs.150.1.0141.
- Taylor, A., R. Goldring, and S. Gowland, 2003, Analysis and application of ichnofabrics: *Earth-Science Reviews*, v. 60, no. 3–4, p. 227–259, doi:10.1016/S0012-8252(02)00105-8.
- Tonkin, N. S., D. McIlroy, R. Meyer, and A. Moore-Turpin, 2010, Bioturbation influence on reservoir quality: A case study from the Cretaceous Ben Nevis Formation, Jeanne d'Arc Basin, offshore Newfoundland, Canada: *AAPG Bulletin*, v. 94, no. 7, p. 1059–1078, doi:10.1306/12090909064.
- Watters, W. A., and J. P. Grotzinger, 2001, Digital reconstruction of calcified early metazoans, terminal Proterozoic Nama Group, Namibia: *Paleobiology*, v. 27, no. 1, p. 159–171.
- Wetzel, A., and R. G. Bromley, 1994, *Phycosiphon incertum* revisited: *Anconichnus horizontalis* is junior subjective synonym: *Journal of Paleontology*, v. 68, no. 6, p. 1396–1402.
- Wetzel, A., and A. Uchman, 1998, Deep-sea benthic food content recorded by ichnofabrics: A conceptual model based on observations from Paleogene flysch, Carpathians, Poland: *Palaaios*, v. 13, no. 6, p. 533–546, doi:10.2307/3515345.
- Wetzel, A., and A. Uchman, 2001, Sequential colonization of muddy turbidites in the Eocene Beloveza Formation, Carpathians, Poland: *Paleogeography, Paleoclimatology, Paleoecology*, v. 168, no. 1–2, p. 171–186, doi:10.1016/S0031-0182(00)00254-6.
- Wetzel, A., and F. Werner, 1980, Morphology and ecological significance of *Zoophycos* in deep-sea sediments off NW Africa: *Paleogeography, Paleoclimatology, Paleoecology*, v. 32, p. 185–212, doi:10.1016/0031-0182(80)90040-1.

4.10. Appendices

In order to control an interactive model (Appx 4.3):

1) click on the chosen three-dimensional reconstruction to activate the interactive content; 2) Use tools that are listed on the bar at the top of the activated area; 3) choose between available views to explore spatial geometry of the three-dimensional object and their chosen components; 4) use Model Tree panel in order to display or hide chosen components.

Appendix 4.1. Symbols and equations of the variables describing trace fossils and ichnofabric geometry and structure.

Symbol	Variable name	Equation
VA	Volume available (the box bounding the burrow/s)	$VA = a \cdot b \cdot c$
d	Space diagonal (of the box)	$d = \sqrt{a^2 + b^2 + c^2}$
VU	Volume utilized	$VU = Vh + Vc$
VE	Volume exploited	$VE = VU \cdot 100 / VA$
%Vh	Halo volume (%)	$\%Vh = Vh \cdot 100 / VA$
%Vc	Core volume (%)	$\%Vc = Vc \cdot 100 / VA$
CM	Core multiplicand (for halo estimation)	$CM = Vh / Vc$
Lc	Core length	$L_C = \sum_{i=0}^n s_i = s_1 + s_2 + s_3 + \dots + s_n$
T	Tortuosity index	$T = d / L_C$
Li	Burrow length index	$L_i = L_M / L_C$

Appendix 4.2. General description of examined samples containing phycosiphoniform burrows.

Ph1 = sample containing phycosiphoniform burrows from Rosario formation; Ph3 = sample containing *Phycosiphon s.s.*; Ph7 = sample containing *Nereites* burrows

Phycosiphoniform	Age	Formation	Lithology	Sedimentary structures, remaining primary fabric	BI	Methods	Accompanying trace fossils
Ph1	Upper Cretaceous	Rosario Formation, Mexico	Siltstone	Subtle lamination	3-6	- Serial grinding (displacement 0.5 mm, 59 slices, 2.95 cm-thick slab) - 3D reconstruction	Rare <i>Planolites</i>
Ph3	Lower Jurassic	Staithes Sandstone Formation, Yorkshire, UK	Siltstone	Solid, no lamination; underlain by sandstone packed by bivalves	3-4	- Serial grinding (displacement 0.2 mm, 59 slices, 1.18 cm-thick slab) - 3D reconstruction	Rare <i>Chondrites</i>
Ph7	Mississippian	Yoredale Sandstone Formation, Northumberland, UK	Siltstone	Subtle lamination	2-3	- Serial grinding (displacement 0.2 mm, 249 slices, 4.96 cm-thick slab) - 3D reconstruction	—

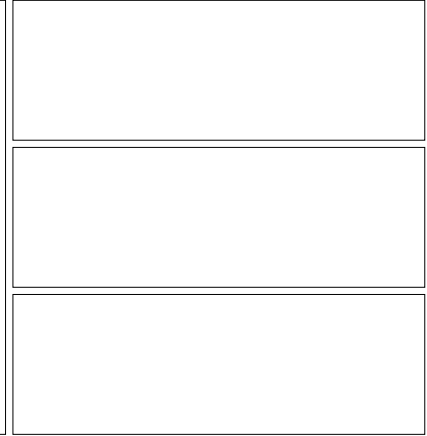
Appendix 4.3. Three-dimensional interactive models of reconstructed phycosiphoniform burrows.

Phycosiphoniform burrows from the Upper Cretaceous Rosario Formation, Mexico (Ph1)

Scale: 15 mm

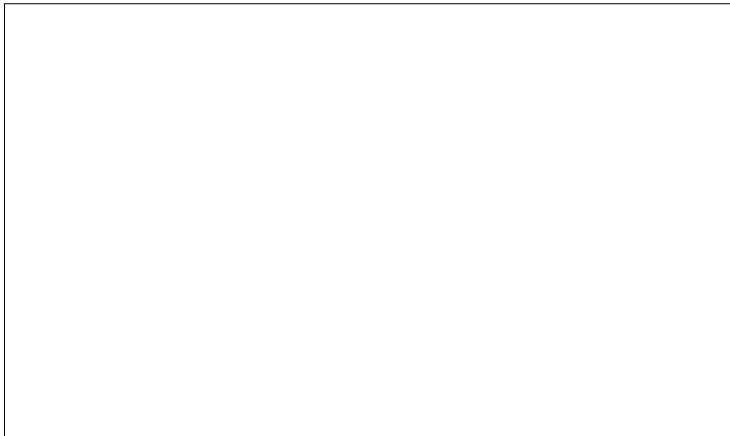


Scale: 15 mm

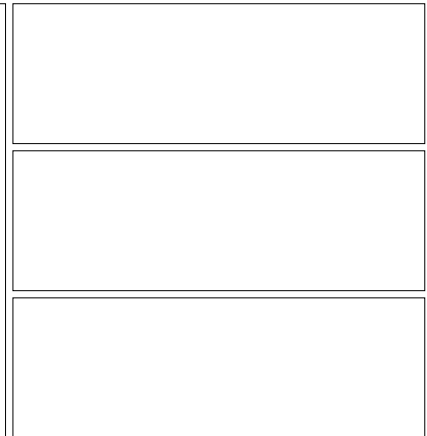


Phycosiphon sensu stricto from the Lower Jurassic Staithes Sandstone Formation, Yorkshire, UK (Ph3)

Scale: 5 mm

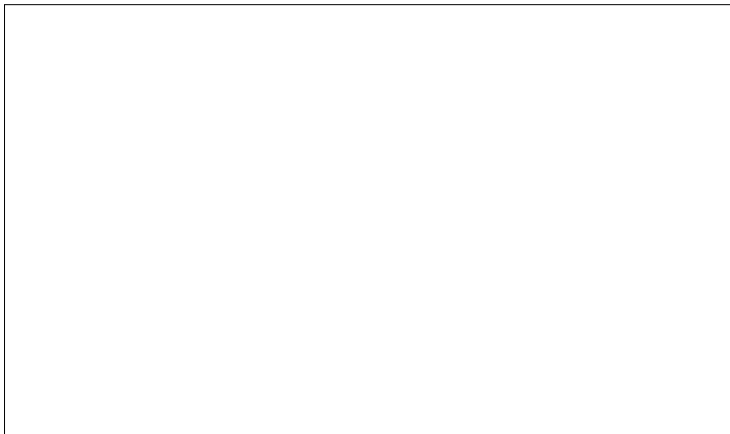


Scale: 2 mm

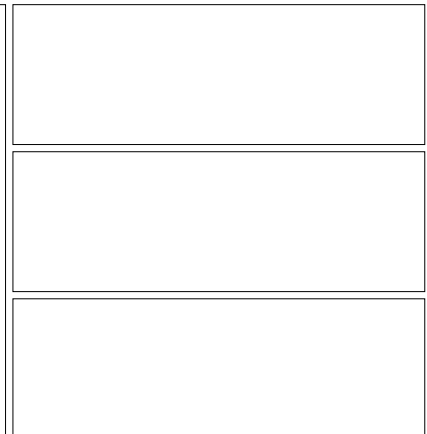


Nereites isp. from the Lower Carboniferous Yoredale Sandstone Formation, Northumberland, UK (Ph7)

Scale: 20 mm



Scale: 20 mm



CHAPTER 5

Organism-sediment interactions in shale-hydrocarbon reservoir facies - three-dimensional reconstruction of complex ichnofabric geometries and pore-networks

Małgorzata Bednarz and Duncan McIlroy

This paper will be submitted to *International Journal of Coal Geology*

5.1. Abstract

The lithological and mineralogical characteristics of mudstones and siltstones -and their stress-strain behaviour at the meter to nanometer scale – can play a critical role in the exploitation of unconventional shale reservoirs. Shale fabrics that result from bioturbation can produce extensive interconnected networks of biologically redistributed sediment grains within reservoir mudstone facies. The presence of biologically-generated heterogeneities may substantially affect reservoir stimulation and thus production from shale facies. This study presents volumetric evaluation of phycosiphoniform and aff. *Chondrites* ichnofabrics, and provides insights into the impact of trace fossils on the rheological and petrophysical characteristics of mudstones. It is calculated that in addition to creating significant volumes of silty (clay-poor) zones of enhanced porosity

and permeability, trace fossils create interpenetrating frameworks of brittle material that reduce communication distances from the low-permeability matrix to the higher permeability silt-rich burrows. Reducing communication distances to less than 1cm increases the potential for diffusive transport of hydrocarbon molecules from the “tight” matrix to the wellbore-connected volumes. This is because shale ichnofabrics create abundant fracture-prone planes of weakness, and increase the surface area of the interface between the hydrocarbon-rich matrix and porous burrow fills, thereby promoting fluid exchange. Understanding of the three-dimensional characteristics of ichnofabrics may form the basis of future modeling of fracture spacing and complexity that is critical to shale gas reservoir characterization.

5.2. Introduction

Gas- and oil-bearing shales are lithologically diverse, including inter-bedded very fine grained sediments e.g., mudstones, siltstones and limestones. Because of the lack of a universal classification system for these lithologically heterogeneous deposits the word ‘shale’ is used in this study in its broader meaning (e.g., Bustin 2012). The lithological and mineralogical characteristics of shales and their stress-strain behaviour at the meter to nanometer scale play a critical role in the exploitation of unconventional shale reservoirs (e.g., Bustin et al. 2008a, 2008b; Ross and Bustin 2008; Bustin and Bustin 2012; Chalmers et al. 2012b; Ding et al. 2012; Josh et al., 2012, Spaw 2013a, b).

The distribution of mineral grains and organic matter particles in mudstones comprise the macroscopic- and microscopic-fabrics (including ichnofabric) that determine the

petrophysical and geomechanical properties of mudstones (e.g., porosity, permeability and brittleness; Josh et al. 2012 and references therein). Individual burrows within an ichnofabric can redistribute sediment grains, thereby influencing both the bulk and small-scale petrophysical properties of the host sediment (e.g., Pemberton and Gingras 2005; Spila et al. 2007; Tonkin et al. 2010; Lemiski et al., 2011; Bednarz and McIlroy 2012; Gingras et al. 2012, 2013). Ichnofabric present in mudstones or siltstones has the potential to create permeability isotropy, e.g., by local destruction of sediment laminae (e.g., Schrieber 2003; Pemberton and Gingras 2005; Lemiski et al. 2011; Bednarz and McIlroy 2012; Gingras et al. 2012).

The spatial geometry of ichnofabrics reflects the cumulative effects of organism-sediment interactions after deposition (McIlroy 2004). In addition to the influence of bioturbation on the spatial distribution of fine-grained minerals, ichnofabric development in a sediment can also affect its mineralogy (McIlroy et al. 2003; Harazim 2013). The tortuosity, connectivity, surface area, volume and spatial distribution of the burrows in an ichnofabric are among the most significant factors determining response of the bioturbated mudstone or siltstone to reservoir stimulation techniques (e.g., Pemberton and Gingras 2005; Gingras et al. 2007, 2012; Bednarz and McIlroy 2012).

In this study, the potential influence of trace fossils on the petrophysical and rheological properties of hydrocarbon-bearing shale facies is presented. In contrast to our earlier work, we here consider the complete ichnofabric present in each studied sample rather than focussing on the reconstruction and quantification of isolated burrows (Bednarz and McIlroy 2009, 2012). The term aff. *Chondrites* is used herein with reference to all

Chondrites s.s. and other trace fossils closely resembling *Chondrites* isp. (cf. Bromley and Ekdale 1984; Wetzel and Wijayananda 1990; Fu and Werner 1994). The interchangeable terms “aff. *Phycosiphon*”, and “phycosiphoniform” burrows relate to an informal grouping of ichnofossils similar to *Phycosiphon* isp. (including *Nereites*), the trace fossils are commonly not identified at the generic level due to unresolved taxonomic issues. All phycosiphoniform burrows are considered to have similar effects on sediment fabric and reservoir quality in shale-hydrocarbon facies (cf. Bednarz and McIlroy 2012).

Ichnofabrics rich in aff. *Phycosiphon* isp. and aff. *Chondrites* isp. are here reconstructed in three dimensions in order to understand the spatial geometry and distribution of biologically redistributed mineral grains and properties in shale-hydrocarbon facies. In this study, we do not attempt to remove compaction of the sediment and its impact on the geometry of the burrows. Compaction affects the geometric relationships within ichnofabrics of gas-shales in a heterogeneous manner, but is beyond the scope of this thesis.

The computer modeled deterministic three-dimensional reconstructions allow volumetric consideration of the biogenic pore networks in the studied ichnofabric. The potential impact of aff. *Chondrites* ichnofabrics is addressed herein for the first time, and involves the same principles as used in our recent consideration of phycosiphoniform burrow volumetrics and morphometrics (see Bednarz and McIlroy 2012). The surface area, density and distribution of three-dimensional architecture of aff. *Phycosiphon* and aff. *Chondrites* ichnofabrics is also assessed herein through the generation of three-

dimensional deterministic models of aff. *Chondrites* and aff. *Phycosiphon* burrows in highly bioturbated sediments.

5.3. Main ichnofabric-forming trace fossils in hydrocarbon shale facies

The productive lithologies within shale-gas reservoirs commonly have inter-bedded layers of dark organic-rich very fine-grained sediments typically marine mudstones, inter-bedded with siltstones. It has been often considered that the black organic rich mudstones that form the basis of shale hydrocarbon plays were deposited in association with anoxia or severe dysoxia (e.g., Tyson 1995; Bohacs 1998; Katz 2005). The necessity for anoxia for black shale deposition has however been challenged (e.g., Schrieber 1994b, 2003, 2011; Wetzel and Uchman 1998b; Macquaker et al., 1999; Macquaker and Bohacs, 2007; Schrieber et al. 2007; Rodríguez-Tovar and Uchman 2010; Ghadeer and Macquaker 2012). A number of recent petrographic studies have demonstrated bioturbation in shale-hydrocarbon reservoir facies that previously seemed to be devoid of ichnofabric (e.g., Schieber 2003; Ghadeer and Macquaker 2012; Egenhoff and Fishman 2013). It may commonly be the case that bioturbation is present at a microscopic scale, and that both core and outcrop studies lack the resolution to determine such small structures, that commonly have subtle color contrast (cf. Wetzel and Uchman 1998a; Schrieber 2003; Egenhoff and Fishman 2013).

While dysoxic basins are generally considered to be hostile to macrobenthic organisms, the organic-rich sediments that are deposited host abundant small endobenthic organisms that are tolerant of dysoxic to anoxic pore waters (e.g., Bromley and Ekdale 1984; Savrda

and Bottjer 1991; Middelburg and Levin 2009). Such organisms with extreme tolerance to low-oxygen content (e.g., foraminifera) and/or small benthic organisms tolerant even to episodic total anoxia (e.g. nematodes, polychaetes, pogonophores, sipunculoid worms and bivalves) are responsible for bioturbation of organic-rich muds (e.g., Seilacher 1990; Savrda and Bottjer 1991; Dufour and Felbeck 2003; Stewart et al. 2005; Arndt-Sullivan et al. 2008; Dando et al., 2008; Dubilier et al. 2008; Middelburg and Levin 2009). The resulting trace fossil assemblages are typical of stressed ecosystems, in having low diversity, but commonly high abundance (e.g., Goldring et al., 1991; Bottjer 1993; Angulo and Buatois 2012a, b). The chemosymbiotic organisms (i.e. organisms having microbial symbionts capable of anaerobic respiration) from among the abovementioned phyla are the most likely to be candidate producers of *Chondrites* and *Trichichnus* (e.g., Swinbanks and Shirayama 1984; Seilacher 1990, 2007; Fu 1991; Zuschin et al. 2001). Both *Chondrites* and *Trichichnus* are deep tier trace fossils, most commonly recorded from anoxic mudstones, where they are often present in monospecific assemblages (e.g., Romero-Wetzel 1987; McBride and Picard 1991; Fu and Werner 1994; Rodríguez-Tovar and Uchman 2010). Of these two only *Chondrites* is a common ichnofabric-forming trace fossil (Callow and McIlroy 2011). The producer of *Chondrites* is usually inferred to be a chemosymbiotic organism and is used as an indicator of anoxic or dysoxic settings (e.g., Bromley and Ekdale 1984; Seilacher 1990, 2007; Fu 1991).

Phycosiphoniform trace fossils and *Chondrites*-like burrows that are the focus of this study, are amongst the most frequent ichnofabric-forming trace fossils observed in organic- and clay-rich siliciclastic marine deposits including both conventional and

Table 5.1. Examples of black/gray, organic-rich shale intervals, currently producing and potential shale-gas reservoirs with recognized presence of trace fossils. WCSB = Western Canadian Sedimentary Basin.

Organic-rich shale succession	<i>Chondrites</i>	<i>Phycosiphon-like traces</i>	<i>Helminthopsis</i>	<i>Paleophycus</i>	<i>Planolites</i>	<i>Rhizocorallium</i>	<i>Teichichnus</i>	<i>Trichichnus</i>	<i>Terebellina</i>	<i>Zoophycos</i>
New Albany Shales , Illinois Basin, USA (Cluff, 1980; Schieber, 2003; Lazar and Schieber 2004)	X	X			X					X
Fayetteville Shale , (AR, OK) Arkoma Basin, USA (Ceron and Slatt 2012)					X		X			
Woodford Shale , (OK), Anadarko Basin (Spaw 2013)	X									
Marcellus Shale , Appalachian Basin, USA (Spaw 2012)	X									
Ohio Shales , Appalachian Basin, USA (Lazar and Schieber 2004)	X				X	X	X			X
Chattanooga Shale , (TN) Black Warrior Basin, USA (Schieber 1994a, b)	X				X		X			
Bakken Formation , Williston basin, USA, Canada (Kasper 1992; Pemberton et al. 1992; Sonnenberg and Pramudito 2009; Angulo and Buatois 2011; Egenhoff and Fishman 2013; Gingras et al. 2013)	X	X	X		X		X			
Exshaw Formation , WCSB, Canada (Caplan and Bustin, 2001; Angulo and Buatois 20011)			X	X	X	X	X			X
Barnett Shale , Fort Worth Basin, USA (Loucks and Ruppel 2007; Ottmann and Bohacs, 2010)	X	X	X	X	X		X			X
Mancos Shale , Uinta Basin, USA (Macquaker et al., 2007; Bhattacharya and MacEachern 2009, Bednarz and McIlroy 2012)	X	X		X	X	X	X		X	
Mowry Shale , (WY) USA (Bohacs, 1998; Bohacs et al., 2005)	X	X	X	X	X	X	X		X	
Niobrara Shale , (KS) Denver-Julesburg Basin, USA (Jackson and Hasiotis 2013)	X				X		X			X
Kimmeridge Clay Formation , UK (Macquaker and Gawthorpe 1993; Morgans-Bell et al. 2001)	X				X		X			
Cleveland Ironstone and Whitby Mudstone Formations , UK (Ghadeer 2011; Ghadeer and Macquacker 2012)	X	X			X	X				
Alderson Member , (SK) WCSB Canada, (Hovikoski 2008; Lemiski et al. 2011)	X	X	X		X					X
Medicine Hat Member , (AB) WCSB, Canada (La Croix et al. 2013)	X	X	X	X	X	X	X			X
Montney Formation , (BC) Dawson Creek Region, Canada (Proverb et al. 2010)	X	X		X	X		X	X		X
Posidonia Shale , Germany (Savrda and Bottjer 1989; Seilacher 2007)	X									
Silurian shales of the East European Platform, Lublin Basin, Poland, (Porebski et al. 2013)	X	X			X		X			
Rosario Formation , Baja California, Mexico (Bednarz and McIlroy 2009, 2012, Callow et al. 2013a, b)	X	X	X		X					X

unconventional reservoir facies (Tab. 5.1; e.g., Cluff 1980; Wetzel and Bromley 1994; Pemberton and Gingras, 2005; Callow and McIlroy 2011; Leminski et al. 2011; Bednarz and McIlroy, 2012; La Croix et al. 2013). Other prominent trace fossils in organic-rich shale intervals are *Planolites*, *Zoophycos*, *Trichichnus*, *Helminthopsis*, *Paleophycus* and *Teichichnus* (e.g., Cluff 1980; Wetzel and Werner 1980; Callow and McIlroy 2011).

5.3.1. *Chondrites* ichnofabrics

Chondrites burrows are complex root-like systems of branching tunnels penetrating down with more or less vertical tunnel(s) from an opening at the sediment-water interface (e.g., Osgood 1970; Wetzel 1983, 2011; Löwemark et al. 2006; Wetzel and Reisdorf 2007; Pemberton et al. 2009). *Chondrites* and aff. *Chondrites* ispp. are common in very fine-grained sediments, such as organic-rich dark mudstones. In vertical cross section, the tunnels of *Chondrites* range from a fraction of a millimeter up to several millimetres in diameter, forming abundant circular spots. In organic-matter rich shale-hydrocarbon facies *Chondrites* burrows are generally filled by coarser-grained silty or very fine sandy material, depending on the lithology of the sediment overlaying the burrowed deposit. Where the infill is clay-rich, there is usually some colour contrast (e.g., Schieber 2003). Since the *Chondrites* producer was probably chemosymbiotic (thiotrophic and/or methanotrophic), it would likely have been able to survive and prosper in sediment with sulfidic pore waters, but would have had to have been connected to the sediment-water interface where at least some oxygen was available (cf. Bromley and Ekdale 1984; Seilacher 1990; Fu 1991; Stewart et al. 2005; Dando et al. 2008). *Chondrites* is

commonly the only macroscopic trace fossil found in black mudstones (e.g., Bromley and Ekdale 1984; Bottjer, 1993; cf. Schieber, 2003).

5.3.2. Phycosiphoniform ichnofabric

Phycosiphoniform burrows are produced by grain-selective deposit feeders and are most common in comparatively less organic-rich siltstones and silty mudstones (e.g., Goldring et al. 1991; Wetzel and Bromley 1994, Bromley 1996; Wetzel 2002, 2011; Bednarz and McIlroy 2009, 2012; cf. Egenhoff and Fishman 2013) than those with monotypic assemblages of *Chondrites*. These trace fossils have a mudstone-rich fecal core surrounded by a silt-grade light-colored quartzose halo (e.g., Bromley 1996; Wetzel and Bromley 1994; Wetzel 2002; Bednarz and McIlroy 2009, 2012; Callow et al. 2013a, b). The host sediment most probably had oxygenated or at least dysoxic interstitial waters to allow continuous burrowing without maintenance of a connection to the sediment-water interface (e.g., Wetzel and Uchman 1998 b, 2001; Wetzel 2002; Bednarz and McIlroy 2009, 2012). Phycosiphoniform-dominated ichnofabrics are common in silty hydrocarbon-bearing facies (e.g., Spila et al. 2007; Lemiski et al. 2011; Bednarz and McIlroy 2012 and reference therein; Egenhoff and Fishman 2013). In organic-rich shale settings phycosiphoniform burrows may commonly form monospecific ichnofabric, although *Phycosiphon-Nereites* or *Phycosiphon-Chondrites* or *Phycosiphon-Nereites-Chondrites* ichnofabrics are frequently observed (e.g., Goldring et al. 1991; Bottjer 1993, Wetzel and Uchman 2001; Angulo and Buatois 2012a, b; Callow et al. 2013a, b).

5.4. Methods

Samples of rocks containing *Chondrites*-like and phycosiphoniform burrows were serial ground with computer-controlled milling machine HAAS VF-3 CNC Vertical Machining Center. Serial grinding creates regularly spaced parallel surfaces that are photographed. The photographs were graphically processed in order to obtain consecutive digital images from which the burrows can be selected. The set of prepared images form the data from which a computer-based 3D reconstruction can be created (cf. Sutton et al.2001; Naruse and Nifuku 2008; Bednarz and McIlroy 2009, 2012, Bednarz et al. in press). Five spatial reconstructions of ichnofabrics were prepared and measured. All measurements were done on deterministic models of the ichnofabrics with no compensation for compaction.

Selected discrete burrows as well as specifically distinctive parts of spatial models enclosed in digital interactive 3D files were artificially colored for clarity and to examine burrow interrelations (Appx 5.1).

5.4.1. Volumetrics

The volumetric calculations provided herein are deterministic as they were made on the basis of the three-dimensional burrows at their natural scale. It should be noted that, because of algorithms used to optimize the mesh of the objects, the calculations include a small degree of error. These errors mostly give volume underestimates due to shrinking the mesh in the “mesh decimation” process (cf. Bednarz and McIlroy 2012; in press).

Quantitative analysis of the reconstructed burrow associations involves investigation of the three-dimensional models. The following variables are used herein to characterize the ichnofabrics considered herein (following Plat et al. 2010; Bednarz and McIlroy 2012; Bednarz et al. in press):

Volume available (VA) is the volume of the smallest rectangular prism (width = x , height = y and length = z) that encloses the burrow or burrow association. It represents the total volume of the sample that the examined burrows are enclosed within (Fig. 5.1A).

Volume utilized (VU) is the volume of the sediment reworked by the trace maker(s) and it is expressed in cubic units.

Volume exploited (VE) is the volume utilized presented as a percentage of the volume available to be bioturbated. It describes the efficiency of volume usage by the trace maker(s).

In the case of phycosiphoniform burrows, volume utilized can be subdivided into the mineralogically-different component parts of the trace fossil (silty halo and clayey fecal core; Fig. 5.2C, D). These are expressed as volume of halo ($\%Vh$) and volume of core ($\%Vc$). These measurements allowed for calculation of *core multiplicand (CM)* – a variable that captures the relative volumes of the silty burrow halo relative to that of the clay-rich fecal burrow core.

Surface area (SA) is a measurement of the total surface area of examined 3D models of ichnofabric. It is calculated by the visualizing software, and is given in square units.

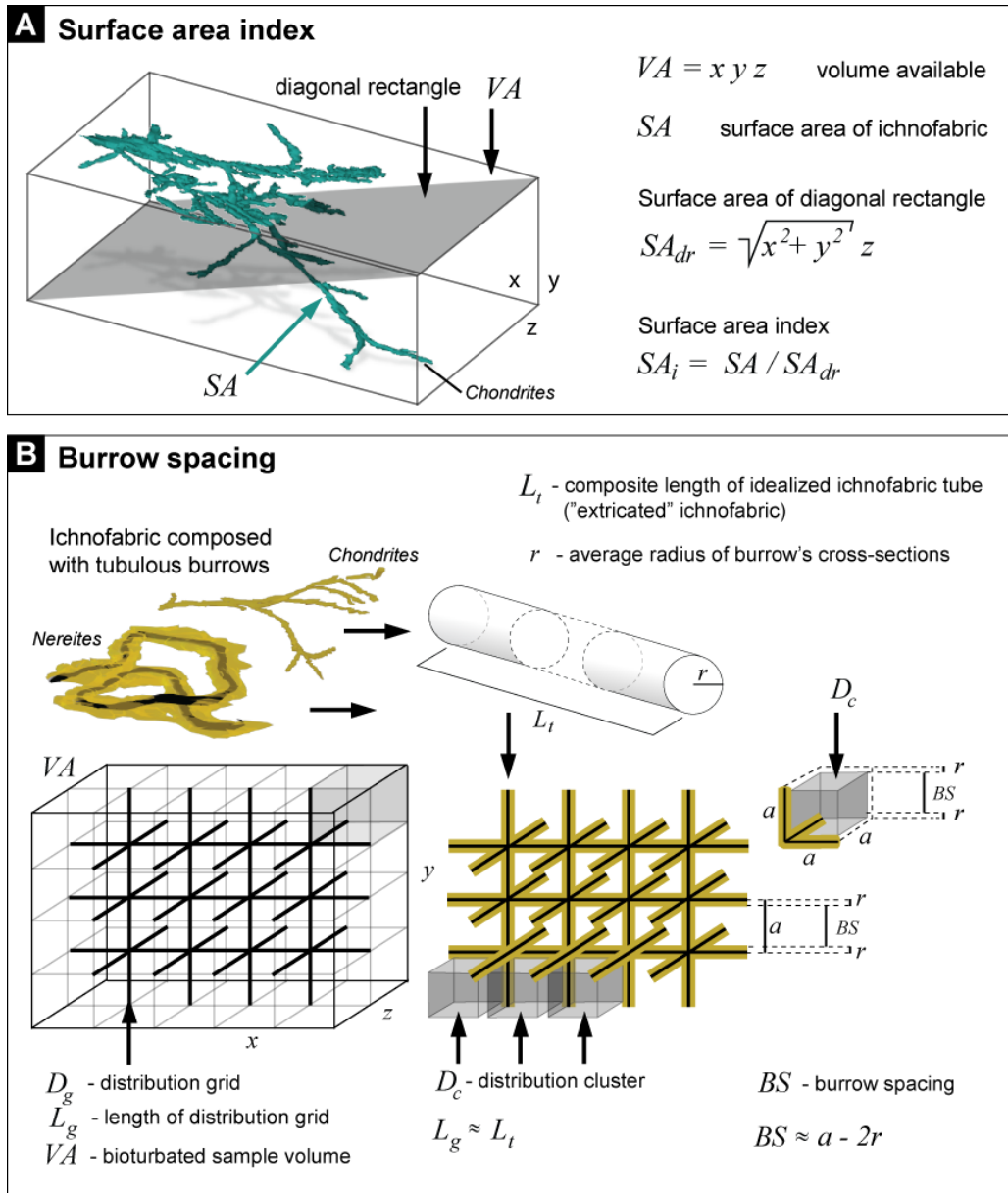


Fig. 5.1. Explanation of variables used to assess volumetric characteristics of the examined ichnofabrics. **A.** Surface area index explained. Surface area index illustrates how many times the surface area of ichnofabric is larger than the area that is shadowed by the ichnofabric (the horizontal section of the block). Surface area index additionally considers the volume of the bioturbated block through the value of the space diagonal of the block that is incorporated in the block section calculation. Example built on 3D model of a single aff. *Chondrites* burrow from Staithes. **B.** Burrow spacing explained. Distribution cluster is a box bounded by the edges of the modelled regular square-shape grid composed of idealized cylinders which summarized length corresponds to the total length of the ichnofabric tubes within the given size of volume available. *BS* – burrow spacing (spacing between burrow tubes) - describes the path length of hydrocarbon molecule transport through the matrix. *VDc* – volume of distribution cluster. Top 3D models illustrate representative individual burrows of *Nereites* from Craster and aff. *Chondrites* from Staithes.

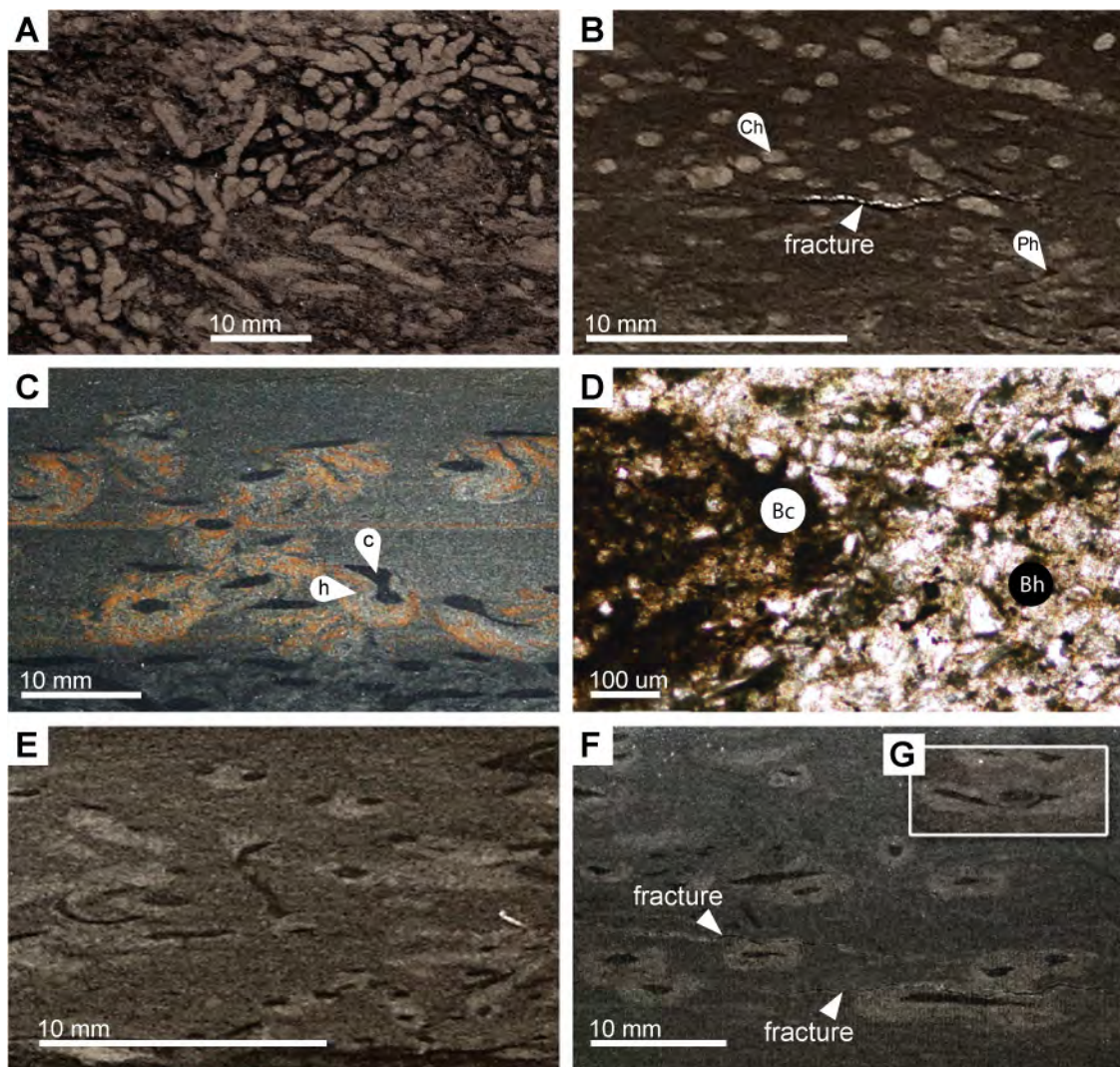


Fig. 5.2. Examined *Phycosiphon*-like and *Chondrites*-like ichnofabric.

A. Aff. *Chondrites* from Upper Cretaceous Mancos Shale, Muddy Creek, Utah; **B.** Aff. *Chondrites* from the Lower Jurassic Staithes Sandstone Formation, Yorkshire coast, UK; **C.** *Phycosiphon*iform burrows from the Upper Cretaceous Rosario Formation, Baja California, Mexico; **D.** Microscopy image showing clay-composed burrow core (c) and silty quartz-enriched halo (h); **E.** *Phycosiphon* s.s. from the Lower Jurassic Staithes Sandstone Formation, Yorkshire coast, UK; **F.** *Nereites* from the Mississippian Yoredale Sandstone Formation, Northumberland, UK; **G.** Cross-cutting relation of two burrows of *Nereites* from Craster. c – core; h – halo; Ch – *Chondrites*; Ph – *Phycosiphon*.

Surface area index (SA_i) is a unitless variable illustrating the ratio of burrow or ichnofabric surface area to the surface area of the rectangle that is diagonal to the box enclosing the ichnofabric (S_{Adr}). S_{Adr} reflects the rectangle surface area that is shadowed by the ichnofabric or burrow model (surface area of horizontal section of the sample block) and additionally it takes into consideration the vertical dimension of the block through its diagonal (Fig. 5.1A). Surface area index (SA_i) illustrates how many times the surface area of the ichnofabric or burrow is larger than the surface area of a shadowed horizontal interface such as mudstone bed or lamina.

Distribution cluster (D_c) is an individual segment of the unbioturbated rock matrix within a sample block which was cut by a square grid created with idealized cylinders representing extricated ichnofabric built by tubular burrows (Fig.5.1B).

Distribution cluster is presented as a volume (V_{Dc}) in cubic units and/or as a box of a calculated edge length ($a-2r$; Fig. 5.1B). Except for the most external clusters, each distribution cluster is bounded by the tubes composing the distribution grid (D_g). The total length of the distribution grid (L_g) approximately equals the total length of the extricated tubular burrows (L_t) constituting the ichnofabric volume (Appx 5.2). Distribution grid and distribution clusters illustrate burrow spacing.

Burrow spacing (BS) i.e. spacing between burrows (Fig. 5.1B). It is the length of the distribution cluster edge. Burrow spacing illustrates the approximate distance between the closest permeable fluid flow paths (burrow tunnels) to be reached by the hydrocarbon molecule travelling through the unbioturbated matrix (distribution cluster). The quantitative values of regular burrow spacing calculated in this study are intended for

comparison in order to grade the significance of burrow network present in gas- or oil-bearing shale, and do not reflect irregularity of the ichnofabric that is presented herein graphically as three-dimensional interactive models (Appx 5.1). Because of the irregularity of the ichnofabric, calculations of values of burrow spacing are intended to be considered as approximations.

5.5. Results

Samples containing aff. *Chondrites* and phycosiphoniform ichnofabrics were collected from deep-marine sedimentary facies that are comparable in grain size to many shale hydrocarbon reservoirs including the Mancos Shale studied from field-samples herein (see Bednarz and McIlroy 2012 and references therein).

The material was collected from the following localities:

1. Upper Cretaceous (Turonian) Ferron Sandstone Member of the Mancos Shale Formation, Muddy Creek, Utah (aff. *Chondrites* ichnofabric);
2. The Upper Cretaceous Rosario Formation, Baja California, Mexico (aff. *Phycosiphon* ichnofabric);
3. The Lower Jurassic Staithes Sandstone Formation, the Yorkshire coast, UK (ichnofabrics dominated by aff. *Chondrites* and *Phycosiphon s.s.* in two separate samples);
4. The Mississippian Yoredale Sandstone Formation, Craster, Northumberland UK (*Nereites* ichnofabric).

5.5.1. Examined aff. *Chondrites* ichnofabric

5.5.1.1. *Chondrites*-like ichnofabric from Upper Cretaceous Mancos Shale, Muddy Creek, Utah

One sample with dense aff. *Chondrites* ichnofabric was collected from the Ferron Sandstone Member of the Mancos Shale Formation in the canyon of Muddy Creek, East-Central Utah. The sample is composed of dark gray mudstone and is characterized by the presence of irregular bodies of light-colored sandy siltstone inferred to result from soft-sediment deformations that are typical of several Ferron Sandstone Member facies (e.g., loading structures and convolute bedding, see Bhattacharya and MacEachern 2009). This heterogeneous mudstone also contains aff. *Chondrites* burrows composed of the same silt-grade material as the irregular bodies (Fig. 5.2A). The mudstone was poorly lithified and had to be tightly taped to hold its consistency for the duration of transport and was encased in plaster for serial grinding. During serial grinding, plucking of the mudstone enhanced the contrast between the silty burrows and host sediment. The *Chondrites*-like form from Muddy Creek is relatively large. The average diameter of the tunnels is between 1 and 2 mm. The sample was serially sectioned with constant increment of 0.2 mm. The slab of the rock containing reconstructed ichnofabric can be bound in a box of 12.28 x 9.26 x 1.85 cm and is 210 cm³ (*VA*).

The high surface area index ($SA_i = 25.3$) illustrates significant degree of mudstone penetration by the *Chondrites*-like form from Muddy Creek. The volume of the total ichnofabric material (*VE*) present in the examined sample was only 7.5%, but it

interpenetrated the sample volume (VA) to a substantial degree (Fig. 5.3A; Appx 5.1A). The summarized length of all the tubes of the *Chondrites*-like trace present in this sample is approximately 8900 mm (almost 9 m), which accounts for an extremely long silt-filled tube considering the hand-sized sample volume. If such extremely long tube were to be used to create an idealized three-dimensional regular grid within the size of the sample from Muddy Creek it would cut the remaining 92.5% of unbioturbated matrix to distribution clusters (Dc) of volumes of about 122 mm³. Burrow spacing (BS) in this sample is approximately 5 mm (Tab. 5.2).

The outlines of the burrows in vertical cross section range from circular to elongated ellipses, strings, and also upward and downward branching structures that give the initial impression of burrow geometries and direction of burrow propagation (Fig. 5.2A). The frequent obliquely, upwardly directed or even vertically orientated burrows with dense branching suggest deposit feeding behaviour, rather than exclusively sulfide-mining by a chemosymbiotic organism as previously suggested (cf. Bromley and Ekdale 1984; Fu 1991, Kotake 1991; Callow and McIlroy 2011). The sample is densely bioturbated (BI IV \approx 70%), with almost all burrows being interconnected. The character of the burrow-burrow contact is therefore difficult to be precisely recognized but it is considered to be mostly the result of frequently adjoining walls of adjacent burrows. No obvious cross-cutting relationships between *Chondrites*-like burrows were observed on the image slices even where the bioturbation intensity was very high.

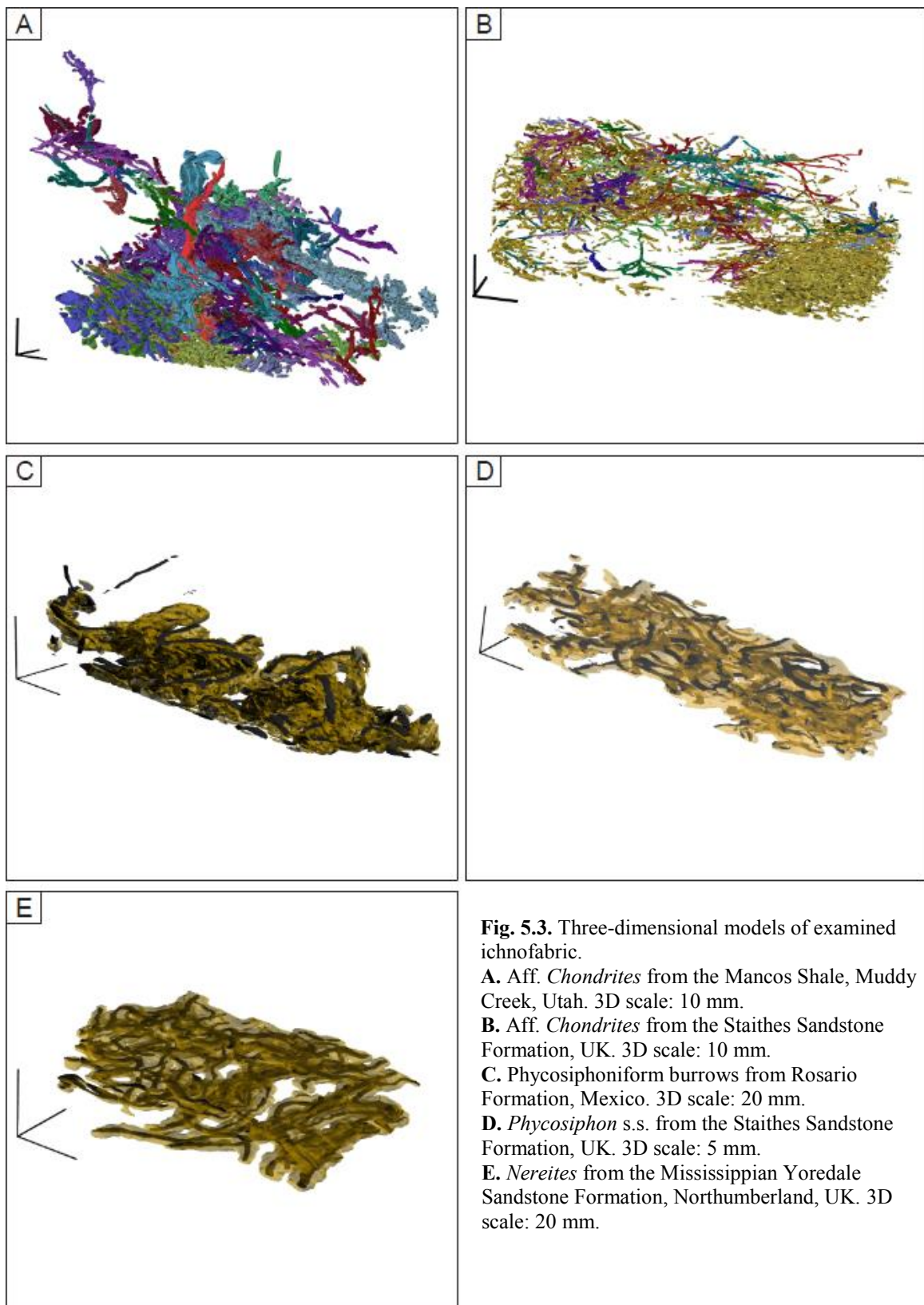


Table 5.2. Measurements of examined three-dimensional ichnofabric.

BI = bioturbation index; VA = volume available; VU = volume utilized; VE = volume exploited; $\%Vh$ = volume of the burrow halo(s); $\%Vc$ = volume of the burrow core(s); CM = core multiplicand; SA_i = surface area index; BS = burrow spacing; VDc = volume of distribution cluster; $2r$ = average diameter of burrows' cross sections; L_g = length of distribution grid.

Ichnofabric	Prism dimension			BI	VA	VU	VE			SAi	BS	VDc	2r	Lg
	x	y	z											
	mm													
Aff. Chondrites ichnofabric Upper Cretaceous Mancos Shale, Muddy Creek, Utah	122.8	92.6	18.5	IV (70%)	210.45	15.74	7.5			25.3	5.0	122.8	1.5	891.3
Aff. Chondrites ichnofabric Lower Jurassic Staithes Sandstone Formation, Yorkshire, UK	83.9	23.2	39.6	IV (65%)	77.04	2.62	3.4			20.5	4.5	90.5	1	333.8
Phycosiphoniform ichnofabric Upper Cretaceous Rosario Formation, Baja California, Mexico	152.0	33.7	29.5	III (35%)	151.08	29.17	%Vh	%Vc	CM	9.5	8.6	636.1	8	58.0
							19.3		6.5					
							16.7	2.6						
Phycosiphon s.s. ichnofabric Lower Jurassic Staithes Sandstone Formation, Yorkshire, UK	39.5	6.0	11.8	IV (65%)	2.78	0.87	31.3		4.8	5.3	1.6	4.1	2.5	17.9
							25.9	5.4						
							14.7							
Nereites isp. ichnofabric Mississippian Yoredale Sandstone Formation, Craster, UK	98.6	27.9	49.6	II – III (30%)	136.41	20.07	13.3	1.4	4.8	9.5	843.9	6	71	

5.5.1.2. *Chondrites*-like ichnofabric from the Lower Jurassic Staithes Sandstone Formation, Yorkshire coast, UK

A sample containing dense aff. *Chondrites* burrows was collected from the lower part of the Jurassic Staithes Sandstone Formation, North Yorkshire, UK. The burrows are in a dark gray to black silty mudstone containing some very light gray siltstone layers.

The sample is densely bioturbated ($BI\ IV \approx 65\%$). In vertical cross section *Chondrites*-like burrows are seen mainly as rounded and ellipsoidal shapes of 1 mm in diameter on average. The burrows are filled with light gray silt and visually contrast with the dark gray host sediment. The sample contains a fracture that runs sub-parallel to bedding, but its geometry is modified by shape of *Chondrites*-like tubes (Fig. 5.2B). Aff. *Chondrites* systematically postdates and cross-cuts the *Phycosiphon s.s.* in the examined sample, mostly where silty material is in elevated concentrations (Fig. 5.2B; cf. Bednarz and McIlroy 2012). *Phycosiphon s.s.* from the same formation, but from a different sample, was also reconstructed.

The sample was serially sectioned with constant increment of 0.2 mm. The slab of the rock containing reconstructed ichnofabric can be inscribed in the box of size of 8.39 x 2.32 x 3.96 cm (i.e. 77 cm³; VA). The high surface area index ($SA_i = 20.5$) illustrates the significant degree of mudstone penetration by the ichnofabric built of burrows of aff. *Chondrites* from Staithes. The volume of the ichnofabric in this sample constitutes only 3.4% (VE , Tab. 5.2) of the total volume of the sample. The summarized length of all the tubes of the *Chondrites*-like trace present in this sample was calculated and it is

approximately 3335 mm (3.3 m), which accounts for an extremely long silt-filled tube considering the small size of the sample. The idealized three-dimensional regular grid created with this tube would cut the remaining 96.6% of unbioturbated matrix to distribution clusters (D_c) of volumes of about 90 mm³. Burrow spacing (BS) is approximately 4.5 mm (Tab. 5.2).

The branched systems constituting this type of *Chondrites*-like burrows diverge essentially horizontally, with a variable angle of downward, and also upward, inclination relative to bedding. The presence of obliquely- and vertically-directed branches, coupled with the intense bioturbation of this sample has significant influence on the vertical connectivity of the burrows enclosed within it (Appx 5.1B, view: vertical branching). The resultant ichnofabric is a network of vertically and horizontally interconnected silt-filled tunnels that densely penetrate the hosting mudstone from the top to the bottom of the examined sample (Fig. 5.3B; Appx 5.1 B). Burrow tunnels principally neither cross-cut themselves, nor any other burrow. The burrow-burrow contact has mainly the character of locally adjoining walls of adjacent burrows and is most probably the effect of the sediment compaction. Additionally, connectivity of the burrows is enhanced through the presence of composite master shafts of the aff. *Chondrites*. Such mostly horizontal master shafts were identified as having multiple bundled and adherent tubes coalescing often into one thicker tubular, branching, structure (Fig. 5.4; Appx 5.1B, view: bundled master shafts).

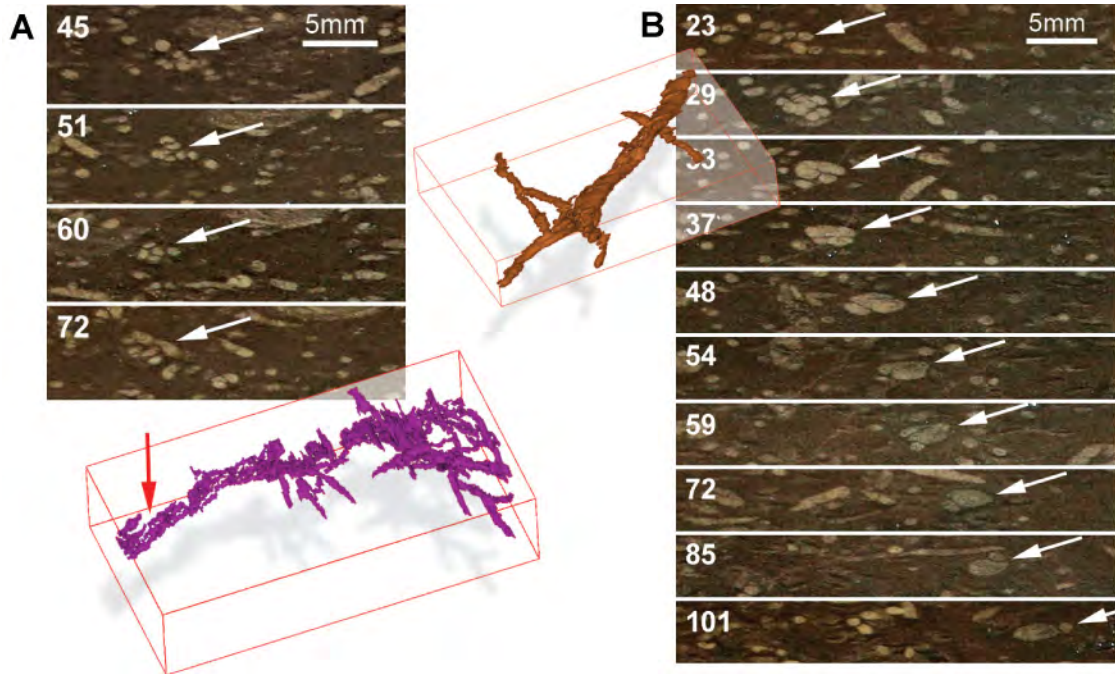


Fig. 5.4. Composite master shafts of burrows of aff. *Chondrites* from Staithes.

The numbers on the left side of the photos stand for the slice numbers. The master shafts are positioned horizontally. **A.** Master shaft composed of multiple bundled tunnels of diameters the same as the average diameter of branches (~ 1 mm); **B.** Master shaft composed of several tunnels of the average diameter (~ 1 mm) merging into one of a significantly larger diameter (up to 400% larger).

5.5.2. Examined *Phycosiphon*-like ichnofabrics

The detailed volumetric three-dimensional reconstructions of the phycosiphoniform burrows were recently presented and analyzed (Bednarz and McIlroy 2009, 2012). The results of this analysis are incorporated in this study and along with the new data and calculations are subject of further interpretation.

5.5.2.1. Phycosiphoniform burrows from the Upper Cretaceous Rosario Formation, Baja California, Mexico

A sample containing dense *Phycosiphon*-like ichnofabric was collected from coastal exposures of the Upper Cretaceous (Maastrichtian) Rosario Formation. The rock hosting the ichnofabric is a laminated, organic-rich turbiditic siltstone (see Bednarz and McIlroy 2009, 2012; Callow et al. 2013a, b). An isolated fragment of a tube of *Bathysiphon* was observed in the examined sample. This agglutinated foraminifer has been found to abundantly occur in muddy deposits of Rosario Formation (Callow et al. 2013a). The *Phycosiphon*-like ichnofabric from Rosario Formation is composed of anomalously large burrows, with the average major axis of the burrow cross section being 8 mm (Fig. 5.2C). Bioturbation is moderately intense (BI III or 35%).

The silty quartz- and feldspar-dominated burrow halo is essentially lacking clay-sized components (<10%) and structured organic matter what results in the higher porosity compared to the host sediment (0-5% and about 30% respectively; Harazim, 2013). The core material is found to contain elevated amounts of organic carbon compared to matrix (average TOC values equal 1.8 wt% and 0.6 wt% respectively; Harazim, 2013).

The volume of burrow halo material can reach as much as about 17% of the total sample volume (Tab. 5.2). The volume of the halo material is on average 6.5 times greater than the volume of the burrow core (*CM*), which constitutes 2.6% of the total volume of the sample. Un-branched black clay-rich cores of individual burrows never cross-cut themselves or any other burrow core constructing continuous and tortuous isolated cylindrical strings often arranged in vertical loops. Contrary, silty haloes of adjacent burrows are widely connected in vertical and/or horizontal direction dependently on the burrows' spatial arrangement and locally elevated or decreased burrow density (Fig. 5.3C; Appx 5.1C).

The volumetric assessment of the sample with phycosiphoniform ichnofabric from Rosario Formation shows that, even with moderate density of bioturbation, the ichnofabric creates highly interconnected framework of silt-rich and porous zones (Fig. 5.3C; Appx 1 C). Distinct difference in mineralogy and grain size of burrow and matrix material generates moderately large surface area of the ichnofabric-matrix interface - the surface area index is calculated as being 9.5. The idealized three-dimensional regular grid created with the idealized burrow tube would cut the remaining 80.7% of unbioturbated hosting sediment into distribution clusters (*Dc*) of volumes of about 636 mm³. Burrow spacing (*BS*) is approximately 8.6 mm.

5.5.2.2. *Phycosiphon sensu stricto* from the Lower Jurassic Staithes Sandstone Formation, Yorkshire coast, UK

A sample with *Phycosiphon s.s.* burrows was collected from the lower part of the Jurassic Staithes Sandstone Formation, North Yorkshire, UK - the same locality as the sample of dark mudstone containing *Chondrites* ichnofabric described above. The *Phycosiphon* traces are hosted in a light gray fine-grained muddy siltstone (Fig. 5.2E).

The volume of rock containing the reconstructed ichnofabric is small 2.78 cm^3 (VA). The average major axis of cross sections from the elliptical burrows was 2.5 mm. Volumetric examination of the reconstructed *Phycosiphon* from Staithes shows that the volume of the halo material is on average 4.5 times greater than the volume of the burrow core (CM). The quartzose burrow halo material (%Vh) measured for the entire volume of the bioturbated rock sample (with BI 4 or 65%) constitutes almost 26% of this volume. Despite the very high burrow density the unbranched burrow cores never crosscut themselves or any other burrow. Silty haloes of adjacent burrows are widely connected in vertical and/or horizontal direction (Fig. 5.3D; Appx 5.1D). The surface area of the burrow-matrix interface created by the *Phycosiphon* ichnofabric from Staithes is moderately large - the surface area index is calculated as being 5.3. The idealized three-dimensional regular grid created with *Phycosiphon* tube would cut the unbioturbated sediment to distribution clusters (Dc) of volumes of about 4.1 mm^3 . Burrow spacing (BS) is approximately 1.6 mm.

5.5.2.3. *Nereites* isp. from the Mississippian Yoredale Sandstone Formation, Northumberland, UK

A sample containing *Nereites* ichnofabric was collected from the coastal exposure of Mississippian Yoredale Sandstone Formation, Northumberland, UK. The intensity of the bioturbation in the sample is low (BI II-III or 30%). The bioturbation cross-cuts a gray parallel laminated siltstone (Fig. 5.2F). The burrows are relatively large, average length of a major axis of the cross section is 6 mm.

The clay-rich cores of *Nereites* from Craster never crosscut themselves. However there has been found one case when the burrow core of larger diameter cross cuts the one of smaller size (Fig. 5.2G; Appx 5.1E, view: cross cut). The crosscutting relationships are clearly visible in vertical cross section, and cannot be explained by the effect of the compaction. Silty haloes of adjacent burrows are widely connected in vertical and/or horizontal direction (Fig. 5.3E; Appx 5.1E).

Volumetric data indicate that the volume of a burrow halo is about 8 times larger than the volume of core material (*CM*). The volume of quartzose halo material in this sample is 13.3% (*%Vh*). The surface area index is moderately large and is calculated as being 4.8. The idealized three-dimensional regular grid created with the observed *Nereites* tubes would cut the remaining 85.3% of unbioturbated matrix to distribution clusters (*Dc*) of volumes of about 844 mm³. Burrow spacing (*BS*) is approximately 9.5 mm.

The sample has natural fractures that run sub-parallel to bedding, but where fractures intersect burrow haloes, the fracture plane is changed (Fig. 5.2F).

5.6. Discussion - The effect of ichnofabric on mudstone properties and shale reservoir potential

5.6.1. Porosity and permeability of the bioturbated reservoir facies

The tortuous and interconnected geometries of *Phycosiphon*- and *Chondrites*-like ichnofabric that occur in hydrocarbon-bearing shales are frequently composed of coarser-grained, quartzose brittle material. Cemented or not, these burrows may provide additional pore volumes either through development of natural (micro)fractures (fracture porosity) and/or from inter-granular porosity inherited by the porous nature of silt-grade material respectively. In either case, the ichnofabric would make the facies dual-porosity or dual-permeability flow media (sensu Gingras et al. 2007, 2012). Porosity of silty and sandy ichnofabric material in bioturbated intervals may also constitute an additional space for hydrocarbon molecules concentration thereby improving capacity and storativity of the reservoir (Pemberton and Gingras 2005; Gingras et al. 2007, 2012; Bednarz and McIlroy 2012; La Croix et al. 2013).

Phycosiphon-like ichnofabric has been proven in the laboratory to show orders of magnitude greater permeabilities than the surrounding muddy matrix (Spila et al. 2007; Lemiski et al. 2011; Gingras et al. 2012, 2013; La Croix et al. 2013). The vertical connectivity of *Phycosiphon*-like and *Chondrites*-like ichnofabrics breaches impermeable horizontal barriers of originally layered hosting shale reservoir intervals that are typically composed of interbedded mudstones and siltstones. This results in homogenisation of the bulk volume of sediment at the macro-scale causing porosity and permeability isotropy

due to obliteration of otherwise impermeable horizontal lithological barriers (equalizing vertical permeability [k_v] with horizontal permeability [k_h]; Pemberton and Gingras 2005; Spila et al. 2007; Lemiski 2011; Bednarz and McIlroy 2012; Gingras et al. 2012; La Croix et al. 2013).

The biogenic pore-networks representing primary or additional fluid flow paths may constitute a significant volume of the shale interval - up to 26% of the total rock volume in case of phycosiphoniform ichnofabric. If burrows do not significantly contribute to the volume of silty material within the host sediment (3.5 – 7.5% in case of *Chondrites*), they may provide vast and tortuous planes of weakness promoting development of fracture porosity additionally enhancing burrow-to-matrix interactions through their deeply penetrative nature (Fig. 5.5).

At the millimetric scale, ichnofabrics can increase heterogeneity in the form of localized concentrations of - for example: 1) silt- and sand-grade grains of brittle minerals; and/or 2) clay-grade particles (Fig. 5.2D) that are present in an immediate vicinity to the organic-rich mudstone matrix thereby improving the efficiency of complex fluid flow mechanisms typical for low-permeability mudstones (Fig. 5.6). It may be particularly important within organic rich and hydrocarbon prone black mudstones that are the richest sources of gas or oil within the reservoir and that are typified with very low porosities and ultra-low permeabilities. The majority of the porosity within such organic rich mudstones is considered to be located within particles of organic matter e.g., kerogen (e.g., Passey et.al. 2010; Swami 2012; Bust 2013). If bioturbated, such mudstones may have additional porosity within silty-rich burrow tubes or natural micro-fractures and

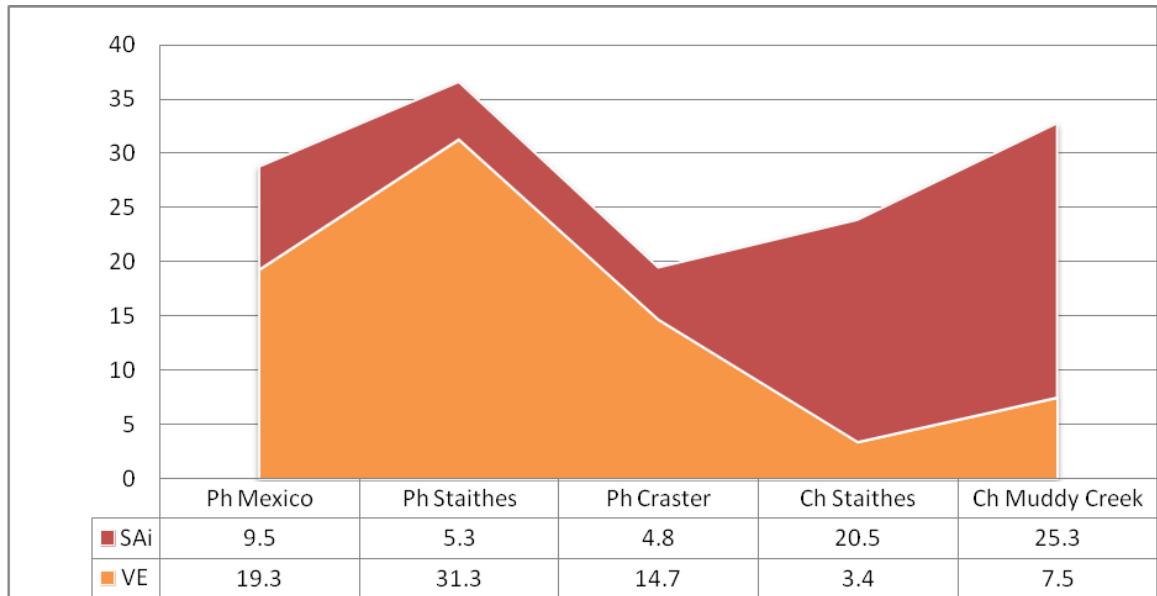


Fig. 5.5. Chart illustrating relation of volume exploited (VE) to surface area (SA_i) of *Phycosiphon*- and *Chondrites*-like ichnofabric.

Phycosiphon-like ichnofabric constitutes significant volume of the bioturbated samples but has smaller surface area relative to *Chondrites*-like ichnofabric that has extensive surface area (potential planes of weakness) associated even with a small volume of the ichnofabric.

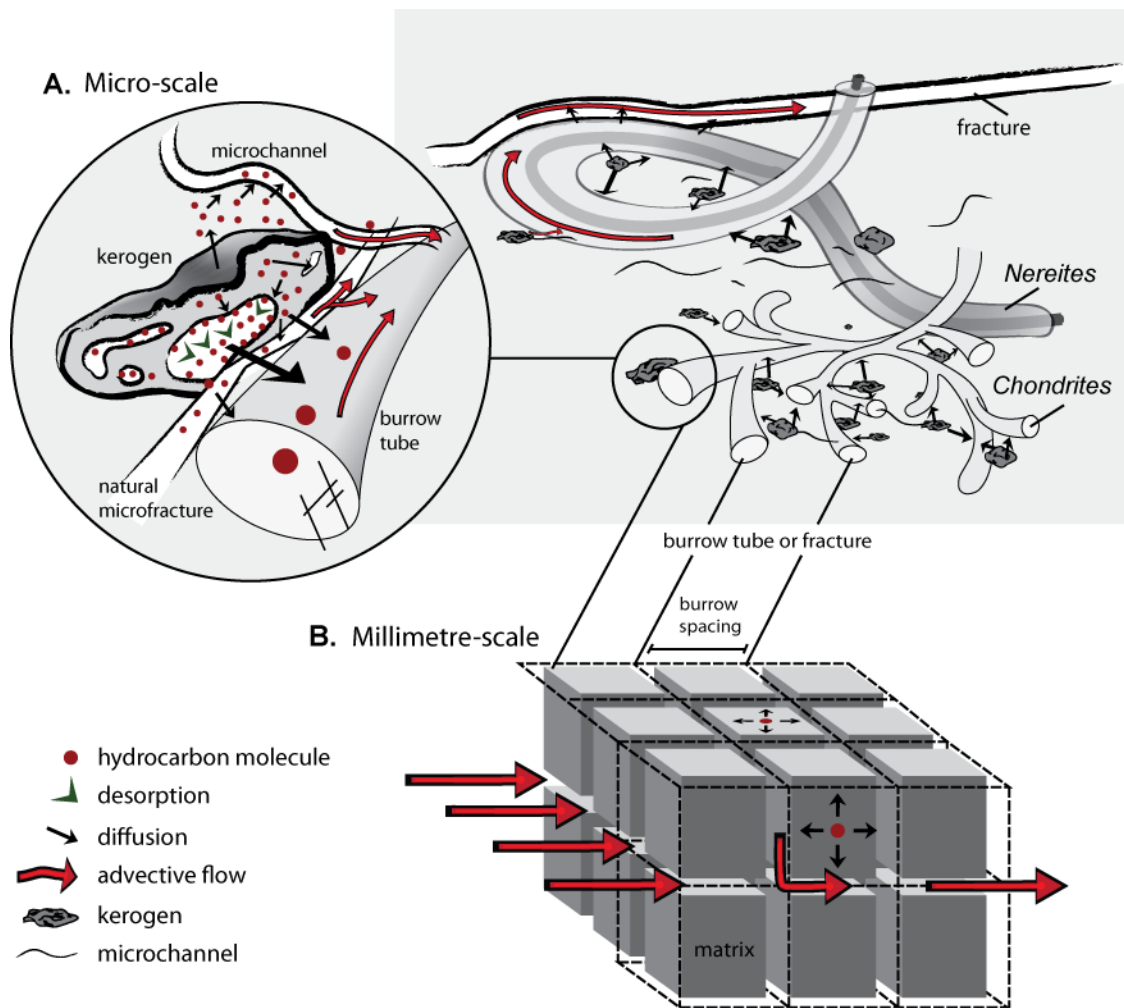


Fig. 5.6. Schematic illustration presenting stages of the fluid flow within bioturbated, gas-charged tight mudstone.

A. Micro-scale. With pressure drop hydrocarbon molecules enter the organo-porosity through desorption from pore walls and kerogen material. If the pore is connected to the (micro)fracture or microchannel, molecules travel through the conductive flow paths to the well bore. If there is no fracture or microchannel connected to the organoporosity, the molecules travel to the fracture network or permeable flow path through diffusion.

B. Millimetre-scale (modified from Bustin et al. 2008a). Efficiency of the flux of the diffusively migrating molecules into the fracture network is dependent on the distance from oil- or gas-charged pore to the closest fracture or permeable flow path. Dense ichnofabric network minimize the distance of the diffusive flow through partitioning the hosting rock with permeable and brittle silty tubes and may also improve fracture spacing and/or complexity.

Inspired by reservoir studies by Bustin et al. 2008a.

“micro-channels” developed along and/or within the brittle burrow fill (cf. Schrieber 2003; Slatt and O’Brien 2011). Therefore fossils of quasi-anaerobic biofacies (sensu Savrda and Bottjer 1991) can substantially contribute to the improvement of the porosity and vertical permeability of source rock even if present in a microscale.

5.6.2. Brittleness of bioturbated shale.

The mineralogically-based brittleness of any shale depends on ratio of a sum of quartz and all other brittle minerals content (e.g., feldspars or carbonates) and clay-mineral content (e.g., Jarvies et al. 2007; Bust et al. 2013). This proportion has to be favourable in its brittle mineral content (mainly quartz) in order to consider a rock brittle and thus fracturable. If clay minerals are predominant in relation to brittle minerals the mudrock is ductile and will not respond efficiently to fracturing. The fracturability is a determining factor for effective petroleum producibility from the well (e.g., Narr and Currie 1982; Jacobi et al. 2008; Jenkins and Boyer 2008; Ross and Bustin 2009; Bust et al. 2013). The quartz-dependent brittleness of the rock combines rock ability to fail under stress and to maintain the fracture once the rock fractures (Rickman et al. 2008). Even as small amount as 3.4% of biogenically concentrated silty and quartz-rich material within the total volume of a clay-dominated mudstone thereby may create a dense irregular boxwork of fracture-prone material (see aff. *Chondrites* ichnofabric from Staithes, Tab. 5.2). Thus, mudstones that are generally considered as ductile, if bioturbated, may have potential to be fractured and possibly also to maintain the micro-fractures created within quartzose burrow microenvironment which is devoid of clay particles that could cause fracture

“healing”. Networks of the narrow quartzose tubular burrows distributed within a clay-rich matrix may be fractured on a microscopic scale during initial phases of deformation if such conditions occur during mudstone burial history. Consequently, micro-fractures have the potential to coalesce into a single through-going macroscopic fracture and may therefore enhance the brittle failure characteristics of the bulk volume (Petley 1999).

The stress-strain behaviour of bioturbated mudstones has not yet been studied in either the laboratory or the field. It is considered herein to be the next frontier for ichnological studies of shale-hydrocarbon reservoirs. The anisotropic horizontal stresses that result from laminated structure of shales may also have severe consequences for drilling if not addressed (Khan et al. 2011). Since ichnofabric obliterates the primarily laminated structure of most shales and thus improves both permeability and stress isotropy (e.g., Pemberton and Gingras 2005; Gingras et al. 2012), it is realistic to imply that the presence of dense and interconnected network of thin brittle tubes embedded within a clay-rich matrix will alter the response of mudstone to applied stress regimes. The predominant volume of the clay-rich matrix of bioturbated mudstone or siltstone (~ 75% - 96%), with its inherited susceptibility to compaction, may respond to applied stress through extensive shattering of regions with thin, brittle silty tubes that commonly constitute mudstone ichnofabrics.

Millimetre scale ichnofabric-induced fracturability, when upscaled to the reservoir scale, can be considered to be a potential major influence on shale hydrocarbon reservoirs. This assumes that the lateral distribution of the bioturbated facies is large and continuous; such information is not yet known, but seems likely from qualitative field observations (e.g.,

Cluff 1980; McIlroy 2007; Angulo et al., 2008; Hovikoski et al., 2008; Lemiski et al., 2011; Angulo and Buatois, 2012a, 2012b; Gingras et al. 2012; Callow et al., 2013a; Egenhoff and Fishman 2013).

5.6.3. Impact of ichnofabric on fracture spacing and complexity

The presence of planes of weakness, pre-existing natural fractures or sediment fabrics within shales generates geometrically complex induced hydraulic fractures (e.g., Cipolla et al. 2009; Fan et al., 2010; Palmer and Moschovidis 2010; Bustin and Bustin 2012). Inducing the largest possible complexity of man-made fracture network that maximizes the surface area of the reservoir that is connected to the well-bore is the key factor for improved drainage and well productivity (e.g., Cipolla et al. 2009, 2010; Wang et al. 2009; Fan et al. 2010; Khan et al. 2011, 2012; Bust et al. 2013). In order to achieve this, recognition and activation of pre-existing natural fractures and/or planes of weakness and/or rock fabric within the stimulated interval is crucial (e.g., Bowker et al. 2007; Cipolla et al. 2009, 2010; Bustin and Bustin 2012). The complex geometry of the ichnofabric, and its inherently large surface area, functions as a cylindrical, tortuous three-dimensional surface of weakness that separates brittle silty burrow infill from relatively ductile muddy matrix. Quartz-rich ichnofabrics may therefore propagate natural and/or induced fractures in dense, complex geometries, and improves fracture spacing (Fig. 1B; Fig. 5.6; burrow spacing may be a framework for modeling of effective fracture spacing). *Chondrites*-like ichnofabrics may create such dense ichnofabrics even though

this type of ichnofabric usually constitutes low sediment volume (Fig. 5.5; e.g., aff. *Chondrites* from Staithes with its summarized tube length of 3.3 m constitutes only 3.4% of the total sample volume of 77 cm³ and it partitions the host rock with burrow spacing of 4.5 mm; Tab. 5.2).

However, even the most complex fracture network may be uneconomical without sufficient conductivity (the ability to transport fluid through e.g., “un-propped” porous material) (Cipolla et al. 2009). It is possible that the silty tubes of *Chondrites*-like and *Phycosiphon*-like networks, being exceptionally interconnected both horizontally and vertically, would play a considerable role in providing conductive fluid flow pathways in addition to fractures. This additional connected pore-volume would increase gas production, which is known to increase with permeability enhancement and is inherently linked with fracture spacing and conductivity within the stimulated reservoir volume (cf. Palmer et al. 2010).

5.6.4. Impact on fluid flow within bioturbated shale

The advective flow of free gas from matrix porosity and natural fractures is possible because of permeability and conductivity generated through hydraulic fracturing that increases the surface area in contact with hydrocarbon-charged porosity (cf. Ballard et al. 1994). This type of flow from source rock to the well bore is responsible for the enhanced production rates from the well in the first months after reservoir stimulation (e.g., Cipolla et al. 2009; Fan et al. 2010). After this time it is usually the case that well performance will still be economically producing and surprisingly long term production is observed in

some wells (e.g., Swami 2012; Swami et al. 2012). This phenomenon is explained by desorption of hydrocarbon molecules from organic matter or clay minerals triggered by pressure drop during production (e.g., Javadpour et al. 2007; Cipolla et al. 2009; Fan et al. 2010; Swami 2012; Swami and Settari 2012). It is considered that the hydrocarbons released from their dissolved and/or sorbed state can constitute the majority of the total hydrocarbons in place, and may be more than 50% of gas produced, especially in shallow to moderate reservoir depths (e.g., Cipolla et al. 2009; Fan et al. 2010; Swami 2012; Swami and Settari 2012). It is thus crucial that organo-porosity is connected to the fracture network, and/or that fracture spacing is improved such that the distance of diffusive hydrocarbon flow through the sediment is minimized (Bustin and Bustin 2012). The tight mudstone matrix is the main attenuator for diffusive gas molecule flow as this sluggish process is dependent not on pressure, but on available pore space and pore volume, pore-throat size and pore distribution within the mudstone (Ballard et al. 1994; Swami 2012; Swami et al. 2012). Decreasing communication distances to a few millimetres between kerogen particles and silt-rich ichnofabrics may considerably improve the bulk diffusive potential of the mudstone (Fig. 5.6). *Chondrites* ichnofabric, though not sizable in volume, has a disproportionately large surface area and connectivity, creating closely-packed three-dimensional conduits composed of very thin silt-composed tubes surrounding small volumes of petroliferous mudstone (with burrow spacing of 4.5 - 5 mm; Fig. 5.5). Accordingly a shortcut is created for sluggish diffusional flow from matrix into the porous trace fossils and associated loci of potential micro-fractures (Fig. 5.6B; cf. Bustin et al. 2008a; Bustin and Bustin 2012).

Small burrows may not be a well-recognized conduit for transport of desorbed gas and thus elevated producibility but it is possible that burrows provide improved dispersivity (i.e. rock property related to hydrodynamic spreading of a solute or phase that is intensified by the heterogeneity of the porous medium; see Gingras et al. 2012) of otherwise ultra-tight and ductile mudstones (cf. Schrieber 2003).

5.7. Conclusion

The burrow architecture of *Chondrites*-like forms shows an adaptation that maximizes the surface area of the burrow system for enhanced solute exchange. Feeding strategy of producers of *Chondrites*-like burrows is usually considered to rely on substrate exchange (sulphide mining sensu Seilacher 1990; Fu 1991) in order to gather as much substrates for chemoautotrophic symbionts as possible. The most effective burrow architecture for such purpose is one that offers extensive surface area penetrating large volumes of ambient sulfide-rich pore waters.

The architecture of *Phycosiphon*-like burrows shows an adaptation that maximizes the volume of the host-sediment exploited. *Phycosiphon*-like ichnofabric may provide the bioturbated interval with up to 25% of brittle, quartz-rich material that may be up to 30 times more porous than the surrounding matrix. The small volumes of phycosiphoniform burrow cores (~ 1 -5%) may contain high concentrations of low reactivity organic carbon and should therefore be considered during interpretation of TOC values from shale-hydrocarbon reservoir facies with such burrows.

From the well stimulation point of view it is crucial to understand volumetric relation between brittle silty ichnofabric and ductile clay-rich matrix. The interrelated structural and mineralogical heterogeneities typical for aff. *Phycosiphon*, *Nereites* and aff. *Chondrites* influence shale gas reservoir quality in a number of ways:

- 1) By introducing or concentration of various volumes (3.5% - 26%) of silty material in form of homogenous quartz-rich and clay-depleted burrow fills, thereby creating preferential fluid flow paths and improving bulk-volume brittleness;
- 2) By creation of brittle and/or porous burrow fills throughout the vertical extent of the tight muddy—often laminated—host rock, thereby improving permeability isotropy ($k_h \approx k_v$) and increasing stress isotropy;
- 3) By creating tortuously distributed, disproportionally large, burrow-sediment interfaces that act as fracture-prone planes of weakness and form the basis for improved matrix-solute exchange, thereby improving bulk shale fracturability and dispersivity respectively;
- 4) By creating dense, highly interconnected brittle boxworks that improve fracture-spacing and fracture connectivity. Burrow spacing (millimeters long) should form the basis for future modeling of fracture spacing and assessment of fracture complexity in stimulated gas- or oil-shale intervals with bioturbation;
- 5) By partitioning the petroliferous shale matrix to small volumes (around 1 cm³), thereby enhancing bulk diffusive efficiency of hydrocarbon flow to the well-bore, consequently improving productivity.

5.8. References

- Algeo, T.J., L. Schwark, and J.C. Hower, 2004, High-resolution geochemistry and sequence stratigraphy of the Hushpuckney Shale (Swope Formation, Eastern Kansas): Implications for climato-environmental dynamics of the Late Pennsylvanian Midcontinent Seaway: *Chemical Geology*, v. 206, p. 259-288.
- Angulo, S., and L.A. Buatois, 2011, Petrophysical characterization of sedimentary facies from the upper Devonian-Lower Mississippian Bakken Formation in the Williston Basin, Southeastern Saskatchewan, In: *Summary of Investigations 2011*, v.1, Saskatchewan Geological Survey, Sask. Ministry of Energy and Resources, Misc. Rep. 2011-4.1, Paper A-6, 16p.
- Angulo, S., and L.A. Buatois, 2012a, Ichnology of a Late Devonian–Early Carboniferous low-energy seaway: The Bakken Formation of subsurface Saskatchewan, Canada: Assessing paleoenvironmental controls and biotic responses, *Palaeogeography, Palaeoclimatology, Palaeoecology*, v. 315–316, p. 46–60, doi: 10.1016/j.palaeo.2011.11.007.
- Angulo, S., and L.A. Buatois, 2012b, Integrating depositional models, ichnology, and sequence stratigraphy in reservoir characterization: The middle member of the Devonian–Carboniferous Bakken Formation of subsurface southeastern Saskatchewan revisited, *AAPG Bulletin*, v. 96, no. 6, p. 1017–1043
- Arndt-Sullivan, C., J.P. Lechaire, and H. Felbeck, 2008. Extreme tolerance to anoxia in the *Lucinoma aequizonata* symbiosis, *Journal of Shellfish Research*, v. 27, no. 1, p. 119–127.
- Ballard, T.J., S.P. Beare, and T.A. Lawless, 1994, Fundamentals of Shale Stabilisation: Water Transport Through Shales, *SPE Formation Evaluation*, v. 9, no. 2, p. 129-134.
- Bednarz, M., and D. McIlroy, 2009, Three-dimensional reconstruction of "phycosiphoniform" burrows: implications for identification of trace fossils in core: *Palaeontologia Electronica* v. 12, no. 3. http://palaeo-electronica.org/2009_3/195/index.html
- Bednarz, M., and D. McIlroy, 2012, Effect of phycosiphoniform burrows on shale hydrocarbon reservoir quality: *AAPG Bulletin*, v. 96, no. 10, p. 1957-1977, doi:10.1306/02221211126.
- Bednarz, M., L. G. Herringshaw, C. Boyd, M. Leaman, E. Kahlmeyer, and D. McIlroy, (in press), Precision serial grinding and volumetric 3D reconstruction of large

- ichnological specimens: Post-Ichnia 2012 Volume - Book of collected papers, Memorial University of Newfoundland and Geological Association of Canada.
- Bhattacharya, J., and J. MacEachern, 2009, Hyperpycnal rivers and prodeltaic shelves in the Cretaceous seaway of North America: *Journal of Sedimentary Research*, v. 79, p. 184-209.
- Bockelie, J. F., 1991, Ichnofabric mapping and interpretation of Jurassic reservoir rocks in the Norwegian North Sea: *Palaios*, v. 6, no. 3, p. 206–215, doi:10.2307/3514902.
- Bohacs, K.M., 1998, Contrasting expressions of depositional sequences in mudrocks from marine to non-marine environs. In: Schieber, J., Zimmerle, W., Seth, P.S. (Eds.), *Shales and Mudstones: Basin Studies Sedimentology and Palaeontology*. Schweizerbart'sche Verlagsbuchhandlung, Stuttgart, p. 33-78.
- Bohacs, K.M., G. J. Grabowski Jr, A.R. Carroll, P. J. Mankiewicz, K. J. Miskell-Gerhardt, J.R. Schwalbach, M. B. Wegner, and J. A. Simo, 2005, Production, destruction, and dilution: The many paths to source rock development, in N. B. Harris, ed., *The deposition of organic carbon-rich sediments: Models, mechanisms, and consequences*: SEPM, Special Publication 82, p. 61–101.
- Bowker, K.A., 2007, Barnett Shale gas production, Fort Worth Basin: Issues and discussion: *AAPG Bulletin*, v. 91, no. 4, p. 523–533.
- Bromley, R. G., 1996, *Trace fossils: Biology, taphonomy and applications*: London, Chapman and Hall, 361 p.
- Bromley, R.G. and A.A. Ekdale, 1984, *Chondrites*; a trace fossil indicator of anoxia in sediments: *Science*, v. 224, no. 4651, p. 872-874.
- Bust, V.K., A.A. Majid, J.U. Oletu, and P.F. Worthington, 2013, The petrophysics of shale gas reservoirs: Technical challenges and pragmatic solutions: *Petroleum Geoscience*, v. 19, no 2, p. 91–103, DOI: 10.1144/petgeo2012-031.
- Bustin, R.M., 2012, Shale gas and shale oil petrology and petrophysics: *International Journal of Coal Geology*, v. 103, p. 1-2.
- Bustin, A.M.M., R.M. Bustin, and X. Cui, 2008a, Importance of Fabric on the Production of Gas Shales: Society of Petroleum Engineers Unconventional Reservoirs Conference, 10-12 February 2008, Keystone, Colorado, US, doi: 10.2118/114167-MS
- Bustin, R.M., A.M.M. Bustin, X. Cui, D.J.K. Ross, and V.S.M. Pathi, 2008b, Impact of Shale Properties on Pore Structure and Storage Characteristics: Society of Petroleum Engineers Shale Gas Production Conference, 16-18 November 2008, Fort Worth, Texas, USA, doi: 10.2118/119892-MS
- Bustin, A.M.M. and R.M. Bustin, 2012, Importance of rock properties on the producibility of gas shales: *International Journal of Coal Geology*, v. 103, p. 132-147.

- Callow, R.H.T., and D. McIlroy, 2011, Ichnofabrics and ichnofabric forming trace fossils in Phanerozoic turbidites: *Bulletin of Canadian Petroleum Geology*, v. 59, no. 2, p. 103-111.
- Callow, R.H.T., D. McIlroy, B. Kneller, and M. Dykstra, 2013a, Integrated ichnological and sedimentological analysis of a Late Cretaceous submarine channel-levee system: the Rosario Formation, Baja California, Mexico: *Marine and Petroleum Geology*, v. 41, p. 277-294. DOI: 10.1016/j.marpetgeo.2012.02.001.
- Callow, R.H.T., D. McIlroy, B. Kneller, and M. Dykstra, 2013b, Ichnology of late Cretaceous turbidites from the Rosario Formation, Baja California, Mexico: *Ichnos*, v. 20, no. 1, p. 1-14. DOI: 10.1080/10420940.2012.734763.
- Caplan, M.L., and R.M. Bustin, 2001, Palaeoenvironmental and palaeoceanographic controls on black, laminated mudrock deposition: example from Devonian-Carboniferous strata, Alberta, Canada: *Sedimentary Geology*, v. 145, p. 45-72
- Ceron, C.R., and R.M. Slatt, 2012, Gas Shales Characterization: Upper Mississippian Fayetteville Shale, Arkoma Basin, a Case Study: AAPG Search and Discovery Article #90142, 2012 AAPG Annual Convention and Exhibition, April 22-25, 2012, Long Beach, California
- Chalmers, G.R., R.M. Bustin, and I.M. Power, 2012a, Characterization of gas shale pore systems by porosimetry, pycnometry, surface area, and field emission scanning electron microscopy/transmission electron microscopy image analyses: examples from the Barnett, Woodford, Haynesville, Marcellus, and Doig units: *AAPG Bulletin*, v. 96, no. 6 p. 1099–1119, DOI:10.1306/10171111052.
- Chalmers, G.R., D.J. Ross, and R.M. Bustin, 2012b, Geological controls on matrix permeability of Devonian Gas Shales in the Horn River and Liard basins, northeastern British Columbia, Canada: *International Journal of Coal Geology*, v. 103, p. 120-131.
- Cipolla, C.L., E.P. Lonon, and M.J. Mayerhofer, 2009, Reservoir Modeling and Production Evaluation in Shale-Gas Reservoirs: Conference Paper, International Petroleum Technology Conference, 7-9 December 2009, Doha, Qatar, doi:10.2523/13185-MS.
- Cipolla, C., M. Mack, and S. Maxwell, 2010, Reducing Exploration and Appraisal Risk in Low-Permeability Reservoirs Using Microseismic Fracture Mapping: Conference Paper, Canadian Unconventional Resources and International Petroleum Conference, 19-21 October 2010, Calgary, Alberta, Canada, doi: 10.2118/137437-MS.
- Cluff, R.M., 1980, Paleoenvironment of the New Albany Shale Group (Devonian-Mississippian) of Illinois: *Journal of Sedimentary Petrology*, September, 1980, v. 50, no. 3, p.767-780.

- Dando P.R., A.J. Southward, E.C. Southward, P. Lamont, R. Harvey, 2008, Interactions between sediment chemistry and frenulate pogonophores (Annelida) in the north-east Atlantic: *Deep-Sea Research*, v. 55, p: 966–996.
- De Gibert, J.M., and A.A. Ekdale, 1999, Trace fossil assemblages reflecting stressed environments in the Middle Jurassic Carmel Seaway of Central Utah: *Journal of Paleontology*, v. 73, p. 711-720.
- Ding, W., C. Li, Ch. Li, C. Xu, K. Jiu, W. Zeng, and L. Wu, 2012, Fracture development in shale and its relationship to gas accumulation: *Geoscience Frontiers*, v. 3, no. 1, p: 97-105.
- Dubilier, N., C. Bergin, and C. Lott, 2008. Symbiotic diversity in marine animals: the art of harnessing chemosynthesis: *Nature Reviews Microbiology*, v. 6, p. 725-740, doi:10.1038/nrmicro1992.
- Dufour, S.C., and H. Felbeck, 2003, Sulphide mining by the superextensile foot of symbiotic thyasirid bivalves: *Nature*, v. 426, p. 65-67.
- Egenhoff S.O., and N.S. Fishman, 2013, Traces in the dark: sedimentary processes and facies gradients in the upper shale member of the Upper Devonian-Lower Mississippian Bakken Formation, Williston Basin, North Dakota, U.S.A: *Journal of Sedimentary Research*, v. 83, p. 803 – 824.
- Ekdale, A.A. and T.R. Mason, 1988. Characteristic trace-fossil associations in oxygen-poor sedimentary environments: *Geology*, v.16, p.720-723.
- Fan, L., J.W. Thompson, and J.R. Robinson, 2010, Understanding Gas Production Mechanism and Effectiveness of Well Stimulation in the Haynesville Shale Through Reservoir Simulation: Conference Paper, Canadian Unconventional Resources and International Petroleum Conference, 19-21 October 2010, Calgary, Alberta, Canada, Society of Petroleum Engineers, doi: 10.2118/136696-MS
- Fu, S., 1991, Funktion, Verhalten und Einteilung fucoider und lophocteniider Lebensspuren. *Cour. Forsch. Inst. Senckenberg* v. 135, p. 1–79.
- Fu, S., and F. Werner, 1994, Distribution and composition of biogenic structures on the Iceland-Faeroe Ridge; relation to different environments: *Palaos*, vol. 9, no. 1, p. 92-101
- Ghadeer, S., 2011, An investigation of the sediment dispersal operating to control lithofacies variability and organic carbon preservation in an ancient mud-dominated succession: a case study of the Lower Jurassic mudstone dominated succession exposed in the Cleveland Basin (North Yorkshire): PhD thesis, The University of Manchester, UK.
- Ghadeer, S.G., and J.H.S. Macquaker, 2012, The role of event beds in the preservation of organic carbon in fine-grained sediments: Analyses of the sedimentological processes operating during deposition of the Whitby Mudstone Formation

- (Toarcian, Lower Jurassic) preserved in northeast England: *Marine and Petroleum Geology*, v. 35, no 1, p. 309-320.
- Gingras, M. K., S. G. Pemberton, F. Henk, J. A. MacEachern, C. Mendoza, B. Rostron, R. O'Hare, M. Spila, and K. Konhauser, 2007, Applications of ichnology to fluid and gas production in hydrocarbon reservoirs, in J. A. MacEachern, S. G. Pemberton, M. K. Gingras, K. L. Bann, eds., *Applied ichnology: SEPM Short Course Notes* 52, p. 131–147.
- Gingras M.K., G. Baniak, J. Gordon, J. Hovikoski, K.O. Konhauser, A. La Croix, R. Lemiski, C. Mendoza, S.G. Pemberton, C. Polo, and J-P. Zonneveld, 2012, Porosity and Permeability in Bioturbated Sediments, In: *Developments in Sedimentology: Trace Fossils as Indicators of Sedimentary Environments*, Eds. Knaust, D. and Bromley, R.G., v. 64, p. 837-868.
- Gingras, M. K., Angulo, S., and L.A. Buatois, 2013, Biogenic Permeability in the Bakken Formation: Search and Discovery Article #50905, Extended abstract, AAPG Annual Convention and Exhibition, Pittsburgh, Pennsylvania, May 19-22, 2013.
- Goldring, R., J. E. Pollard, and A. M. Taylor, 1991, *Anconichnus horizontalis*: A pervasive ichnofabric-forming trace fossil in post-Paleozoic offshore siliciclastic facies: *Palaaios*, v. 6, no. 3, p. 250–263, doi:10.2307/3514905.
- Harazim, D., 2013, High-energy seafloor processes and biological reworking as first-order controls on mudstone composition and geochemistry: Ph.D. Thesis, Memorial University of Newfoundland, Canada.
- Hovikoski, J., R. Lemiski, M. K. Gingras, S. G. Pemberton, and J. A. MacEachern, 2008, Ichnology and sedimentology of a mud-dominated deltaic coast: Upper Cretaceous Alderson Member (Lea Park Formation), western Canada: *Journal of Sedimentary Research*, v. 78, no. 12, p. 803–824, doi:10.2110/jsr.2008.089.
- Jackson, A.M., and S.T. Hasiotis, 2013, Ichnology of the Upper Cretaceous Greenhorn and Niobrara Formations of the Amoco Production Company Rebecca K Bounds #1 Well, Greeley County, KS, Kansas: Interdisciplinary Carbonates Consortium Proposal – June 2013.
- Jacobi, D., M. Gladkikh, B. LeCompte, G. Hursan, F. Mendez, J. Longo, S. Ong, M. Bratovich, G. Patton, B. Hughes, and P. Shoemaker, 2008, Integrated Petrophysical Evaluation of Shale Gas Reservoirs: Conference Paper, CIPC/SPE Gas Technology Symposium 2008 Joint Conference, 16-19 June 2008, Calgary, Alberta, Canada, Society of Petroleum Engineers doi: 10.2118/114925-MS.
- Javadpour, F., D. Fisher, and M. Unsworth, 2007, Nanoscale Gas Flow in Shale Gas Sediments, *Journal of Canadian Petroleum Technology*, vol. 46, no. 10, p. 55-61; doi: 10.2118/07-10-06.
- Jenkins, C.D., and C. M. Boyer, 2008, Coalbed and shale gas reservoirs: *Journal of Petroleum Technology*, v. 60, no. 2, p. 92-99.

- Kasper, D., 1992, Stratigraphy and Sedimentology of the Bakken Formation of West-central Saskatchewan: A Preliminary Report, Summary of Investigations 1992, Saskatchewan Geological Survey, Sask. Energy Mines, Misc. Rep. 92-4
- Katz, B.J., 2005, Controlling factors on source rock development: a review of productivity, preservation, and sedimentation rate. In: Harris, N.B. (Ed.), The Deposition of Organic Carbon-rich Sediments: Models, Mechanisms, and Consequences. (SEPM) Society for Sedimentary Geology, Special Publication, p. 7-16.
- Khan, S., S. Ansari, H. Han, and N. Khosravi, 2011, Importance of Shale Anisotropy in Estimating In-Situ Stresses and Wellbore Stability Analysis in Horn River Basin: Canadian Unconventional Resources Conference, 15-17 November 2011, Alberta, Canada, Society of Petroleum Engineers, doi: 10.2118/149433-MS.
- Khan, S., R. Williams, S. Ansari, and N. Khosravi, 2012, Impact of Mechanical Anisotropy on Design of Hydraulic Fracturing in Shales: Abu Dhabi International Petroleum Conference and Exhibition, 11-14 November 2012, Abu Dhabi, UAE, Society of Petroleum Engineers, doi: 10.2118/162138-MS.
- Kotake, N., 1991, Packing process for the filling material in *Chondrites*: Ichnos, v.1, no. 4, p. 277-285.
- La Croix, A.D., M.K. Gingras, S.G. Pemberton, C.A. Mendoza, J.A. MacEachern, R.T. Lemiski, 2013, Biogenically enhanced reservoir properties in the Medicine Hat gas field, Alberta, Canada: Marine and Petroleum Geology, v. 43, p. 464-477.
- Lazar, O.R., and J. Schieber, 2004, New Albany and Ohio Shales: An Introduction. In: Devonian Black Shales of the Eastern U.S.: New Insights into Sedimentology and Stratigraphy from the Subsurface and Outcrops in the Illinois and Appalachian Basins. Field Guide for the 2004 Great Lakes Section SEPM Annual Field Conference, J. Schieber and O.R. Lazar (eds.), Indiana Geological Survey Open File Study 04-05, p. 31-34.
- Lemiski, R.T., J. Hovikoski, S.G. Pemberton, and M.K. Gingras, 2011, Sedimentological, ichnological and reservoir characteristics of the low-permeability, gas-charged Alderson Member (Hatton gas field, southwest Saskatchewan): Implications for resource development: Bulletin of Canadian Petroleum Geology, v. 59, p. 27-53, doi:10.2113/gscpgbull.59.1.27.
- Leszczyński, S., and A. Uchman, 1993, Biogenic structures of organic-poor sediments: examples from the Paleogene variegated shales, Polish Outer Carpathians: Ichnos, v. 2, p. 267-275
- Loucks, G.G., and S.C. Ruppel, 2007, Mississippian Barnett Shale: Lithofacies and depositional setting of a deep-water shale-gas succession in the Fort Worth Basin, Texas: AAPG Bulletin, v. 91, no. 4, p. 579-601.
- Loucks, R.G., R.M. Reed, S.C. Ruppel, and U. Hammes, 2012, Spectrum of pore types and networks in mudrocks and a descriptive classification for matrix-related

- mudrock pores: AAPG Bulletin, v. 96, no. 6, p. 1071–1098, DOI:10.1306/08171111061.
- Macquaker, J.H.S. and R.L. Gawthorpe, 1993, Mudstone lithofacies in the Kimmeridge Clay Formation, Wessex Basin, southern England: Implications for the origin and controls of the distribution of mudstones, *Journal of Sedimentary Research*, v. 63, no. 6, p. 1129–1143.
- Macquaker, J.H.S., M.A. Keller, and K.G. Taylor, 1999, Sequence Stratigraphic Analysis of the Lower Part of the Pebble Shale Unit, Canning River, northeastern Alaska: Chapter SS (Sequence Stratigraphy of the Pebble Shale Unit), in *The Oil and Gas Resource Potential of the Arctic National Wildlife Refuge 1002 Area, Alaska*, by ANWR Assessment Team: U.S. Geological Survey Open-File Report 98-34, Version 1.0, p. SS1–SS28.
- Macquaker, J. H. S., and K. M. Bohacs, 2007, On the accumulation of mud: *Science*, v. 318, no. 5857, p. 1734–1735, doi:10.1126/science.1151980.
- Macquaker, J.H.S., K.G. Taylor, and R.L. Gawthorpe, 2007, High-resolution facies analyses of mudstones; implications for paleoenvironmental and sequence stratigraphic interpretations of offshore ancient mud-dominated successions: *Journal of Sedimentary Research*, v. 77, no. 4, p. 324–339, doi:10.2110/jsr.2007.029
- McBride, E.,F., and M.D. Picard, 1991, Facies implications of *Trichichnus* and *Chondrites* in turbidites and hemipelagites, Marnosoarenacea Formation (Miocene), Northern Apennines, Italy: *Palaos*, v. 6, p. 281–290.
- McIlroy, D., 2004, Some ichnological concepts, methodologies, applications and frontiers, in D. McIlroy, ed., *The application of ichnology to paleoenvironmental and stratigraphic analysis*: Geological Society (London) Special Publication 228, p. 3–29.
- McIlroy, D., 2007, Lateral variability in shallow marine ichnofabrics: implications for the ichnofabric analysis method: *Journal of the Geological Society*, v. 164; p. 359–369.
- McIlroy, D., R.H. Worden, and S. J. Needham, 2003, Faeces, clay minerals and reservoir potential: *Journal of the Geological Society (London)*, v. 160, no. 3, p. 489–493, doi:10.1144/0016-764902-141.
- Middelburg, J.,J., and L.A. Levin, 2009. Coastal hypoxia and sediment biogeochemistry: *Biogeosciences*, v. 6, p. 1273–1293, ISSN 1726-4170.
- Morgans-Bell, H.S., A.L. Coe, S.P. Hesselbo, H.C. Jenkyns, G.P. Weedon, J.E.A. Marshall, R.V. Tyson, and C.J. Williams, 2001, Integrated stratigraphy of the Kimmeridge Clay Formation (Upper Jurassic) based on exposures and boreholes in south Dorset, UK: *Geological Magazine*, vol. 138, no. 5, p. 511–539.

- Narr, W., and J. B. Currie, 1982, Origin of fracture porosity: Example from Altamont field, Utah: AAPG Bulletin, v. 66, no. 9, p. 1231–1247.
- Naruse, H., and K. Nifuku, 2008, Three-dimensional morphology of the ichnofossil *Phycosiphon incertum* and its implication for paleoslope inclination: Palaios, v. 23, no. 5, p. 270–279, doi:10.2110/palo.2007.p07-020r.
- Osgood, R.G. Jr. 1970. Trace fossils of the Cincinnati area: Palaeontographica Americana, v. 6, no. 41, p. 328–340.
- Ottmann, J.D., and K.M. Bohacs, 2010, The Barnett Shale - A sequence stratigraphic view of depositional controls, reservoir distribution and resource density: AAPG Search and Discovery, AAPG Hedberg Conference, December 5–10, 2010, Austin, Texas.
- Palmer, I., and Z. Moschovidis, 2010, New Method To Diagnose and Improve Shale Gas Completions: Conference Paper, SPE Annual Technical Conference and Exhibition, 19–22 September 2010, Florence, Italy, Society of Petroleum Engineers, doi: 10.2118/134669-MS
- Passey, Q.R., K.M. Bohacs, W.L. Esch, R. Klimentidis, and S. Sinha, 2012, From Oil-Prone Source Rock to Gas-Producing Shale Reservoir - Geologic and Petrophysical Characterization of Unconventional Shale Gas Reservoirs: Society of Petroleum Engineers, Conference Paper, International Oil and Gas Conference and Exhibition in China, 8–10 June 2010, doi.org/10.2118/131350-MS.
- Pedersen, T.F., and S.E. Calvert, 1990, Anoxia vs. productivity: what controls the formation of organic-carbon-rich sediments and sedimentary rocks?: AAPG Bulletin, v. 74, p. 454–466.
- Pemberton, S. G., 1992, Applications of ichnology to petroleum exploration: SEPM Core Workshop 17, 429 p.
- Pemberton, S. G., and M. K. Gingras, 2005, Classification and characterizations of biogenically enhanced permeability: AAPG Bulletin, v. 89, p. 1493–1517, doi:10.1306/07050504121.
- Pemberton, S.G., J.A. MacEachern, M.K., Gingras, and K.L. Bann, 2009. Atlas of Trace Fossils: The Recognition of Common Trace Fossils in Outcrop and Cores, Elsevier Science Ltd., ISBN 9780444532329.
- Petley, D.N., 1999, Failure envelope of mudrocks at high confining pressures. In: Aplin, A.C., Fleet, A.J., Macquaker, J.H.S. (Eds.), Muds and Mudstones: Physical and Fluid Flow Properties, Geological Society (London) Special Publications, v. 158, p. 61–71.
- Pieńkowski, G., 1985, Early Liassic trace fossil assemblages from The Holy Cross Mountains, Poland: their distribution in continental and marginal marine environments. In: H. Allen Curran (Ed): Biogenic Structures: their use in

- interpreting depositional environments: SEPM, Spec. Publ. 35, p. 37-51; doi: 10.2110/pec.85.35.0037
- Platt, B. F., S. T. Hasiotis, and D.R. Hirmas, 2010, Use of low-cost multistripe laser triangulation (MLT) scanning technology for three-dimensional, quantitative paleoichnological and neoichnological studies: *Journal of Sedimentary Research*, v. 80, no. 7, p. 590–610, doi:10.2110/jsr.2010.059.
- Porębski, J., W. Prugar, and J. Zacharski, 2013, Silurian shales of the East European Platform in Poland – some exploration problems: *Przegląd Geologiczny*, v. 61, no. 11/1, 2013.
- Proverbs, I.P., K.L. Bann, and C. Fratton, 2010, Integrated Sedimentology, Ichnology and Petrography of Unconventional Gas Reservoirs of the Montney Formation; Dawson Creek Region, Northeastern B.C.: GeoCanada 2010 – Working with the Earth, Conference Core Abstracts, Retrieved from: http://cseg.ca/assets/files/resources/abstracts/2010/core/0798_GC2010_Integrated_Sedimentology.pdf
- Rickman, R., M. Mullen, E. Petre, B. Grieser, and D. Kundert, 2008, A Practical Use of Shale Petrophysics for Stimulation Design Optimization: All Shale Plays Are Not Clones of the Barnett Shale: Society of Petroleum Engineers, SPE Annual Technical Conference and Exhibition, 21-24 September 2008, Denver, Colorado, USA, Conference Paper, doi: 10.2118/115258-MS.
- Rodríguez-Tovar, F.J. and A. Uchman, 2010, Ichnofabric evidence for the lack of bottom anoxia during the Lower Toarcian Oceanic Anoxic Event (T-OAE) in the Fuente de la Vidriera section, Betic Cordillera, Spain: *Palaios*, v. 25, p.576-587.
- Romero-Wetzel, M.B., 1987, Sipunculans as inhabitants of very deep, narrow burrows in deep-sea sediments: *Marine Biology* v. 96, p. 87–91.
- Ross, D.J.K., and R.M. Bustin, 2009, The importance of shale composition and pore structure upon gas storage potential of shale gas reservoirs: *Marine and Petroleum Geology*, v. 26, p. 916-927, doi:10.1016/j.marpetgeo.2008.06.004
- Savrdá, C.E. and D.J. Bottjer, 1989, Anatomy and implications of bioturbated beds in 'black shale' sequences: examples from the Jurassic Posidonienschiefer (southern Germany: *Palaios*, v. 4, p. 330-342.
- Savrdá C.E. and D.J. Bottjer, 1991, Oxygen-related biofacies in marine strata: An overview and update. In: Tyson R.V. & Pearson T.H. (Eds.): *Modern and ancient continental shelf anoxia*. Geol. Soc. London Spec. Publ. No. 58, 202-219.
- Savrdá, C.E., and D.J. Bottjer, 1994, Ichnofossils and ichnofabrics in rhythmically bedded pelagic/hemi-pelagic carbonates: recognition and evaluation of benthic redox and scour cycles: *Special Publications, International Association of Sedimentologists*, v. 19, p. 195-210.

- Schieber, J., 1994a, Evidence for high-energy events and shallow-water deposition in the Chattanooga Shale, Devonian, central Tennessee, USA: *Sedimentary Geology*, v. 93, no. 3–4, p. 193–208.
- Schieber, J., 1994b, Reflection of deep vs shallow water deposition by small scale sedimentary features and microfabrics of the Chattanooga Shale in Tennessee: *Canadian Society of Petroleum Geologists*, v. 17, p. 773-784.
- Schieber, J., 2003, Simple gifts and hidden treasures – Implications of finding bioturbation and erosion surfaces in black shales: *The Sedimentary Record*, v. 1, p. 4-8.
- Schieber, J., 2011, Reverse engineering mother nature — Shale sedimentology from an experimental perspective: *Sedimentary Geology*, v. 238, no. 1-2, p. 1-22.
- Schieber, J., J. Southard, and K. Thaisen, 2007, Accretion of mudstone beds from migrating floccule ripples: *Science*, v. 318, no. 5857, p. 1760–1763, doi:10.1126/science.1147001.
- Seilacher, A., 1990, Aberrations in bivalve evolution related to photo- and chemosymbiosis: *Historical Biology*, v. 3, p. 289-311.
- Seilacher, A., 2007, *Trace Fossil Analysis*: Springer-Verlag, Berlin, Heidelberg, New York, 226p.
- Slatt, R.M., and N.R. O'Brien, 2011, Pore types in the Barnett and Woodford gas shales: Contribution to understanding gas storage and migration pathways in fine-grained rocks: *AAPG Bulletin*, v. 95, no. 12, p. 2017–2030, DOI:10.1306/03301110145
- Sonnenberg, S. A., and A. Pramudito, 2009, Petroleum geology of the giant Elm Coulee Field, Williston Basin: *AAPG Bulletin*, v. 93, no. 9, p. 1127-1153, doi:10.1306/05280909006
- Spaw, J.M., 2013a, Recognition of ichnofacies distributions and their contributions to matrix heterogeneity in mudstones: *Unconventional Resources Technology Conference (URTeC)*, Denver, Colorado, USA, 12-14 August 2013.
- Spaw, J.M., 2013b, Microfacies analysis: an integrated petrologic approach to characterizing mudrock heterogeneity: *Unconventional Resources Technology Conference (URTeC)*, Denver, Colorado, USA, 12-14 August 2013
- Spila, M. V., S. G. Pemberton, B. Rostron, and M. K. Gingras, 2007, Biogenic textural heterogeneity, fluid flow and hydrocarbon production: Bioturbated facies, Ben Nevis Formation, Hibernia field, offshore Newfoundland, in J. A. MacEachern, K. L. Bann, M. K. Gingras, and G. S. Pemberton, eds., *Applied ichnology: SEPM Short Course Notes 52*, p. 363–380.
- Stewart, F.J., I.L. Newton, and C.M. Cavanaugh, 2005, Chemosynthetic endosymbioses: adaptations to oxic-anoxic interfaces. In: *Trends Microbiology*, vol. 13, no.9, p. 439-48.

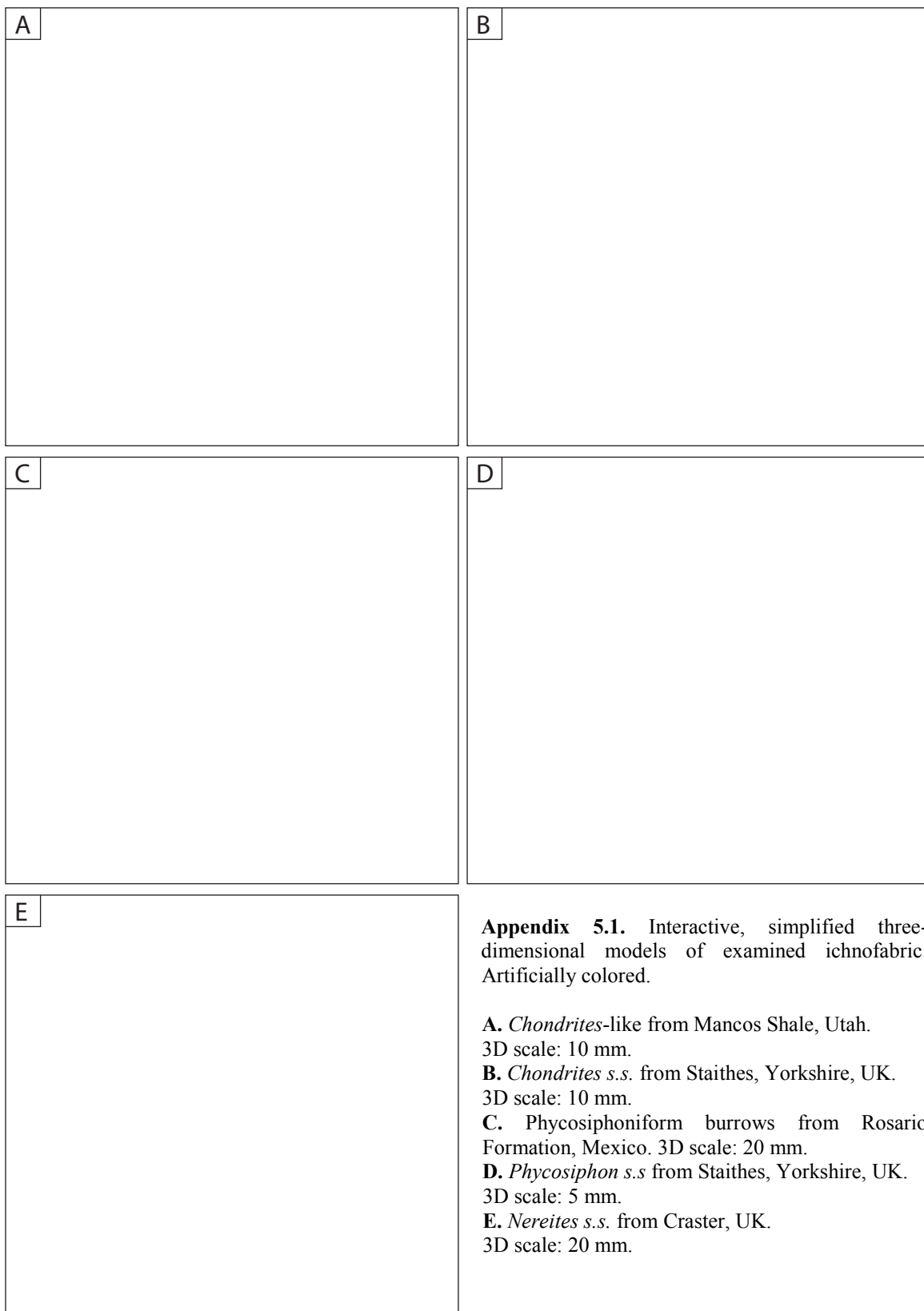
- Sutton, M.D., D.E.G. Briggs, D.J. Siveter, and D.J. Siveter, 2001, Methodologies for the visualization and reconstruction of three-dimensional fossils from the Silurian Herefordshire Lagerstätte: *Palaeontologia Electronica*, v. 4, no. 1, p. 1-17, 1MB; http://palaeo-electronica.org/2001_1/s2/issue1_01.htm
- Swami, V., 2012, Shale Gas Reservoir Modeling: From Nanopores to Laboratory: Society of Petroleum Engineers, Conference Paper, SPE Annual Technical Conference and Exhibition, 8-10 October 2012, San Antonio, Texas, USA. doi.org/10.2118/163065-STU
- Swami, V., and A. Settari, 2012, Pore Scale Gas Flow Model for Shale Gas Reservoir: SPE Americas Unconventional Resources Conference, 5-7 June 2012, Pittsburgh, Pennsylvania USA, Society of Petroleum Engineers, doi: 10.2118/155756-MS
- Swami, V., C.R. Clarkson, and A. Settari, 2012, Non-Darcy Flow in Shale Nanopores: Do We Have a Final Answer?: SPE Canadian Unconventional Resources Conference, 30 October-1 November 2012, Calgary, Alberta, Canada, Society of Petroleum Engineers, doi: 10.2118/162665-MS
- Swinbanks, D.D., and Y. Shirayama, 1984, Burrow stratigraphy in relation to manganese diagenesis in modern deep-sea carbonates, In: *Deep-Sea Research. Part A: Oceanographic Research Papers*, v. 31, no. 10A, p.1197-1223,
- Tonkin, N.S., D. McIlroy, R. Meyer, and A. Moore-Turpin, 2010, Bioturbation influence on reservoir quality; a case study from the Cretaceous Ben Nevis Formation, Jeanne d'Arc Basin, offshore Newfoundland, Canada: *AAPG Bulletin*, v. 94, no. 7, p. 1059-1078, doi:10.1306/12090909064.
- Tyson, R.V., 1995, *Sedimentary Organic Matter: Organic Facies and Palynofacies*, First ed. Chapman & Hall, London. 615p.
- Uchman, A., R. Mikulas, V. Housa, 2003, The trace fossil *Chondrites* in Uppermost Jurassic–Lower Cretaceous deep cavity fills from The Western Carpathians (Czech Republic): *Geologica Carpathica*, v. 54, no. 3, p. 181-187.
- Uchman, A., 2010, A new ichnogenus *Skolichnus* for *Chondrites hoernesii* Ettingshausen, 1863, a deep-sea radial trace fossil from the Upper Cretaceous of the Polish Flysch Carpathians: Its taxonomy and palaeoecological interpretation as a deep-tier chemichnion: *Cretaceous Research*, v. 31, no.5, p. 515-523.
- Wang F.P., R.M. Reed, J.A. Jackson and K.G. Jackson, 2009, Pore Networks and Fluid Flow in Gas Shales: Conference Paper, SPE Annual Technical Conference and Exhibition, 4-7 October 2009, New Orleans, Louisiana, doi: 10.2118/124253-MS
- Weaver, P.P.E., and P.J. Schultheiss, 1983, Vertical open burrows in deep-sea sediments 2 m in length: *Nature*, v. 301, p. 329 – 331, doi:10.1038/301329a0.
- Wetzel, A., 1983, Biogenic sedimentary structures in a modern upwelling region: NW African continental margin. In: Thiede, J., Suess, E. (Eds.), *Coastal Upwelling*

- and Its Sediment Record: Sedimentary Records of Ancient Coastal Upwelling, Part B, Plenum, New York, p. 123-144.
- Wetzel, A., 2002, Modern *Nereites* in the South China Sea- ecological association with redox conditions in the sediment: *Palaios*, v. 17, no. 5, p. 507-515.
- Wetzel, A., and F. Werner, 1980, Morphology and ecological significance of *Zoophycos* in deep-sea sediments off NW Africa: *Palaeogeography, Palaeoclimatology, Palaeoecology*, v. 32, p. 185-212, doi:10.1016/0031-0182(80)90040-1.
- Wetzel, A. and N.P. Wijayananda, 1990, Biogenic sedimentary structures in outer Bengal fan deposits drilled during LEG 116, 1524. In Cochran, J.R. and Stow, D.A.V., (eds.), *Proceedings of the Ocean Drilling Program, Scientific Results 116*.
- Wetzel, A., and R.G. Bromley, 1994, *Phycosiphon incertum* revisited: *Anconichnus horizontalis* is junior subjective synonym: *Journal of Paleontology*, v. 68, no. 6, p.1396-1402.
- Wetzel, A., and A. Uchman, 1998 a, Biogenic sedimentary structures in mudstones - an overview, In: Schieber, J., Zimmerle, W. & Sethi, P.S. (eds.), *Shales & Mudstones. I. Basin Studies, Sedimentology, and Paleontology*. E. Schweitzerbart, Stuttgart, p. 351-369. Stuttgart.
- Wetzel, A., and A. Uchman, 1998 b, Deep-sea benthic food content recorded by ichnofabrics: A conceptual model based on observations from Paleogene flysch, Carpathians, Poland: *Palaios*, v. 13, no. 6, p. 533-546.
- Wetzel, A., and A. Uchman, 2001, Sequential colonization of muddy turbidites in the Eocene Beloveza Formation, Carpathians, Poland: *Paleogeography, Paleoclimatology, Paleocology*, v. 168, no. 1-2, p. 171-186, doi:10.1016/S0031-0182(00)00254-6.
- Wetzel, A., R. Tjallingii, and M.G. Wiesner, 2011, Bioturbational structures record environmental changes in the upwelling area off Vietnam (South China Sea) for the last 150,000 years: *Palaeogeography, Palaeoclimatology, Palaeoecology*, v. 311, no. 3-4, p. 256-267.
- Wightman, D.M., S.G., Pemberton, and C. Singh, 1987, Depositional modelling of The Upper Mannville (Lower Cretaceous), East Central Alberta: Implications for the recognition of brackish water deposits. In: Tillman, R.W. and Wber, K.J. (Eds.): *Reservoir sedimentology*. SEPM, Special Publications v. 40, p. 189-220; doi: 10.2110/Pec.87.40.0189
- Zuschin, M., O. Mandic, M. Harzhauser, P. Pervesler, 2001, Fossil evidence for chemoautotrophic bacterial symbiosis in the thyasirid bivalve *Thyasira michelottii* from the middle miocene (Badenium) of Austria: *Historical Biology* v. 15, p. 123-134

5.9. Appendices

In order to control the interactive model embedded in PDF file (Appx 5.1):

1) Click on the chosen three-dimensional reconstruction to activate the interactive content; 2) Use tools that are listed on the bar at the top of the activated area; 3) choose between available views to explore spatial geometry of the three-dimensional object and their chosen components; 4) use Model Tree panel in order to display or hide chosen components.



Appendix 5.2. Calculation of burrow spacing (*BS*).

1. Known variables (see Fig. 5.1):

VU = volume of ichnofabric (volume utilized);

r = averaged radius of burrow cross sections;

x, y, z = lengths of the edges of the prism containing the ichnofabric (corresponds to dimensions of volume available [VA]).

2. The length of distribution grid (L_g) is calculated from the equation:

$$L_g = \frac{VU}{\pi r^2}$$

3. The length of the distribution grid (L_g) is composed of a number of cylinders of the length of a (see Fig. 5.1B). The length of a is calculated from the equation:

$$L_g = x\left(\frac{y}{a} - 1\right)\left(\frac{z}{a} - 1\right) + y\left(\frac{x}{a} - 1\right)\left(\frac{z}{a} - 1\right) + z\left(\frac{x}{a} - 1\right)\left(\frac{y}{a} - 1\right)$$

$$L_g a^2 = x(y - a)(z - a) + y(x - a)(z - a) + z(x - a)(y - a)$$

$$L_g a^2 = xyz - xya - xza + xa^2 + xyz - xya - yza + ya^2 + xyz - xza - yza - za^2$$

$$L_g a^2 = (x + y + z)a^2 - 2(xy + xz + yz)a + 3xyz$$

$$(L_g - x - y - z)a^2 + 2(xy + xz + yz)a - 3xyz = 0$$

It is a quadratic equation because of a .

$$\Delta = 4(xy + xz + yz)^2 + 12xyz(L_g - x - y - z) = 4[(xy + xz + yz)^2 + 3xyz(L_g - x - y - z)]$$

$$\sqrt{\Delta} = 2\sqrt{(xy + xz + yz)^2 + 3xyz(L_g - x - y - z)}$$

$$a = \frac{-2(xy + xz + yz) + 2\sqrt{(xy + xz + yz)^2 + 3xyz(L_g - x - y - z)}}{2(L_g - x - y - z)}$$

$$a = \frac{-xy - xz - yz + \sqrt{(xy + xz + yz)^2 + 3xyz(L_g - x - y - z)}}{L_g - x - y - z}$$

4. Burrow spacing BS is approximately equal to a with subtracted averaged diameter of the burrow cross sections:

$$BS \approx a - 2r$$

CHAPTER 6

Three-dimensional reconstruction of ichnofabrics in shale gas reservoirs: discussion and conclusions

To generate a more complete understanding of the role that organisms have in controlling the porosity, permeability and fracture-susceptibility of shale-gas reservoir intervals a three-dimensional volumetric study of the most common ichnofabrics in these facies has been performed. In order to investigate the complex three-dimensional burrow fabrics, precise serial grinding and volumetric ichnofabric analysis of the reconstructed burrows was undertaken. Formulation and standardization of volumetric calculations and description of a burrow or ichnofabric presented in this study aims to contribute to the emerging field of quantitative three-dimensional ichnology. There is an emerging need to be able to predict the distribution of ichnofabric-associated trends, and thus reservoir quality, in bioturbated hydrocarbon reservoirs especially the shale-hydrocarbon reservoirs that are hosted in ultra-low permeability mudstones. This study helps to delineate these trends through the investigation of the deterministic three-dimensional reconstructions of some ichnotaxa typical of shale-gas reservoir facies. Five samples of organic rich bioturbated mudstones and siltstones have been investigated in the course of this thesis in order to create three-dimensional reconstructions of some typical trace fossils and the ichnofabrics that they produce. These studies demonstrate the potential for trace fossils to affect shale-hydrocarbon reservoir quality and producibility, and to provide insights

into some of the underlying precepts that might influence reservoir quality and its regional prediction.

6.1. Achievements of the thesis and summary of conclusions

6.1.1. Formulation of methodology for the deterministic volumetric 3D reconstructions and analysis of ichnological specimens.

This study presents a new methodology that was developed for obtaining precise, deterministic three-dimensional reconstructions of large or complex trace fossils and ichnofabrics and further analytical approach to the spatial reconstructions in order to provide detailed, morphological and volumetric characterization of the studied ichnological specimens (Chapter 2).

The novelty of the methodology of 3D reconstruction and analysis of ichnofossils based on serial sectioning is founded on a combination of:

- 1) High resolution of serial sectioning and employment of precise, automated computer-controlled grinding machinery capable of grinding to a precision of fractions of millimetre;
- 2) Digital image-processing for optimal interpretation of lithology of different components of trace fossils, and also in some cases the near-burrow environment, in volume-visualizing software;
- 3) Generation and optimization of the polygonal surface(s) of visualized trace fossils (and their different morphological components present) at a 1:1 scale;

- 4) Volumetric and descriptive analysis of the acquired 3D reconstructions that represent the ichnological specimens at their real-scale;
- 5) Formulation of case-specific proxies and calculations for volumetric characterization;
- 6) Presentation of the resultant reconstructions as interactive objects in popular file formats or software (e.g., PDF, Internet browsers).

This PhD thesis presents application of the above methodology to the five ichnofabrics in order to characterize the true geometry, spatial distribution, and volumetric assessment of *Nereites*, aff. *Phycosiphon*, and aff. *Chondrites* ichnofabrics. Consideration of multiple ichnological samples allowed for formulation and standardization of procedures, such that all the samples were processed the same way and the results are directly comparable (Tab. 5.2).

The wide variety of possible measurements and calculations that can be applied to the deterministic three-dimensional reconstructions of ichnological data provides the means to characterize burrows and complex ichnofabrics. The methodology presented is based on serial grinding and is especially useful for 3D examination of the ichnofabric contained in mudstones and muddy siltstones where the application of non-destructive methods such as CT scanning or MRI is impossible owing to the petrological characteristics of the rock (e.g., low burrow-matrix density difference). Although destructive, the methodology presented herein results in the generation of the reconstructed ichnofabric in the form of three-dimensional polygonal mesh that once created, may be presented as interactive object (e.g., Appx 2.1 and Appx 4.3). The

availability of the interactive 3D models enables their manipulation and/or modification in order to explore the three-dimensional arrangement of burrows and allows for their artificial slicing in order to provide a set of search templates for the identification of trace fossils in core and thin section (Appx 2.1: section views; cf. Fig. 2.5).

Realistic quantification of burrow volumes, together with the improved understanding of their spatial arrangement and distribution may help to elucidate possible trace maker behaviours, especially when the impact on the near-burrow environment and distribution relative to host sediment heterogeneities is considered. This is considered to be especially true for complex burrows when volumetric and morphological arrangements of the compartment burrow elements may reflect their classification as demonstrated in this study (Fig. 4.2). Quantification of burrow parameters such as those that reflect sediment-exploitation efficiency allows consideration of the differences between burrows of the same taxon in different sediments, and comparison between similar taxa in the same sediment (Tab. 4.2). Such parameters as the proximity of a burrow to a sediment heterogeneity (e.g., sediment layer or patch of a concentrated food resource) or a biogeochemical stimulus may significantly affect both behaviour and burrow volumetrics.

This study is focussed on linking the detailed 3D geometries of ichnofabrics and burrows with lithology, volumetric evaluation of the burrows, and in some cases their petrologically/petrophysically disparate components and, as such, has its application to reservoir characterization. It is considered that the measurements and calculations based on the volume of the sediment processed by the trace maker (volume exploited),

burrow(s) surface area, and the quantitative assessment of the approximate density of the distribution of the ichnofabric-forming burrows within a sample (burrow spacing, Fig. 5.1) are among the most valuable and informative ichnologically-based quantifications of relevance to the hydrocarbon-reservoir characterization.

6.1.2. Understanding morphological diversity of common shale-gas reservoir trace fossils in the light of their 3D reconstructions

***Aff. Phycosiphon* trace fossils**

The three types of phycosiphoniform burrows examined in this study significantly differ from each other despite having the characteristic “frogspawn” texture in vertical cross section (Fig. 4.2; cf. Bromley 1996). The deterministic three-dimensional reconstructions of the three examined trace fossils allow for detailed examination of the spatial geometry and volumetrics of these complex trace fossils (Tabs 4.1, 5.2; Appx 4.3). This is important because they are composed of mineralogically and petrographically different elements (dark clay-rich fecal burrow cores and light silty burrow halos) whose spatial and volumetric inter-relations allow for taxonomic and palaeobiological considerations as well as may have significant influence on the reservoir quality.

It is demonstrated herein that the geometry of *Phycosiphon* s.s. burrows from Staithes Sandstone Formation, may be explained by the pre-existing palaeobiological model for *Phycosiphon incertum* (Wetzel and Bromley 1994; Bromley 1996; Fig. 3.4). This material may therefore be attributed to *Phycosiphon incertum* s.s. Burrows of aff.

Phycosiphon from the Upper Cretaceous Rosario Formation, Mexico, are found to be morphologically distinct from *Phycosiphon* s.s. Similarly to the *Phycosiphon* s.s. the geometry of phycosiphoniform burrows from the Rosario Formation is principally based on loops that commonly results in paired core ellipses in vertical cross section. Similar amount of halo material is present below both of the core ellipses of the single burrow loops from Rosario Formation. This makes the form from Rosario Formation distinguishable from *Phycosiphon* s.s., which is characterized by halo material being present only between the two core ellipses (Figs 4.2A-E, 4.4 and 4.5). *Nereites* ichnofabrics also ostensibly resemble the phycosiphoniform “frog-spawn” pattern, especially where vertical cross sections of individual burrows are connected by their haloes (Figs 4.2G, H and 5.2F). This juxtaposition may lead to erroneous impression of the presence of looped tubes that may be thus interpreted as composing a halo-sealed loop similar to that of *Phycosiphon*. Three-dimensional reconstruction of *Nereites* shows that the elliptical, dark grey burrow cores are seldom looped, and are completely surrounded by light grey silty halo material. It is illustrated that *Nereites* is characterized by the least tortuous burrows considered in this study, however it is illustrated that many species of this type of phycosiphoniform burrows do have closely guided—bedding parallel—meanders.

It is documented herein that without exception, every fecal burrow of aff. *Phycosiphon* from Rosario Formation creates a lobe that is bent vertically (Fig. 4.3). No horizontal loops have been observed in the sample from Rosario Formation; whereas such geometry is frequent for lobes of *Phycosiphon* s.s. and prevalent in the meanders of *Nereites* from

Craster. In contrast to the core strings, the silty haloes of adjacent phycosiphoniform burrows are widely connected in the vertical and/or horizontal places, significantly influencing the vertical connectivity of these permeable and/or brittle volumes within tight matrix.

Detailed analysis of the spatial geometry of the three phycosiphoniform burrows examined in this study allows for consideration of the trace makers burrowing behavior. The producers of aff. *Phycosiphon* and *Nereites* burrows are considered to be worm-like, subsurface grain-selective deposit feeders, ingesting organic-rich sediment, using oxygen from interstitial pore waters for respiration (e.g., Wetzel and Bromley 1994; Bromley 1996; Wetzel 2002). *Phycosiphon*-like burrows commonly occur as monotaxic assemblages that are taken to imply stressed seafloor environments (e.g., dysoxia; e.g., Wetzel 2002) or the early, opportunistic colonization of food-rich sediments (e.g., turbiditic deposits; e.g., Stow and Wetzel 1990; Wetzel and Uchman 2001). All of the three ichnotaxa considered herein (aff. *Phycosiphon*, *Phycosiphon* s.s., and *Nereites*) have been found to occur together in the same sediment interval (Callow et al., 2013a, b). The illustrated morphologic/geometric differences between the three ichnotaxa are most likely the result of biomechanical and/or behavioral adaptations, which may result from the trace making organism(s) morphological, digestive, respiratory and sensory adaptations (cf. Wetzel and Uchman 2001; Wetzel 2002). In the light of the three-dimensional reconstructions it is suggested that the producers of all the three trace fossil types processed the largest possible volume of sediment possible within the limits of their biomechanics and food availability. The volumetric studies of these trace fossils

presented herein indicate that the producers of *Nereites* (from Craster) and phycosiphoniform burrows (from the Rosario Formation) were more efficient at processing large volumes of sediment compared to the *Phycosiphon* s.s. trace maker. This is illustrated by the core multiplicand for halo estimation (*CM*), a variable that describes volumetric relation of halo to core material (Tab. 4.1 and 4.2). Average core multiplicand of *Phycosiphon* s.s. was calculated to be 4.5 whereas the phycosiphoniform burrows from the Rosario Formation was 6.5 and *Nereites* (from Craster) was up to 8 (Bednarz and McIlroy 2012). The persistent presence of the silty clay-poor material of halo around each fecal string or externally from lobes suggests that *Nereites* and phycosiphoniform burrows from Rosario were formed by grain-selective sediment feeding, at the anterior of the burrow, during periods of continuous burrowing. In contrast, burrows of *Phycosiphon* s.s. with their diagnostic clay-rich marginal tube are most likely to result from successive probing (Wetzel and Bromley 1994; Bromley 1996; Bednarz and McIlroy 2009). The looping architecture of phycosiphoniform burrows from the Rosario Formation and *Phycosiphon* s.s. from Staithes may indicate positive thigmotaxis detecting the proximity of clean (bioturbated) sediment (see Wetzel and Bromley 1994). The suggestion of phototaxis as a sensory adaptation of the producers of phycosiphoniform burrows (Callow et al. 2013a) can be supported by the observation herein that almost none of the reconstructed burrows self-cross-cut even when tracked in the most tortuous of three dimensional ichnofabrics burrow cores densely distributed in three dimensions (Appx 5.1C–D, views: burrow cores). Only one instance was observed where the burrow core of large diameter *Nereites* demonstrably cross-cuts that of a *Nereites* of smaller size (Fig.

5.2G, Appx 5.1E, view: cross cut). If any of the three types of phycosiphoniform burrows co-occur within the same sediment volume they have been found to (probably phobotactically) avoid the previously produced fecal cores (Callow et al., 2013a) with few exceptions. In contrast, the cleaned sediment halos of phycosiphoniform burrows are found to be highly connected (Appx 4.3, chapter 4). Such spatial relations may support geochemical study of the Rosario Formation phycosiphoniform burrows that were found to have only trace amounts of organic matter preserved in the burrow halo (Harazim 2013). The organic matter contained within the fecal cores was likely refractory (Harazim 2013). Phobotactic avoidance of burrow crossing is considered to contribute to optimization of space usage, especially in the areas of high burrow density.

Aff. *Chondrites* trace fossils

This study also presents three-dimensional reconstructions of two *Chondrites*-like ichnofabrics (Appx 5.1A, B). *Chondrites*-like burrows have been found to produce burrow geometries of small volume but with a disproportionally large surface area (Fig. 5.5). Volumetric examination of the *Chondrites*-like ichnofabrics presented in this study indicates the significant potential of this type of ichnofabric to thoroughly penetrate the bioturbated sediment even when the total ichnofabric volume is small (calculated to be 3.5 – 7.5% of the total sample volume, Tab. 5.2). Thin (1-2 mm in diameter) tubes constituting root-like burrow systems of *Chondrites* were likely designed to maximize the area of solute exchange between burrow microenvironment and pore waters of the surrounding sediment. This strategy was probably employed by the *Chondrites* trace maker in order to collect the dispersed hydrogen sulfide needed for chemosynthetic

activity of its symbionts (i.e. sulfide mining; Seilacher 1990; Fu, 1991; Bromley and Ekdale 1994; Bromley 1996; Uchman 1999). The function of *Chondrites* burrows and the ethology, and biology of the *Chondrites* trace maker have remained unresolved but highly debated for more than a century (e.g., Salter 1866; Nathorst 1881; Fush 1895; Simpson 1956; Osgood 1970; Seilacher 1990; Fu 1991; Kotake 1991; Ekdale 1992; Seilacher 2007). Full palaeobiological exploration of *Chondrites* palaeobiology is beyond the scope of this study.

The two examined aff. *Chondrites* burrows show significant differences in architecture. The burrows from Staithes and from Muddy Creek show anomalous burrow architecture that precludes confident assignment to *Chondrites* (Appx 5.1A, B). However, both of these trace fossils produce *Chondrites*-like ichnofabrics (Fig. 5.2A, B). The most striking feature of the aff. *Chondrites* burrows from Muddy Creek is the abundant vertical branching seen in the distal branches (Appx 5.1A, e.g., view: vertical branching). This is, however, not part of the ichnogenic diagnosis of *Chondrites*, nor is it widely documented in the literature (cf. Osgood, 1970).

6.1.3. Understanding the impact of trace fossils on shale–hydrocarbon reservoir

This research project aims to generate a more complete understanding of the role that organisms have in controlling the rheology and petrophysical properties of shale-gas and shale-oil reservoir intervals. The study is built around deterministic 3D reconstructions of aff. *Phycosiphon*, *Nereites* and aff *Chondrites* ichnofabrics that allowed for 1) quantitative assessment of the ichnological contribution to the examined volume of the

organic-rich mudstone; and 2) recognition of spatial distribution of petrophysical trends associated with burrows lithology.

Through the creation of porous and permeable volumes within sediments, silty burrows may provide effective fluid flow conduits and increase primary and fracture-related porosity and permeability in shale-hydrocarbon reservoirs. It has been observed that burrows of *Chondrites*-like forms and the halo of the neighboring phycosiphoniform burrows are highly connected in three-dimensions (Fig. 5.3, Appx 5.1). The strong vertical connectivity of the trace fossils studies may improve producibility at the macro-scale ($k_h \approx k_v$) (Tab. 4.2). It is the burrow halo of phycosiphoniform burrows that most significantly participates in the volumetric enhancement of porosity and permeability in bioturbated mudstones (from 17% up to 25%; Tab. 4.1; Fig. 5.5). This type of ichnofabric creates porosity enhancement that is up to 30 times that of the host sediment (cf. Gingras et al., 2013; Harazim 2013).

It has been demonstrated in this study that the tortuous geometries of the interconnected silty burrows create a large surface area for release of gas into the porous ichnofabric network. Since the porous burrow fills are directly associated with source rocks, the communication distances from sediment to pore-networks is greatly decreased (Fig. 5.6) and producibility/deliverability is increased. Additionally, the interconnected quartz-rich burrow fills of aff. *Chondrites* and the burrow halos of phycosiphoniform burrows form a framework of brittle material in otherwise non-brittle mudstones (Fig. 5.2B, F). The burrow fills may themselves undergo diagenetic cementation (e.g., by carbonate or quartz cements), further increasing brittleness but decreasing primary porosity. The

interconnected burrow surfaces are likely to be planes of weakness for both natural and induced fractures, thereby improving fracturability, particularly vertical connectivity/permeability. It is the aff. *Chondrites* ichnofabric that contribute most significantly to the generation of the fracture-prone interfaces as the surface area of the burrows may be more than 25 times larger than the surface area of the horizontal plane of the bioturbated volume (Tab. 5.2).

The millimetric burrow spacing that characterizes some mudstone ichnofabrics (between 1.6 – 9.5 mm in the examined samples) should be investigated for its impact on fracture spacing and complexity in hydraulically-stimulated reservoir facies (Fig. 5.6, Tab. 5.2). Millimetre scale fracture spacing is, however, considered the most effective fracture density that allows for efficient contact with the reservoir rock (cf. Bustin and Bustin 2012). Ichnofabric development would intuitively constitute the most likely means to meet these criteria.

6.2. Avenues for future research

Three-dimensional volumetric analysis of ichnofabric as a tool for assessing the impact of bioturbation on reservoir quality has been formulated and used herein for the first time. It can be further linked with detail petrography, geochemistry (cf. Harazim 2013) and mini-permeability measurements (cf. Leaman 2013), and may shed more light on the mudstone depositional processes that are still not well understood. While this study is focused on centimeter-scale analysis of the ichnofabric, the results may be up-scaled when linked

with stratigraphic understanding of reservoir shale-hydrocarbon play (cf. Macquaker et al. 2007; McIlroy 2007; Slatt and Abousleiman 2011; Spaw 2012, 2013).

Because of the fact that the currently available technology of production from shale-hydrocarbon reservoirs depends on the effectiveness of the hydraulic fracturing, the significant impact that the ichnofabric has on the distribution and alternation of the rheological properties of shales should not be ignored. This study illustrated cases of burrow-controlled fracturing along ichnofabric-generated planes of weakness and shows the need of experimentation focused on the fracture propagation and possible fracture coalescence to be applied to trace fossil studies. If the results of such geo-mechanical experiments are linked with ichnofabric analysis, then modeling of fracture propagation and fracture spacing has the potential to improve shale-hydrocarbon reservoir characterization. Incorporating ichnology into shale-hydrocarbon reservoir characterization may be especially helpful for reservoir optimization since the commonly used surfactants will be significantly affected by trace-fossil mediated reservoir wettability characteristics.

It is considered herein that bioturbated reservoir facies may be preferential targets for application of various production optimization technologies (e.g., acidization; use of surfactants etc.). The inter-relationship between ichnology and shale-hydrocarbon reservoirs is still little explored. This thesis provides one of the first attempts at realistic 3D reservoir ichnology in shale-hydrocarbon plays, and should be the basis for further detailed studies incorporating mineralogy, petrophysics, experimental fracturing and flow-modeling.

6.3. References

- Bednarz, M., and D. McIlroy, 2009, Three-dimensional reconstruction of "phycosiphoniform" burrows: implications for identification of trace fossils in core: *Palaeontologia Electronica* v. 12, no. 3. http://palaeo-electronica.org/2009_3/195/index.html
- Bednarz, M., and D. McIlroy, 2012, Effect of phycosiphoniform burrows on shale hydrocarbon reservoir quality: *AAPG Bulletin*, v. 96, no. 10, p. 1957-1977, doi:10.1306/02221211126.
- Bromley, R. G., 1996, *Trace fossils: Biology, taphonomy and applications*: London, Chapman and Hall, 361 p.
- Bromley, R.G. and A.A. Ekdale, 1984, Chondrites; a trace fossil indicator of anoxia in sediments: *Science*, v. 224, no. 4651, p. 872-874.
- Bustin, A.M.M. and R.M. Bustin, 2012, Importance of rock properties on the producibility of gas shales: *International Journal of Coal Geology*, v. 103, p. 132-147.
- Callow, R.H.T., D. McIlroy, B. Kneller, and M. Dykstra, 2013a, Integrated ichnological and sedimentological analysis of a Late Cretaceous submarine channel-levee system: the Rosario Formation, Baja California, Mexico: *Marine and Petroleum Geology*, v. 41, p. 277-294. DOI: 10.1016/j.marpetgeo.2012.02.001.
- Callow, R.H.T., D. McIlroy, B. Kneller, and M. Dykstra, 2013b, Ichnology of late Cretaceous turbidites from the Rosario Formation, Baja California, Mexico: *Ichnos*, v. 20, no. 1, p. 1-14. DOI: 10.1080/10420940.2012.734763.
- Ekdale, A.A., 1992, Mudcracking and mudslinging, the joys of deposit-feeding, In: C.G. Maples and R.R. West (eds), *Trace Fossils: Paleontological Society Short Courses in Paleontology* v.5 p.145-171.
- Fu, S., 1991, Funktion, Verhalten und Einteilung fucoider und lophocteniider Lebensspuren. *Cour. Forsch. Inst. Senckenberg* 135, p. 1–79.
- Fuchs, T., 1895. Studien fiber Fucoiden und Hieroglyphen. *Denkschr: Akad. Wiss. Wien*, v. 62, p. 369-448.
- Gingras, M. K., Angulo, S., and L.A. Buatois, 2013, Biogenic Permeability in the Bakken Formation: Search and Discovery Article #50905, Extended abstract, AAPG Annual Convention and Exhibition, Pittsburgh, Pennsylvania, May 19-22, 2013.
- Harazim, D., 2013, High-energy seafloor processes and biological reworking as first-order controls on mudstone composition and geochemistry: Ph.D. Thesis, Memorial University of Newfoundland, Canada.
- Kotake, N., 1991, Packing process for the filling material in *Chondrites*: *Ichnos*, v.1, no. 4, p. 277-285.

- La Croix, A.D., M.K. Gingras, S.E. Dashtgard, and S.G. Pemberton, 2012, Computer modeling bioturbation: The creation of porous and permeable fluid-flow pathways, AAPG Bulletin, v. 96, no. 3, pp. 545–556.
- Leaman, M., 2013, Three-Dimensional Morphology of *Diplocraterion* and *Ophiomorpha* and their impact on reservoir properties: M.Sc. Thesis, Memorial University of Newfoundland, Canada.
- Macquaker, J.H.S., K.G. Taylor, and R.L. Gawthorpe, 2007, High-resolution facies analyses of mudstones; implications for paleoenvironmental and sequence stratigraphic interpretations of offshore ancient mud-dominated successions: Journal of Sedimentary Research, v. 77, no. 4, p. 324-339, doi:10.2110/jsr.2007.029.
- McIlroy, D. 2007, Lateral variability in shallow marine ichnofabrics: implications for the ichnofabric analysis method: Journal of the Geological Society, v. 164; p. 359-369.
- Michalík, J., and V. Šimo, 2010, A new spreite trace fossil from Lower Cretaceous limestone (Western Carpathians, Slovakia): Earth and Environmental Science Transactions of the Royal Society of Edinburgh, v. 100, no. 4, p. 417-427.
- Naruse, H., and K. Nifuku, 2008, Three-dimensional morphology of the ichnofossil *Phycosiphon incertum* and its implication for paleoslope inclination: Palaios, v. 23, no. 5, p. 270–279, doi:10.2110/palo.2007.p07-020r.
- Nathorst, A. G., 1881. Om spår af några evertebrerade djur m. och deras palaeontologiska betydelse, Kongliga Svenska Vetenskapsakademien Handlingar, v. 18; no. 7, p. 1-104.
- Osgood, R.G. Jr. 1970. Trace fossils of the Cincinnati area: Palaeontographica Americana, v. 6, no. 41, p. 328-340.
- Salter, J. W., 1866, On the fossils of North Wales: In Ramsey, A. C., The geology of North Wales: Geol. Surv., Great Britain v. 3.
- Seilacher, A., 1990, Aberrations in bivalve evolution related to photo- and chemosymbiosis: Historical Biology, v. 3, p. 289-311.
- Seilacher, A., 2007, Trace Fossil Analysis: Springer-Verlag, Berlin, Heidelberg, New York, 226p.
- Šimo, V., and A. Tomašových, 2013, Trace-fossil assemblages with a new ichnogenus in “spotted” (Fleckenmergel—Fleckenkalk) deposits: a signature of oxygen-limited benthic communities: Geologica Carpathica, v. 64, no. 5, p. 355-374 doi: 10.2478/geoca-2013-0024
- Simpson, S., 1956, On the trace fossil *Chondrites*, Quarterly Journal of the Geological Society of London, v. 112.

- Slatt, R.M., and Y. Abousleiman, 2011, Multi-scale, brittle-ductile couplets in unconventional gas shales: merging sequence stratigraphy and geomechanics: Poster presentation at AAPG Annual Convention and Exhibition, Houston, Texas, USA, April 10-13, 2011, Search and Discovery Article #80181.
- Spaw, J.M., 2012, Identification, integration and upscaling of mudrock types - a pathway to unlocking shale plays: SPE/EAGE European Unconventional Resources Conference and Exhibition, 20-22 March, Vienna, Austria, doi.org/10.2118/153111-MS.
- Spaw, J.M., 2013, Recognition of ichnofacies distributions and their contributions to matrix heterogeneity in mudstones: Unconventional Resources Technology Conference (URTeC), Denver, Colorado, USA, 12-14 August 2013.
- Stow, D.A.V., and A. Wetzel, 1990, Hemiturbidite: a new type of deep-water sediment, In: Cochran J R, et al. (eds), Scientific Results Ocean Drilling Program, v.116, College Station, Texas, Ocean Drilling Program, p. 25-34.
- Uchman, A., 1999, Ichnology of the Rhenodanubian Flysh (Lower Cretaceous-Eocene) in Austria and Germany: Beringeria, v. 25, p. 67-173.
- Wetzel, A., 2002, Modern Nereites in the South China Sea: Ecological associations with redox conditions in the sediment: Palaios, v. 17, p. 507–515.
- Wetzel, A., and R.G. Bromley, 1994, *Phycosiphon incertum* revisited: *Anconichnus horizontalis* is junior subjective synonym: Journal of Paleontology, v. 68, no. 6, p.1396-1402.
- Wetzel, A., and A. Uchman, 2001, Sequential colonization of muddy turbidites in the Eocene Beloveza Formation, Carpathians, Poland: Paleogeography, Paleoclimatology, Paleoecology, v. 168, no. 1–2, p. 171–186, doi:10.1016/S0031-0182(00)00254-6.